ENHANCING THE PHYTOTECHNOLOGIES TOOLKIT: FROM POLLUTANT PRIORITIZATION TO ASSESSING THE WATER RELATIONS OF *POPULUS* L. GENOTYPES GROWN FOR PHYTOREMEDIATION

A Dissertation

presented to

the Faculty of the Graduate School

at the University of Missouri-Columbia

In Partial Fulfillment

of the Requirements for the Degree

Doctor of Philosophy

---

by

ELIZABETH ROGERS

Dr. Chung-Ho Lin, Dissertation Supervisor

JULY 2025

The undersigned, appointed by the dean of the Graduate School, have examined the dissertation entitled

ENHANCING THE PHYTOTECHNOLOGIES TOOLKIT:
FROM POLLUTANT PRIORITIZATION TO ASSESSING THE WATER RELATIONS OF *POPULUS* L. GENOTYPES GROWN FOR PHYTOREMEDIATION

presented by Elizabeth Rogers,

a candidate for the degree of Doctor of Philosophy,

and hereby certify that, in their opinion, it is worthy of acceptance.

_____

Dr. Chung-Ho Lin

_____

Dr. Ronald S. Zalesny Jr.

_____

Dr. Noel Aloysius

_____

Dr. Jeffrey Wood

_____

Dr. Jeanne Dollinger

DEDICATION

This dissertation is dedicated to my parents, Amy and Jeff Rogers, for your unconditional love and support, for listening to countless phyto conversations over the years, for encouraging me to chase my dreams, even if it meant moving to Missouri, and for all the calls, texts, notes, and care packages through my grad school journey that gave me joy during stressful times and made the distance feel a little shorter; to my favorite brother, Nathaniel Rogers, for giving me a grounded perspective, and inspiring me to be silly when I needed it most; to my bonus family, my father- and mother-in-law, Glenn and Jill Vinhal, and my brother- and sister-in-law, Matt and Taylor Duszak, for the advice, support, and encouragement you have given me over the years, and to my new nephew, Henry Duszak, for your adorable photos that made me smile despite my nerves on the morning of my defense; and to my husband, Ryan Vinhal, for picking up the slack caused by my many nights at the computer, especially over the past six months, for lighting the way forward for me with your fierce optimism when things were challenging, and for your unwavering belief in me. Finally, to the Dolly Parton's America podcast, for getting me through many miles of highway between northern Wisconsin and Missouri, and for assuring me that I would eventually see the light of a clear blue morning.

ACKNOWLEDGEMENTS

First, I would like to express my sincerest gratitude to my co-advisors, Dr. Chung-Ho Lin and Dr. Ronald Zalesny. Your guidance, expertise, and enthusiasm for research shone a light on the way forward for me in my own research. Thank you both for your patience with me and for always making time to answer the many questions I have asked you over the course of my PhD program. Though you are incredibly productive and busy scientists, you never made me feel like my questions were a burden. I would also like to thank the members of my dissertation committee, Dr. Noel Aloysius, Dr. Jeanne Dollinger, and Dr. Jeffrey Wood, for sharing your precious time, invaluable knowledge, and constructive feedback on my research.

This research would not be possible without all the collaborators, partners, and colleagues that I have had the pleasure of working with over the last few years. I am indebted to Mike Peterson and Raymond Seegers for kindly allowing me to collect samples at your landfill sites, and to Dave Henderson for allowing site access to the Manitowoc field site and your wonderful collaboration on the poplar phytoremediation planting at the site. Thank you to Larry Buechel for being open to the idea of phytoremediation at landfills, your wonderful partnership with the phyto team, and for the valuable knowledge that you have graciously shared with us on landfill design and operation. I also owe my eternal thanks to Caroline Todd for always being willing to share your advice and for amazing assistance with everything from conference planning, to managing laboratory orders, to organizing travel accommodations. Additionally, this work would not be possible without the funding provided by the Great Lakes Restoration

Initiative, the University of Missouri Center for Agroforestry, the USDA/ARS Dale Bumpers Small Farm, nor without the support of the USDA Forest Service.

I would also like to thank Edmund Bauer, Dr. Joel Burken, Brent DeBauche, Dr. Chung-Ho Lin, Paul Manley, Dr. Andrej Pilipović, Ryan Vinhal, Adam Wiese, and Dr. Ronald Zalesny for contributing to data collection during the physiological measurement campaign of the sap flow field study. My gratitude moreover goes to Brent DeBauche and Ryan Vinhal for assistance collecting landfill groundwater and leachate samples, site maintenance of the Manitowoc poplar planting, and contributions in establishing and maintaining the sap flow and weather station systems at the Manitowoc field site. Additionally, thank you to Brent for persevering through grueling predawn leaf area index measurements for the sake of science. To Faythe Erdmann and Molly Wagler, thank you for your friendship and kindness that have spanned from our first summer in the field working together on Forest Service phytoremediation projects all the way through to my time at the University of Missouri as I navigated the challenges and triumphs of my PhD program.

I am fortunate to have had multiple mentors over the years of my program who have helped guide me along my path to become a scientist. To Stephanie Connolly, thank you for teaching me that although we are not able to choose what happens to us, our power instead is in how we respond to the challenges that we are faced with. You are such a source of positivity, light, and confidence. You use your voice to elevate others, and you truly lead by example. Thank you for taking a chance on me and allowing me to work with you on the General Technical Report, and for the advice you have shared with me over the years. To Dr. Nancy Sonti, you also took a chance on me, a girl from a small

town in Wisconsin, and invited me to learn from you and the wonderful work you are doing with fast-growing trees in Baltimore, MD. You willingly shared your research with me and provided me with opportunities to grow as a scientist in an urban environment that was unfamiliar to me. That trip left a great impression on me and has served to broaden my view of what is possible, not only as a researcher but in life. I am fortunate to have you as a role model. To Liza Paqueo, thank you for opening my eyes to the world of international partnerships, urban conservation, and community engagement. I'm very fortunate to have worked with you and received your guidance throughout the whole process of developing and implementing the Phytoremediation Training Academy curriculum. You openly shared your wealth of knowledge, and you encouraged me to think about science communication in different ways. You inspire me to find ways to meld science with art and creativity, to see the forest beyond the trees, and to Phyto the Good Fight.

I am forever grateful to all the members of the Lin Lab at the University of Missouri who took me in and patiently trained and guided me in the ways of laboratory work. To Dr. Lin, Dr. Hsin-Yeh Hsieh, Shu-Yu Hsu, Mohamed Bayati, Sally Qasim, and Amanda Dwikarina, thank you all for being willing to share your knowledge with me and taking time to help me feel confident in what I was doing. To you all as well as the other members of the lab, Nahom Ghile, Enji Mohamed Jamil, Isa Kupke, and Ruth Williamson, thank you for your kindness, comradery, and insight throughout my program. You all have made Missouri feel like a second home.

There are numerous people from the Forest Service to which I also owe many thanks. Thank you to Beth Larry for supporting all of my Forest Service endeavors, and

for making time to help me to better understand the agency as a whole, and my place within it. Thank you to Dr. Deahn Donnerwright, not only for your support, but also for welcoming me into NRS-13, and for always encouraging me to take advantage of opportunities to grow as a researcher. To my other lab home, the Institute for Applied Ecosystem Studies, thank you to all the staff for supporting me and for helping to keep my spirits up over the years that I have been at the lab. I have enjoyed getting to learn about the important work that you are doing and getting to know you all through the lab wide Safety Day potluck lunches. The passion that you demonstrate on a daily basis, not only for research, but towards caring for the land and serving people, is admirable. It truly has been a privilege working alongside you all.

I would like to thank the many teachers and professors that I have had over my academic career who have left lasting impressions on me. From Rhinelander High School, my gratitude goes to Mrs. Linda Goldsworthy, for showing me what I was capable of, Mrs. Allie Johnson, for helping me to hone my writing skills and introducing me to inspirational literature like Animal, Vegetable, Miracle, and Mrs. Connie Piasecki, for teaching me that music would always be an important part of my life. From Northern Michigan University and the University of Missouri, thank you to the many inspiring professors I had, who are too numerous to list, for sharing your passions and expertise, and furthering my love of learning.

Finally, my heartfelt gratitude goes to my family members for everything they have provided me over the years to get to this point. To my parents, Amy and Jeff Rogers, thank you for instilling in me a love of nature from a young age, and for helping me to appreciate the small miracles of the natural world. You have supported me without

question or doubt from the beginning of this journey. Thank you for raising me to be the person that I am today and for always believing in me. To my brother, Nathaniel Rogers, thank you for your perspective when things got stressful, and for being willing to help with field data collection at 4:30 am, no questions asked. Your willingness to help means a lot to me. To my father- and mother-in-law, Glenn and Jill Vinhal, thank you for your encouragement and support as I worked through this long journey, and for allowing me to work on my research at your kitchen table, without questioning my sanity. To my brother- and sister-in-law, Matt and Taylor Duszak, thank you for your support in this endeavor, and for your patience with the challenges of scheduling get-togethers around busy field seasons. To my husband, Ryan, thank you for being you throughout everything. Your positivity, calm demeanor, and patience with this whole process have kept me grounded and motivated. Thank you for reviewing countless drafts of papers with your incredible attention to detail. Thank you for compiling never-ending citations into Zotero and using that same attention to detail to make sure each one was properly formatted. Thank you for always being willing to have a discussion on research and for sharing your perspective with me on everything from experimental design to data management to fieldwork and everything in between. You are my sounding board for ideas and more importantly, you are my best friend. I couldn't have done this without you.

TABLE OF CONTENTS

ACKNOWLEDGEMENTS ii
LIST OF TABLES xi
LIST OF FIGURES xiii
LIST OF ABBREVIATIONS xv
ABSTRACT xvii
CHAPTER 1. INTRODUCTION 1
1.1 Background 1
1.2 Dissertation overview 5
1.3 Research objectives 7
1.4 References 8
CHAPTER 2. A SYSTEMATIC APPROACH FOR PRIORITIZING LANDFILL POLLUTANTS BASED ON TOXICITY: APPLICATIONS AND OPPORTUNITIES 19
Abstract 19
2.1 Introduction 20
2.2 Materials and methods 24
2.2.1 A literature search for chemicals in landfill leachate 24
2.2.2 Collection and analysis of toxicity data for landfill leachate chemicals 24
2.2.2.1 ECOTOX database 25
2.2.2.2 ToxCast screening library 25
2.2.2.3 CTV predictor 26
2.2.2.4 Data integration and prioritization using ToxPi 27
2.2.3 Prioritization scheme customization 30
2.2.3.1 Incorporating additional datasets 30
2.2.3.2 Applying weighting schemes 31
2.2.4 Comparison to regulatory lists 31
2.3 Results 32
2.3.1 Availability of toxicity data 32
2.3.2 ToxPi contaminant prioritization: general scheme 32
2.3.3 ToxPi contaminant prioritization: general + ED data scheme 34
2.3.4 ToxPi contaminant prioritization: cancer weighted scheme 35

2.3.5 ToxPi contaminant prioritization: ED weighted scheme 36
2.3.6 ToxPi contaminant prioritization: flora and fauna weighted scheme 36
2.3.7 Comparison with regulatory lists 37
2.4 Discussion 37
2.4.1 ToxPi leachate contaminant prioritization schemes 37
2.4.2 Pollutant prioritization and landfill regulatory lists 39
2.4.3 Future work to build upon the developed prioritization approach 40
2.5 Conclusion 41
2.6 Funding and acknowledgements 42
APPENDIX A 57
2.7 References 80
CHAPTER 3. PRIORITIZING LANDFILL POLLUTANTS TO TARGET WITH PHYTOREMEDIATION: A CASE STUDY IN SOUTHEASTERN WISCONSIN, USA 100
Abstract 100
3.1 Introduction 101
3.2 Materials and methods 106
3.2.1 Sample collection 106
3.2.2 Sample preparation 108
3.2.3 LC-HRMS analysis 109
3.2.4 XCMS data processing 109
3.2.4.1 Reverse searching 110
3.2.4.2 Forward searching 111
3.2.5 Contaminant prioritization 112
3.3 Results 113
3.3.1 Reverse searching 113
3.3.2 Forward searching 114
3.3.3 Toxicity prioritization 115
3.4 Discussion 117
3.5 Conclusion 123
APPENDIX B. 138
3.6 References 149

CHAPTER 4. INTRINSIC AND EXTRINSIC FACTORS INFLUENCING *POPULUS* WATER USE: A LITERATURE REVIEW 161
Abstract 161
4.1 Introduction 162
4.2 Materials and methods 165
4.2.1 Literature review and article selection 165
4.2.2 Water use data transformation 166
4.2.3 Comparative analysis based on experimental factors 167
4.2.3.1 Hybrid *Populus*: intrinsic factors 168
4.2.3.2 Hybrid *Populus*: extrinsic factors 169
4.2.3.3 Non-hybrid *Populus*: intrinsic factors 170
4.2.3.4 Non-Hybrid *Populus*: extrinsic factors 171
4.2.4 Exclusion of meteorological variables from the present review 171
4.2.5 Exclusion of soil type from the present review 172
4.2.6 Statistical analysis 173
4.3 Results 174
4.3.1 Article selection 174
4.3.2 Sap flow methodologies 175
4.3.3 *Populus* water use 176
4.3.3.1 Hybrids 177
4.3.3.2 Non-hybrids 180
4.4 Discussion 182
4.4.1 Sap flow methodologies 182
4.4.2 Hybrid *Populus* water use 183
4.4.3 Non-hybrid *Populus* water use 185
4.5 Conclusions 187
4.6 Funding and acknowledgements 188
APPENDIX C. 201
4.7 References 202
CHAPTER 5. WATER RELATIONS OF THREE HYBRID *POPULUS* GENOTYPES GROWN FOR PHYTOREMEDIATION IN EASTERN WISCONSIN, USA 238
Abstract 238

5.1 Introduction 239
5.2 Materials and methods 246
5.2.1 Experimental site, poplar material, establishment 246
5.2.2 Environmental measurements 248
5.2.3 Sap flow measurements 249
5.2.4 Leaf area index 252
5.2.5 Canopy conductance 253
5.2.6 Leaf water potential and hydraulic conductance 254
5.2.7 Statistical analysis 255
5.3 Results 257
5.3.1 Environmental conditions 257
5.3.2 Stand characteristics 257
5.3.3 Water use and sap flux 259
5.3.4 Stomatal sensitivity to vapor pressure deficit 260
5.3.5 Leaf water potential and hydraulic conductance 261
5.4 Discussion 261
5.4.1 Water use and sap flux 261
5.4.2 Water use and leaf retention 264
5.4.3 Stomatal sensitivity 266
5.4.4 Hydraulic conductance and leaf water potential 268
5.5 Conclusion 269
APPENDIX D. 283
5.6 References 284
CHAPTER 6. CONCLUSIONS AND FUTURE WORK 300
6.1 Conclusions 300
6.2 Future work 303
6.2.1 Targeted analysis of landfill leachate 303
6.2.2 Investigations of the phytoremediation efficacy of poplars 304
VITA 307

LIST OF TABLES

Table 2.1. Uses, sources, and health impacts of compounds in landfill leachate ranked by their potential toxicity according to ToxPi analysis. 44
Table 2.2. Concentration range of compounds in landfill leachate ranked by their potential toxicity according to ToxPi analysis. 47
Table 2.3. Top 40 most potentially toxic landfill leachate chemicals according to the general + endocrine disruption data prioritization scheme 49
Table 2.4. Top 40 most potentially toxic landfill leachate chemicals according to the cancer weighted prioritization scheme 50
Table 2.5. Top 40 most potentially toxic landfill leachate chemicals according to the endocrine disruption weighted prioritization scheme 51
Table 2.6. Top 40 most potentially toxic landfill leachate chemicals according to the flora and fauna weighted prioritization scheme 52
Table 2.7. Top 40 most potentially toxic landfill leachate chemicals according to the general prioritization scheme 53
Table A1. Landfill leachate contaminants identified in a literature review 57
Table A2. Landfill information for studies that reported leachate contaminant concentrations 66
Table A3. Toxicity profiles generated in ToxPi of the 40 most toxic contaminants in landfill leachate according to the general prioritization scheme 68
Table A4. Health impacts and associated references of the 40 most toxic contaminants in landfill leachate according to ToxPi analysis using the general prioritization scheme 73
Table A5. Top 40 most toxic chemicals found in landfill leachate according to the flora and fauna weighted prioritization scheme 75
Table A6. Top 40 most toxic chemicals found in landfill leachate according to the cancer weighted prioritization scheme 76
Table A7. Top 40 most toxic chemicals found in landfill leachate according to the endocrine disruption weighted prioritization scheme 77
Table A8. Top 40 most toxic chemicals found in landfill leachate according to the general + endocrine disruption data prioritization scheme 78
Table 3.1. Landfill characteristics of two landfills in Southeastern Wisconsin, USA, where samples were collected for the present study 125
Table 3.2. XCMS Online pairwise job parameters and feature information for groundwater and leachate samples collected from two landfills in Southeastern Wisconsin 126
Table 3.3. Landfill leachate compounds from the literature review of Rogers et al. (2021) that were putatively identified in the present study 127

Table 3.4. Landfill leachate compounds from regulatory lists that were putatively identified in the present study 128
Table 3.5. Top 25 compounds putatively identified in groundwater and leachate samples from two landfills in Southeastern Wisconsin using XCMS Online 129
Table 3.6. Uses of top 25 compounds putatively identified in groundwater and leachate samples from two landfills in Southeastern Wisconsin using XCMS Online 130
Table B1. Data processing parameters used in XCMS Online jobs 138
Table B2. Toxicity parameters, their definitions, and their transformations in ToxPi 139
Table B3. ToxPi toxicity rankings, hierarchical cluster groupings, and relative intensities for 242 compounds putatively identified in groundwater and leachate samples 140
Table 4.1. Definitions of intrinsic and extrinsic factors analyzed in a quantitative comparison of *Populus* water use reported in the literature 190
Table 4.2. Summary of studies that used sap flow methodologies to quantify hybrid *Populus* water use (n = 18 articles)..... 191
Table 4.3. Hybrid *Populus* genotype parentages from *Populus* water use studies (n = 18) reported in the literature..... 192
Table 4.4. Summary of studies that used sap flow methodologies to quantify non-hybrid *Populus* water use (n = 33 articles)..... 193
Table 4.5. *Populus* species and authorities from non-hybrid *Populus* water use studies (n = 33)..... 194
Table C1. Sap flow methodologies implemented in *Populus* water use studies..... 201
Table 5.1. Genomic groups and plant material sources for the three hybrid poplar genotypes investigated in the current study 271
Table 5.2. Soil physicochemical properties of the study site in Eastern Wisconsin 272
Table 5.3. Tree growth and leaf area characteristics in the middle of the study period (DOY 207; 7/26/21) for 'NM2' (*Populus nigra* × *P. maximowiczii*), '9732-11' (*P. deltoides* × *P. nigra*), and 'DN34' (*P. deltoides* × *P. nigra*) in their fourth growing season..... 273
Table 5.4. Parameters estimated from linear regression equations fitted to the canopy stomatal conductance (G_S; mol m^{-2} s^{-1}) vs. natural log of vapor pressure deficit [ln(VPD); kPa] relationship for 'NM2' (*Populus nigra* × *P. maximowiczii*), '9732-11' (*P. deltoides* × *P. nigra*), and 'DN34' (*P. deltoides* × *P. nigra*) 274
Table 5.5. Tree leaf water potential (Ψ; MPa) and leaf-specific whole-plant hydraulic conductance (K_l; kg m^{-2} h^{-1} MPa^{-1}) for 'NM2' (*Populus nigra* × *P. maximowiczii*), '9732-11' (*P. deltoides* × *P. nigra*), and 'DN34' (*P. deltoides* × *P. nigra*) measured within low ($\theta < 0.2$ m^3 m^{-3}) and high ($\theta > 0.2$ m^3 m^{-3}) soil moisture conditions..... 275
Table D1. Parameters used in Baseliner preprocessing of sap flow data..... 283

LIST OF FIGURES

Figure 2.1. ToxPi prioritization schemes 54
Figure 2.2. Data availability for 322 landfill leachate contaminants identified in the literature and prioritized using ToxPi..... 55
Figure 2.3. Distribution dot plot of ToxPi Scores for all 322 landfill leachate contaminants using the general prioritization scheme 56
Figure A1. Distribution dot plot of ToxPi scores for all contaminants, including outlier 2,3,7,8-TCDD, which was removed from further analysis..... 79
Figure 3.1. Location of two landfill sites in Southeastern Wisconsin, USA where samples were collected 131
Figure 3.2. Comprehensive approach for putative identification of landfill contaminants 132
Figure 3.3. Representative cloud plots of pairwise jobs in XCMS Online..... 133
Figure 3.4. Representative 3D PCA plot of Landfill A and Landfill B samples..... 134
Figure 3.5. Toxicity data availability for 1,321 putatively identified landfill contaminants 135
Figure 3.6. ToxPi model (A) and hierarchical cluster analysis for 242 landfill contaminants putatively identified using a comprehensive data-based and list-based approach in XCMS Online (B) 136
Figure 3.7. ToxPi toxicity score rank plot for 242 putatively identified landfill contaminants 137
Figure 4.1. Flow chart of literature review article selection process 195
Figure 4.2. Sap flow methodologies used to quantify *Populus* sap flow reported in the literature (n = 133 articles)..... 196
Figure 4.3. Hybrid *Populus* transpiration rates (mm/day) reported in 18 articles according to intrinsic factors (i.e., hybrid type and tree age) 197
Figure 4.4. Hybrid *Populus* transpiration rates (mm/day) reported in 18 articles according to extrinsic factors (i.e., planting density and water availability)..... 198
Figure 4.5. Non-hybrid *Populus* transpiration rates (mm/day) reported in 33 articles according to intrinsic factors (i.e., species and tree age) 199
Figure 4.6. Non-hybrid *Populus* transpiration rates (mm/day) reported in 33 articles according to extrinsic factors (i.e., planting density, experimental context, and water availability) 200
Figure 5.1. Location of the sap flow study site..... 276
Figure 5.2. Installation of thermal dissipation sap flow probes in hybrid poplar trees... 277
Figure 5.3. Map of phytoremediation buffer planting (A) and schematic of LAI measurement scheme (B-C)..... 278
Figure 5.4. Climatic conditions measured at the study site in Eastern Wisconsin, USA during the study period (DOY 176-251, 6/25/21-9/8/21)..... 279

Figure 5.5. Monthly leaf area index (LAI; m^2 m^{-2}) of 'NM2' (*Populus nigra* × *P. maximowiczii*), '9732-11' (*P. deltoides* × *P. nigra*), and 'DN34' (*P. deltoides* × *P. nigra*) in their fourth growing season 280
Figure 5.6. Tree-level monthly (A, B) and season (C) water use (kg $tree^{-1}$) of three hybrid poplars ('9732-11', 'DN34', and 'NM2') in their fourth growing season 281
Figure 5.7. Canopy stomatal conductance (G_S; mol m^{-2} s^{-1}) vs. the natural log of vapor pressure deficit (ln VPD; ln kPa) for three poplar genotypes ('9732-11', 'DN34', and 'NM2') within (A) low soil moisture conditions ($\theta < 0.2$ m^3 m^{-3}) and (B) average-to-high soil moisture conditions ($\theta > 0.2$ m^3 m^{-3}) 282

LIST OF ABBREVIATIONS

AC50	Concentration which gives 50% activation in a bioassay (μM)
ANOVA	Analysis of variance
ATSDR	Agency for Toxic Substances and Disease Registry
BMD	Benchmark dose; dose of a compound which elicits a predetermined change in the response rate of a negative effect (mg $kg^{-1}_{body\ weight}$ day^{-1})
BMDL	Benchmark dose lower limit; the lower limit of a one-sided 95% confidence interval on the BMD (mg $kg^{-1}_{body\ weight}$ day^{-1})
BRRTS on the Web	WI DNR database of information on contaminated sites and associated cleanup and redevelopment activities in Wisconsin
CASRN	Chemical Abstracts Service Registry Number
CEC	Contaminant of emerging concern
CFR	Code of Federal Regulations
CHP	Compensation heat pulse
CPV	Cancer potency value; a California EPA-specific OSF (risk per mg $kg^{-1}_{body\ weight}$ day^{-1})
CTV Predictor	Conditional Toxicity Value Predictor; generates predicted *in silico* human toxicity values based on chemical structure
DBH	Diameter at breast height (cm)
EC50	Concentration of a toxicant that induces a response halfway between the baseline and maximum (mg L^{-1})
ECOTOX	US EPA toxicity database of *in vivo* toxicity data
ED	Endocrine disruption
EDKB	Endocrine Disruptor Knowledge Base
E_l	Leaf-level transpiration (kg $m^{-2}_{leaf\ area}$ s^{-1} ; kg $m^{-2}_{leaf\ area}$ h^{-1})
EPA	Environmental Protection Agency
G_S	Canopy conductance (m s^{-1}; mol m^{-2}_{canopy} s^{-1})
G_S sensitivity	Negative slope of the relationship between canopy conductance and lnVPD
$G_{S,ref}$	Reference canopy conductance at VPD = 1 kPa
HPV	Heat pulse velocity
HRMS	High resolution mass spectrometry
J_S	Sap flux (kg H_2O $m^{-2}_{sapwood\ area}$ s^{-1})
K_G	Coefficient calculated as 115.8 + 0.4226 × air temperature (°C)
K_l	Leaf-specific whole-plant hydraulic conductance (kg $m^{-2}_{leaf\ area}$ h^{-1} MPa^{-1})
K_{OC}	Soil organic carbon-water partition coefficient
LAI	Leaf area index ($m^2_{leaf\ area}$ $m^{-2}_{ground\ area}$)
LC	Liquid chromatography
LC-HRMS	Liquid chromatography coupled with high-resolution mass spectrometry
LC-MS	Liquid chromatography coupled with mass spectrometry
LLE	Liquid-liquid extraction
log K_{OW}	n-octanol-water partition coefficient
METLIN	Mass spectral database

MS/MS	Tandem mass spectrometry
MSW	Municipal solid waste
NCTR	National Center for Toxicological Research
NO(A)EL	No observed adverse effect level; the highest dose of a compound for which there are no observed negative effects (mg $kg^{-1}_{body\ weight}$ day^{-1})
NOAA	National Oceanic and Atmospheric Administration
OSF	Oral slope factor; an estimate of the increased cancer risk from oral exposure to a dose of 1 mg kg^{-1} day^{-1} for a lifetime (risk per mg $kg^{-1}_{body\ weight}$ day^{-1})
PCB	Polychlorinated biphenyl
PFAS	Per- and polyfluoroalkyl substances
Q-TOF	Quadrupole-time-of-flight
RBA	Relative binding activity
RCRA	Resource Conservation and Recovery Act
RfD	Reference dose; an estimate of the daily exposure to a compound that is likely to be without negative effects (mg $kg^{-1}_{body\ weight}$ day^{-1})
RP	Relative potency
RPP	Relative proliferation potency
Scaled G_S sensitivity	G_S sensitivity / $G_{S,ref}$
SHB	Stem heat balance
SHWIMS on the Web	Solid and Hazardous Waste Information Management System; former WI DNR database used to track information about solid and hazardous waste disposal sites in Wisconsin
SRC	Short-rotation coppice
SRWC	Short rotation woody crop
T3DB	Toxin and Toxin-Target Database
TDP	Thermal dissipation probe
ToxCast	US EPA toxicity database of *in vitro* assay data
ToxPi	Toxicological Prioritization Index
UHPLC	Ultra-high performance liquid chromatography
USDA	US Department of Agriculture
VOC	Volatile organic compound
VPD	Vapor pressure deficit (kPa)
VWC ; θ	Soil volumetric water content (m^3 m^{-3})
WI DNR	Wisconsin Department of Natural Resources
XCMS Online	Data processing platform for non-targeted mass spectral data
ΔT	Temperature difference between thermal dissipation probes at a particular timepoint
ΔT_{max}	Maximum temperature difference between thermal dissipation probes when sap flow is zero
Ψ	Leaf water potential (MPa)
Ψ_{md}	Midday leaf water potential (MPa)
Ψ_{pd}	Predawn leaf water potential (MPa)
$\Delta\Psi$	Difference in predawn and midday leaf water potential (MPa)

ENHANCING THE PHYTOTECHNOLOGIES TOOLKIT:
FROM POLLUTANT PRIORITIZATION TO ASSESSING THE WATER RELATIONS OF *POPULUS* L. GENOTYPES GROWN FOR PHYTOREMEDIATION

Elizabeth Rogers

Dr. Chung-Ho Lin, Dissertation Supervisor

ABSTRACT

Phytoremediation is a cost-effective technology that has been gaining momentum over the past few decades as a sustainable option for environmental pollution remediation. However, challenges remain to the optimization of phytoremediation systems, including: 1) selecting which pollutants to target with remediation systems, and 2) selecting ideal tree genotypes that both fulfill remediation objectives and are resilient to variable climatic conditions. To address the first challenge, an approach was developed for toxicity-based prioritization of contaminants to target with remediation systems. The comprehensive approach was then applied to a case study of Wisconsin landfills, wherein it was augmented with non-targeted analysis of high-resolution mass spectrometry data for putative identification of candidate compounds in landfill samples. To address the second challenge, a meta-analysis of *Populus* water use reported in the literature was conducted, and its influential factors were identified and compared. Then, a field trial was conducted to investigate the water use strategies of three hybrid poplar genotypes ('DN34', *Populus deltoides* Bartr. ex. Marsh × *P. nigra* L.; '9732-11', *P. deltoides* × *P. nigra*; 'NM2', *P. nigra* × *P. maximowiczii* A. Henry) in their fourth growing season that were grown for phytoremediation at a waste dumping site in Wisconsin. The approaches and results presented here can enable standardized pollutant prioritization and inform the selection of resilient poplar genotypes for phytoremediation applications.

CHAPTER 1. INTRODUCTION

1.1 Background

Interest in phytoremediation and other phytotechnologies has increased substantially since its recognition as a science in the 1990s (Dessureault-Rompré, 2022; Gerhardt et al., 2017; McCutcheon and Schnoor, 2003; Mench et al., 2010). Phytoremediation, the use of plants to clean contaminated soil and water, is considered a cost-effective, aesthetically pleasing, green technology for environmental pollution remediation (Gerhardt et al., 2017; Pivato et al., 2018). Within phytoremediation systems, natural physiological and microbiological processes of trees and their associated microbiomes are harnessed to degrade, sequester, uptake, or immobilize pollutants in water and soils (McCutcheon and Schnoor, 2003; Mench et al., 2010; Tsao, 2003). Tree transpiration is a key component that drives the success of phytoremediation systems. Not only does tree water use enable the uptake and further remediation of bioavailable contaminants from the soil (Davis et al., 2002; Landmeyer, 2012), but it also can enable site managers to gain hydraulic control of contaminated sites (Ferro et al., 2003), and facilitates mass flow of contaminants toward the microbially-active rhizosphere (Ferro et al., 1994; Trapp and Karlson, 2001; Wenzel, 2009). Because of the importance of tree water use in phytoremediation systems, fast-growing trees with elevated water use, including *Populus* L., *Salix* L., and *Eucalypts* L'Hér, are commonly selected for phytoremediation systems (Marmiroli et al., 2011; McCutcheon and Schnoor, 2003; Tripathi et al., 2016; Zalesny et al., 2019a). *Populus* hybrids are a popular option in North America for phytoremediation applications (McCutcheon and Schnoor, 2003; Zalesny et al., 2019b). In addition to their elevated water use (Ferro et al., 2001; Rogers et al., 2023;

Zalesny et al., 2006), hybrid poplars propagate readily from dormant hardwood cuttings (Dickmann et al., 2001), exhibit rapid growth and biomass production (Bradshaw et al., 2000; Laurent et al., 2015), and have extensive genetic diversity (Dickmann et al., 2001; Stettler et al., 1996), all of which make them ideal candidates for phytoremediation systems. Because of these traits, the remediation capacity of hybrid poplars has been investigated for heavy metals (Kovačević et al., 2025; Li et al., 2024; Prouzová et al., 2024) and organic contaminants (BenIsrael et al., 2019; Doty et al., 2017; Ferro et al., 2013; Gordon et al., 1998; Landmeyer and Effinger, 2016) across a range of site types and ecosystems.

Despite the positive momentum for phytotechnologies over the past few decades, challenges to the optimization of phytoremediation systems remain. For instance, it has been challenging to select which pollutants to target with remediation systems, particularly when contaminated media have complex chemical compositions. Landfill leachate is one such matrix that is composed of a dynamic mixture of chemicals, with co-occurring factors such as landfill age, management operations, waste composition, and climatic conditions all influencing its composition (Wang and Qiao, 2024). Successful leachate phytoremediation requires data-driven, non-biased prioritization of pollutants to target with remediation systems, so that optimal tree genotypes that are ideally suited to the contaminants can be tested and selected (Zalesny et al., 2007, 2021). However, priority compounds are often selected based on regulatory lists, which can be outdated (e.g., Appendices I and II, 40 C.F.R. § 258, 1991); literature on landfill leachate (Rogers et al., 2021), which may have varying relevance; heuristic evidence; and limited site-specific information. Such an approach for identifying priority pollutants not only lacks

quantitative prioritization, but it also can neglect other potentially harmful pollutants within leachate, such as organic pollutants like pharmaceuticals, PFAS, personal care products, and other emerging contaminants of concern (Masoner et al., 2016, 2020; Tolaymat et al., 2023; Yu et al., 2020). A comprehensive framework that combines global chemical profiling of site-specific samples with toxicity-based prioritization of leachate pollutants to target with remediation systems does not exist but is needed to enhance the efficacy of phytoremediation systems.

Another challenge facing the field of phytotechnologies regards selection of ideal poplar genotypes that both fulfill remediation objectives and are resilient to variable climatic conditions. There are a multitude of available poplar genotypes resulting from tree breeding and tree improvement programs of the last half century (Isebrands and Zalesny, 2021; Nelson et al., 2021; Riemenschneider et al., 2001), however, the water use strategies of many of these genotypes, including the quantity of water that is used on a tree-level basis, and associated strategy for stomatal regulation, are unknown. Variability in water use strategies has been found among poplar genotypes, from isohydric responses to water stress, in which stomatal conductance decreases during dry periods in order to maintain a relatively constant leaf water potential (Attia et al., 2015; Lüttschwager et al., 2016; Navarro et al., 2018; Schmidt-Walter et al., 2014; Tardieau and Simonneau, 1998), to anisohydric responses, in which stomatal conductance increases and leaf water potential concurrently decreases during dry periods (Attia et al., 2015; Babi et al., 2019; Lüttschwager et al., 2016; Navarro et al., 2018; Orság et al., 2024; Rovida Kojima et al., 2024; Zenone et al., 2015), to near-isohydric, and near-anisohydric responses that fall somewhere in the middle of the isohydricity spectrum (Rovida Kojima et al., 2023; 2024;

Tang et al., 2024). The isohydricity of a genotype can affect its productivity (Tang et al., 2024; Rovida Kojima et al., 2024) as well as its overall water use. Some isohydric poplars can recover transpiration rates after severe water stress sooner and more completely than more anisohydric genotypes (Attia et al., 2015). On the other hand, elevated transpiration has been documented for anisohydric trees compared to isohydric trees (Navarro et al., 2018). Implementing trees of the same isohydricity (strictly anisohydric or strictly isohydric) in phytoremediation systems may lead to unfavorable results. For example, anisohydric poplars may exhibit greater water use than isohydric poplars (Navarro et al., 2018) but may also have reduced productivity and water use efficiency compared to strictly using isohydric genotypes (González-González et al., 2017), as well as increased risk of cavitation and hydraulic failure (Attia et al., 2015; McDowell et al., 2008). Alternatively, isohydric poplars may be a less risky option under severe drought conditions (Attia et al., 2015; Schmidt-Walter et al., 2014), but their lower water use relative to that of anisohydric trees should also be considered (Navarro et al., 2018). With tree water use being a critical component affecting the efficacy of phytoremediation systems (Vose et al., 2000), information on tree water use strategies of regionally relevant genotypes is important for maximizing phytoremediation success. However, few studies have investigated the relationships between poplar isohydricity and phytoremediation implications (Babi et al., 2019; Grimond et al., 2024; Stojnić et al., 2021). Planning for resilient phytoremediation systems will require knowledge of water use strategies to select complementary genotypes that maximize water use and productivity in the short-term and promote system survival in the long-term.

1.2 Dissertation overview

The overarching objective of this work is to provide relevant and necessary information on two aspects of phytoremediation systems that are critical components of success, namely, pollutant prioritization and the water relations of fast-growing trees implemented in such systems. To accomplish this, a combination of meta-analyses of available literature, laboratory work, and field work were conducted. Laboratory and field results were based on case studies of municipal solid waste landfills and other waste-dumping sites in Wisconsin, USA.

Chapter Two presents a meta-analysis of contaminants reported to exist in municipal solid waste landfill leachate. In addition, a landfill pollutant prioritization approach was developed for prioritization of leachate contaminants to target with remediation systems based on potential toxicity to human health and/or the environment. The developed approach was then implemented to prioritize leachate contaminants identified in the literature. The main content of this chapter is from the following publication:

Rogers, E.R., Zalesny, R.S., Lin, C.-H., 2021. A systematic approach for prioritizing landfill pollutants based on toxicity: applications and opportunities. J. Environ. Manage. 284, 112031. https://doi.org/10.1016/j.jenvman.2021.112031.

In Chapter Three, the pollutant prioritization approach was augmented by the addition of non-targeted analysis of high-resolution mass spectrometry data. A combination of list-based forward searching and data-based reverse searching are implemented in the non-targeted analysis to putatively identify candidate compounds in environmental samples. The developed framework for putative pollutant identification

and prioritization was applied to groundwater and leachate samples collected from two Southeastern Wisconsin municipal solid waste landfills.

Chapter Four presents a meta-analysis of the water use of *Populus* species and genotypes reported in the literature. Common methodologies for quantifying *Populus* water use were evaluated. Intrinsic and extrinsic factors influencing the water use of *Populus* were identified, water use data were compared among the factors, and the most influential factors were discussed. The main content of this chapter is from the following publication:

Rogers, E.R., Zalesny, R.S., Lin, C.-H., Vinhal, R.A., 2023. Intrinsic and extrinsic factors influencing *Populus* water use: a literature review. J. Environ. Manage. 348, 119180. https://doi.org/10.1016/j.jenvman.2023.119180.

In Chapter Five, the water use strategies are investigated for three hybrid poplar genotypes in their fourth growing season that are grown for phytoremediation at a waste-dumping site in Eastern Wisconsin. Tree water use during a 75-day study period was quantified and compared among the genotypes. Morphological and physiological parameters related to water use strategies (i.e., leaf area index; stomatal conductance; stomatal sensitivity to vapor pressure deficit; leaf water potential; leaf-specific whole-plant hydraulic conductance) were also measured. Implications for genotype selection for phytoremediation systems are discussed.

Chapter Six presents overall conclusions from this work and describes the future work that can build upon this research.

1.3 Research objectives

The work reported in the dissertation below has the following specific objectives:

1. Develop a pollutant prioritization approach based on potential toxicity that is flexible and broadly applicable for use in phytotechnologies applications.
2. Develop a comprehensive framework for putative contaminant identification and prioritization and implement the framework in a landfill case study.
3. Synthesize available literature on *Populus* water use and identify influential intrinsic and extrinsic factors that affect it.
4. Assess the water use and water use strategies of three hybrid *Populus* genotypes in their fourth growing season that are grown for phytoremediation.

1.4 References

Appendix I to 40 C.F.R. § 258, 1991. Appendix I to Part 258—Constituents for detection monitoring. https://www.ecfr.gov/current/title-40/part-258/appendix-Appendix I to Part 258.

Appendix II to 40 C.F.R. § 258, 1991. Appendix II to Part 258—List of hazardous inorganic and organic constituents. https://www.ecfr.gov/current/title-40/part-258/appendix-Appendix II to Part 258.

Attia, Z., Domec, J.-C., Oren, R., Way, D.A., Moshelion, M., 2015. Growth and physiological responses of isohydric and anisohydric poplars to drought. J. Exp. Bot. 66, 4373–4381. https://doi.org/10.1093/jxb/erv195.

Babi, K., Guittonny, M., Larocque, G.R., Bussière, B., 2019. Effects of spacing and herbaceous hydroseeding on water stress exposure and root development of poplars planted in soil-covered waste rock slopes. Écoscience 26, 149–163. https://doi.org/10.1080/11956860.2018.1538591.

BenIsrael, M., Wanner, P., Aravena, R., Parker, B.L., Haack, E.A., Tsao, D.T., Dunfield, K.E., 2019. Toluene biodegradation in the vadose zone of a poplar phytoremediation system identified using metagenomics and toluene-specific stable carbon isotope analysis. Int. J. Phytoremediat. 21, 60–69. https://doi.org/10.1080/15226514.2018.1523873.

Bradshaw, H.D., Ceulemans, R., Davis, J., Stettler, R., 2000. Emerging model systems in plant biology: poplar (*Populus*) as a model forest tree. J. Plant Growth Regul. 19, 306–313. https://doi.org/10.1007/s003440000030.

Davis, L.C., Castro-Diaz, S., Zhang, Q., Erickson, L.E., 2002. Benefits of vegetation for soils with organic contaminants. Crit. Rev. Plant Sci. 21, 457–491. https://doi.org/10.1080/0735-260291044322.

Dessureault-Rompré, J., 2022. Restoring soil functions and agroecosystem services through phytotechnologies. Front. Soil Sci. 2, 927148. https://doi.org/10.3389/fsoil.2022.927148.

Dickmann, D.I., Isebrands, J.G., Eckenwalder, J.E., Richarson, J. (Eds.), 2001. Poplar culture in North America. NRC Research Press, Ottawa, Ontario.

Doty, S.L., Freeman, J.L., Cohu, C.M., Burken, J.G., Firrincieli, A., Simon, A., Khan, Z., Isebrands, J.G., Lukas, J., Blaylock, M.J., 2017. Enhanced degradation of TCE on a superfund site using endophyte-assisted poplar tree phytoremediation. Environ. Sci. Technol. 51, 10050–10058. https://doi.org/10.1021/acs.est.7b01504.

Ferro, A., Chard, J., Kjelgren, R., Chard, B., Turner, D., Montague, T., 2001. Groundwater capture using hybrid poplar trees: evaluation of a system in Ogden, Utah. Int. J. Phytoremediat. 3, 87–104. https://doi.org/10.1080/15226510108500051.

Ferro, A., Gefell, M., Kjelgren, R., Lipson, D.S., Zollinger, N., Jackson, S., 2003. Maintaining hydraulic control using deep rooted tree systems, in: Tsao, D.T. (Ed.), Phytoremediation. Springer Berlin Heidelberg, Berlin, Heidelberg, pp. 125–156.

Ferro, A.M., Adham, T., Berra, B., Tsao, D., 2013. Performance of deep-rooted phreatophytic trees at a site containing total petroleum hydrocarbons. Int. J. Phytoremediat. 15, 232–244. https://doi.org/10.1080/15226514.2012.687195.

Ferro, A.M., Sims, R.C., Bugbee, B., 1994. Hycrest crested wheatgrass accelerates the degradation of pentachlorophenol in soil. J. Env. Qual. 23, 272–279. https://doi.org/10.2134/jeq1994.00472425002300020008x.

Gerhardt, K.E., Gerwing, P.D., Greenberg, B.M., 2017. Opinion: taking phytoremediation from proven technology to accepted practice. Plant Sci. 256, 170–185. https://doi.org/10.1016/j.plantsci.2016.11.016.

González-González, B.D., Oliveira, N., González, I., Cañellas, I., Sixto, H., 2017. Poplar biomass production in short rotation under irrigation: a case study in the Mediterranean. Biomass Bioenerg. 107, 198–206. https://doi.org/10.1016/j.biombioe.2017.10.004.

Gordon, M., Choe, N., Duffy, J., Ekuan, G., Heilman, P., Muiznieks, I., Ruszaj, M., Shurtleff, B.B., Strand, S., Wilmoth, J., Newman, L.A., 1998. Phytoremediation of trichloroethylene with hybrid poplars. Environ. Health Perspect. 106, 1001–1004. https://doi.org/10.1289/ehp.98106s41001.

Grimond, L., Rivest, D., Bilodeau-Gauthier, S., Khlifa, R., Elferjani, R., Bélanger, N., 2024. Novel soil reconstruction leads to successful afforestation of a former asbestos mine in southern Quebec, Canada. New Forest. 55, 477–503. https://doi.org/10.1007/s11056-023-09989-3.

Isebrands, J.G., Zalesny, R.S., 2021. Reflections on the contributions of *Populus* research at Rhinelander, Wisconsin, USA. Can. J. For. Res. 51, 139–153. https://doi.org/10.1139/cjfr-2020-0248.

Kovačević, B., Milović, M., Kesić, L., Pajnik, L.P., Pekeč, S., Stanković, D., Orlović, S., 2025. Interclonal variation in heavy metal accumulation among poplar and willow clones: implications for phytoremediation of contaminated landfill soils. Plants 14, 567. https://doi.org/10.3390/plants14040567.

Landmeyer, J.E., 2012. Introduction to phytoremediation of contaminated groundwater: historical foundation, hydrologic control, and contaminant remediation. Springer Netherlands, Dordrecht. https://doi.org/10.1007/978-94-007-1957-6.

Landmeyer, J.E., Effinger, T.N., 2016. Effect of phytoremediation on concentrations of benzene, toluene, naphthalene, and dissolved oxygen in groundwater at a former manufactured gas plant site, Charleston, South Carolina, USA, 1998–2014. Environ. Earth Sci. 75, 605. https://doi.org/10.1007/s12665-016-5408-9.

Laurent, A., Pelzer, E., Loyce, C., Makowski, D., 2015. Ranking yields of energy crops: a meta-analysis using direct and indirect comparisons. Renew. Sustain. Energ. Rev. 46, 41–50. https://doi.org/10.1016/j.rser.2015.02.023.

Li, M., Heng, Q., Hu, C., Wang, Z., Jiang, Y., Wang, X., He, X., Yong, J.W.H., Dawoud, T.M., Rahman, S.U., Fan, J., Zhang, Y., 2024. Phytoremediation efficiency of poplar hybrid varieties with diverse genetic backgrounds in soil contaminated by multiple toxic metals (Cd, Hg, Pb, and As). Ecotoxicol. Environ. Safe. 283, 116843. https://doi.org/10.1016/j.ecoenv.2024.116843.

Lüttschwager, D., Ewald, D., Atanet Alía, L., 2016. Consequences of moderate drought stress on the net photosynthesis, water-use efficiency and biomass production of

three poplar clones. Acta Physiol. Plant. 38, 27. https://doi.org/10.1007/s11738-015-2057-7.

Marmiroli, M., Pietrini, F., Maestri, E., Zacchini, M., Marmiroli, N., Massacci, A., 2011. Growth, physiological and molecular traits in Salicaceae trees investigated for phytoremediation of heavy metals and organics. Tree Physiol. 31, 1319–1334. https://doi.org/10.1093/treephys/tpr090.

Masoner, J.R., Kolpin, D.W., Cozzarelli, I.M., Smalling, K.L., Bolyard, S.C., Field, J.A., Furlong, E.T., Gray, J.L., Lozinski, D., Reinhart, D., Rodowa, A., Bradley, P.M., 2020. Landfill leachate contributes per-/poly-fluoroalkyl substances (PFAS) and pharmaceuticals to municipal wastewater. Environ. Sci.: Water Res. Technol. 6, 1300–1311. https://doi.org/10.1039/D0EW00045K.

Masoner, J.R., Kolpin, D.W., Furlong, E.T., Cozzarelli, I.M., Gray, J.L., 2016. Landfill leachate as a mirror of today's disposable society: pharmaceuticals and other contaminants of emerging concern in final leachate from landfills in the conterminous United States. Environ. Toxicol. Chem. 35, 906–918. https://doi.org/10.1002/etc.3219.

McCutcheon, S.C., Schnoor, J.L. (Eds.), 2003. Phytoremediation: transformation and control of contaminants, 1st ed. Wiley-Interscience, Hoboken, New Jersey. https://doi.org/10.1002/047127304X.

McDowell, N., Pockman, W.T., Allen, C.D., Breshears, D.D., Cobb, N., Kolb, T., Plaut, J., Sperry, J., West, A., Williams, D.G., Yepez, E.A., 2008. Mechanisms of plant survival and mortality during drought: why do some plants survive while others

succumb to drought? New Phytol. 178, 719–739. https://doi.org/10.1111/j.1469-8137.2008.02436.x.

Mench, M., Lepp, N., Bert, V., Schwitzguébel, J.-P., Gawronski, S.W., Schröder, P., Vangronsveld, J., 2010. Successes and limitations of phytotechnologies at field scale: outcomes, assessment and outlook from COST Action 859. J. Soils Sediments 10, 1039–1070. https://doi.org/10.1007/s11368-010-0190-x.

Navarro, A., Portillo-Estrada, M., Arriga, N., Vanbeveren, S.P.P., Ceulemans, R., 2018. Genotypic variation in transpiration of coppiced poplar during the third rotation of a short-rotation bio-energy culture. GCB Bioenergy 10, 592–607. https://doi.org/10.1111/gcbb.12526.

Nelson, N.D., Berguson, W.E., McMahon, B.G., Jackson, J., Buchman, D., DuPlissis, J., White, T.W., 2021. Intellectual property in the NRRI hybrid poplar program – inventory, commercialization plan, and progress report (Technical Report No. NRRI/TR-2021/07). University of Minnesota Duluth, Duluth, Minnesota. https://conservancy.umn.edu/items/b5cb6f2f-ccbe-4a63-a057-b3c57f1e0a30.

Orság, M., Berhongaray, G., Fischer, M., Klem, K., Ceulemans, R., King, J.S., Hlaváčová, M., Trnka, M., 2024. Elevated CO_2 concentration alleviates the negative effect of vapour pressure deficit and soil drought on juvenile poplar growth. Centr. Eur. For. J. 70, 51–61. https://doi.org/10.2478/forj-2024-0017.

Pivato, A., Garbo, F., Moretto, M., Lavagnolo, M.C., 2018. Energy crops on landfills: functional, environmental, and costs analysis of different landfill configurations.

Environ. Sci. Pollut. Res. 25, 35936–35948. https://doi.org/10.1007/s11356-018-1452-1.

Prouzová, N., Kubátová, P., Mercl, F., Száková, J., Najmanová, J., Tlustoš, P., 2024. Biomass yield and metal phytoextraction efficiency of *Salix* and *Populus* clones harvested at different rotation lengths in the field experiment. Chem. Biol. Technol. Agric. 11, 78. https://doi.org/10.1186/s40538-024-00600-1.

Riemenschneider, D.E., Isebrands, J.G., Berguson, W.E., Dickmann, D.I., Hall, R.B., Mohn, C.A., Stanosz, G.R., Tuskan, G.A., 2001. Poplar breeding and testing strategies in the north-central U.S.: demonstration of potential yield and consideration of future research needs. Forest. Chron. 77, 245–253. https://doi.org/10.5558/tfc77245-2.

Rogers, E.R., Zalesny, R.S., Lin, C.-H., 2021. A systematic approach for prioritizing landfill pollutants based on toxicity: applications and opportunities. J. Environ. Manage. 284, 112031. https://doi.org/10.1016/j.jenvman.2021.112031.

Rogers, E.R., Zalesny, R.S., Lin, C.-H., Vinhal, R.A., 2023. Intrinsic and extrinsic factors influencing *Populus* water use: a literature review. J. Environ. Manage. 348, 119180. https://doi.org/10.1016/j.jenvman.2023.119180.

Rovida Kojima, E.A., Gonzalez, C.V., Mundo, I.A., Guevara, A., Biruk, L.N., Giordano, C.V., 2023. Differential responses of *Populus deltoides* and *Populus* × *canadensis* clones to short-term water deficit. New Forest. 54, 421–437. https://doi.org/10.1007/s11056-022-09929-7.

Rovida Kojima, E.A., González, C.V., Mundo, I.A., Guevara, A., Giordano, C.V., 2024. Mechanisms of drought resistance in *Populus deltoides* and *P.* × *canadensis* clones to possible situations of water restriction in irrigated systems in drylands. Trees 38, 1267–1281. https://doi.org/10.1007/s00468-024-02551-4.

Schmidt-Walter, P., Richter, F., Herbst, M., Schuldt, B., Lamersdorf, N.P., 2014. Transpiration and water use strategies of a young and a full-grown short rotation coppice differing in canopy cover and leaf area. Agric. Forest Meteorol. 195–196, 165–178. https://doi.org/10.1016/j.agrformet.2014.05.006.

Stettler, R.F., Bradshaw, H.D.Jr., Heilman, P.E., Hinckley, T.M. (Eds.), 1996. Biology of *Populus* and its implications for management and conservation. NRC Research Press, Ottawa, Ontario, Canada.

Stojnić, S., Bojović, M., Pilipović, A., Orlović, S., 2021. Selecting tree species for reclamation of coal mine tailings based on physiological parameters. Topola 27–38. https://doi.org/10.5937/topola2108027S.

Tang, L., Cao, P., Zhang, S., Liu, X., Ge, X., Tang, L., 2024. Two male poplar clones (*Populus* × *euramericana* 'Siyang-1' and *Populus deltoides* 'Nanlin 3804') exhibit distinctly different physiological responses to soil water deficit. Forests 15, 1142. https://doi.org/10.3390/f15071142.

Tardieu, F., Simonneau, T., 1998. Variability among species of stomatal control under fluctuating soil water status and evaporative demand: modelling isohydric and anisohydric behaviours. J. Exp. Bot. 49, 419–432. https://doi.org/10.1093/jxb/49.Special_Issue.419.

Tolaymat, T., Robey, N., Krause, M., Larson, J., Weitz, K., Parvathikar, S., Phelps, L., Linak, W., Burden, S., Speth, T., Krug, J., 2023. A critical review of perfluoroalkyl and polyfluoroalkyl substances (PFAS) landfill disposal in the United States. Sci. Total Environ. 905, 167185. https://doi.org/10.1016/j.scitotenv.2023.167185.

Trapp, S., Karlson, U., 2001. Aspects of phytoremediation of organic pollutants. J. Soils Sediments 1, 37–43. https://doi.org/10.1007/BF02986468

Tripathi, V., Edrisi, S.A., Abhilash, P.C., 2016. Towards the coupling of phytoremediation with bioenergy production. Renew. Sustain. Energ. Rev. 57, 1386–1389. https://doi.org/10.1016/j.rser.2015.12.116.

Tsao, D.T., 2003. Overview of phytotechnologies, in: Tsao, D.T. (Ed.), Phytoremediation, Advances in Biochemical Engineering/Biotechnology. Springer Berlin Heidelberg, Berlin, Heidelberg, pp. 1–50. https://doi.org/10.1007/3-540-45991-X_1.

Vose, J.M., Swank, W.T., Harvey, G.J., Clinton, B.D., Sobek, C., 2000. Leaf water relations and sapflow in eastern cottonwood (*Populus deltoides* Bartr.) trees planted for phytoremediation of a groundwater pollutant. Int. J. Phytoremediat. 2, 53–73. https://doi.org/10.1080/15226510008500030.

Wang, J., Qiao, Z., 2024. A comprehensive review of landfill leachate treatment technologies. Front. Environ. Sci. 12, 1439128. https://doi.org/10.3389/fenvs.2024.1439128.

Wenzel, W.W., 2009. Rhizosphere processes and management in plant-assisted bioremediation (phytoremediation) of soils. Plant Soil 321, 385–408. https://doi.org/10.1007/s11104-008-9686-1.

Yu, X., Sui, Q., Lyu, S., Zhao, W., Liu, J., Cai, Z., Yu, G., Barcelo, D., 2020. Municipal solid waste landfills: an underestimated source of pharmaceutical and personal care products in the water environment. Environ. Sci. Technol. 54, 9757–9768. https://doi.org/10.1021/acs.est.0c00565.

Zalesny, J.A., Zalesny, R.S., Wiese, A.H., Hall, R.B., 2007. Choosing tree genotypes for phytoremediation of landfill leachate using phyto-recurrent selection. Int. J. Phytoremediat. 9, 513–530. https://doi.org/10.1080/15226510701709754.

Zalesny, R.S., Berndes, G., Dimitriou, I., Fritsche, U., Miller, C., Eisenbies, M., Ghezehei, S., Hazel, D., Headlee, W.L., Mola-Yudego, B., Negri, M.C., Nichols, E.G., Quinn, J., Shifflett, S.D., Therasme, O., Volk, T.A., Zumpf, C.R., 2019a. Positive water linkages of producing short rotation poplars and willows for bioenergy and phytotechnologies. WIREs Energy Environ. 8, e345. https://doi.org/10.1002/wene.345.

Zalesny, R.S., Headlee, W.L., Gopalakrishnan, G., Bauer, E.O., Hall, R.B., Hazel, D.W., Isebrands, J.G., Licht, L.A., Negri, M.C., Nichols, E.G., Rockwood, D.L., Wiese, A.H., 2019b. Ecosystem services of poplar at long-term phytoremediation sites in the Midwest and Southeast, United States. WIREs Energy Environ. 8, e349. https://doi.org/10.1002/wene.349.

Zalesny, R.S., Pilipović, A., Rogers, E.R., Burken, J.G., Hallett, R.A., Lin, C.-H., McMahon, B.G., Nelson, N.D., Wiese, A.H., Bauer, E.O., Buechel, L., DeBauche, B.S., Peterson, M., Seegers, R., Vinhal, R.A., 2021. Establishment of regional phytoremediation buffer systems for ecological restoration in the Great Lakes Basin, USA. I. Genotype × environment interactions. Forests 12, 430. https://doi.org/10.3390/f12040430.

Zalesny, R.S., Wiese, A.H., Bauer, E.O., Riemenschneider, D., 2006. Sapflow of hybrid poplar (*Populus nigra* L. × *P. maximowiczii* A. Henry 'NM6') during phytoremediation of landfill leachate. Biomass Bioenerg. 30, 784–793. https://doi.org/10.1016/j.biombioe.2005.08.006.

Zenone, T., Fischer, M., Arriga, N., Broeckx, L.S., Verlinden, M.S., Vanbeveren, S., Zona, D., Ceulemans, R., 2015. Biophysical drivers of the carbon dioxide, water vapor, and energy exchanges of a short-rotation poplar coppice. Agric. Forest Meteorol. 209–210, 22–35. https://doi.org/10.1016/j.agrformet.2015.04.009.

CHAPTER 2. A SYSTEMATIC APPROACH FOR PRIORITIZING LANDFILL POLLUTANTS BASED ON TOXICITY: APPLICATIONS AND OPPORTUNITIES

Adapted from: **Rogers, E.R.**, Zalesny, R.S., and Lin, C-H. 2021. A systematic approach for prioritizing landfill pollutants based on toxicity: Applications and opportunities. J. Environ. Manage. 284, 112031. https://doi.org/10.1016/j.jenvman.2021.112031.

Abstract

Landfills in the United States produce leachate that can pose risks to human health and the environment if it comes into contact with ground and surface water. Current environmental regulations require detection and/or monitoring assessments of landfill leachate for contaminants that have been deemed particularly harmful. However, the lists of contaminants to be monitored are not comprehensive. Further, landfill leachate composition varies over space and time, and thus the contaminants, and their corresponding toxicity, are not consistent across or within landfills. One of the main objectives of this study was to prioritize contaminants found in landfill leachate using a systematic, toxicity-based prioritization scheme. A literature review was conducted, and from it, 484 landfill leachate contaminants with available CAS numbers were identified. *In vitro*, *in vivo*, and predicted human toxicity data were collected from ToxCast, ECOTOX, and CTV Predictor, respectively. These data were integrated using the Toxicological Priority Index (ToxPi) for the 322 contaminants which had available toxicity data from at least two of the databases. Four modifications to this general prioritization scheme were developed to demonstrate the flexibility of this scheme for addressing varied research and applied objectives. The general scheme served as a basis for comparison of the results from the modified schemes and allowed for identification of

contaminants uniquely prioritized in each of the schemes. The schemes outlined here can be used to identify the most harmful contaminants in environmental media in order to design the most relevant mitigation strategies and monitoring plans. Finally, future research directions involving the combination of these prioritization schemes and non-target global metabolomic profiling are discussed.

2.1 Introduction

Landfills in the United States produce large volumes of leachate each year, which represents an important source of chemicals that must be monitored and treated to prevent environmental contamination. Though current comprehensive data do not exist, the U.S. Environmental Protection Agency (EPA) reported that the nearly 2,000 active landfills in the U.S. generate leachate flows ranging from 3.8 L per day to over 2 million L per day (U.S. EPA, 2000). Additionally, 163 landfills were identified as generating contaminated groundwater, with daily flows ranging from 22.7 L per day to over 3.7 million L per day, and a median daily flow of about 48,000 L. The physicochemical and biological composition of landfill leachate varies widely, depending on waste characteristics, moisture content of the waste, hydrogeology of the site, and landfill age (Chu et al., 1994; Kulikowska and Klimiuk, 2008; Moody and Townsend, 2017). Landfill leachate composition is dynamic and fluctuates over time due to a combination of physical and societal factors. Recently, growing awareness of contaminants of emerging concern [CECs, xenobiotic compounds such as personal care products, pharmaceuticals, and PFAS (per- and polyfluoroalkyl substances)] within the environment, and their harmful effects, have prompted research of their existence in landfill leachate (Masoner et

al., 2016). Further research regarding the fate, degradation, and transport of CECs in landfill leachate is needed (Masoner et al., 2014).

Landfill pollutants pose an immediate threat to human health and the environment if leached offsite via groundwater or surface water flow. Human health risks from contaminated water sources are dictated by leachate composition and the extent of the exposure, and can include elevated cancer risk, acute toxicity, and genotoxicity (Mukherjee et al., 2015), though health risks from exposure to newer classes of pollutants like CECs have yet to be classified comprehensively (Ramakrishnan et al., 2015). Incidental ingestion, dermal contact, and inhalation of volatilized leachate contaminants from water contaminated with leachate (i.e., drinking water or recreational water sources), as well as consumption of fish and other aquatic organisms living in contaminated water are the main pathways of human exposure to landfill leachate contaminants (Schiopu and Gavrilescu, 2010). Older "historic" landfills which do not contain modern landfill liners and/or were constructed in low-lying floodplains pose a particular pollution risk to surrounding communities (Brand et al., 2018).

Current Monitoring Guidelines under Code of Federal Regulations (CFR) Title 40, Part 258: Criteria for Municipal Solid Waste Landfills require landfill operators to perform Detection Monitoring at all groundwater monitoring wells for the 62 compounds listed in Appendix I of Part 258 (40 CFR § 258.54, 1991). The chief administrative official responsible for implementing the state permitting program may modify the list of pollutants a site must test for, including deletion of Appendix I compounds or development of an alternative list. If a statistically significant increase over the background concentration for the site is detected for one or more of the compounds, the

site manager must move into the Assessment Monitoring phase. In this phase, groundwater is sampled and analyzed for all 213 compounds listed in Appendix II of Part 258 (40 CFR § 258.55, 1991). In addition, the Effluent Limitations stipulated in CFR Title 40, Part 445 require any wastewater discharged from non-hazardous waste landfills to meet maximum daily concentration requirements for nine physical and chemical parameters. Effluent limitations are selected based on ability to meet them with application of the best practicable control technology currently available (40 C.F.R. § 445.21, 2000).

Mitigation strategies for landfill water pollution depend on location of the polluted water (surface runoff, water in the vadose zone, or groundwater) and on the physical and chemical properties of the pollutants therein. In general, landfill pollution abatement has consisted of waste containment with barriers and liners and offsite treatment of leachate, with varying degrees of success (Allen, 2001). Increased interest in sustainability along with recent technological and scientific advancements in pollution remediation have led to changes in the design and remediation of landfills (Townsend et al., 2015). Many site managers have elected to implement onsite landfill remediation, which can take a variety of forms, such as permeable reactive barriers, electrokinetic remediation, microbial remediation, or *in situ* injection treatments (Ye at al., 2019), in addition to the longer-scale phytoremediation (Nagendran et al., 2006; Tao et al., 2018). Onsite remediation efforts have typically adopted a target approach in which systems are designed to detect, quantify, and remediate pollutants of known existence at a site. Target approaches like these have often relied on 1) groundwater and leachate composition information generated through landfill monitoring procedures and 2) regulatory lists of

monitored compounds developed by traditional targeted analytical approaches, both of which can be limited in scope, as well as 3) decision of most important pollutants to target based on word of mouth or anecdotal evidence. Such methods have failed to consider all the potentially harmful contaminants at a site, especially the emerging contaminants that result from the modern lifestyle. Further, these methods do not quantitatively account for the potential risks the contaminants pose to human health and the environment.

A standardized method for pollutant prioritization, based on toxicity, does not exist but could help mitigation efforts by targeting the most potentially harmful pollutants. Current methods of pollutant prioritization include health risk assessments (Hoang et al., 2016), as well as prioritization based on regulatory standards (Von der Ohe et al., 2011), degradation half-life (Gramatica and Papa, 2007), and signal intensities and frequency in high resolution mass spectrometry (HRMS) spectra (Park et al., 2018). In addition, toxicity data are housed in multiple databases and comprise an array of endpoints (Guillén et al., 2012). This mosaic of prioritization methodologies and toxicity information has led to fragmented, site-specific pollutant mitigation efforts, which discourages cross-study comparison and cohesivity. Here, we present the utility of the toxicity prioritization scheme outlined in Danforth et al. (2020), and modifications thereof, in prioritizing landfill leachate contaminants based on available toxicity data. The original prioritization scheme presented in Danforth et al. (2020) prioritizes contaminants based on toxicity data from three databases: ECOTOX, ToxCast, and Conditional Toxicity Value (CTV) Predictor.

The objectives of the current study were to: 1) prioritize landfill leachate contaminants that have been reported in the literature using a prioritization scheme based on multiple toxicity endpoints; 2) describe possible modifications to the scheme, including the use of additional datasets and/or different weighting schemes; and 3) provide recommendations on broader applications of the general scheme. The approach outlined here establishes the means for systematic prioritization of contaminants in landfill leachate or contaminated groundwater which can aid in subsequent monitoring, remediation and/or treatment, and research.

2.2 Materials and methods

2.2.1 A literature search for chemicals in landfill leachate

Literature regarding municipal solid waste landfill leachate composition was reviewed, and a list of over 500 contaminants was compiled (Table A1). All contaminants that were detected at least once in landfill leachate, and with a reported concentration, were included. Basic descriptive information for the landfills in the identified studies is included in Table A2. This list is not intended to be all-inclusive but rather serves as a starting point for further research involving landfill leachate contaminants. Contaminants that did not have available Chemical Abstracts Service (CAS) numbers were not included in further analysis. Therefore, toxicity data to use in prioritization analyses were collected for the 484 compounds with available CAS numbers (Table A1).

2.2.2 Collection and analysis of toxicity data for landfill leachate chemicals

The compound toxicity ranking schemes developed in the current study are based on the methods of Danforth et al. (2020), whereby compounds are prioritized according

to toxicity values from three databases: ECOTOX, ToxCast, and the Conditional Toxicity Value (CTV) Predictor. These three databases provide a robust approach in covering the spectrum of toxicity data, including *in vivo* data, *in vitro* assay data, and predicted *in silico* human toxicity values, respectively. The predicted human toxicity values component is especially powerful, as it allows for the characterization of compounds that may not yet have regulatory standards.

2.2.2.1 ECOTOX database

ECOTOX is a U.S. EPA database that contains *in vivo* toxicity data (i.e., compound effects on a whole, live organism) for aquatic and terrestrial organisms (U.S. EPA, 2020a). Toxicity data for over 12,000 compounds and over 13,000 species of aquatic organisms and terrestrial plants and wildlife are reported in ECOTOX. In the database, values are reported as individual toxicity values for given chemical-organism combinations. Each chemical does not necessarily have at least one toxicity value for every species in the database. As in Danforth et al. (2020), data for the half-maximal effective concentration (EC50, mg L^{-1}; the concentration of the toxicant that induces a response halfway between the baseline and maximum) were collected from ECOTOX, as this was the most data-rich endpoint. In the present study, the minimum EC50 value across all species in the database was collected for each compound. This approach, though conservative, accounts for sensitive species for which data are not reported, and for sensitive endpoints not represented in this scheme.

2.2.2.2 ToxCast screening library

The ToxCast library is another U.S. EPA database (Richard et al., 2016) and is housed under the CompTox Dashboard (Williams et al., 2017). *In vitro* assay toxicity data

from bioassays of varied types (e.g., cell type, design, bioactivity type) are reported in ToxCast. Particularly, bioactivity (i.e., active or inactive) and half maximal activity concentration values (AC50, μM; the concentration which gives 50% activation in a bioassay) are reported for 4,746 compounds (U.S. EPA, 2018, 2020b). In the current study, the minimum AC50 value as well as the percentage of active assays for each compound were collected from CompTox. Like the approach of selecting the minimum EC50 values from ECOTOX, we recorded minimum AC50 values as a conservative way to account for sensitive species whose AC50 data are not reported in ToxCast.

2.2.2.3 CTV predictor

The CTV Predictor is a web-based tool that generates human health risk data through a quantitative structure activity relationship (QSAR) model-based *in silico* approach (Wignall et al., 2018). Briefly, the QSAR models employed by the CTV Predictor were developed using human health toxicity values publicly available by the US EPA or the California EPA. First, researchers calculated mathematical chemical descriptors based on compound structure for each chemical using the Chemistry Development Kit (CDK) in R (Wignall et al., 2018). Random forests machine learning models were implemented to predict toxicity values of compounds based on their CDK descriptors, and the resulting models were validated and cross-validated; it is these models that the CTV Predictor is based on. The toxicity predictions generated by the CTV Predictor were shown to have smaller deviations from regulatory values than predictions based on high-throughput screening (HTS) assays and *in vitro* to *in vivo* extrapolation (IVIVE) (Wignall et al. 2018). In the current study, data for the following toxicity parameters were collected from the CTV predictor: 1) reference dose (RfD, mg

kg^{-1} day^{-1}; an estimate of the daily exposure to a compound that is likely to be without negative effects), 2) reference dose benchmark dose (BMD, mg kg^{-1} day^{-1}; dose of a compound which elicits a predetermined change in the response rate of a negative effect), 3) reference dose benchmark dose lower limit (BMDL, mg kg^{-1} day^{-1}; the lower limit of a one-sided 95% confidence interval on the BMD), 4) reference dose no observed adverse effect level (NO(A)EL, mg kg^{-1} day^{-1}; the highest dose of a compound for which there are no observed negative effects), 5) oral slope factor (OSF, risk per mg kg^{-1} day^{-1}; an estimate of the increased cancer risk from oral exposure to a dose of 1 mg kg^{-1} day^{-1} for a lifetime), and 6) cancer potency value (CPV, risk per mg kg^{-1} day^{-1}; a California EPA-specific OSF) (Danforth et al. 2020; U.S. EPA 2020c; Wignall et al. 2018). These parameters were selected because they involve oral exposure, and the primary means of potential exposure to the contaminants is through ingestion of contaminated water. Existing toxicity values were collected from CTV Predictor when possible, otherwise predicted toxicity values were collected.

2.2.2.4 Data integration and prioritization using ToxPi

All toxicity data were uploaded into the Toxicological Prioritization Index (ToxPi), a Java-based program that integrates multiple sources of toxicity data into one dimensionless index score (Marvel et al. 2018). ToxPi is a visualization software consisting of modified iconographic displays that were developed using the R packages *graphics*, *gdata*, and *lattice* (Reif et al., 2010). Index scores are calculated in ToxPi through the weighted or unweighted combination of data from multiple sources and are represented as unit circles made up of slices of data from different domains (Figure 2.1). The width of each slice corresponds to the user-defined weight of that domain, while the

slice length represents how potent the toxic effect is of the domain, for the particular chemical (Reif et al., 2010). ToxPi was used to calculate a toxicity score for each compound by integrating toxicity data from the three databases described above (sections 2.2.2.1, 2.2.2.2, and 2.2.2.3), specifically: EC50 (ECOTOX); AC50 and percentage of active assays (ToxCast); BMD, BMDL, CPV, NO(A)EL, OSF, RfD (CTV Predictor). Higher toxicity scores generated by ToxPi correspond to greater potential toxicity relative to other compounds in the dataset. Data for some of the parameters were transformed to ensure that higher values represented greater toxicity. The negative log was taken of EC50, AC50, RfD, BMD, BMDL, and NO(A)EL values, while remaining parameters (i.e., percentage of active assays, CPV, OSF) were linearly scaled. Toxicity profiles [i.e., visual representations of how each component (slice) influences the overall toxicity score] were generated in ToxPi for all compounds. Equal weights were given to all toxicity parameters (slices) in the analysis (Figure 2.1A). Hereafter, this scheme is referred to as the "general prioritization scheme." To summarize, the general prioritization scheme prioritizes chemicals based on all the following toxicity parameters: EC50, AC50, percentage of active assays, RfD, BMD, BMDL, NO(A)EL, OSF, and CPV.

This scheme is closely based on the scheme reported in Danforth et al. (2020), except that: 1) in the current study, the negative log is taken of toxicity parameters (EC50, AC50, RfD, BMD, BMDL, NO(A)EL) and others were linearly scaled (percentage of active assays, CPV, OSF) to aid in comparisons and interpretability of the effects of the parameters on the final ToxPi profiles, and 2) the minimum EC50 value across all species and the minimum AC50 values were used in the current study, rather than the Quantile 1 values used in Danforth et al. (2020), which provides a more

conservative estimate of potential toxicity. The schemes in subsequent sections demonstrate other modifications which can be made to this general scheme.

An important consideration is that the databases utilized here consider contaminants in water. Therefore, the results presented here do not consider all the possible synergistic or antagonistic effects that could occur within the complex landfill leachate matrix. Such a comparison was out of the scope of the present study, though could be addressed in future research.

Only contaminants for which there were available toxicity data from at least two of the three toxicity databases (i.e., ECOTOX, ToxCast, CTV Predictor) were included in ToxPi analysis. Further, one of the compounds identified in the literature review, 2,3,7,8-TCDD was found to have significantly larger toxicity parameter values than all other contaminants (Figure A1). As ToxPi assigns relative scores for each parameter based on the values of the other contaminants in the dataset, the extremely high values of 2,3,7,8-TCDD led to artificially low toxicity scores for a majority of the contaminants. Upon further review of the literature, it was found that this contaminant is associated with landfills which largely accept incinerator fly ash, or industrial wastes (Baderna et al., 2011; Choi and Lee, 2006; Murphy, 1989; Smith et al., 1983) which is not representative of municipal solid waste landfills. For both of these reasons, 2,3,7,8-TCDD was removed from the analysis. Thus, 322 contaminants (those for which there were available toxicity data from at least two of the three databases and excluding 2,3,7,8-TCDD) were prioritized in ToxPi (Table A1).

2.2.3 Prioritization scheme customization

The general prioritization scheme outlined above can be customized according to applied and research objectives. Two options for customization include the incorporation of toxicity data from additional datasets and the application of weighting schemes in ToxPi analysis. The following sections detail how these options were implemented in the current study.

2.2.3.1 Incorporating additional datasets

To illustrate the option of prioritization scheme customization, endocrine disruption (ED) data from the Endocrine Disruptor Knowledge Base (EDKB) were collected for the 322 contaminants in this study. The EDKB is an online database developed by the U.S. Food and Drug Administration (FDA) National Center for Toxicological Research (NCTR) (U.S. FDA, 2019). Since its inception in 1997, the EDKB has been accessed by users from government, academic, and private sectors to fulfill a variety of compound evaluation- and prioritization-related objectives (Ding et al., 2010). Rat, mouse, and human assay data for over 1800 compounds are reported in EKDB. Specifically, data for three parameters are presented in the database: relative binding activity (RBA), relative potency (RP), and relative proliferation potency (RPP). The largest value for each parameter was collected for all 322 contaminants in the current study. Contaminants were then prioritized in ToxPi according to the general scheme with the additional ED parameters. Hereafter, this scheme will be referred to as the "general + ED data" scheme (Figure 2.1B). All parameters were given equal weight, as the objective of this scheme was to demonstrate the utility of incorporating other data into the general scheme. Adding toxicity data from more domains, while keeping all weights constant, is

the most basic form of scheme modification. To summarize, the general + ED data scheme prioritizes chemicals based on the following parameters: EC50, AC50, percentage of active assays, RfD, BMD, BMDL, NO(A)EL, OSF, CPV, RBA, RP, and RPP.

2.2.3.2 Applying weighting schemes

Different weighting schemes may be implemented to further customize the prioritization scheme in order to meet research and applied objectives. In the current study, we designed three example weighting schemes to demonstrate this option: 1) cancer risk [parameters OSF and CPV were given 5x weights (Figure 2.1C)], 2) risk to flora and fauna [the EC50 parameter was given 5x weights (Figure 2.1D)], and 3) endocrine disruption risk [endocrine parameters (RP, RPP, RBA) were given 5x weights (Figure 2.1E)]. Hereafter, these schemes will be referred to as "cancer weighted scheme," "flora and fauna weighted scheme," and "endocrine disruption weighted scheme."

2.2.4 Comparison to regulatory lists

There are certain regulatory standards that landfills in the United States must meet regarding monitoring of chemicals released. Title 40, Part 258 of the CFR establishes minimum criteria for all municipal solid waste landfill units according to the Resource Conservation and Recovery Act (RCRA) (40 C.F.R. §258.1, 1991). These criteria serve to ensure protection of human health and the environment. Appendix I to Part 258, Constituents for Detection Monitoring, contains a list of 62 chemicals which must be monitored at all groundwater monitoring wells at all municipal solid waste units. If a statistically significant increase over the background level is detected for any of the

Appendix I chemicals, an assessment monitoring program must be established, in which chemicals listed in Appendix II to Part 258, List of Hazardous Inorganic and Organic Constituents, must be monitored (40 CFR § 258.55, 1991). In the present study, both appendices were examined, and data were collected on whether each of the 322 landfill leachate contaminants was included.

2.3 Results

2.3.1 Availability of toxicity data

Toxicity data availability from each of the four databases (i.e., ECOTOX, ToxCast, CTV Predictor, and EDKB) for all compounds is summarized in Figure 2.2. Toxicity data were available from all three databases (i.e., CTV Predictor, ToxCast, and ECOTOX) for a majority (>81%) of the 322 contaminants. Therefore, identifying contaminants for which toxicity data are available in at least two of the three major databases was an effective way to select data-rich contaminants. On the other hand, ED data from the EDKB were not as available. Each of the individual ED parameters (RP, RBA, RPP) had available data for less than 26% of the compounds. This low availability of ED data is likely due to endocrine disruption characterization, testing, and reporting being in relatively earlier stages compared to other toxicity endpoints (Karthikeyan et al., 2019). In addition, not all the contaminants are EDs, and therefore do not have existing data.

2.3.2 ToxPi contaminant prioritization: general scheme

Toxicity data from ECOTOX, ToxCast, and the CTV Predictor were integrated and prioritized using the ToxPi platform. It is important to note that ToxPi assigns relative

toxicity rankings to compounds in a dataset according to the toxicity data that is input. This study focused on 322 contaminants identified in the literature; every possible landfill leachate contaminant was not investigated. The results of ToxPi analysis using the general prioritization scheme are displayed in Figure 2.3. Toxicity profiles for the top 3 most toxic compounds (endrin, aldrin, and dieldrin) were very similar, exhibiting large scores for parameters BMD, BMDL, NO(A)EL, and RfD. For each of these three compounds, BMD scores were greater than 0.9373, BMDL scores were greater than 0.9493, NO(A)EL scores were greater than 0.8719, and RfD scores were greater than 0.8039 (with a value of 1 being the largest possible value). Clotrimazole, ranked 4th, demonstrated a balanced toxicity profile with relatively moderate scores for most parameters (each parameter besides BMD and BMDL had a score between 0.3827 and 0.6910), while oxytetracycline, ranked 5th, exhibited a toxicity profile dominated by the human toxicity values from CTV Predictor (BMD score = 0.8092, BMDL score = 0.8314, NO(A)EL score = 0.6180). Toxicity profiles for the top 40 contaminants according to the general scheme are listed in Table A3.

According to the general prioritization scheme, the 40 most toxic landfill leachate contaminants are listed in Table 2.1. The top 40 compounds are comprised of: 12 components of pesticides, fungicides, or their metabolites (endrin, dieldrin, aldrin, chlordane, heptachlor, p,p'-DDE, 4,4'-DDD, heptachlor epoxide, endosulfan I, endosulfan sulfate, lindane, tebuconazole); 8 pharmaceuticals (clotrimazole, oxytetracycline, tetracycline, doxycycline, chlortetracycline, enrofloxacin, codeine, ofloxacin); 8 industrial byproducts/ cigarette ingredients (indeno(123cd)pyrene, 1,2,3,4,7,8-hexaCDD, benzo(a)pyrene, benzo(ghi)perylene, benzo(b)fluoranthene,

dibenz(ah)anthracene, benzo(k)fluoranthene, benz(a)anthracene); 4 coolants and lubricants (PCB-187, PCB-153, PCB-128, PCB-105); 3 flame retardants (BDE-47, BDE-99, BDE-100); and 5 multi-use compounds (tetrabromobisphenol-A, p,p'-DDT, 2,3,7,8-TCDF, pentachlorophenol, pentachlorobenzene) (Table 2.1). Health impacts are compound-specific, and many of the compounds can produce multiple negative effects (Table 2.1). Of the top 40 compounds, 21 were reported as potential or confirmed endocrine disruptors, 14 as potential or confirmed human carcinogens, and 12 as causing neurological impacts.

A wide range of concentrations in landfill leachate have been reported for these 40 contaminants (Table 2.2). Pesticides and their metabolites exhibited the largest reported concentrations of over 1×10^4 ng L^{-1} (i.e., endrin, dieldrin, endosulfan I, and pentachlorophenol). However, the lowest concentrations of less than 1×10^{-1} ng L^{-1} were reported for compounds with a range of sources and uses (i.e., p,p'-DDE [pesticide], endosulfan sulfate [metabolite of pesticide ingredient], BDE-47 [flame retardant], PCB-153 [coolant and lubricant in transformers], PCB-128 [coolant and lubricant in transformers], PCB-105 [coolant and lubricant in transformers], and pentachlorobenzene [fungicide, flame retardant, industrial by-product]). Within individual compounds, the range between minimum and maximum landfill leachate concentration varied from as low as 0.5 ng L^{-1} (clotrimazole and tebuconazole) to greater than 1.3×10^5 ng L^{-1} (dieldrin).

2.3.3 ToxPi contaminant prioritization: general + ED data scheme

Table 2.3 lists the top 40 most toxic compounds according to the general + ED data scheme. Thirty-nine compounds were found in the top 40 of both the general and the

+ED schemes; bisphenol A was the only compound unique to the top 40 of the general + ED data scheme. The average change in rank between the top 40 of the general scheme and that of the general + ED data scheme was ± 3.2. A majority of the compounds in the top 40 (i.e., 95%) exhibited a change in toxicity rank of less than 7 places. p,p'-DDT and bisphenol A had rank changes of 10 and 58 places, respectively. As the only difference between the two schemes is the addition of ED data in the general + ED data scheme, it can be concluded that these changes in rank are due to p,p'-DDT and bisphenol A having endocrine disruption activity. This is not unexpected; both compounds have been reported as endocrine disruptors (Rubin, 2011; Munier et al., 2016).

2.3.4 ToxPi contaminant prioritization: cancer weighted scheme

Table 2.4 lists the top 40 most toxic landfill leachate contaminants according to the cancer weighted scheme. 1,2,3,7,8-pentaCDD, ampicillin, fluoranthene, and amoxicillin were in the top 40 of the cancer weighted scheme, but not the general scheme. The average change in toxicity rank between the general scheme and the cancer weighted scheme was 12.7. Twenty contaminants in the top 40 of the cancer weighted scheme exhibited a change in rank of over 10 places, while 9 contaminants had a rank change of over 20 places. The largest rank changes were exhibited by codeine (32 places) and fluoranthene (51 places). Those contaminants that exhibit large changes in rank have an enhanced risk of cancer compared to their overall general toxicity. Site managers could use a combination approach when determining which chemicals to target with remediation efforts, by choosing to target compounds with large rank changes like codeine and fluoranthene (greater risk of cancer), as well as those that rank highly in both the general and the cancer weighted schemes, such as oxytetracycline, clotrimazole, and

indeno(123cd)pyrene (they represent both large cancer risk and large toxicity risks overall).

2.3.5 ToxPi contaminant prioritization: ED weighted scheme

Table 2.5 lists the top 40 most toxic landfill leachate contaminants according to the ED weighted scheme. Three contaminants were in the top 40 of the ED weighted scheme, but not that of the general scheme: bisphenol A, octyl phenol, and butylparaben. For the top 40, the average change in toxicity rank between the general scheme and the ED weighted scheme was 10.4, and 93% of contaminants exhibited a change in rank of 10 or less places. The three largest rank changes were 64 (bisphenol A), 91 (octyl phenol), and 113 places (butylparaben). These three contaminants have much greater potential to negatively impact organisms' endocrine systems compared to their overall toxicity (i.e., their ranks are closer to "1" in the ED weighted scheme than the general scheme). Further, this weighted scheme has proven to be more effective in identifying endocrine-disrupting contaminants in leachate than the general + ED data scheme, based on the greater magnitude of change in rank between the ED weighted scheme and the general scheme than that of the general + ED data scheme.

2.3.6 ToxPi contaminant prioritization: flora and fauna weighted scheme

Table 2.6 lists the top 40 most toxic landfill leachate contaminants according to the flora and fauna weighted scheme. Nine contaminants were in the top 40 of the flora and fauna weighted scheme, but not of the general scheme (naphthalene, atrazine, propiconazole, triclocarban, hexachlorobenzene, triclosan, MCPA, hexazinone, and dichlorobenzene). The average change in toxicity rank between the general scheme and the flora and fauna weighted scheme for these 40 compounds was 14 places. 43% of

compounds exhibited a change in rank of 10 or more places, while 5 compounds had a change in rank of 20 or more. Naphthalene, atrazine, hexazinone, and dichlorobenzene all exhibited a change in rank of over 50 places, suggesting that these four contaminants all have large potential to negatively impact the flora and fauna of a site and a relatively lower overall toxicity risk (according to the general prioritization scheme).

2.3.7 Comparison with regulatory lists

Only one contaminant identified in the top 40 by one of the prioritization schemes in the current study is listed in Appendix I of 40 C.F.R 258: dichlorobenzene (flora and fauna weighted scheme, Table A5). Between 60-63% of the top 40 contaminants from each scheme are included in Appendix II of 40 C.F.R. 258 (see Table 2.7 and Tables A5-A8).

2.4 Discussion

2.4.1 ToxPi leachate contaminant prioritization schemes

The general landfill leachate pollutant prioritization scheme presented here is widely applicable for diverse environmental applications as it includes *in vivo* assay data, *in vitro* assay data, and *in silico* human toxicity data. Such an integration of toxicity data allows for the identification of contaminants that pose the greatest possible threats to surrounding human and wildlife populations (Danforth et al., 2020). Landfill site managers and researchers can take advantage of this robust method of prioritization when determining contaminants to target with remediation efforts. It should be noted, however, that the occurrence of contaminants with extremely large toxicity parameters (such as 2,3,7,8-TCDD) can influence the relative toxicity values of the rest of the dataset. Such

compounds may be removed from analysis so as not to skew the final results, yet should be recognized if prioritization is being done in the interest of selecting compounds to remediate.

The incorporation of other toxicity datasets in addition to those implemented in the general prioritization scheme provides another layer of specificity in meeting specific research and community objectives. For example, specific toxicity endpoints may be included (e.g., reproductive toxicity, developmental toxicity) if certain health problems are of particular concern in a community. However, as evidenced by the minimal changes in rank between the general scheme and the general + ED data scheme, weighting may need to be applied in order to identify a greater number of compounds that exhibit the toxic effects of interest. Weighted prioritization schemes such as those outlined above add another dimension of selectivity in meeting site objectives. These or similar weighting schemes are particularly useful to communities in which there are defined health concerns or priorities. For example, a scheme like the cancer weighted scheme would best be implemented in an area where cancer was of greater concern, such as “Cancer Alley” in the Southern United States (Singer, 2011). On the other hand, if a community was experiencing high rates of infertility or other problems related to the endocrine system, a scheme like the ED weighted scheme would be the most prudent. The flora and fauna weighted scheme lends itself well to implementation in an area where animal and plant life is of high importance or value, for example: pristine natural areas, locations with endangered species, or places where human consumption of animals (through hunting or fishing) is common.

Comparison of the most toxic compounds ranked according to both the general scheme and weighted schemes can aid in determining those that are most harmful according to research and community objectives. Compounds that exhibit a large change in rank between schemes, as well as those that exhibit low ranks across schemes, could then be targeted for further research on potential and known impacts to the health of humans and/or flora and fauna. In addition, though not implemented here, prioritization approaches can also incorporate pollutant concentration information, if it is available, whether as an additional endpoint in ToxPi analyses, or as a decision-support metric after ToxPi prioritization. The variability in landfill contaminant concentrations reported in the literature (Table 2.2) highlights the importance of utilizing site-specific concentration data whenever possible to ensure that any decisions made using concentration data are relevant to the site of interest.

2.4.2 Pollutant prioritization and landfill regulatory lists

Only one contaminant in the top 40 most potentially harmful pollutants of the prioritization schemes implemented here is listed in Appendix I of 40 C.F.R 258, while 60-63% of the top 40 contaminants from each scheme are included in Appendix II of 40 C.F.R. 258. Generally, Appendix II compounds are not expected to be monitored unless detection of an Appendix I compound permits it (40 C.F.R. §258.54, 1991). Neither appendix has been modified since 2005 (70 FR 34555), and accordingly, more recently recognized CECs are not represented therein. Further, regulations which target industrial compounds and related carcinogens may not address the complexity of emerging contaminants. While traditional industrial carcinogens commonly exhibit a linear relationship between level of exposure and toxicity, some CECs and EDs cause

deleterious effects at much lower concentrations or exhibit nonlinear dose responses (Lagarde et al., 2015; U.S. EPA, 2017; Vandenberg et al., 2013). The results of the prioritizations in this study suggest that updating landfill groundwater monitoring requirements to reflect the evolving understanding of landfill leachate composition (and toxicity of the pollutants within it) could be useful and effective, as this leachate may pose risks to groundwater through offsite transport. In addition, these results underscore the importance of gathering comprehensive, site-specific pollutant information to make informed decisions about leachate remediation, and that site monitoring data based on regulatory lists may not provide a complete picture of leachate composition.

2.4.3 Future work to build upon the developed prioritization approach

A large range in concentrations was reported in the literature for the top 40 contaminants of the general prioritization scheme. Large variation in landfill leachate composition is likely due to the inherent variability between landfills. Landfill age and design, as well as demographic, climatic, and geographic characteristics of the area, all impact the type and concentration of contaminants within leachate (Kjeldsen et al., 2002). Because of this natural variation, the 322 landfill leachate contaminants identified in the literature and analyzed here are not likely to be detected in every leachate or groundwater sample. Therefore, site-specific data including identified contaminants and their concentrations are crucial to accurate, relevant prioritization, and incorporating site-specific contaminant data when applying the prioritization schemes outlined in this study will provide the most accurate and applicable results.

A combination of methods including global chemical profiling and quantitative targeted analysis could be implemented to generate necessary site-specific landfill

leachate composition data. Non-targeted analysis using high-resolution mass spectrometry (HRMS) (Arrebola-Liébanas et al., 2017), coupled with HRMS data processing platforms that perform peak detection, integration, and annotation such as XCMS Online (Domingo-Almenara et al., 2018; Smith et al., 2006) could generate comprehensive, site-specific information on the relative intensities and putative identities of compounds within leachate. Targeted approaches that apply analytical reference standard-derived calibration curves then would provide absolute identification and quantification of select compounds (Sargent, 2013). The prioritization scheme described in this paper could be integrated seamlessly into these approaches, whether following non-targeted analysis to identify the most potentially harmful compounds to conduct targeted analysis of, following targeted analysis to identify compounds to target with remediation, or both. In this manner, both the chemical profile and the potential health risks of contaminants identified at a site are considered. Mitigation efforts can then be designed accordingly to target contaminants which are not only the most abundant, but the most harmful as well.

2.5 Conclusion

Landfills contain many harmful chemicals which may leach offsite into groundwater. It is not feasible nor economically viable to monitor and remediate all possible contaminants. Prioritization schemes that incorporate numerous sources of toxicity data, such as those described here, provide the means for cost-effective identification of contaminants most relevant to community priorities and concerns. The general prioritization scheme depicted here is also highly flexible and can be easily customized. Included parameters can be modified and weighting schemes can be added

or adjusted to best meet diverse objectives, as shown by the four modified schemes presented here. Out of the original 322 contaminants analyzed in this study, 56 were identified in the top 40 most toxic contaminants of all five schemes. The flora and fauna weighted scheme had the largest average change in rank (± 14 places) when compared to the general scheme, and the general + ED data scheme had the smallest average rank change (± 3.2 places). A combination of rank and change in rank can be implemented when deciding which contaminants to target with remediation efforts. Further, though the original scheme was designed particularly for pollutants in aqueous solutions, it can be modified for applications with air pollutants as well. This method holds promise for implementation in environmental pollutant mitigation, especially when used to prioritize global metabolomic data generated through HRMS non-target analysis. Landfill leachate is a continuously evolving media, both due to internal processes (e.g., waste decomposition) and external factors, such as societal change, which alter the composition of waste deposited in landfills. Future research directions, therefore, include comprehensive assessments of CECs and their impacts on human health and the environment, and implementation of the prioritization schemes defined here to monitor landfill leachate toxicity as a function of time.

2.6 Funding and acknowledgements

This work was supported by the Great Lakes Restoration Initiative, Template Number 738 (Landfill Runoff Reduction), the Center for Agroforestry at the University of Missouri, and the USDA/ARS Dale Bumpers Small Farm Research Center under cooperative agreement (58-6020-6-001) with the USDA Agricultural Research Service.

The findings and conclusions in this publication are those of the authors and should not be construed to represent any official USDA or U.S. Government determination or policy. We thank Mohamed Bayati and anonymous journal reviewers who critiqued earlier versions of this manuscript. We thank Brent DeBauche, Molly Wagler, and Ryan Vinhal for their assistance in data collection. We would like to thank the USDA-Forest Service, Center for Agroforestry at the University of Missouri, and USDA/ARS Dale Bumpers Small Farm Research Center for their support.

Table 2.1. Uses, sources, and health impacts of compounds in landfill leachate ranked by their potential toxicity according to ToxPi analysis. The top 40 most potentially toxic compounds, ranked according to the general prioritization scheme, are included.

Rank	Contaminant	CASRN[a]	Uses/Sources[b]	Health Impacts[e]
1	Endrin	72-20-8	pesticide[c]	neurological, endocrine
2	Dieldrin	60-57-1	pesticide[c]	developmental, endocrine, hepatic, immunological, neurological
3	Aldrin	309-00-2	pesticide[c]	developmental, endocrine, hepatic, immunological, neurological
4	Clotrimazole	23593-75-1	antifungal medication	potential endocrine disruptor
5	Oxytetracycline	79-57-2	antibiotic to treat bacterial infections	potential endocrine disruptor
6	Chlordane	12789-03-6	pesticide[c]	endocrine disruption
7	Indeno(123cd)pyrene	193-39-5	industrial by-product; cigarette ingredient	animal carcinogen, possible human carcinogen
8	Heptachlor	76-44-8	insecticide[c]	developmental, reproductive, endocrine
9	Tetrabromobisphenol-A	79-94-7	flame retardant; epoxy resins of printed circuit boards	potential endocrine disruptor, neurotoxicity
10	p,p'-DDE	72-55-9	component of DDT; pesticide	developmental, endocrine, hepatic, neurological, reproductive
11	p,p'-DDT	50-29-3	component of DDT; pesticide; cigarette ingredient	developmental, endocrine, hepatic, neurological, reproductive
12	1,2,3,4,7,8-hexaCDD	39227-28-6	industrial by-product[c]	probable carcinogen
13	Tetracycline	60-54-8	antibiotic to treat bacterial infections	endocrine disruption
14	4,4'-DDD	72-54-8	component of DDT; pesticide	developmental, endocrine, hepatic, neurological, reproductive
15	Benzo(a)pyrene	50-32-8	industrial by-product; cigarette ingredient	probable human carcinogen

Rank	Contaminant	CASRN[a]	Uses/Sources[b]	Health Impacts[e]
16	Benzo(ghi)perylene	191-24-2	industrial by-product; cigarette ingredient	not classified
17	Benzo(b)fluoranthene	205-99-2	industrial by-product; cigarette ingredient	probable human carcinogen
18	Dibenz(ah)anthracene	53-70-3	industrial by-product; cigarette ingredient	probable human carcinogen
19	Heptachlor epoxide	1024-57-3	metabolite of heptachlor[c]	developmental, reproductive
20	PCB-187	52663-68-0	coolants and lubricants in transformers and capacitors[c]	carcinogenic to humans, endocrine
21	Benzo(k)fluoranthene	207-08-9	industrial by-product; cigarette ingredient	possible human carcinogen
22	Doxycycline	564-25-0	antibacterial drug; antimalarial	possible endocrine disruptor
23	Benz(a)anthracene	56-55-3	industrial by-product; cigarette ingredient	probable human carcinogen
24	Endosulfan I	959-98-8	insecticide[d]	possible human carcinogen, neurological
25	Endosulfan sulfate	1031-07-8	metabolite of endosulfan	neurological, possible carcinogen
26	2,3,7,8-TCDF	51207-31-9	industrial by-product; insecticide	possible neurological
27	BDE-47	5436-43-1	flame retardant	neurotoxicity
28	Chlortetracycline	57-62-5	veterinary antibiotic[d]	possible endocrine disruptor
29	PCB-153	35065-27-1	coolants and lubricants in transformers and capacitors[c]	carcinogenic to humans, endocrine
30	BDE-99	60348-60-9	flame retardant	neurotoxicity
31	PCB-128	38380-07-3	coolants and lubricants in transformers and capacitors[c]	endocrine
32	Lindane	58-89-9	insecticide	possible carcinogen, endocrine
33	PCB-105	32598-14-4	coolants and lubricants in transformers and capacitors[c]	carcinogenic to humans, endocrine

Rank	Contaminant	CASRN[a]	Uses/Sources[b]	Health Impacts[e]
34	Enrofloxacin	93106-60-6	antibiotic to treat bacterial infections[d]	not classified
35	Pentachlorophenol	87-86-5	pesticide; wood preservative	developmental, endocrine, reproductive
36	Codeine	76-57-3	pain-relief; antidiarrheal; cough suppressant	not classified
37	Tebuconazole	80443-41-0	fungicide[d]	possible human carcinogen
38	BDE-100	189084-64-8	flame retardant	endocrine
39	Ofloxacin	82419-36-1	antibiotic to treat bacterial infections[d]	toxic to mammalian cells in culture
40	Pentachlorobenzene	608-93-5	fungicide; flame retardant; industrial by-product[d]	hepatic, urinary

[a] Chemical Abstracts Service Registry Number
[b] T3DB
[c] ATSDR
[d] pubchem
[e] For details, see Table A4.

Table 2.2. Concentration range of compounds in landfill leachate ranked by their potential toxicity according to ToxPi analysis. The top 40 most potentially toxic compounds, ranked according to the general prioritization scheme, are included.

Rank	Contaminant	CASRN[a]	Concentration Range[b] (ng L^{-1})	References
1	Endrin	72-20-8	7-50000	Assmuth, 1996; Chilton and Chilton, 1992; Palma-Fleming et al., 2000
2	Dieldrin	60-57-1	5-130600	Argun et al., 2017; Assmuth, 1996; Murray and Beck, 1990
3	Aldrin	309-00-2	3-333	Assmuth, 1996; Murray and Beck, 1990; Palma-Fleming et al., 2000
4	Clotrimazole	23593-75-1	1-1.5	Peng et al., 2014; Shi et al., 2020
5	Oxytetracycline	79-57-2	0.7-1070	Andrews et al., 2011; Wu et al., 2015; Wu et al., 2017
6	Chlordane	12789-03-6	15-40	Andrews et al., 2011; Ferrell and Smith, 1995; Kadlec and Zmarthie, 2010
7	Indeno(123cd)pyrene	193-39-5	2-50	Öman and Junestedt, 2008; Oturan et al., 2015; Smol et al., 2016
8	Heptachlor	76-44-8	6-350	Kadlec and Zmarthie, 2010; Palma-Fleming et al., 2000; Reinhart and Grosh, 1998
9	Tetrabromobisphenol-A	79-94-7	4.5-1227	Öman and Junestedt, 2008; Osako et al., 2004; Zhou et al., 2013
10	p,p'-DDE	72-55-9	0.01-13.2	Palma-Fleming et al., 2000; Wang and Kelly, 2017; Xu et al., 2008
11	p,p'-DDT	50-29-3	22-220	Assmuth, 1996; Chilton and Chilton, 1992; Xu et al., 2008
12	1,2,3,4,7,8-hexaCDD	39227-28-6	1-47	Dudzinska et al., 2004; Dudzinska et al., 2008; Wenzel et al., 1999
13	Tetracycline	60-54-8	50-2470	Andrews et al., 2011; Fang et al., 2020; Topal and Arslan Topal, 2015
14	4,4'-DDD	72-54-8	40-130	Assmuth, 1996; Denton et al., 2005; Kadlec and Zmarthie, 2010
15	Benzo(a)pyrene	50-32-8	1-200	Andrews et al., 2011; Xu et al., 2008; Oturan et al., 2015
16	Benzo(ghi)perylene	191-24-2	10-120	Oturan et al., 2015; Welander and Henrysson, 1998; Xu et al., 2008
17	Benzo(b)fluoranthene	205-99-2	11-2050	Smol et al., 2016; Welander and Henrysson, 1998; Xu et al., 2008
18	Dibenz(ah)anthracene	53-70-3	1-200	Koc-Jurczyk, 2014; Öman and Junestedt, 2008; Smol et al., 2016
19	Heptachlor epoxide	1024-57-3	0.2-<50	Gardiner et al., 2002; Oturan et al., 2015; Palma-Fleming et al., 2000

Rank	Contaminant	CASRN[a]	Concentration Range[b] (ng L^{-1})	References
20	PCB-187	52663-68-0	0.1407	Kõrgmaa et al., 2011
21	Benzo(k)fluoranthene	207-08-9	<3-2000	Klimiuk and Kulikowska, 2004; Smol et al., 2016; Welander and Henrysson, 1998
22	Doxycycline	564-25-0	6-541.9	Andersson et al., 2006; Andrews et al., 2011; Qi et al., 2018
23	Benz(a)anthracene	56-55-3	1-960	Kadlec and Zmarthie, 2010; Oturan et al., 2015; Xu et al., 2008
24	Endosulfan I	959-98-8	18-760400	Argun et al., 2017; Palma-Fleming et al., 2000; Wang and Kelly, 2017
25	Endosulfan sulfate	1031-07-8	0.044-190	Kõrgmaa et al., 2011; Palma-Fleming et al., 2000; Wang and Kelly, 2017
26	2,3,7,8-TCDF	51207-31-9	2-111.15	Dudzinska et al., 2004; Dudzinska et al., 2008; Wenzel et al., 1999
27	BDE-47	5436-43-1	0.041-6750	Daso et al., 2017; Wang and Kelly, 2017; Zhou et al., 2013
28	Chlortetracycline	57-62-5	12.6-912	Andrews et al., 2011; Fang et al., 2020; Wu et al., 2015
29	PCB-153	35065-27-1	0.012-24	Kõrgmaa et al., 2011; Oturan et al., 2015; Wang and Kelly, 2017
30	BDE-99	60348-60-9	3.41-14620	Daso et al., 2017; Kõrgmaa et al., 2011; Zhou et al., 2013
31	PCB-128	38380-07-3	0.1-2	Kängsepp, 2008; Kõrgmaa et al., 2011
32	Lindane	58-89-9	5-950	Andrews et al., 2011; Chilton and Chilton, 1992; Oturan et al., 2015
33	PCB-105	32598-14-4	0.003-0.5105	Kõrgmaa et al., 2011; Wang and Kelly, 2017
34	Enrofloxacin	93106-60-6	17.95-4026.67	Andrews et al., 2011; Wu et al., 2015; You et al., 2018
35	Pentachlorophenol	87-86-5	200-470000	Assmuth, 1996; Chilton and Chilton, 1992; Masoner et al., 2014
36	Codeine	76-57-3	44.9-728	Andrews et al., 2011; Lu et al., 2016; Masoner et al., 2014
37	Tebuconazole	80443-41-0	0.3-0.8	Peng et al., 2014
38	BDE-100	189084-64-8	<0.15-1590	Daso et al., 2017; Kõrgmaa et al., 2011; Zhou et al., 2013
39	Ofloxacin	82419-36-1	9.1-79.5	Peng et al., 2014
40	Pentachlorobenzene	608-93-5	0.042-56	Matejczyk et al., 2011; Wang and Kelly, 2017

[a] Chemical Abstracts Service Registry Number
[b] Concentration range in landfill leachate reported in the literature.

Table 2.3. Top 40 most potentially toxic landfill leachate chemicals according to the general + endocrine disruption data prioritization scheme. Bolded chemicals exhibited a change in rank between the general and the general + ED scheme of 10 or more.

General + ED Data Rank	General Rank[a]	Contaminant	CASRN
1	**11**	**p,p'-DDT**	**50-29-3**
2	1	Endrin	72-20-8
3	10	p,p'-DDE	72-55-9
4	2	Dieldrin	60-57-1
5	3	Aldrin	309-00-2
6	4	Clotrimazole	23593-75-1
7	**65**	**Bisphenol A**	**80-05-7**
8	5	Oxytetracycline	79-57-2
9	6	Chlordane	12789-03-6
10	8	Heptachlor	76-44-8
11	7	indeno(123cd)pyrene	193-39-5
12	9	Tetrabromobisphenol-A	79-94-7
13	12	1,2,3,4,7,8-hexaCDD	39227-28-6
14	14	4,4'-DDD	72-54-8
15	13	Tetracycline	60-54-8
16	15	Benzo (a) pyrene	50-32-8
17	16	Benzo(ghi)perylene	191-24-2
18	17	Benzo(b)fluoranthene	205-99-2
19	18	dibenz(ah)anthracene	53-70-3
20	19	Heptachlor epoxide	1024-57-3
21	20	PCB-187	52663-68-0
22	21	benzo(k)fluoranthene	207-08-9
23	22	Doxycycline	564-25-0
24	23	Benz(a)anthracene	56-55-3
25	24	Endosulfan I	959-98-8
26	25	Endosulfan sulfate	1031-07-8
27	26	2,3,7,8-TCDF	51207-31-9
28	29	PCB-153	35065-27-1
29	27	BDE-47	5436-43-1
30	28	Chlorotetracycline	57-62-5
31	30	BDE-99	60348-60-9
32	31	PCB-128	38380-07-3
33	32	Lindane	58-89-9
34	33	PCB-105	32598-14-4
35	34	Enrofloxacin	93106-60-6
36	35	Pentachlorophenol	87-86-5
37	36	Codeine	76-57-3
38	37	Tebuconazole	80443-41-0
39	38	BDE-100	189084-64-8
40	39	Ofloxacin	82419-36-1

[a] Toxicity rankings according to the general prioritization scheme.

Table 2.4. Top 40 most potentially toxic landfill leachate chemicals according to the cancer weighted prioritization scheme. Bolded chemicals exhibited a change in rank between the general scheme and the cancer weighted scheme of 10 or more.

Cancer Weighted Rank	General Rank[a]	Contaminant	CASRN
1	5	Oxytetracycline	79-57-2
2	**22**	**Doxycycline**	**564-25-0**
3	**13**	**Tetracycline**	**60-54-8**
4	**36**	**Codeine**	**76-57-3**
5	4	Clotrimazole	23593-75-1
6	7	Indeno(123cd)pyrene	193-39-5
7	16	Benzo(ghi)perylene	191-24-2
8	**28**	**Chlorotetracycline**	**57-62-5**
9	18	Dibenz(ah)anthracene	53-70-3
10	1	Endrin	72-20-8
11	2	Dieldrin	60-57-1
12	3	Aldrin	309-00-2
13	17	Benzo(b)fluoranthene	205-99-2
14	15	Benzo (a) pyrene	50-32-8
15	23	Benz(a)anthracene	56-55-3
16	21	Benzo(k)fluoranthene	207-08-9
17	**39**	**Ofloxacin**	**82419-36-1**
18	**34**	**Enrofloxacin**	**93106-60-6**
19	12	1,2,3,4,7,8-hexaCDD	39227-28-6
20	**44**	**1,2,3,7,8-pentaCDD**	**40321-76-4**
21	**31**	**PCB-128**	**38380-07-3**
22	29	PCB-153	35065-27-1
23	26	2,3,7,8-TCDF	51207-31-9
24	20	PCB-187	52663-68-0
25	33	PCB-105	32598-14-4
26	**10**	**p,p'-DDE**	**72-55-9**
27	**8**	**Heptachlor**	**76-44-8**
28	27	BDE-47	5436-43-1
29	**11**	**p,p'-DDT**	**50-29-3**
30	**9**	**Tetrabromobisphenol-A**	**79-94-7**
31	**14**	**4,4'-DDD**	**72-54-8**
32	**19**	**Heptachlor epoxide**	**1024-57-3**
33	**46**	**Ampicillin**	**69-53-4**
34	**6**	**Chlordane**	**12789-03-6**
35	**86**	**Fluoranthene**	**206-44-0**
36	30	BDE-99	60348-60-9
37	**24**	**Endosulfan I**	**959-98-8**
38	**25**	**Endosulfan sulfate**	**1031-07-8**
39	38	BDE-100	189084-64-8
40	**66**	**Amoxicillin**	**26787-78-0**

[a] Toxicity rankings according to the general prioritization scheme.

Table 2.5. Top 40 most potentially toxic landfill leachate chemicals according to the endocrine disruption weighted prioritization scheme. Bolded chemicals exhibited a change in rank between the general scheme and the weighted scheme of 10 or more.

Endocrine Disruption Weighted Rank	General Rank[a]	Contaminant	CASRN
1	**65**	**Bisphenol A**	**80-05-7**
2	11	p,p'-DDT	50-29-3
3	10	p,p'-DDE	72-55-9
4	**95**	**Octyl phenol**	**1806-26-4**
5	1	Endrin	72-20-8
6	2	Dieldrin	60-57-1
7	3	Aldrin	309-00-2
8	4	Clotrimazole	23593-75-1
9	5	Oxytetracycline	79-57-2
10	8	Heptachlor	76-44-8
11	6	Chlordane	12789-03-6
12	7	Indeno(123cd)pyrene	193-39-5
13	14	4,4'-DDD	72-54-8
14	9	Tetrabromobisphenol-A	79-94-7
15	12	1,2,3,4,7,8-hexaCDD	39227-28-6
16	13	Tetracycline	60-54-8
17	15	Benzo(a)pyrene	50-32-8
18	16	Benzo(ghi)perylene	191-24-2
19	**29**	**PCB-153**	**35065-27-1**
20	**133**	**Butylparaben**	**94-26-8**
21	17	Benzo(b)fluoranthene	205-99-2
22	18	Dibenz(ah)anthracene	53-70-3
23	19	Heptachlor epoxide	1024-57-3
24	20	PCB-187	52663-68-0
25	24	Endosulfan I	959-98-8
26	21	Benzo(k)fluoranthene	207-08-9
27	22	Doxycycline	564-25-0
28	23	Benz(a)anthracene	56-55-3
29	25	Endosulfan sulfate	1031-07-8
30	26	2,3,7,8-TCDF	51207-31-9
31	27	BDE-47	5436-43-1
32	28	Chlorotetracycline	57-62-5
33	32	Lindane	58-89-9
34	30	BDE-99	60348-60-9
35	31	PCB-128	38380-07-3
36	33	PCB-105	32598-14-4
37	34	Enrofloxacin	93106-60-6
38	35	Pentachlorophenol	87-86-5
39	36	Codeine	76-57-3
40	37	Tebuconazole	80443-41-0

[a] Toxicity rankings according to the general prioritization scheme.

Table 2.6. Top 40 most potentially toxic landfill leachate chemicals according to the flora and fauna weighted prioritization scheme. Bolded chemicals exhibited a change in rank between the general scheme and the weighted scheme of 10 or more.

Flora and Fauna Weighted Rank	General Rank[a]	Contaminant	CASRN
1	1	Endrin	72-20-8
2	2	Dieldrin	60-57-1
3	3	Aldrin	309-00-2
4	12	1,2,3,4,7,8-hexaCDD	39227-28-6
5	**15**	**Benzo (a) pyrene**	**50-32-8**
6	11	p,p'-DDT	50-29-3
7	8	Heptachlor	76-44-8
8	4	Clotrimazole	23593-75-1
9	**26**	**2,3,7,8-TCDF**	**51207-31-9**
10	10	p,p'-DDE	72-55-9
11	7	Indeno(123cd)pyrene	193-39-5
12	14	4,4'-DDD	72-54-8
13	16	Benzo(ghi)perylene	191-24-2
14	6	Chlordane	12789-03-6
15	18	Dibenz(ah)anthracene	53-70-3
16	9	Tetrabromobisphenol-A	79-94-7
17	**5**	**Oxytetracycline**	**79-57-2**
18	17	Benzo(b)fluoranthene	205-99-2
19	23	Benz(a)anthracene	56-55-3
20	**32**	**Lindane**	**58-89-9**
21	24	Endosulfan I	959-98-8
22	**111**	**Naphthalene**	**91-20-3**
23	**77**	**Atrazine**	**1912-24-9**
24	21	Benzo(k)fluoranthene	207-08-9
25	**13**	**Tetracycline**	**60-54-8**
26	30	BDE-99	60348-60-9
27	33	PCB-105	32598-14-4
28	**38**	**BDE-100**	**189084-64-8**
29	**42**	**Propiconazole**	**60207-90-1**
30	35	Pentachlorophenol	87-86-5
31	27	BDE-47	5436-43-1
32	**51**	**Triclocarban**	**101-20-2**
33	**48**	**Hexachlorobenzene**	**118-74-1**
34	**49**	**Triclosan**	**3380-34-5**
35	**55**	**MCPA**	**94-74-6**
36	**137**	**Hexazinone**	**51235-04-2**
37	**92**	**Dichlorobenzene**	**106-46-7**
38	**25**	**Endosulfan sulfate**	**1031-07-8**
39	**40**	Pentachlorobenzene	608-93-5
40	**22**	**Doxycycline**	**564-25-0**

[a] Toxicity rankings according to the general prioritization scheme.

Table 2.7. Top 40 most potentially toxic landfill leachate chemicals according to the general prioritization scheme. A star indicates inclusion in Appendix I or Appendix II, 40 C.F.R. § 258.

Rank	CAS	Contaminant	40 C.F.R. 258. App. I	40 C.F.R. 258. App. II
1	72-20-8	Endrin		*
2	60-57-1	Dieldrin		*
3	309-00-2	Aldrin		*
4	23593-75-1	Clotrimazole		
5	79-57-2	Oxytetracycline		
6	12789-03-6	Chlordane		*
7	193-39-5	Indeno(123cd)pyrene		*
8	76-44-8	Heptachlor		*
9	79-94-7	Tetrabromobisphenol-A		
10	72-55-9	p,p'-DDE		*
11	50-29-3	p,p'-DDT		*
12	39227-28-6	1,2,3,4,7,8-hexaCDD		
13	60-54-8	Tetracycline		
14	72-54-8	4,4'-DDD		*
15	50-32-8	Benzo(a)pyrene		*
16	191-24-2	Benzo(ghi)perylene		*
17	205-99-2	Benzo(b)fluoranthene		*
18	53-70-3	Dibenz(ah)anthracene		*
19	1024-57-3	Heptachlor epoxide		*
20	52663-68-0	PCB-187		*
21	207-08-9	Benzo(k)fluoranthene		*
22	564-25-0	Doxycycline		
23	56-55-3	Benz(a)anthracene		*
24	959-98-8	Endosulfan I		*
25	1031-07-8	Endosulfan sulfate		*
26	51207-31-9	2,3,7,8-TCDF		*
27	5436-43-1	BDE-47		
28	57-62-5	Chlortetracycline		
29	35065-27-1	PCB-153		
30	60348-60-9	BDE-99		*
31	38380-07-3	PCB-128		
32	58-89-9	Lindane		*
33	32598-14-4	PCB-105		*
34	93106-60-6	Enrofloxacin		*
35	87-86-5	Pentachlorophenol		
36	76-57-3	Codeine		*
37	80443-41-0	Tebuconazole		
38	189084-64-8	BDE-100		
39	82419-36-1	Ofloxacin		
40	608-93-5	Pentachlorobenzene		

Figure 2.1. ToxPi prioritization schemes. For definitions of each scheme, refer to Sections 2.2.2 and 2.2.3. Each contaminant was analyzed using these combinations of data from multiple domains, which are represented by slices of a similar color: *in vivo* ecotoxicology endpoints (blue), *in vitro* high throughput screening assays (aqua), known or conditional human health toxicity values (red), and endocrine disruption assay data (gold). Individual slices represent data for the corresponding parameter. The distance of each slice from the center indicates the normalized value of the component. The angle of the slice represents how that component is weighted relative to the other components in the overall ToxPi calculation. BMD: reference dose benchmark dose; BMDL: reference dose benchmark dose lower limit; CPV: cancer potency value; NO(A)EL: reference dose no observed adverse effect level; OSF: oral slope factor; RfD: reference dose; RBA: relative binding activity; RP: relative potency; RPP: relative proliferation potency; AC50: half maximal activity concentration; % Active Assays: percentage of active assays; EC50: half-maximal effective concentration.

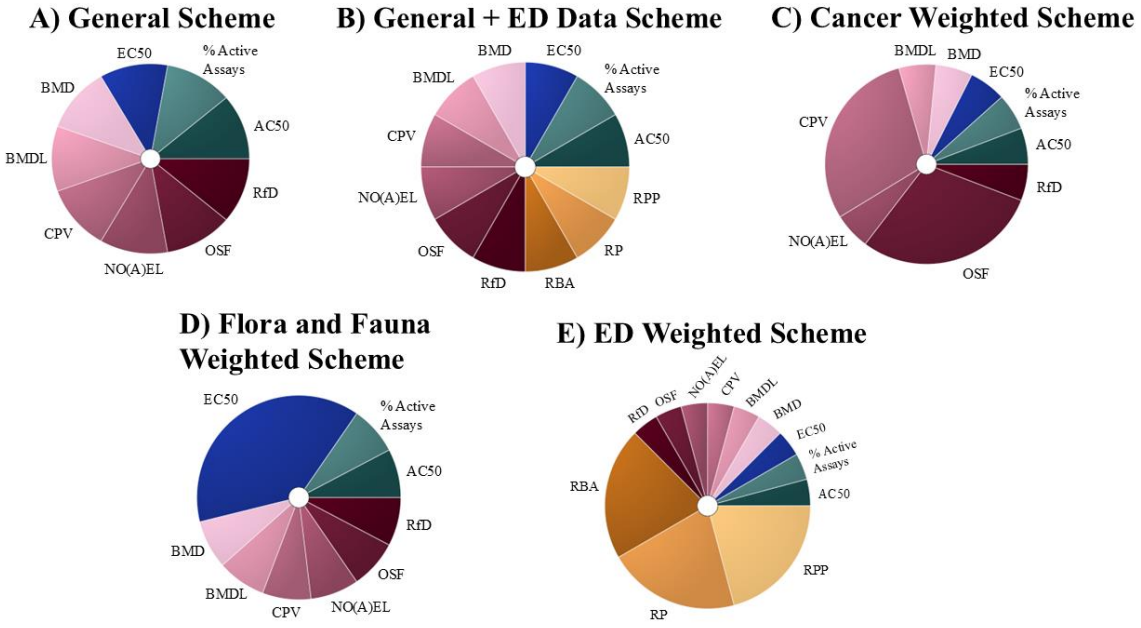

Figure 2.2. Data availability for 322 landfill leachate contaminants identified in the literature and prioritized using ToxPi. (A) Availability of all parameters reported in the Conditional Toxicity Value (CTV) predictor. (B) Availability of the half-maximal activity concentrations (AC50) reported in ToxCast. (C) Availability of the half-maximal effective concentrations (EC50) reported in ECOTOX. (D), (E), and (F) were collected from the EDKB and are defined as follows: relative potency (RP), relative binding activity (RBA), and relative proliferation potency (RPP), respectively.

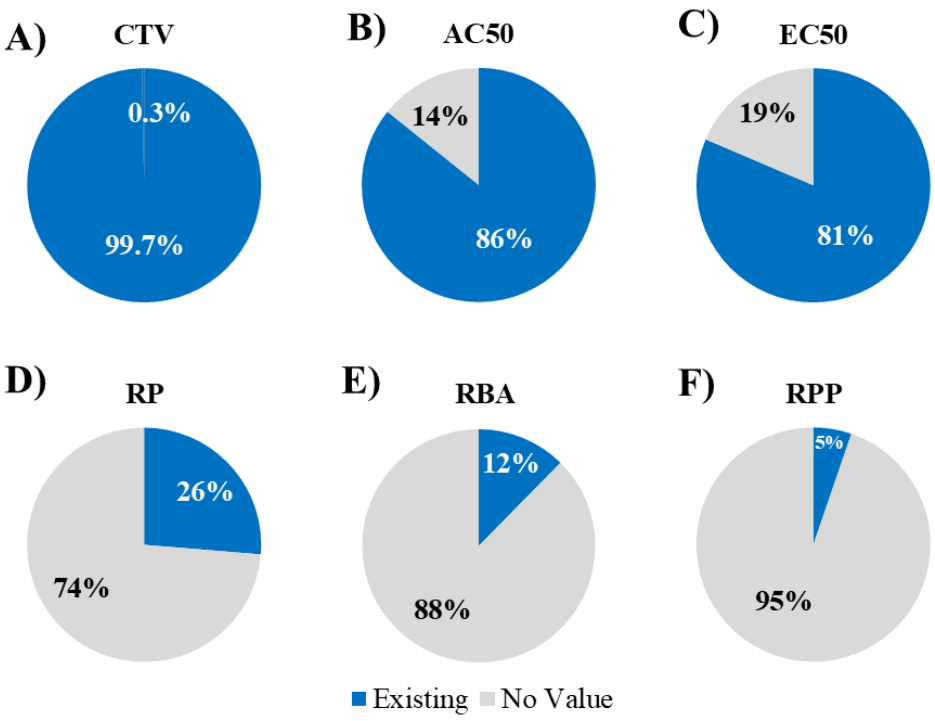

Figure 2.3. Distribution dot plot of ToxPi Scores for all 322 landfill leachate contaminants using the general prioritization scheme. Dots represent individual contaminants. Black and blue dots represent contaminants listed in Appendices I and II of 40 C.F.R 258, respectively, while yellow dots represent contaminants that are not included in either Appendix. ToxPi toxicity profiles for the five most toxic contaminants and the least toxic contaminant are displayed in the insets.

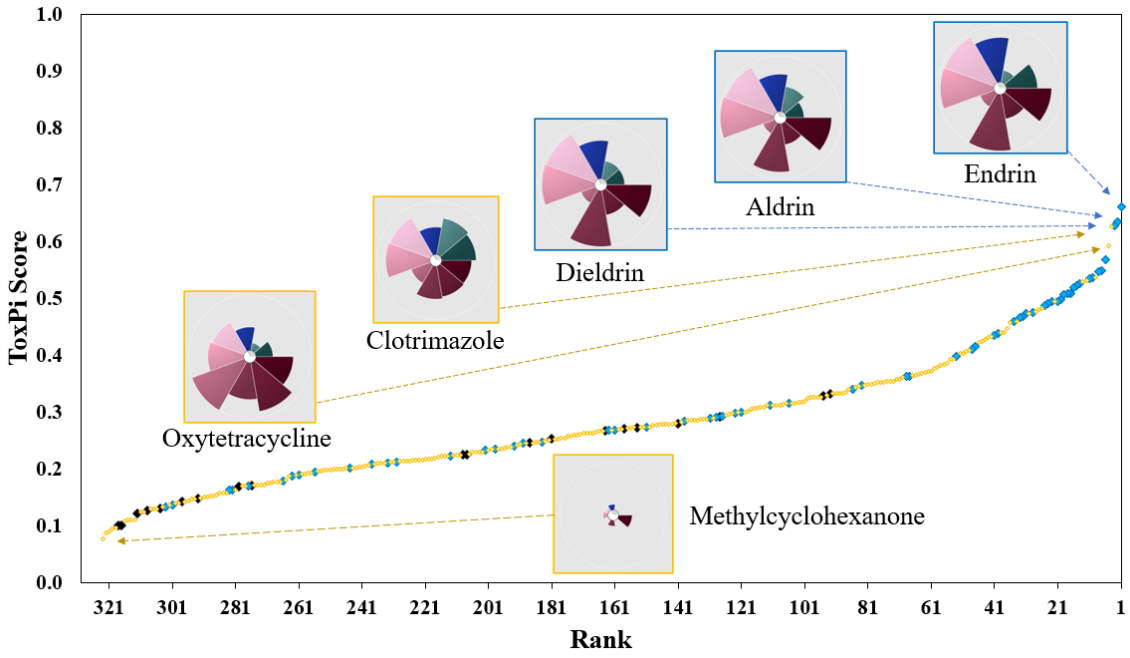

APPENDIX A

Table A1. Landfill leachate contaminants identified in a literature review. Of the 584 contaminants, 484 had existing CAS numbers. The 322 contaminants with existing toxicity data from at least two of the following databases: ECOTOX, ToxCast, and CTV Predictor, were prioritized in ToxPi analysis (bolded).

Contaminant	CASRN
4-Nitrophenol	**100-02-7**
Methylhydroxybenzoic acid	**100-09-4**
Terephthalic acid	**100-21-0**
Ethylbenzene	**100-41-4**
Styrene	**100-42-5**
Triclocarban	**101-20-2**
Chlorpropham	**101-21-3**
Diphenylether	**101-84-8**
Heptachlor epoxide	**1024-57-3**
Endosulfan sulfate	**1031-07-8**
Bis(2-ethylhexyl)adipate	**103-23-1**
n-Propylbenzene	**103-65-1**
Phenylacetic acid	**103-82-2**
Nonylphenol	**104-40-5**
2,4-Dimethylphenol	**105-67-9**
p-Xylene	**106-42-3**
p-Cresol	**106-44-5**
Dichlorobenzene	**106-46-7**
4-Chloroaniline (p-chloroaniline)	**106-47-8**
4-Chlorophenol	**106-48-9**
p-Toluidine	**106-49-0**
1,2-Dibromoethane	**106-93-4**
Glyphosate	**1071-83-6**
Glycol	**107-21-1**
Di-n-butyl phosphate	**107-66-4**
Butyric acid	**107-92-6**
m-Xylene	**108-38-3**
m-Cresol	**108-39-4**
3-Chlorophenol	**108-43-0**
m-Toluidine	**108-44-1**
1,3,5-Trimethylbenzene	**108-67-8**
3,5-Dimethylphenol	**108-68-9**
Toluene	**108-88-3**

Contaminant	CASRN
Fumaric acid	**110-17-8**
Pyridine	**110-86-1**
Glutaric acid	**110-94-1**
Branched heptanoic acid	**111-14-8**
Pimelic acid	**111-16-0**
Sebacic acid	**111-20-6**
Heptanol	**111-70-6**
Pelargonic acid	**112-05-0**
Oleic acid	**112-80-1**
Erythromycin	**114-07-8**
Propoxur	**114-26-1**
Phosphoric acid, triphenyl ester	**115-86-6**
Tris(2-chloroethyl)phosphate	**115-96-8**
BDE-209	**1163-19-5**
Bis(2-ethylhexyl)phthalate (DEHP)	**117-81-7**
Bis(2-methoxyethyl)phthalate	**117-82-8**
Bis(2-butoxyethyl)phthalate	**117-83-9**
Di-n-octyl phthalate	**117-84-0**
Hexachlorobenzene	**118-74-1**
Dichlobenil	**1194-65-6**
Benzophenone	**119-61-9**
2,3,4-tetrahydronaphthalene	**119-64-2**
Anthracene	**120-12-7**
2,4-DP (Dichloroprop)	**120-36-5**
Ethylparaben	**120-47-8**
1H-Indole	**120-72-9**
2,4-Dichlorophenol	**120-83-2**
Isophthalic acid	**121-91-5**
Iso-Propylbenzaldehyde	**122-03-2**
Simazine	**122-34-9**
Azelaic acid	**123-99-9**
Adipic acid	**124-04-9**
Branched octanoic acid	**124-07-2**

Contaminant	CASRN
Chlorobenzene	108-90-7
Phenol	108-95-2
Thiophenol	108-98-5
Valeric acid	109-52-4
Tetrahydrofuran	109-99-9
Furan	110-00-9
Succinic acid	110-15-6
Pyrene	129-00-0
Dimethyl phthalate	131-11-3
Di-n-amyl phthalate	131-18-0
Monobutylphthalate (MbutP)	131-70-4
Dibenzofuran	132-64-9
Diethyltoluamide (DEET)	134-62-3
Tris(1-chloropropan-2-yl)phosphate	13674-84-5
Tris(1,3-dichloropropan-2-yl)phosphate	13674-87-8
Limonene	138-86-3
Menthone	14073-97-3
Malonic acid	141-82-2
Hexanoic acid	142-62-1
Lauric acid	143-07-7
Sulfamethizole	144-82-1
Sulfapyridine	144-83-2
Diclofenac	15307-86-5
1,2-Dichloroethene	156-59-2
Sulpiride	15676-16-1
Cephalexin	15686-71-2
Ibuprofen	15687-27-1
2-Methyl-4-chlorophenol	1570-64-5
Chloridazon	1698-60-8
2,3,7,8-TCDD	1746-01-6
Perfluorooctanesulfonic acid	1763-23-1
Octyl phenol	1806-26-4
BDE-100	189084-64-8
Atrazine	1912-24-9
Benzo(ghi)perylene	191-24-2

Contaminant	CASRN
Tri-(2-methylpropyl)-phosphate	126-71-6
Phosphoric acid, tributyl ester	126-73-8
Tetrachloroethylene	127-18-4
Diphenylsulfone	127-63-9
Sulfamerazine	127-79-7
Chlordane	12789-03-6
Ionol	128-37-0
Tridemorph	24602-86-6
Bentazone	25057-89-0
Monobenzylphthalate (MbenzP)	2528-16-7
Gemfibrozil	25812-30-0
Amoxicillin	26787-78-0
Perfluoropentanoic acid	2706-90-3
2-perfluorooctylethanoic acid	27854-31-5
Pyrazine	290-37-9
Atenolol	29122-68-7
Bis(2-ethylhexyl)phosphate	298-07-7
Carbamazepine	298-46-4
Perfluorohexanoic acid	307-24-4
Perfluorododecanoic acid	307-55-1
Aldrin	309-00-2
Octabromodiphenyl ether	32536-52-0
PCB-105	32598-14-4
Decanoic acid	334-48-5
Perfluorooctanoic acid	335-67-1
Perfluorodecanoic acid	335-76-2
Triclosan	3380-34-5
Isoproturon	34123-59-6
PCB-153	35065-27-1
N-Butylbenzenesulfonamide	3622-84-2
Perfluorobutanoic acid	375-22-4
Perfluorobutane sulfonamido acetic acid	375-73-5
Perfluoroheptanoic acid	375-85-9
Perfluorononanoic acid	375-95-1
Perfluorotetradecanoic acid (PFTeDA)	376-06-7

Contaminant	CASRN
Indeno(123cd)pyrene	193-39-5
2,6-dichlorobenzamide (BAM)	2008-58-4
Perfluoroundecanoic acid	2058-94-8
Benzo(b)fluoranthene	205-99-2
Fluoranthene	206-44-0
Benzo(k)fluoranthene	207-08-9
Acenaphthylene	208-96-8
Hydroxyatrazine	2163-68-0
Chrysene	218-01-9
Ketoprofen	22071-15-4
Naproxen	22204-53-1
Miconazole	22916-47-8
Monoethylphthalate (MEP)	2306-33-4
Clotrimazole	23593-75-1
Methyl-6,7-dihydro-5H-cyclopentapyrazine	23747-48-0
Hexazinone	51235-04-2
Trimethyl phosphate	512-56-1
2,4-Dinitrophenol	51-28-5
Tripropyl phosphate	513-08-6
Metoprolol	51384-51-1
Sulfisomidine	515-64-0
5β-Cholestan-3α-ol	516-92-7
Propranolol	525-66-6
PCB-187	52663-68-0
1,2,3-Trimethylbenzene	526-73-8
2,3-Dimethylphenol	526-75-0
Dibenz(ah)anthracene	53-70-3
2-perfluorohexylethanoic acid	53826-12-3
Indomethacin	53-86-1
Decamethylcyclopentasiloxane	541-02-6
Nicotine	54-11-5
BDE-47	5436-43-1
Myristic acid	544-63-8
Octamethylcyclotetrasiloxane	556-67-2

Contaminant	CASRN
PCB-128	38380-07-3
1,2,3,4,7,8-hexaCDD	39227-28-6
1,2,3,7,8-pentaCDD	40321-76-4
BDE-28	41318-75-6
Bezafibrate	41859-67-0
Monoethylhexylphthalate (MEHP)	4376-20-9
Branched hexanoic acid	4536-23-6
Camphorquinone	465-29-2
1,8-Cineole	470-82-6
Cotinine	486-56-6
Tetrachlorophenol	4901-51-3
Indane	496-11-7
p,p'-DDT	50-29-3
Benzo(a)pyrene	50-32-8
2,3,7,8-TCDF	51207-31-9
Pentachlorobenzene	608-93-5
2-Ethyltoluene	611-14-3
Methylbenzamide	613-93-4
2-Phenylpropan-2-ol	617-94-7
4-Ethyltoluene	622-96-8
Aniline	62-53-3
Sulfanilamide	63-74-1
Branched pentanoic acid	646-07-1
Benzoic acid	65-85-0
Ketamine	6740-88-1
Fenpropimorph	67564-91-4
Acetone	67-64-1
Chloroform (trichloromethane)	67-66-3
Palmitic acid	67701-03-5
Sulfadiazine	68-35-9
BDE-153	68631-49-2
Ampicillin	69-53-4
Chloromethylpyridine	6959-47-3
Salicylic acid	69-72-7

Contaminant	CASRN
Tetrachloromethane	56-23-5
Doxycycline	564-25-0
Benz(a)anthracene	56-55-3
Chloramphenicol	56-75-7
Stearic acid	57-11-4
Chlorotetracycline	57-62-5
2,6-Dimethylphenol	576-26-1
Sulfaguanidine	57-67-0
Sulfadimidine (Sulfamethazine)	57-68-1
Caffeine	58-08-2
Di-methyl-naphthalene	581-42-0
Methylcyclohexanone	583-60-8
2,5-Dichlorophenol	583-78-8
Lindane (γ-HCH)	58-89-9
3,5-dichlorophenol	591-35-5
Acyclovir	59277-89-3
Sulfaquinoxaline	59-40-5
4-Chlor-o/m-cresol	59-50-7
Propiconazole	60207-90-1
Linoleic acid	60-33-3
BDE-99	60348-60-9
Tetracycline	60-54-8
Dieldrin	60-57-1
2,6-Dinitrotoluene	606-20-2
Branched butyric acid	79-31-2
Oxytetracycline	79-57-2
Tetrabromobisphenol-A	79-94-7
Bisphenol A	80-05-7
Roxithromycin	80214-83-1
Sulfamethoxypyridazine	80-35-3
n-Ethyl-p-toluenesulfonamide	80-39-7
Tebuconazole	80443-41-0
Clarithromycin	81103-11-9
3-Perfluoroheptyl propanoic acid	812-70-4
Ganciclovir	82410-32-0
Ofloxacin	82419-36-1
Acenaphthene	83-32-9

Contaminant	CASRN
Norfloxacin	70458-96-7
2H-perfluoro-2-decenoic acid	70887-84-2
2H-perfluoro-2-octenoic acid	70887-88-6
Benzene	71-43-2
1,1,1-Trichloroethane	71-55-6
2,6-Di-tert-butylchinone	719-22-2
Sulfathiazole	72-14-0
Endrin	72-20-8
Sulfamethoxazole	723-46-6
4,4'-DDD	72-54-8
p,p'-DDE	72-55-9
Florfenicol	73231-34-2
Trimethoprim	738-70-5
4-Chlorobenzoic acid	74-11-3
Dichloromethane (methylene chloride)	75-09-2
1,1-Dichloroethene	75-35-4
Camphor	76-22-2
Heptachlor	76-44-8
Codeine	76-57-3
Phosphoric acid	7664-38-2
Triethyl phosphate	78-40-0
Tris(2-ethylhexyl)phosphate	78-42-2
1,2-Dichloropropane	78-87-5
Glycolic acid	79-14-1
Enrofloxacin	93106-60-6
Benzothiazolone	934-34-9
MCPP (Mecoprop)	93-65-2
2,4,5-Trichlorophenoxyacetate (2,4,5-Trichlorophenoxyacetic acid)	93-76-5
Phenylbenzoate	93-99-2
Propylparaben	94-13-3
Butylparaben	94-26-8
MCPA	94-74-6
2,4-Dichlorophenoxyacetic acid	94-75-7
Benzothiazole	95-16-9
o-Xylene	95-47-6
o-Cresol	95-48-7
1,2-Dichlorobenzene	95-50-1

Contaminant	CASRN
3-Methylindole, skatole	**83-34-1**
Ametryn	**834-12-8**
24-Ethyl-cholest-5,22-dien-3β-ol	**83-48-7**
Di-cyclohexyl phthalate	**84-61-7**
Diethyl phthalate	**84-66-2**
Di-isobutyl phthalate	**84-69-5**
Dibutyl phthalate (di-n-butyl phthalate)	**84-74-2**
Di-n-hexyl phthalate	**84-75-3**
Di-n-nonyl phthalate	**84-76-4**
Phenanthrene	**85-01-8**
Benzylbutylphthalate (BBP)	**85-68-7**
Fluconazole	**86386-73-4**
Fluorene (9H Fluorene)	**86-73-7**
3,3,5-Trimethylcyclohexanone	**873-94-9**
1H-Indoleacetic acid	**87-51-4**
2,6-Dichlorophenol	**87-65-0**
Pentachlorophenol	**87-86-5**
Clofibric acid	**882-09-7**
2-Nitrophenol	**88-75-5**
Phthalic acid	**88-99-3**
Thymol	**89-83-8**
2-Methoxyphenol	**90-05-1**
1-Methyl-naphthalene	**90-12-0**
2-Hydroxybiphenyl (2-phenylphenol)	**90-43-7**
Naphtalene	**91-20-3**
3-Perfluoropentyl propanoic acid	**914637-49-3**
2-Methyl-naphthalene	**91-57-6**
Biphenyl (1,1'-Biphenyl)	**92-52-4**
Octylfenol-diethoxylate	1173020-69-3
Fenchone	1195-79-5
Sulfanilic acid	121-57-3
Sulfamonomethoxine	1220-83-3
Monomethylphthalate (MMP)	1276197-40-0
Xylene	128686-03-3
Carvomenthone	13163-73-0
4:2 disubstituted polyfluoroalkyl phosphate	135098-69-0

Contaminant	CASRN
o-Chloroaniline	**95-51-2**
o-Toluidine	**95-53-4**
2-Chlorophenol	**95-57-8**
Monochlorophenol	**95-57-8**
1,2,4-Trimethylbenzene	**95-63-6**
3,4-Dimethylphenol	**95-65-8**
3,4-Dichlorophenol	**95-77-2**
2,5-Dimethylphenol	**95-87-4**
Trichloro-phenol	**95-95-4**
Endosulfan I	**959-98-8**
t-Butylbenzene	**98-06-6**
Lomefloxacin	**98079-51-7**
Boronic acid	**98-80-6**
Isopropylbenzene (cumene)	**98-82-8**
Acetophenone	**98-86-2**
Nitrobenzene	**98-95-3**
Methylparaben	**99-76-3**
Perfluorohexane sulfonamido acetic acid (FHxSAA)	1003193-99-4
Perfluoroheptane sulfonamido acetic acid	1003194-00-0
Methylperfluoropentane sulfonamido acetic acid	1003194-04-4
Methyl perfluoroheptane sulfonamido acetic acid	1003194-05-5
Nonylphenol-monoethoxylate	104-35-8
n-Ethyl-o-toluene-sulfonamide	1077-56-1
Perfluorohexane sulfonate	108427-53-8
Methylpyridine	109-06-8
Thiophene	110-02-1
Squalene	111-02-4
8:2/10:2 disubstituted polyfluoroalkyl phosphate	1158182-60-5
PCB-8	34883-43-7
PCB-138	35065-28-2
PCB-180	35065-29-3
PCB-170	35065-30-6
3-Perfluoropropyl propanoic acid	356-02-5
PCB-52	35693-99-3
1,2,3,4,6,7,8-heptaCDD	35822-46-9
Perfluoroheptane sulfonate	375-92-8

Contaminant	CASRN
3-Perfluorononyl propanoic acid (9:3)	143260-97-3
Methyl perfluorobutane sulfonamido acetic acid	159381-10-9
Hydroxy-iso-propyl-acetophenone	1634-36-2
Perfluorooctadecanoic acid	16517-11-6
n-Phenylbenzenesulfonamide	1678-25-7
Dehydroabietinic acid	1740-19-8
Perfluoropentane sulfonate	175905-36-9
Pentabromodiphenyl ether	182346-21-0
1,2,3,7,8,9-hexaCDD	19408-74-3
PCB-209	2051-24-3
BDE-154	207122-15-4
BDE-183	207122-16-5
Tri-methyle-naphthalene	2245-38-7
Trans-1,2-Cyclohexanedicarboxylic acid	2305-32-0
Methylperfluorooctane sulfonamido acetic acid (NMeFOSAA)	2355-31-9
Nopinone	24903-95-5
Branched heptanoic acid	25103-52-0
2,6-dichlorophenoxypropionic acid	25140-90-3
Hydroxysimazine	2599-11-3
Econazole	27220-47-9
Perfluorooctane sulfonamido acetic acid	2806-24-8
p-Aminobenzoate	2906-28-7
Ethylperfluorooctane sulfonamido acetic acid	2991-50-6
Ephedrine	299-42-3
Amphetamine	300-62-9
Chloromethylphenol	30915-79-8
PCB-118	31508-00-6
PCB-66	32598-10-0
OctaCDD	3268-87-9
4-chlorophenoxypropionic acid	3307-39-9
Perfluorodecane sulfonate	335-77-3
Cyclopentane carboxylic acid	3400-45-1

Contaminant	CASRN
PCB-18	37680-65-2
PCB-101	37680-73-2
Norborn-5-ene-2,3-dicarboxylic acid	3813-52-3
Dimethyl-6,7-dihydro-5H-cyclopentapyrazine	38917-61-2
1,2,3,4,6,7,8-heptaCDF	38998-75-3
OctaCDF	39001-02-0
PCB-206	40186-72-9
PCB-44	41464-39-5
MDMA	42542-10-9
Hexabromodiphenyl ether	446255-03-4
m-Aminobenzoate	4518-10-9
Perfluorobutane sulfonate	45187-15-3
Perfluorononane sulfonate	474511-07-4
Propyphenazone	479-92-5
Biphenyl-2,2-dicarboxylic acid	482-05-3
Hydroxypivalinic acid	4835-90-9
Methylisophthalic acid	499-49-0
Bis(perfluorooctyl)phosphinate	500776-69-2
Borneol	507-70-0
2,4-Dichlorobenzoic acid	50-84-0
Bis(perfluorobutyl)phosphinate	52299-25-9
5,5-Diallylbarbituric acid	52-43-7
3,3-Dimethylnorbornane-2-carboxclic acid	52557-97-8
PCB-195	52663-78-2
1,2,4-Benzenetricarboxylic acid	528-44-9
Cyclohexylacetic acid	5292-21-7
Methamphetamine	537-46-2
Dichloroethylene	540-59-0
Dodecamethylcyclohexasiloxane	540-97-6
Benzamide	55-21-0
Coumaranone	553-86-6
1,2,3,4,7,8,9-heptaCDF	55673-89-7

Contaminant	CASRN
Heroin	561-27-3
2,3,4,7,8-pentaCDF	57117-31-4
1,2,3,7,8-pentaCDF	57117-41-6
1,2,3,6,7,8-hexaCDF	57117-44-9
Perfluoroheptadecanoic acid	57475-95-3
Methyl-1,2-cyclohexane dicarboxylicacid	57567-84-7
1,2,3,6,7,8-hexaCDD	57653-85-7
6:2 disubstituted polyfluoroalkyl phosphate	57677-95-9
24-Ethyl-cholest-5-en-3β-ol	5779-62-4
Cholest-5-en-3β-ol	57-88-5
n-Heptacosane	593-49-7
Podocarpic acid	5947-49-9
N;N;4-Trimethylbenzenesulfonamide	599-69-9
5β-Cholestan-3-one	601-53-6
Bis(2-ethoxyethyl)phthalate	605-54-9
2,3,4,6,7,8-hexaCDF	60851-34-5
Cis-1,2-Cyclohexanedicarboxylic acid	610-09-3
Perfluorohexylperfluorooctyl phosphinate	610800-34-5
Dimethylbenzamide	611-74-5
p-Toluamide	619-55-6
n-Pentacosane	629-99-2
n-Hexacosane	630-01-3
n-Octacosane	630-02-4
n-Nonacosane	630-03-5
Di-iso-butyl phosphate	6303-30-6
Nonabromodiphenyl ether	63387-28-0
Phenylsuccinic acid	635-51-8
n-Tricosane	638-67-5
n-Triacontane	638-68-6
iso-Propylacetophenone	645-13-6
n-Tetracosane	646-31-1
Perfluoropentane sulfonamido acetic acid	647-43-8
8:2 disubstituted polyfluoroalkyl phosphate	678-41-1
Perfluorohexadecanoic acid	67905-19-5
Heptabromodiphenyl ether	68928-80-3

Contaminant	CASRN
Pefloxacin	70458-92-3
Bis(perfluorohexyl)phosphinate	70609-44-8
1,2,3,4,7,8-hexaCDF	70648-26-9
Methyl perfluorohexane sulfonamido acetic acid	715646-50-7
Bis(1,3-dichloropropan-2-yl)phosphate	72236-72-7
Perfluorotridecanoic acid (PFTrDA)	72629-94-8
1,2,3,7,8,9-hexaCDF	72918-21-9
Branched nonanoic acid	7540-70-7
Hexyl 2-ethylhexyl phthalate	75673-16-4
α-amino-3-hydroxy-5-methyl-4-isoxazolepropionic acid (AMPA)	77521-29-0
2-Methyl-2-n-propyl-1,3-propanediol	78-26-2
Tricresyl phosphate	78-32-0
Tris (2-butoxyethyl) phosphate	78-51-3
Trichloroethylene	79-01-6
Levopimaric acid	79-54-9
5α-Cholestan-3β-ol	80-97-7
Bicyclo[2.2.1]heptenedicarbonicacid	824-62-4
Bis(4-methyl-2-pentyl)phthalate	84-63-9
Thiamphenicol	847-25-6
6-Cl-o-cresol	87-64-9
Benzyl succinic acid	884-33-3
o-Aminobenzoate	9031-59-8
Cholest-5,22-dien-3β-ol	92218-20-7
Propiophenone	93-55-0
Hydroxyphenylpropionic acid	938-96-5
Phenoxypropionic acid	940-31-8
6:2/8:2 disubstituted polyfluoroalkyl phosphate	943913-15-3
7-Acetyl-2-hydroxy-2-methyl-5-iso-propylbicyclo[4.3.0.]nonane	96093-81-1
Cyclohexane carboxylic acid	98-89-5
∑12PAHs	
∑16PAHs	
∑20 Sterol	
∑8PAEs	
∑8PBDEs	
1-(1-Ethoxyisopropoxy)-2-propanol	

Contaminant	CASRN
Ethylperfluoropentane sulfonamido acetic acid	68957-31-3
Ethylperfluorohexane sulfonamido acetic acid	68957-32-4
Ethylperfluorobutane sulfonamido acetic acid	68957-33-5
Ethylperfluoroheptane sulfonamido acetic acid	68957-63-1
PCB-28	7012-37-5
1-hydroxy-undecamethylcyclohexasiloxane	
2-(2-Hydroxyphenyl)-2-(4-hydroxyphenyl)propane	
2,4-Dichlorobenzene	
24-Ethyl-5α-cholest-22-en-3β-ol	
24-Ethyl-5α-cholestan-3β-ol	
24-Ethyl-5β-cholestan-3α-ol	
24-Methylcholest-5-en-3β-ol	
24-Ethyl-5β-cholestan-3β-ol	
24-Ethyl-5β-colestan-22-en-3α-ol	
24-Ethyl-5β-colestan-22-en-3β-ol	
24-Methyl-5α-cholestan-3β-ol	
27-Nor-24-methyl-cholesta-5,22-dien-3β-ol	
2H-Perfluoro-2-dodecenoic acid	
2H-Perfluoro-2-hexenoic acid	
2-Perfluorobutylethanoic acid	
2-Perfluorodecylethanoic acid	
4,6-Dichlorocresol	
4:2 Fluorotemomer sulfonate	
4:2/6:2 disubstituted polyfluoroalkyl phosphate	
4α,23,24-Trimethyl-5α-cholest-22-en-3α-ol	
6:2 Fluorotelomer mercaptoalkyl phosphate diester	
6:2 Fluorotemomer sulfonate	
6:2/8:2 Fluorotelomer mercaptoalkyl phosphate diester	
8:2 Fluorotelomer mercaptoalkyl phosphate diester	
8:2 Fluorotemomer sulfonate	
8:2/10:2 Fluorotelomer mercaptoalkyl phosphate diester	
a-Campholenic acid	
C1-Benzoic acid	
C2-Benzoic acid	
C2-Hydroxybutyric acid	

Contaminant	CASRN
1,3-Dichlorobenzene	
1,4-Dimethylnaphthalene	
10:2 disubstituted polyfluoroalkyl phosphate	
10:2 fluorotelomer mercaptoalkyl phosphate diester	
1-hydroxy-nonamethylcyclopentasiloxane	
C4-Pyrazine	
C5-Pyrazine	
Cyclohexane dicarboxylic acid	
Dichloroaniline	
Dihydroxybutyric acid	
Dihydroxydihydrocinnamic acid	
FM2	
Hydroxybutyric acid	
Hydroxycinnamic acid	
Hydroxycyclohexane carboxylic acid	
Hydroxyheptanoic acid	
Hydroxyindolecarboxylic acid	
Hydroxypentanoic acid	
Hydroxyphenylacetic acid	
Hydroxyphenylbutyric acid	
Methylnopinone	
Methylphenylbutyric acid	
NEtFOSAA	
N-ethyl perfluorooctane-sulfonamido-ethanol-based phosphate diester	
Nonchlorinated carbanilide	
Perfluorobutyl perfluorohexyl phosphinate	
Perfluoropentadecanoic acid	
PFBA	
PFBS	
PFDA	
PFDoA	
PFHpA	
PFHxA	
PFHxS	
PFNA	

Contaminant	CASRN
C2-Phenol	
C3-Benzene	
C3-Benzoic acid	
C3-Phenol	
C3-Pyrazine	
C4-Benzene	
C4-Benzoic acid	
C4-Phenol	
Sulfonamide	
Terpineol	
Tetrabromodiphenyl ethers	
Tetrahydrohydroxynaphthoic acid	
Tetrahydroretene	
Thiocresol	
Thiophencarboxylic acid	

Contaminant	CASRN
PFOA	
PFOS	
PFPeA	
PFPrA	
PFUnA	
Phenylbutyric acid	
Phenylpropionic acid	
Propylphenazone	
Toluenesulfonamide	
Trichlorobenzenes	
Trichloroethene	
Trimethyl-6,7-dihydro-5H-cyclopentapyrazine	
Trimethylbenzenes	
Trimethyltetralin	

Table A2. Landfill information for studies that reported leachate contaminant concentrations.

Source	Location	Description
Andersson et al., 2006	Sweden	9 landfills
Andrews et al., 2011	Oklahoma, USA	2 landfills: one closed (in operation early 1900s-1985, served 100,000), one active (Oklahoma City metropolitan area)
Argun et al., 2017	Konya Region, Turkey	Samples collected from active detention pond, municipal landfill recieves 706 tons of waste per year
Assmuth, 1996	Finland	43 waste sites, operational and closed municipal mixed-waste landfills, 23-year average length of period of use
Baun et al., 2003	Vejen, Denmark	Closed landfill, operated 1962-1981, 4×10^5 tons of waste
Baun et al., 2004	Denmark	10 landfills: 6 active, 4 closed, 1.5×10^5- 50×10^5 m^3 of waste
Chilton and Chilton, 1992	United States	Summary reports of average concentrations of harmful substances in municipal solid waste landfill leachate
Daso et al., 2017	Guauteng Province, South Africa	8 landfills
Denton et al., 2005	Ordot, Guam	Active landfill, over 50 years old, 24 ha, receives 71 m^3 of waste per day
Dudzinska et al., 2004	Lublin, Poland	Active landfill constructed in 1994, 39.19 ha, population served: 400,000
Dudzinska et al., 2008	Lublin, Poland	Active landfill constructed in 1994, 39.19 ha, population served: 400,001
Fang et al., 2020	Northern Zhejiang Province, China	3 landfills: 2 active, 1 closed
Ferrell and Smith, 1995	Mecklenburg County, North Carolina, USA	5 active and closed landfills, 4-30 years old, 11.33-151.76 ha
Gardiner et al., 2002	Selma, Virginia, USA	Closed landfill, operated 1972-1990, 10 ha, 860,000 tons total waste
Holm et al., 1995	Grindsted, Denmark	Closed landfill, active from 1930-1977
Kadlec and Zmarthie, 2010	Saginaw, MI, USA	12 ha landfill, closed in early 1980s
Kängsepp, 2008	Sweden and Estonia	4 landfills: two in Sweden, 2 in Estonia
Klimiuk and Kulikowska, 2004	Wysieka, Poland	Mature, active landfill
Koc-Jurczyk, 2014	Northeastern Poland	Closed landfill that had operated for 7 years
Kõrgmaa et al., 2011	Estonia	Active landfill, 4,300 m^3 leachate/year, population served: 100,000
Kulikowska and Klimiuk, 2008	Wysieka, Poland	Active landfill operated since 1996, 22 ha, over 7,000 tons of waste per year
Lang et al., 2017	United States	18 landfills: 1 closed, 17 active, 8-24 years old
Lu et al., 2016	Central Taiwan	4 landfills: two in urban areas (population served: 830,000 and 1,050,000), one rural area (population served: 56,000) and one suburb (population served: 87,000)

Source	Location	Description
Marttinen et al., 2003	Finland	11 landfills: 8 active, 3 closed, 2-52 ha, 0.3-5 Mm3 waste per year
Masoner et al., 2014	United States	19 active landfills: 12 municipal and 7 private, range in waste loads (1,000 to over 1,000,000 tons annually)
Matejczyk et al., 2011	Southern Poland	22 landfills, 1-22 years old, 1.92-128 ha, 1,800-200,000 Mg waste/year
Murray and Beck, 1990	Lake Charles, Louisiana, USA	Closed, received municipal waste from 1979-1985
Öman and Junestedt, 2008	Sweden	12 landfills, 2-50 years, 10-50 ha
Osako et al., 2004	Japan	7 landfills (active and closed)
Oturan et al., 2015	France	8 landfills
Palma-Fleming et al., 2000	Valdivia, Los Ríos, Chile	Landfill in operation since 1980, closed (113,920 m^3 of waste) and active sections (81,845 m^3 of waste)
Paxéus, 2000	Western Sweden	3 landfills: 2 active (each 8 ha), 1 closed (25 ha)
Peng et al., 2014	Guangzhou, China	2 municipal solid waste landfills: one small, old, and closed (5 million tons), one large, new, and open (opened in 2002, accepting 7,000-9,000 tons per day)
Qi et al., 2018	China	Over 40 landfills
Reinhart and Grosh, 1998	Florida, USA	39 lined landfills
Schwarzbauer et al., 2002	Germany	NA
Shi et al., 2020	Chongqing, China	2 landfills: one large and new that recieves urban waste materials, one small and older
Smol et al., 2016	Częstochowa, Poland	Municipal landfill in operation since 1987, 128.4 ha
Topal and Topal, 2015	Elazığ City, Turkey	Active landfill, 80 ha, 97,000 tons/year, population served: 266,000
Wang and Kelly, 2017	Singapore	Sampling from leachate treatment wetland, original landfill: closed, capacity: 3,000 m^3/day
Welander and Henrysson, 1998	Hyllstofta, Sweden	Active landfill, conventional mixed landfill (1,322,000 total tons of waste at time of sampling)
Wenzel et al., 1999	Germany	N/A
Wu et al., 2015	Shanghai, China	3 active sites (capacity: 1,700 tons/day, 1,500 tons/day, 10,000 tons/day)
Wu et al., 2017	Shanghai, China	Active, receives about 12,000 tons/day
Xu et al., 2008	Beijing, China	Municipal landfill in operation since 1996
You et al., 2018	China	7 active landfills, range of 2,200-10,000 t/d
Zhou et al., 2013	Shanghai, China	Urban landfill, receives around 10,000 tons/day

Table A3. Toxicity profiles generated in ToxPi of the 40 most toxic contaminants in landfill leachate according to the general prioritization scheme.

Rank	Compound	CASRN	Toxicity Profile
1	Endrin	72-20-8	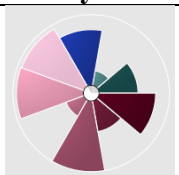
2	Dieldrin	60-57-1	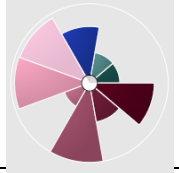
3	Aldrin	309-00-2	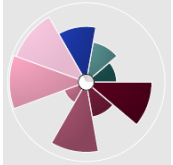
4	Clotrimazole	23593-75-1	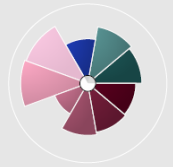
5	Oxytetracycline	79-57-2	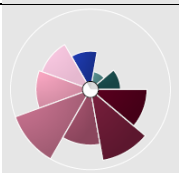
6	Chlordane	12789-03-6	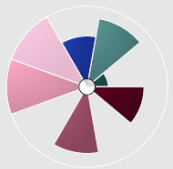
7	Indeno(123cd)pyrene	193-39-5	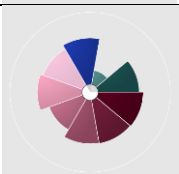
8	Heptachlor	76-44-8	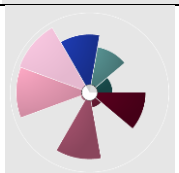
9	Tetrabromobisphenol-A	79-94-7	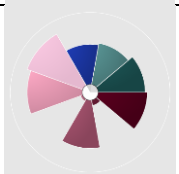

Rank	Compound	CASRN	Toxicity Profile
10	p,p'-DDE	72-55-9	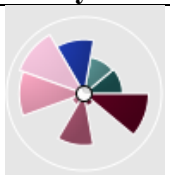
11	p,p'-DDT	50-29-3	
12	1,2,3,4,7,8-hexaCDD	39227-28-6	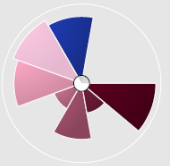
13	Tetracycline	60-54-8	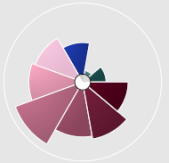
14	4,4'-DDD	72-54-8	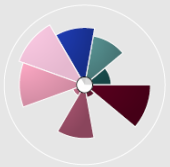
15	Benzo(a)pyrene	50-32-8	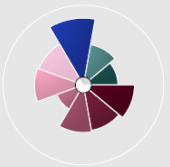
16	Benzo(ghi)perylene	191-24-2	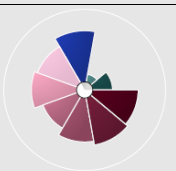
17	Benzo(b)fluoranthene	205-99-2	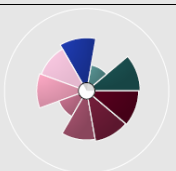
18	Dibenz(ah)anthracene	53-70-3	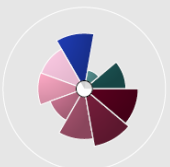

Rank	Compound	CASRN	Toxicity Profile
19	Heptachlor epoxide	1024-57-3	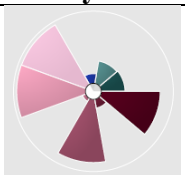
20	PCB-187	52663-68-0	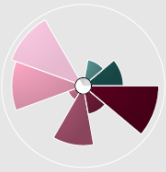
21	Benzo(k)fluoranthene	207-08-9	
22	Doxycycline	564-25-0	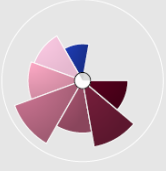
23	Benz(a)anthracene	56-55-3	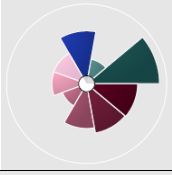
24	Endosulfan I	959-98-8	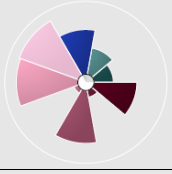
25	Endosulfan sulfate	1031-07-8	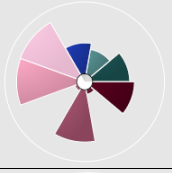
26	2,3,7,8-TCDF	51207-31-9	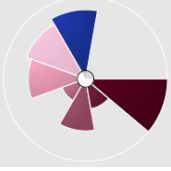
27	BDE-47	5436-43-1	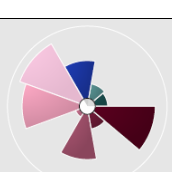

Rank	Compound	CASRN	Toxicity Profile
28	Chlortetracycline	57-62-5	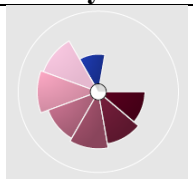
29	PCB-153	35065-27-1	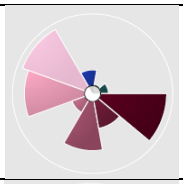
30	BDE-99	60348-60-9	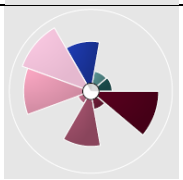
31	PCB-128	38380-07-3	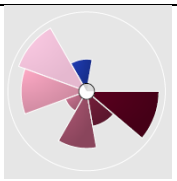
32	Lindane	58-89-9	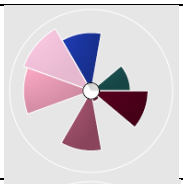
33	PCB-105	32598-14-4	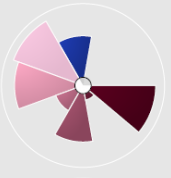
34	Enrofloxacin	93106-60-6	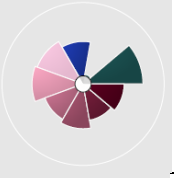
35	Pentachlorophenol	87-86-5	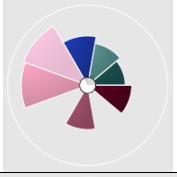
36	Codeine	76-57-3	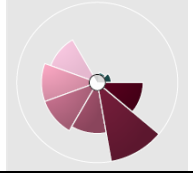

Rank	Compound	CASRN	Toxicity Profile
37	Tebuconazole	80443-41-0	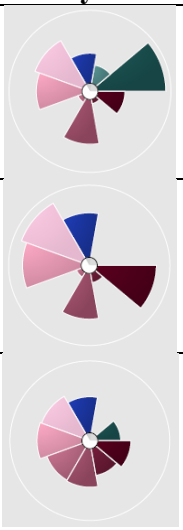
38	BDE-100	189084-64-8	
39	Ofloxacin	82419-36-1	
40	Pentachlorobenzene	608-93-5	

Table A4. Health impacts and associated references of the 40 most toxic contaminants in landfill leachate according to ToxPi analysis using the general prioritization scheme.

Rank	Compound	CASRN[a]	Health Impacts	Reference
1	Endrin	72-20-8	neurological, endocrine	Mnif et al., 2011
2	Dieldrin	60-57-1	developmental, endocrine, hepatic, immunological, neurological	Mnif et al., 2011
3	Aldrin	309-00-2	developmental, endocrine, hepatic, immunological, neurological	Mnif et al., 2011
4	Clotrimazole	23593-75-1	potential endocrine disruptor	Sabourin et al., 2010
5	Oxytetracycline	79-57-2	potential endocrine disruptor	Ji et al., 2010
6	Chlordane	12789-03-6	endocrine disruption	Huang et al., 2004
7	Indeno(123cd)pyrene	193-39-5	Known animal carcinogen, possible human carcinogen	T3DB[b]
8	Heptachlor	76-44-8	developmental, reproductive, endocrine	Mnif et al., 2011
9	Tetrabromobisphenol-A	79-94-7	potential endocrine disruptor, neurotoxicity	Yu et al., 2019
10	p,p'-DDE	72-55-9	developmental, endocrine, hepatic, neurological, reproductive	Mnif et al., 2011
11	p,p'-DDT	50-29-3	developmental, endocrine, hepatic, neurological, reproductive	Mnif et al., 2011
12	1,2,3,4,7,8-hexaCDD	39227-28-6	probable carcinogen	US EPA (a)
13	Tetracycline	60-54-8	endocrine disruption	Zeh et al., 2012
14	4,4'-DDD	72-54-8	developmental, endocrine, hepatic, neurological, reproductive	Mnif et al., 2011
15	Benzo(a)pyrene	50-32-8	probable human carcinogen	ATSDR, 2009
16	Benzo(ghi)perylene	191-24-2	not classified	Kim et al., 2013
17	Benzo(b)fluoranthene	205-99-2	probable human carcinogen	ATSDR, 2009
18	Dibenz(ah)anthracene	53-70-3	probable human carcinogen	ATSDR, 2009
19	Heptachlor epoxide	1024-57-3	developmental, reproductive	Mnif et al., 2011

Rank	Compound	CASRN[a]	Health Impacts	Reference
20	PCB-187	52663-68-0	carcinogenic to humans, endocrine	T3DB[b]; Tijani et al., 2013
21	Benzo(k)fluoranthene	207-08-9	possible human carcinogen	ATSDR, 2009
22	Doxycycline	564-25-0	possible endocrine disruptor	Hou et al., 2019
23	Benz(a)anthracene	56-55-3	probable human carcinogen	ATSDR, 2009
24	Endosulfan I	959-98-8	possible human carcinogen, neurological	T3DB[b]; Singh and Singh, 2014
25	Endosulfan sulfate	1031-07-8	neurological, possible carcinogen	T3DB[b]; Singh and Singh, 2014; Chan et al., 2007
26	2,3,7,8-TCDF	51207-31-9	possible neurological	Pelclova et al., 2018
27	BDE-47	5436-43-1	neurotoxicity	Tagliaferri et al., 2010
28	Chlortetracycline	57-62-5	possible endocrine disruptor	Ji et al., 2010
29	PCB-153	35065-27-1	carcinogenic to humans, endocrine	T3DB[b]; Tijani et al., 2013; Lasserre et al., 2009
30	BDE-99	60348-60-9	neurotoxicity	Tagliaferri et al., 2010
31	PCB-128	38380-07-3	endocrine	Tijani et al., 2013
32	Lindane	58-89-9	possible carcinogen, endocrine	T3DB[b]; Tijani et al., 2013
33	PCB-105	32598-14-4	carcinogenic to humans, endocrine	Tijani et al., 2013
34	Enrofloxacin	93106-60-6	not classified	
35	Pentachlorophenol	87-86-5	developmental, endocrine, reproductive	Mnif et al., 2011
36	Codeine	76-57-3	not classified	
37	Tebuconazole	80443-41-0	possible human carcinogen	Pubchem[c]
38	BDE-100	189084-64-8	endocrine	Hamers et al., 2008
39	Ofloxacin	82419-36-1	toxic to mammalian cells in culture	Kato and Onondera, 1988
40	Pentachlorobenzene	608-93-5	hepatic, urinary	US EPA (b)

[a] Chemical Abstracts Service Registry Number

[b] Toxin and Toxin-Target Database, http://www.t3db.ca/

[c] pubchem.ncbi.nlm.nih.gov

Table A5. Top 40 most toxic chemicals found in landfill leachate according to the flora and fauna weighted prioritization scheme. A star indicates inclusion in Appendix I or Appendix II, 40 C.F.R. § 258.

Flora and Fauna Weighted Rank	Compound	CAS	40 C.F.R. § 258. App. I	40 C.F.R. § 258. App. II
1	Endrin	72-20-8		*
2	Dieldrin	60-57-1		*
3	Aldrin	309-00-2		*
4	1,2,3,4,7,8-hexaCDD	39227-28-6		
5	**Benzo (a) pyrene**	**50-32-8**		*
6	p,p'-DDT	50-29-3		*
7	Heptachlor	76-44-8		*
8	Clotrimazole	23593-75-1		
9	**2,3,7,8-TCDF**	**51207-31-9**		
10	p,p'-DDE	72-55-9		*
11	Indeno(123cd)pyrene	193-39-5		*
12	4,4'-DDD	72-54-8		*
13	Benzo(ghi)perylene	191-24-2		*
14	Chlordane	12789-03-6		*
15	Dibenz(ah)anthracene	53-70-3		*
16	Tetrabromobisphenol-A	79-94-7		
17	**Oxytetracycline**	**79-57-2**		
18	Benzo(b)fluoranthene	205-99-2		*
19	Benz(a)anthracene	56-55-3		*
20	**Lindane**	**58-89-9**		*
21	Endosulfan I	959-98-8		*
22	**Naphthalene**	**91-20-3**		*
23	**Atrazine**	**1912-24-9**		
24	Benzo(k)fluoranthene	207-08-9		*
25	**Tetracycline**	**60-54-8**		
26	BDE-99	60348-60-9		
27	PCB-105	32598-14-4		*
28	**BDE-100**	**189084-64-8**		
29	**Propiconazole**	**60207-90-1**		
30	Pentachlorophenol	87-86-5		*
31	BDE-47	5436-43-1		
32	**Triclocarban**	**101-20-2**		
33	**Hexachlorobenzene**	**118-74-1**		*
34	**Triclosan**	**3380-34-5**		
35	**MCPA**	**94-74-6**		
36	**Hexazinone**	**51235-04-2**		
37	**Dichlorobenzene**	**106-46-7**	*	*
38	**Endosulfan sulfate**	**1031-07-8**		*
39	Pentachlorobenzene	608-93-5		*
40	**Doxycycline**	**564-25-0**		

Table A6. Top 40 most toxic chemicals found in landfill leachate according to the cancer weighted prioritization scheme. A star indicates inclusion in Appendix I or Appendix II, 40 C.F.R. § 258.

Cancer Weighted Rank[a]	Compound	CAS	40 C.F.R. § 258. App. I	40 C.F.R. § 258. App. II
1	Oxytetracycline	79-57-2		
2	Doxycycline	564-25-0		
3	Tetracycline	60-54-8		
4	Codeine	76-57-3		
5	Clotrimazole	23593-75-1		
6	Indeno(123cd)pyrene	193-39-5		*
7	Benzo(ghi)perylene	191-24-2		*
8	Chlorotetracycline	57-62-5		
9	Dibenz(ah)anthracene	53-70-3		*
10	Endrin	72-20-8		*
11	Dieldrin	60-57-1		*
12	Aldrin	309-00-2		*
13	Benzo(b)fluoranthene	205-99-2		*
14	Benzo (a) pyrene	50-32-8		*
15	Benz(a)anthracene	56-55-3		*
16	Benzo(k)fluoranthene	207-08-9		*
17	Ofloxacin	82419-36-1		
18	Enrofloxacin	93106-60-6		
19	1,2,3,4,7,8-hexaCDD	39227-28-6		
20	1,2,3,7,8-pentaCDD	40321-76-4		
21	PCB-128	38380-07-3		*
22	PCB-153	35065-27-1		*
23	2,3,7,8-TCDF	51207-31-9		
24	PCB-187	52663-68-0		*
25	PCB-105	32598-14-4		*
26	p,p’-DDE	72-55-9		*
27	Heptachlor	76-44-8		*
28	BDE-47	5436-43-1		
29	p,p’-DDT	50-29-3		*
30	Tetrabromobisphenol-A	79-94-7		
31	4,4'-DDD	72-54-8		*
32	Heptachlor epoxide	1024-57-3		*
33	Ampicillin	69-53-4		
34	Chlordane	12789-03-6		*
35	Fluoranthene	206-44-0		*
36	BDE-99	60348-60-9		
37	Endosulfan I	959-98-8		*
38	Endosulfan sulfate	1031-07-8		*
39	BDE-100	189084-64-8		
40	Amoxicillin	26787-78-0		

Table A7. Top 40 most toxic chemicals found in landfill leachate according to the endocrine disruption weighted prioritization scheme. A star indicates inclusion in Appendix I or Appendix II, 40 C.F.R. § 258.

Weighted Rank	Compound	CAS	40 C.F.R. § 258. App. I	40 C.F.R. § 258. App. II
1	Bisphenol A	80-05-7		
2	p,p'-DDT	50-29-3		*
3	p,p'-DDE	72-55-9		*
4	Octyl phenol	1806-26-4		
5	Endrin	72-20-8		*
6	Dieldrin	60-57-1		*
7	Aldrin	309-00-2		*
8	Clotrimazole	23593-75-1		
9	Oxytetracycline	79-57-2		
10	Heptachlor	76-44-8		*
11	Chlordane	12789-03-6		*
12	Indeno(123cd)pyrene	193-39-5		*
13	4,4'-DDD	72-54-8		*
14	Tetrabromobisphenol-A	79-94-7		
15	1,2,3,4,7,8-hexaCDD	39227-28-6		
16	Tetracycline	60-54-8		
17	Benzo(a)pyrene	50-32-8		*
18	Benzo(ghi)perylene	191-24-2		*
19	PCB-153	35065-27-1		*
20	Butylparaben	94-26-8		
21	Benzo(b)fluoranthene	205-99-2		*
22	Dibenz(ah)anthracene	53-70-3		*
23	Heptachlor epoxide	1024-57-3		*
24	PCB-187	52663-68-0		*
25	Endosulfan I	959-98-8		*
26	Benzo(k)fluoranthene	207-08-9		*
27	Doxycycline	564-25-0		
28	Benz(a)anthracene	56-55-3		*
29	Endosulfan sulfate	1031-07-8		*
30	2,3,7,8-TCDF	51207-31-9		
31	BDE-47	5436-43-1		
32	Chlorotetracycline	57-62-5		
33	Lindane	58-89-9		*
34	BDE-99	60348-60-9		
35	PCB-128	38380-07-3		*
36	PCB-105	32598-14-4		*
37	Enrofloxacin	93106-60-6		
38	Pentachlorophenol	87-86-5		*
39	Codeine	76-57-3		
40	Tebuconazole	80443-41-0		

Table A8. Top 40 most toxic chemicals found in landfill leachate according to the general + endocrine disruption data prioritization scheme. A star indicates inclusion in Appendix I or Appendix II, 40 C.F.R. § 258.

General + ED Data Rank	Compound	CASRN	40 C.F.R. § 258. App. I[1]	40 C.F.R. § 258. App. II[2]
1	p,p'-DDT	50-29-3		*
2	Endrin	72-20-8		*
3	p,p'-DDE	72-55-9		*
4	Dieldrin	60-57-1		*
5	Aldrin	309-00-2		*
6	Clotrimazole	23593-75-1		
7	Bisphenol A	80-05-7		
8	Oxytetracycline	79-57-2		
9	Chlordane	12789-03-6		*
10	Heptachlor	76-44-8		*
11	indeno(123cd)pyrene	193-39-5		*
12	Tetrabromobisphenol-A	79-94-7		
13	1,2,3,4,7,8-hexaCDD	39227-28-6		
14	4,4'-DDD	72-54-8		*
15	Tetracycline	60-54-8		
16	Benzo (a) pyrene	50-32-8		*
17	Benzo(ghi)perylene	191-24-2		*
18	Benzo(b)fluoranthene	205-99-2		*
19	dibenz(ah)anthracene	53-70-3		*
20	Heptachlor epoxide	1024-57-3		*
21	PCB-187	52663-68-0		*
22	benzo(k)fluoranthene	207-08-9		*
23	Doxycycline	564-25-0		
24	Benz(a)anthracene	56-55-3		*
25	Endosulfan I	959-98-8		*
26	Endosulfan sulfate	1031-07-8		*
27	2,3,7,8-TCDF	51207-31-9		
28	PCB-153	35065-27-1		*
29	BDE-47	5436-43-1		
30	Chlorotetracycline	57-62-5		
31	BDE-99	60348-60-9		
32	PCB-128	38380-07-3		*
33	Lindane	58-89-9		*
34	PCB-105	32598-14-4		*
35	Enrofloxacin	93106-60-6		
36	Pentachlorophenol	87-86-5		*
37	Codeine	76-57-3		
38	Tebuconazole	80443-41-0		
39	BDE-100	189084-64-8		
40	Ofloxacin	82419-36-1		

Figure A1. Distribution dot plot of ToxPi scores for all contaminants, including outlier 2,3,7,8-TCDD, which was removed from further analysis. The toxicity profile for 2,3,7,8-TCDD is displayed in the inset.

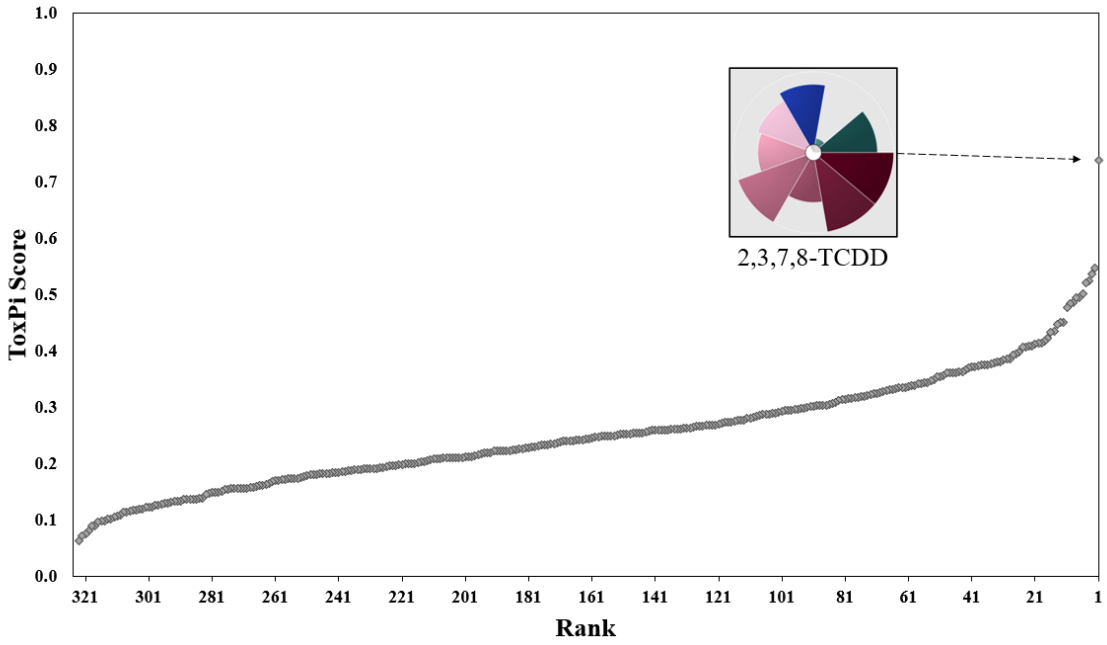

2.7 References

40 C.F.R. §258.1, 1991. Purpose, scope, and applicability. https://www.ecfr.gov/current/title-40/chapter-I/subchapter-I/part-258/subpart-A/section-258.1.

40 CFR § 258.54, 1991. Detection monitoring program. https://www.ecfr.gov/current/title-40/section-258.54.

40 CFR § 258.55, 1991. Assessment monitoring program. https://www.ecfr.gov/current/title-40/section-258.55.

40 C.F.R. § 445.21, 2000. Effluent limitations attainable by the application of the best practicable control technology currently available (BPT). https://www.ecfr.gov/current/title-40/chapter-I/subchapter-N/part-445/subpart-B/section-445.21.

70 FR 34555, 2005. Waste management system; Testing and monitoring activities; Final rule: Methods innovation rule and SW–846 final update IIIB. https://www.govinfo.gov/link/fr/70/34555

Allen, A., 2001. Containment landfills: the myth of sustainability. Eng. Geol. 60 (1-4), 3–19. https://doi.org/10.1016/S0013-7952(00)00084-3.

Andersson, J., Woldegiorgis, A., Remberger, M., Kaj, L., Ekheden, Y., Dusan, B., Svenson, A., Brorström-Lundén, E., Dye, C., Schlabach, M., 2006. Results from the Swedish National Screening Programme 2005, Subreport 1: Antibiotics, Anti-inflammatory substances, and Hormones (IVL Report B1689). Swedish Environmental Research Institute, p. 100. https://www.diva-portal.org/smash/record.jsf?pid=diva2%3A1551907&dswid=3329.

Andrews, W.J., Masoner, J.R., Cozzarelli, I.M., 2011. Emerging contaminants at a closed and an operating landfill in Oklahoma. Groundwater Monitor. and Remed. 32 (1), 120–130. https://doi.org/10.1111/j.1745-6592.2011.01373.x.

Appendix I to 40 C.F.R. § 258, 1991. Appendix I to Part 258—Constituents for detection monitoring. https://www.ecfr.gov/current/title-40/part-258/appendix-Appendix I to Part 258.

Appendix II to 40 C.F.R. § 258, 1991. Appendix II to Part 258—List of hazardous inorganic and organic constituents. https://www.ecfr.gov/current/title-40/part-258/appendix-Appendix II to Part 258.

Argun, M.E., Alver, A., Karatas, M., 2017. Optimization of landfill leachate oxidation at extreme conditions and determination of micropollutants removal. Desal. Water Treatment 90, 130–138. https://doi.org/10.5004/dwt.2017.21241.

Arrebola-Liébanas, F.J., Romero-González, R., Garrido Frenich, A., 2017. HRMS: fundamentals and basic concepts, in: Romero-González, R., Garrido Frenich, A. (Eds.), Applications in High Resolution Mass Spectrometry: Food Safety and Pesticide Residue Analysis. Elsevier Inc., Cambridge, Maine, USA, pp. 1-14. https://www.sciencedirect.com/science/article/abs/pii/B9780128094648000014.

Assmuth, T.W., 1996. Comparative risk analysis of waste site toxicants by indices based on concentration distributions, fluxes, environmental fate and critical effects. J. Hazard. Mater. 48 (1–3), 121–135. https://doi.org/10.1016/0304-3894(95)00139-5.

ATSDR (Agency for Toxic Substances and Disease Registry), 2009. Polycyclic aromatic hydrocarbons (PAHs): what health effects are associated with PAH exposure? Case Studies in Environmental Medicine, Toxicity of Polycyclic Aromatic

Hydrocarbons (PAHs). Course WB 1519. https://www.atsdr.cdc.gov/csem/pah/docs/pah.pdf.

Baderna, D., Maggiono, S., Boriani, E., Gemma, S., Molteni, M., Lombardo, A., Colombo, A., Bordonali, S., Rotella, G., Lodi, M., Benfenati, E., 2011. A combined approach to investigate the toxicity of an industrial landfill's leachate: chemical analyses, risk assessment, and *in vitro* assays. Environ. Res. 111 (4), 603–613. https://doi.org/10.1016/j.envres.2011.01.015.

Baun, A., Ledin, A., Reitzel, L.A., Bjerg, P.L., Christensen, T.H., 2004. Xenobiotic organic compounds in leachates from ten Danish MSW landfills—chemical analysis and toxicity tests. Water Research 38 (18), 3845–3858. https://doi.org/10.1016/j.watres.2004.07.006.

Baun, A., Reitzel, L.A., Ledin, A., Christensen, T.H., Bjerg, P.L., 2003. Natural attenuation of xenobiotic organic compounds in a landfill leachate plume (Vejen, Denmark). J. Contam. Hydrol. 65 (3-4), 269–291. https://doi.org/10.1016/S0169-7722(03)00004-4.

Brand, J.H., Spencer, K.L., O'shea, F.T., Lindsay, J.E., 2018. Potential pollution risks of historic landfills on low-lying coasts and estuaries. WIREs Water 5 (1), e1264. https://doi.org/10.1002/wat2.1264.

Chan, M.P.L., Morisawa, S., Nakayama, A., Yoneda, M., 2007. Evaluation of health risk due to the exposure to endosulfan in the environment. in: Proceedings of the 6th World Congress on Alternatives & Animal Use in the Life Sciences, August 21-25, 2007, Tokyo, Japan. AATEX, 14:543–548.

Chilton, J., Chilton, K., 1992. A critique of risk modeling and risk assessment of municipal landfills based on U.S. Environmental Protection Agency techniques. Waste Manage. Res. 10 (6), 505–516. https://doi.org/10.1016/0734-242X(92)90090-8.

Choi, K-I., Lee, D-H., 2006. PCDD/DF in leachates from Korean MSW landfills. Chemosphere 63 (8), 1353–1360. https://doi.org/10.1016/j.chemosphere.2005.09.028.

Chu, L.M., Cheung, K.C., Wong, M.H., 1994. Variations in the chemical properties of landfill leachate. Environ. Manage. 18, 105–117. https://doi.org/10.1007/BF02393753.

Danforth, C., Chiu, W.A., Rusyn, I., Schultz, K., Bolden, A., Kwiathowski, C., Craft, E., 2020. An integrative method for identification and prioritization of constituents of concern in produced water from onshore oil and gas extraction. Environ. Int. 134, 677–682. https://doi.org/10.1016/j.envint.2019.105280.

Daso, A.P., Rohwer, E.R., Koot, D.J., Okonkwo, J.O., 2017. Preliminary screening of polybrominated diphenyl ethers (PBDEs), hexabromocyclododecane (HBCDD) and tetrabromobisphenol A (TBBPA) flame retardants in landfill leachate. Environ. Monit. Assess. 189 (8), 418. https://doi.org/10.1007/s10661-017-6131-z.

Denton, G.R.W., Golabi, M.H., Iyekar, C., Wood, H.R., Wen, Y., 2005. Mobilization of aqueous contaminants leached from ordot landfill in surface and subsurface flows (Technical Report No. 108). Water and Environmental Research Institute of the Western Pacific University of Guam, Guam. https://ghs-cdn.uog.edu/wp-

content/databases/Library/PDFs/WERI%20TR%20108%20-%20Denton%20et%20al%202005.pdf.

Ding D., Xu L., Fang H., Hong H., Perkins R., Harris S., Bearden E.D., Shi L., Tong, W., 2010. The EDKB: an established knowledge base for endocrine disrupting chemicals. BMC Bioinf. 11 (Suppl 6), S5. https://doi.org/10.1186/1471-2105-11-S6-S5.

Domingo-Almenara, X., Montenegro-Burke, J.R., Ivanisevic, J., Thomas, A., Sidibé, J., Teav, T., Guijas, C., Aisporna, A.E., Rinehart, D., Hoang, L., Nordström, A., Gómez-Romero, M., Whiley, L., Lewis, M.R., Nicholson, J.K., Benton, H.P., Siuzdak, G., 2018. XCMS-MRM and METLIN-MRM: a cloud library and public resource for targeted analysis of small molecules. Nat. Methods 15, 681–684. https://doi.org/10.1038/s41592-018-0110-3.

Dudzińska, M.R., Czerwiński, J., Rut, B., 2004. Comparison of PCDD/Fs levels and profiles in leachates from "new" and "old" municipal landfills, in: Dioxin 2004: 24. International symposium on halogenated environmental organic pollutants and POPs. Proceedings, Organohalogen Compounds, vol. 66, ISBN 3-928379-30-5, p. 4035.

Dudzińska, M.R., Czerwiński,J., Rut, B. 2008. PCDD/F/T in leachates from "young" and "old" municipal landfills. Environ. Engin. Sci. 25 (7), 989–997. https://doi.org/10.1089/ees.2007.0104.

Fang, C., Chen, B., Zhuang, H., Mao, H., 2020. Antibiotics in leachates from landfills in northern Zhejiang Province, China. Bull. Environ. Contam. Toxicol. 105, 36–40. https://doi.org/10.1007/s00128-020-02894-x.

Ferrell, G.M., Smith, D.G., 1995. Water-quality conditions at selected landfills in Mecklenburg County, North Carolina, 1986-92. U.S. Geological Survey. Water Resources Investigations Report, pp. 95-4067.

Gardiner, J., Harris, L., Jacobi, M. (Eds.), 2002. Coastal and estuarine hazardous waste site reports, October 2002. Seattle: Coastal Protection and Restoration Division, Office of Response and Restoration, National Oceanic and Atmospheric Administration, p. 130.

Gramatica, P., Papa, E., 2007. Screening and ranking of POPs for global half-life: QSAR approaches for prioritization based on molecular structure. Environ. Sci. Technol. 41, 2833–2839. https://doi.org/10.1021/es061773b.

Guillén, D., Ginebreda, A., Farré, M., Darbra, R.M., Petrovic, M., Gros, M., Barceló, D., 2012. Prioritization of chemicals in the aquatic environment based on risk assessment: analytical, modeling and regulatory perspective. Sci. Total Environ. 440, 236–52. https://doi.org/10.1016/j.scitotenv.2012.06.064.

Hamers, T., Kamstra, J.H., Sonneveld, E., Murk, A.J., Visser, T.J., Van Velzen, M.J.M., Brouwer, A., Bergman, A., 2008. Biotransformation of brominated flame retardants into potentially endocrine-disrupting metabolites, with special attention to 2,2′,4,4′-tetrabromodiphenyl ether (BDE-47). Mol. Nutr. Food Res. 52 (2), 284–298. https://doi.org/10.1002/mnfr.200700104.

Hoang, T., Castorina, R., Gaspar, F., Maddalena, R., Jenkins, P.L., Zhang, Q., McKone, T.E., Benfenati, E., Shi, A.Y., Bradman, A., 2016. VOC exposures in California early childhood education environments. Indoor Air 27, 609–621. https://doi.org/10.1111/ina.12340.

Holm, V., Rügge, K., Bjerg, P.L., Christensen, T.H., 1995. Occurrence and distribution of pharmaceutical organic compounds in the groundwater downgradient of a landfill (Grinsted, Denmark). Environ. Sci. Technol. 29 (5), 1415–1419.

Hou, X., Zhu, L., Zhang, X., Zhang, L., Bao, H., Tang, M., Wei, R., Wang, R., 2019. Testosterone disruptor effect and gut microbiome perturbation in mice: early life exposure to doxycycline. Chemosphere 222, 722–731. https://doi.org/10.1016/j.chemosphere.2019.01.101.

Huang, D.-J., Wang, S.-Y., Chen, H.-C., 2004. Effects of the endocrine disrupter chemicals chlordane and lindane on the male green neon shrimp (*Neocaridina denticulata*). Chemosphere 57 (11), 1621–1627. https://doi.org/10.1016/j.chemosphere.2004.08.063.

Ji, K., Choi, K., Lee, S., Park, S., Khim, J.S., Jo, E.H., Choi, K., Zhang, X., Giesy, J.P., 2010. Effects of sulfathiazole, oxytetracycline and chlortetracycline on steroidogenesis in the human adrenocarcinoma (H295R) cell line and freshwater fish *Oryzias Latipes*. J. Hazard. Mater. 182 (1-3), 494–502. https://doi.org/10.1016/j.jhazmat.2010.06.059.

Kadlec, R.H., Zmarthie, L.A., 2010. Wetland treatment of leachate from a closed landfill. Ecol. Engin. 36 (7), 946–957. https://doi.org/10.1016/j.ecoleng.2010.04.013.

Kängsepp, P., 2008 Development and evaluation of a filter-bed-based system for full scale treatment of industrial landfill leachate. Ph.D. Dissertation, Department of Analytical Chemistry, Lund. Lund University. https://portal.research.lu.se/en/publications/development-and-evaluation-of-a-filter-bed-based-system-for-full-.

Karthikeyan, B.S., Ravichandran, J., Mohanraj, K., Vivek-Ananth, R.P., Samal, A., 2019. A curated knowledgebase on endocrine disrupting chemicals and their biological systems-level perturbations. Sci. Total Environ. 692, 281–296. https://doi.org/10.1016/j.scitotenv.2019.07.225.

Kato, M., Onondera, T., 1988. Effect of ofloxacin on the uptake of [^{3}H]thymidine by articular cartilage cells in the rat. Toxicol. Lett. 44 (1-2), 131–142. https://doi.org/10.1016/0378-4274(88)90139-7.

Kim, K.-H., Jahan, S.A., Kabir, E., Brown, R.J.C., 2013. A review of airborne polycyclic aromatic hydrocarbons (PAHs) and their human health effects. Environ. Int. 60, 71–80. https://doi.org/10.1016/j.envint.2013.07.019.

Kjeldsen, P. Barlaz, M.A., Rooker, A.P., Baun, A., Ledin, A., Christensen, T.H., 2002. Present and long-term composition of MSW landfill leachate: a review. Crit. Rev. Environ. Sci. Technol. 32, 297–336. https://doi.org/10.1080/10643380290813462.

Klimiuk, E., Kulikowska, D., 2004. Effectiveness of organics and nitrogen removal from municipal landfill leachate in single and two-stage SBR system. Pol. J. Environ. Stud. 13 (5), 525–532.

Koc-Jurczyk, J., 2014. Removal of refractory pollutants from landfill leachate using two-phase system. Water Environ. Res. 86 (1), 74–80. https://doi.org/10.2175/106143013X13807328848810.

Kõrgmaa, V., Laht, M., Põllumäe, A., Volkov, E., Huhtala, S., Munne, P., Nakari, T., Nuutinen, J., Perkola, N., Schultz, E., Zielonka, U., 2011. National report of the Estonian results of the COHIBA WP3 study. Estonian Environmental Research Centre, p. 109.

Kulikowska, D. Klimiuk, E., 2008. The effect of landfill age on municipal leachate composition. Bioresour. Technol. 99 (13), 5981–5985. https://doi.org/10.1016/j.biortech.2007.10.015.

Lagarde, F., Beausoleil, C., Belcher, S.M., Belzunces, L.P., Emond, C., Guerbet, M., Rousselle, C., 2015. Non-monotonic dose–response relationships and endocrine disruptors: a qualitative method of assessment. Environ. Health 14, 13. https://doi.org/10.1186/1476-069X-14-13.

Lang, J.R., Allred, B.M., Field, J.A., Levis, J.W., Barlaz, M.A., 2017. National estimate of per- and polyfluoroalkyl substance (PFAS) release to U.S. municipal landfill leachate. Environ. Sci. Technol. 51 (4), 2197–2205. https://doi.org/10.1021/acs.est.6b05005.

Lasserre, J.P., Fack, F., Revets, D., Planchon, S., Renaut, J., Hoffmann, L., Gutleb, A.C., Miller, C.P., Bohn, T., 2009. Effects of the endocrine disruptors atrazine and PCB 153 on the protein expression of MCF-7 human cells. J. Proteome Res. 8 (12), 5485–5496. https://doi.org/10.1021/pr900480f.

Lu, M-C., Chen, Y.Y., Chiou, M-R., Chen, M.Y., Fan, H-J., 2016. Occurrence and treatment efficiency of pharmaceuticals in landfill leachates. Waste Manage. 55, 257–264. https://doi.org/10.1016/j.wasman.2016.03.029.

Marttinen, S.K., Kettunen, R.H., Rintala, J.A., 2003. Occurrence and removal of organic pollutants in sewages and landfill leachates. Sci. Total Environ. 301 (1-3), 1–12. https://doi.org/10.1016/S0048-9697(02)00302-9.

Marvel SW, To K, Grimm FA, Wright FA, Rusyn I, Reif DM., 2018. ToxPi Graphical User Interface 2.0: dynamic exploration, visualization, and sharing of integrated data models. BMC Bioinf. 19 (1), 80. https://doi.org/10.1186/s12859-018-2089-2.

Masoner, J.R., Kolpin, D.W., Furlong, E.T., Cozzarelli, I.M., Gray, J.L., Schwab, E.A., 2014. Contaminants of emerging concern in fresh leachate from landfills in the conterminous United States. Environ. Sci.: Proc. Imp. 16 (10), 2335–2354. https://doi.org/10.1039/C4EM00124A.

Masoner, J.R., Kolpin, D.W., Furlong, E.T., Cozzarelli, I.M., Gray, J.L., 2016. Landfill leachate as a mirror of today's disposable society: pharmaceuticals and other contaminants of emerging concern in final leachate from landfills in the conterminous United States. Environ. Toxicol. Chem. 35 (4), 906–918. https://doi.org/10.1002/etc.3219.

Matejczyk, M., Plaza, G.A., Naleca-Jawecki, G., Ulfig, K., Markowska-Szczupak, A., 2011. Estimation of environmental risk posed by landfills using chemical, microbiological and ecotoxicological testing of leachates. Chemosphere 82 (7), 1017–1023. https://doi.org/10.1016/j.chemosphere.2010.10.066.

Mnif, W., Hassine, A.I.H., Bouaziz, A., Bartegi, A., Thomas, O., Roig, B., 2011. Effect of endocrine disruptor pesticides: a review. Int. J. Environ. Res. Public Health 8 (6), 2265–2303. https://doi.org/10.3390/ijerph8062265.

Moody, C.M., Townsend, T.G., 2017. A comparison of landfill leachates based on waste composition. Waste Manage. 63, 267–274. https://doi.org/10.1016/j.wasman.2016.09.020.

Mukherjee, S., Mukhopadhyay, S., Hashim, M.A., Sen Gupta, B., 2015. Contemporary environmental issues of landfill leachate: assessment and remedies. Crit. Rev. Environ. Sci. Technol. 45 (5), 472–590. https://doi.org/10.1080/10643389.2013.876524.

Munier, M. Grouleff, J., Gourdin, L., Fauchard, M., Chantreau, V., Henrion, D., Coutant, R, Schiøtt, B., Chabbert, M., Rodien, P., 2016. In vitro effects of the endocrine disruptor p,p'-DDT on human follitropin receptor. Environ. Health Perspect. 124, 991–999. https://doi.org/10.1289/ehp.1510006.

Murphy, B.L., 1989. Modeling the leaching and transport of 2,3,7,8-TCDD from incinerator ash from landfills. Chemosphere 19 (1-6), 433–438. https://doi.org/10.1016/0045-6535(89)90348-2.

Murray, H.E., Beck, J.N., 1990. Concentrations of synthetic organic chemicals in leachate from a municipal landfill. Environ. Pollut. 67 (3), 195–203. https://doi.org/10.1016/0269-7491(90)90186-G.

Nagendran, R., Selvam, A., Joseph, K., Chiemchaisri, C., 2006. Phytoremediation and rehabilitation of municipal solid waste landfills and dumpsites: a brief review. Waste Manage. 26 (12), 1357–1369. https://doi.org/10.1016/j.wasman.2006.05.003.

Öman, C.B., Junestedt, C., 2008. Chemical characterization of landfill leachates—400 parameters and compounds. Waste Manage. 28 (10), 1876–1891. https://doi.org/10.1016/j.wasman.2007.06.018.

Osako, M., Kim, Y., Sakai, S., 2004. Leaching of brominated flame retardants in leachate from landfills in Japan. Chemosphere 57 (10), 1571–1579. https://doi.org/10.1016/j.chemosphere.2004.08.076.

Oturan, N., van Hullebusch, E.D., Zhang, H., Mazeas, L., Budzinski, H., Le Menach, K., Oturan, M.A., 2015. Occurrence and removal of organic micropollutants in landfill leachates treated by electrochemical advanced oxidation processes. Environ. Sci. Technol. 49 (20), 12187–12196. https://doi.org/10.1021/acs.est.5b02809.

Palma-Fleming, H., Quiroz, E. Gutierrez, E. Cristi, E., Jara, B., Keim, M.L., Pino, M., Huber, A., Jaramillo, E., Espinoza, O., Quijon, P., Contreras, H., Ramirez, C., 2000. Chemical characterization of a municipal landfill and its influence on the surrounding estuary system, south central Chile. Bol. Soc. Chil. Quím. 45 (4). http://dx.doi.org/10.4067/S0366-16442000000400005.

Park, N., Choi, Y., Kim, D., Kim, K., Jeon, J., 2018. Prioritization of highly exposable pharmaceuticals via a suspect/non-target screening approach: a case study for Yeongsan River, Korea. Sci. Total Environ. 639, 570–579. https://doi.org/10.1016/j.scitotenv.2018.05.081.

Paxéus, N., 2000. Organic compounds in municipal landfill leachates. Water Sci. Technol. 42 (7-8), 323–333. https://doi.org/10.2166/wst.2000.0585.

Pelclova, D., Urban, P., Fenclova, Z., Vlckova, S., Ridzon, P., Kupka, K., Meckova, Z., Bezdicek, O., Navratil, T., Rosmus, J., Zakharov, S., 2018. Neurological and neurophysiological findings in workers with chronic 2,3,7,8-tetrachlorodibenzo-p-

dioxin intoxication 50 years after exposure. Basic Clin. Pharmacol. Toxicol. 122, 271–277. https://doi.org/10.1111/bcpt.12899.

Peng, X., Ou, W., Wang, C., Wang, Z., Huang, Q., Jin, J., Tan, J., 2014. Occurrence and ecological potential of pharmaceuticals and personal care products in groundwater and reservoirs in the vicinity of municipal landfills in China. Sci. Total Environ. 490, 889–898. https://doi.org/10.1016/j.scitotenv.2014.05.068.

Qi, C., Huang, J., Wang, B., Deng, S., Wang, Y., Yu, G., 2018. Contaminants of emerging concern in landfill leachate in China: a review. Emerg. Contam. 4 (1) 1–10. https://doi.org/10.1016/j.emcon.2018.06.001.

Ramakrishnan, A., Blaney, L., Kao, J., Tyagi, R.D., Zhang, T.C., Surampalli, R.Y., 2015. Emerging contaminants in landfill leachate and their sustainable management. Environ. Earth Sci. 73, 1357–1368. https://doi.org/10.1007/s12665-014-3489-x.

Reif, D.M., Martin, M.T., Tan, S.W., Houck, K.A., Judson, R.S., Richard, A.M., Knudsen, T.B., Dix, D.J., Kavlock, R.F., 2010. Endocrine profiling and prioritization of environmental chemicals using ToxCast data. Environ. Health Perspect. 118 (12), 1714–1720. https://doi.org/10.1289/ehp.1002180.

Reinhart, D.R., Grosh, C. J., 1998. Analysis of Florida MSW landfill leachate quality (Report 97-3). State University System of Florida, Florida Center for Solid and Hazardous Waste Management, Gainesville, Florida.

Richard, A.M., Judson, R.S., Houck, K.A., Grulke, C.M., Volarath, P., Thillainadarajah, I., Yang, C., Rathman, J., Martin, M.T., Wambaugh, J.F., Knudsen, T.B., Kancherla, J., Mansouri, K., Patlewicz, G., Williams, A.J., Little, S.B., Crofton, K.M., Thomas, R.S., 2016. ToxCast chemical landscape: paving the road to 21st

century toxicology. Chem. Res. Toxicol. 29 (8), 1225–1251. https://doi.org/10.1021/acs.chemrestox.6b00135.

Rubin, B.S., 2011. Bisphenol A: an endocrine disruptor with widespread exposure and multiple effects. J. Steroid Biochem.Mol. Biol. 127 (1-2), 27–34. https://doi.org/10.1016/j.jsbmb.2011.05.002.

Sabourin, L. Al-Rajab, A.J., Chapman, R., Lapen, D.R., Topp, E., 2011. Fate of the antifungal drug clotrimazole in agricultural soil. Environ. Toxicol. Chem. 30 (3), 582–587. https://doi.org/10.1002/etc.432.

Sargent, M. (Ed.) 2013. Guide to achieving reliable quantitative LC-MS measurements. RSC Analytical Methods Committee. ISBN 978-0-948926-27-3.

Schiopu, A-M., Gavrilescu, M., 2010. Options for the treatment and management of municipal landfill leachate: common and specific issues. CLEAN-Soil, Air, Water 38 (12), 1101–1110. https://doi.org/10.1002/clen.200900184.

Schwarzbauer, J., Heim, S., Brinker, S., Littke, R., 2002. Occurrence and alteration of organic contaminants in seepage and leakage water from a waste deposit landfill. Water Res. 36 (9), 2275–2287. https://doi.org/10.1016/S0043-1354(01)00452-3.

Shi, Y., Liu, J., Zhuo, L., Yan, X., Cai, F., Luo, W., Ren, M., Liu, Q., Yu, Y., 2020. Antibiotics in wastewater from multiple sources and surface water of the Yangtze River in Chongqing in China. Environ. Monitor. Assess. 192 (3), 159. https://doi.org/10.1007/s10661-020-8108-6.

Singer, M., 2011. Down cancer alley: the lived experience of health and environmental suffering in Louisiana's chemical corridor. Med. Anthropol. Q. 25 (2), 141–63. https://doi.org/10.1111/j.1548-1387.2011.01154.x.

Singh, V., Singh, N. 2014. Uptake and accumulation of endosulfan isomers and its metabolite endosulfan sulfate in naturally growing plants of contaminated area. Ecotoxicol. Environ. Safe. 104, 198–193. https://doi.org/10.1016/j.ecoenv.2014.02.025.

Smith, R.M., O'Keefe, P.W., Aldous, K.M., Hilker, D.R., O'Brien, J.E., 1983. 2,3,7,8-Tetrachlorodibenzo-*p*-dioxin in sediment samples from Love Canal storm sewers and creeks. Environ. Sci. Technol. 17, 6–10. https://doi.org/10.1021/es00107a004.

Smith, C.A., Want, E.J., O'Maille, G., Abagyan, R. Siuzdak, G., 2006. XCMS: processing mass spectrometry data for metabolite profiling using nonlinear peak alignment, matching, and identification. Anal. Chem. 78, 779–787. https://doi.org/10.1021/ac051437y.

Smol, M., Włodarczyk-Makuła, M., Mielczarek, K., Bohdziewicz, J., Włóka, D., 2016. The use of reverse osmosis in the removal of PAHs from municipal landfill leachate. Polycycl. Aromat. Comp. 36 (1), 20–39. https://doi.org/10.1080/10406638.2014.957403.

Tagliaferri, S., Caglieri, A., Goldoni, M., Pinelli, S., Alinovi, R., Poli, D., Pellacani, C., Giordano, G., Mutti, A., Costa, L.G., 2010. Low concentrations of the brominated flame retardants BDE-47 and BDE-99 induce synergistic oxidative stress-mediated neurotoxicity in human neuroblastoma cells. Toxicol. in Vitro 24, 116–122. https://doi.org/10.1016/j.tiv.2009.08.020.

Tao, Z., Wei, S., Liu, Y., Xiaoli, C., 2018. Temporal variation of vegetation at two operating landfills and its implications for landfill phytoremediation. Environ. Technol. 41 (5), 649–657. https://doi.org/10.1080/09593330.2018.1508253.

Tijani, J.O., Fatoba, O.O., Petrik, L.F., 2013. A review of pharmaceuticals and endocrine-disrupting compounds: Sources, effects, removal, and detections. Water Air Soil Pollut. 224, 1770. https://doi.org/10.1007/s11270-013-1770-3.

Topal, M., Arslan Topal, E.I., 2015. Determination and monitoring of tetracycline and degradation products in landfill leachate. CLEAN - Soil, Air, Water 44 (4), 444–450. https://doi.org/10.1002/clen.201400938.

Townsend, T.G., Powell, J., Jain, P., Xu, Q., Tolaymat, T., Reinhart, D., 2015. Sustainable practices for landfill design and operation. Springer, Springer Science + Business Media, New York. https://doi.org/10.1007/978-1-4939-2662-6.

U.S. EPAa (United States Environmental Protection Agency) National Center for Environmental Assessment. (n.d.). Hexachlorodibenzo-p-dioxin (HxCDD), mixture of 1,2,3,6,7,8-HxCDD and 1,2,3,7,8,9-HxCDD; CASRN 57653-85-7 and 19408-74-3. Integrated Risk Information System (IRIS), Chemical Assessment Summary.

U.S. EPAb (United States Environmental Protection Agency) National Center for Environmental Assessment. (n.d.). Pentachlorobenzene; CASRN 608-93-5. Integrated Risk Information System (IRIS), Chemical Assessment Summary.

U.S. EPA (United States Environmental Protection Agency) Office of Water, 2000. Development document for final effluent limitations guidelines and standards for the landfills point source category. EPA-821-R-99-019. https://www.epa.gov/sites/production/files/2015-11/documents/landfills-eg_dd_2000.pdf (accessed 22 July 2020).

U.S. EPA (United States Environmental Protection Agency), 2017. Endocrine disruption research: testing for potential low-dose effects. https://www.epa.gov/chemical-research/endocrine-disruption-research-testing-potential-low-dose-effects (accessed 11 August 2020).

U.S. EPA (U.S. Environmental Protection Agency), 2018. ECOTOX user guide: ECOTOXicology Knowledgebase System. Version 5.0. U.S. Environmental Protection Agency. https://nepis.epa.gov/Exe/ZyPURL.cgi?Dockey=P100VVOB.txt (accessed 20 May 2020).

U.S. EPA. (U.S. Environmental Protection Agency), 2020a. ECOTOX Knowledgebase. https://cfpub.epa.gov/ecotox/search.cfm (accessed 20 May 2020).

U.S. EPA. (U.S. Environmental Protection Agency), 2020b. TOXCAST: EPA ToxCast screening library. https://comptox.epa.gov/dashboard/chemical_lists/toxcast (accessed 20 May 2020).

U.S. EPA (United States Environmental Protection Agency), 2020c. Basic information about the integrated risk information system. IRIS. https://www.epa.gov/iris/basic-information-about-integrated-risk-information-system (accessed 29 June 2020).

U.S. FDA (United States Food and Drug Administration), 2019. Endocrine disruptor knowledge base. https://www.fda.gov/science-research/bioinformatics-tools/endocrine-disruptor-knowledge-base (accessed 16 July 2020).

Vandenberg, L.N., Ehrlich, S. Belcher, S.M., Ben-Jonathan, N., Dolinoy, D.C., Hugo, E.R., Hunt, P.A., Newbold, R.R., Rubin, B.S., Saili, K.S, Soto, A.M., Wang, H-S.,

vom Saal, F.S., 2013. Low dose effects of bisphenol A: an integrated review of in vitro, laboratory animal, and epidemiology studies. Endocr. Disruptors 1, 1. https://doi.org/10.4161/endo.26490.

Von der Ohe, P.C., Dulio, V., Slobodnik, J., De Deckere, E., Kühne, R., Ebert, R.-U., Ginebreda, A., De Cooman, W., Schüürmann, G., Brack, W., 2011. A new risk assessment approach for the prioritization of 500 classical and emerging organic microcontaminants as potential river basin specific pollutants under the European Water Framework Directive. Sci. Total Environ. 409 (11), 2064e2077. https://doi.org/10.1016/j.scitotenv.2011.01.054.

Wang, Q., Kelly, B.C., 2017. Occurrence, distribution and bioaccumulation behaviour of hydrophobic organic contaminants in a large-scale constructed wetland in Singapore. Chemosphere, 183, 257−265. https://doi.org/10.1016/j.chemosphere.2017.05.113.

Welander, U., Henrysson, T., 1998. Degradation of organic compounds in a municipal landfill leachate treated in a suspended-carrier biofilm process. Water Environ. Res. 70 (7), 1236–1241. https://doi.org/10.2175/106143098X123589.

Wenzel, A., Gahr, A., Niessner, R., 1999. TOC-removal and degradation of pollutants in leachate using a thin-film photoreactor. Water Res. 33 (4), 937–946. https://doi.org/10.1016/S0043-1354(98)00302-9.

Wignall, J.A., Muratov, E., Sedykh, A., Guyton, K.Z., Tropsha, A., Rusyn, I., Chiu, W.A., 2018. Conditional Toxicity Value (CTV) Predictor: n *in silico* approach for generating quantitative risk estimates for chemicals. Environ. Health Perspect. 126 (5), 057008. https://doi.org/10.1289/EHP2998.

Williams, A.J., Grulke, C.M., Edwards, J., McEachran, A.D., Mansouri, K., Baker, N.C., Patlewicz, G., Shah, I., Wambaugh, J.F., Judson, R.S., 2017. The CompTox Chemistry Dashboard: a community data resource for environmental chemistry. J. Cheminf. 9, 61. https://doi.org/10.1186/s13321-017-0247-6.

Wu, D., Huang, Z., Yang, K., Graham, D., Xie, B., 2015. Relationships between antibiotics and antibiotic resistance gene levels in municipal solid waste leachates in Shanghai, China. Environ. Sci. Technol. 49 (7), 4122–4128. https://doi.org/10.1021/es506081z.

Wu, D., Huang, X-H., Sun, J-Z., Graham, D.W., Xie, B., 2017. Antibiotic resistance genes and associated microbial community conditions in aging landfill systems. Environ. Sci. Technol. 51 (21), 12859−12867. https://doi.org/10.1021/acs.est.7b03797.

Xu, Y., Zhou, Y., Wang, D., Chen, S., Liu, J., Wang, Z., 2008. Occurrence and removal of organic micropollutants in the treatment of landfill leachate by combined anaerobic-membrane bioreactor technology. J. Environ. Sci. 20 (11), 1281–1287. https://doi.org/10.1016/S1001-0742(08)62222-6.

Ye, J., Chen, X., Chen, C., Bate, B., 2019. Emerging sustainable technologies for remediation of soils and groundwater in a municipal solid waste landfill site - a review. Chemosphere 227, 681–702. https://doi.org/10.1016/j.chemosphere.2019.04.053.

You, X., Wu, D., Wei, H., Xie, B., Lu, J., 2018. Fluoroquinolones and β-lactam antibiotics and antibiotic resistance genes in autumn leachates of seven major

municipal solid waste landfills in China. Environ. Int. 113, 162–169. https://doi.org/10.1016/j.envint.2018.02.002.

Yu, Y., Yu, Z., Chen, H., Han, Y., Xiangm, M., Chen, X., Ma, R., Wang, Z., 2019. Tetrabromobisphenol A: disposition, kinetics and toxicity in animals and humans. Environ. Pollut. 253, 909–917. https://doi.org/10.1016/j.envpol.2019.07.067.

Zeh, J.A., Bonilla, M.M., Adrian, A.J., Mesfin, S. Zeh, D.W., 2012. From father to son: transgenerational effect of tetracycline on sperm viability. Sci Rep. 2, 375. https://doi.org/10.1038/srep00375.

Zhou, X., Guo, J., Lin, K., Huang, K., Deng, J., 2013. Leaching characteristics of heavy metals and brominated flame retardants from waste printed circuit boards. J. Hazard. Mater. 246-247, 96–102. https://doi.org/10.1016/j.jhazmat.2012.11.065.

CHAPTER 3. PRIORITIZING LANDFILL POLLUTANTS TO TARGET WITH PHYTOREMEDIATION: A CASE STUDY IN SOUTHEASTERN WISCONSIN, USA

Abstract

Municipal solid waste landfills in the United States generate a considerable volume of leachate each year. Leachate management and treatment can be costly for landfill managers, especially regarding haul-and-treat offsite treatment approaches. On-site leachate treatment is an attractive option for leachate management, with phytoremediation offering a sustainable approach for mitigating contaminants within leachate. However, it is challenging to identify pollutants within leachate to target with phytoremediation systems. In the past, pollutant prioritization relied upon regulatory lists, which can be outdated and limited in scope, and leachate constituents reported in the literature, which range in relevancy for a particular site of interest. In the present study, a framework for comprehensive landfill leachate evaluation for phytotechnologies applications was developed and applied to landfill groundwater and leachate samples from two Wisconsin landfills. The framework combines non-targeted high-resolution mass spectrometry-based metabolomic data processing with a toxicity-based pollutant prioritization approach developed in the author's previous work (Rogers et al., 2021). Out of 6,699 total features, 242 compounds were putatively identified and prioritized using the framework. ToxPi scores for the 242 compounds ranged from 0.0296 (cimetidine) to 0.6430 (clotrimazole). The top 25 compounds with the greatest potential toxicity to human health and/or the environment included mainly pharmaceuticals (52%) and biocides (28%). The framework presented here represents a first step towards

standardized pollutant prioritization for phytotechnologies applications. Future work can expand on these efforts through 1) targeted analysis of putatively identified compounds using reference analytical standards, 2) incorporation of additional toxicity or physicochemical parameters as well as additional fragment (MS/MS) analysis and mass spectral reference libraries, and 3) through incorporation of modern data curation and machine learning approaches to automate toxicity data collection and standardize selection of toxicity model parameters.

3.1 Introduction

In the United States, nearly 150 million tons of municipal solid waste (MSW) are generated each year (U.S. EPA, 2024a and 2024b). Over 2,600 MSW landfills accept and manage this waste, according to regulations set forth by Subtitle D of the Resource Conservation and Recovery Act (RCRA) (U.S. EPA, 2024c). Amended three times since its establishment in 1976 (amendments occurring in 1984, 1992, and 1996), RCRA sets criteria for MSW landfill location, design, operation, monitoring, and closure that are enforceable by the Environmental Protection Agency (U.S. EPA, 2014, 2024c; 40 C.F.R. § 258, 1991). One of the key points in landfill design criteria is leachate management. Leachate is formed as water, mainly from precipitation, percolates through the waste material over time, leaching contaminants from the waste. Under RCRA, new MSW landfills are required to include liners and leachate collection systems to prevent off-site transport of potentially harmful leachate. Municipal solid waste landfills in the United States generate large volumes of leachate. For instance, in a recent review, Krause et al. (2023) reported 43 Ohio landfills to generate over 1.5 billion liters of leachate per year during 2017-2020, and a total of over 13.8 billion liters of leachate from 2010-2020.

Landfill operators are required by RCRA to manage leachate, whether by storage, recycling, or finally, on-site or off-site treatment and disposal (Jain et al., 2021). Leachate generation does not just occur while a landfill is in active operation but can continue for decades after closure, requiring continued leachate collection and treatment during post-closure care (Tolaymat and Carson, 2020). The treatment of leachate generated during the lifetime of a landfill poses a significant cost for landfill operators, with the most common option, hauling leachate off-site to a wastewater treatment plant, costing $0.01-$0.05 per liter ($0.05-$0.18 per gallon) of leachate (Jain et al., 2021). However, the practicability of the haul-and-treat approach is not certain. The dynamic nature of leachate chemical composition, coupled with increasing concentrations of chemicals of emerging concern, pose challenges for wastewater treatment plants, leading to additional fees for leachate treatment, and even outright rejection of leachate (Jain et al., 2021). Therefore, landfill operators must pivot to identify viable solutions for leachate treatment.

On-site treatment of leachate is an alternative option for leachate management. Among the types of on-site treatment, phytoremediation is a sustainable approach for mitigating contaminants within leachate (Jain et al., 2021; Jones et al., 2006; Justin et al., 2010; Lamb et al., 2014). Driven by evapotranspiration, phytoremediation implements specialized trees on the landscape to remediate inorganic and organic compounds from contaminated soils and water (McCutcheon and Schnoor, 2003). A combination of above- and belowground processes enables the uptake, degradation, sequestration, or microbial detoxification of the pollutants within phytoremediation systems (Kafle et al., 2022; McCutcheon and Schnoor, 2003). Phytoremediation is regarded as a cost-effective approach for leachate management, especially when high-yielding short rotation coppice

(SRC), which could generate a source of income through provision of biomass for bioenergy, are implemented (Pivato et al., 2018). A range in leachate application volume and removal rate of leachate constituents has been reported for phytoremediation systems. In a review of landfill leachate phytoremediation, Jones et al. (2006) found leachate application rates to commonly range from 500-1000 m^3 ha^{-1} yr^{-1} for SRC, with harvested SRC biomass contributing to removals of 50-70 kg N ha^{-1} yr^{-1}, and for heavy metals, 0.08 kg Cu ha^{-1} yr^{-1} and 0.08 Cd ha^{-1} yr^{-1}. Others have reported much higher application rates of 2600 m^3 ha^{-1} yr^{-1} for willows (Guidi Nissim et al., 2014) and up to 4950 m^3 ha^{-1} yr^{-1} for willows and poplars (Guidi Nissim et al., 2021). However, not all tree species respond similarly to the application of leachate. In the case of SRC, different species and genotypes exhibit different tolerances for leachate, emphasizing the importance of species/genotype selection in leachate phytoremediation system design. A variety of responses to leachate irrigation have been reported among SRC, including no significant differences in growth among willow varieties (Aronsson et al., 2010), significant differences in stress responses among willows (Dimitriou et al., 2006), enhanced growth under specific leachate dilutions for two willows and one poplar (Justin et al., 2010), enhanced growth for willows and diminished growth for poplars (Dimitriou and Aronsson, 2010), and broad variability in growth and biomass among poplar genotypes (Zalesny et al., 2007; Zalesny et al., 2009). Selection of trees that are not only able to tolerate the high ionic strength of leachate, but that also have elevated contaminant removal rates and the ability to maintain biomass production when irrigated with leachate, is a crucial component of successful leachate phytoremediation systems.

The success of the phytoremediation strategy often depends on the chemical and physical properties of the pollutants that influence their bioavailability as well as their fate and transport through the soil-plant-atmosphere continuum, such as hydrophobicity and volatility (Pilon-Smits, 2005). It has been challenging to identify pollutants within leachate to target with phytoremediation systems. Leachate is a complex matrix; its chemical composition varies over the age of a landfill, the type of waste it contains, its management operations, and the climate of the site (Wang and Qiao, 2024), all of which make historical data, and even data from other landfills, insufficient for determining priority contaminants for remediation at a given landfill. Often, phytoremediation studies focus on a small number of priority constituents within leachate, including ammonia, chloride, nitrogen, salts, and heavy metals (Aronsson et al., 2010; Jones et al., 2006; Justin et al., 2010; Dimitriou and Aronsson, 2010; Zalesny et al., 2008). Such an approach may neglect other potentially harmful contaminants that exist in the leachate, such as organic pollutants like pharmaceuticals, PFAS, personal care products, and other emerging contaminants of concern (Masoner et al., 2016, 2020; Tolaymat et al., 2023; Yu et al., 2020). One option for broadening the scope of leachate phytoremediation is to test for chemicals contained in landfill leachate regulatory lists (such as Appendices I and II, 40 C.F.R. § 258, 1991). These lists specify the chemical compounds that are required to be tested for under Subpart E of C.F.R. § 258, and as such represent priorities for remediation to fulfill EPA landfill regulations. However, these lists were established in 1991, and together contain 275 compounds, and therefore do not promote an up-to-date, comprehensive assessment of leachate composition.

Another option for identifying priority pollutants is to use available historical site data to select compounds of greatest concern, based on parameters such as concentration, persistence, or potential toxicity. However, while landfill-specific data are the most relevant option for identifying specific pollutants to target with phytoremediation systems, they also pose their own set of challenges. For instance, though online databases, such as GEMS on the Web (WI DNR, 2025c), provide publicly accessible landfill monitoring data, their information is limited by regulatory lists that stipulate which compounds are required to be monitored. Specifically, landfills are required to implement semiannual Detection Monitoring of all groundwater wells for the 62 chemicals identified in App. I of 40 C.F.R. § 258 (40 C.F.R. § 258.54). If a statistically significant higher concentration than the background level is detected for one or more compounds, a landfill operator must implement an Assessment Monitoring Program to annually monitor for the 213 compounds listed in App. II 40 C.F.R. § 258 (40 C.F.R. § 258.55). Therefore, unless Assessment Monitoring is being conducted, only the 62 chemicals from App. I are monitored by landfill operators, and thus, are reported in online landfill databases. Even Assessment Monitoring, which involves the additional 213 chemicals from App. II of 40 C.F.R. § 258, does not represent a complete evaluation of contaminants within landfill leachate, especially with regard to newer landfill contaminants such as pharmaceuticals, PFAS, and other contaminants of emerging concern (Masoner et al., 2016; Tolaymat et al., 2023; Yu et al., 2020). A comprehensive approach for site-specific identification and prioritization of landfill contaminants to target with phytoremediation systems is needed.

Rogers et al. (2021) developed a method for identifying and prioritizing landfill leachate pollutants using ecotoxicological data. In the approach, chemicals are prioritized with the Toxicological Prioritization Index (ToxPi; Marvel et al., 2018) using toxicity data gathered from publicly available toxicity databases. The approach was used to prioritize targeted landfill leachate compounds reported in the literature (Rogers et al., 2021) but has not been applied to an existing dataset generated from non-targeted chemical profiling analysis. The objectives of this study were to 1) apply the prioritization approach in combination with high-resolution mass spectrometry landfill data, and a high-resolution mass spectrometry data processing metabolomic platform, to putatively identify and prioritize landfill leachate chemicals, using a case study of landfills in Wisconsin, and 2) present a framework for comprehensive landfill leachate evaluation for phytotechnologies applications.

3.2 Materials and methods

3.2.1 Sample collection

Leachate and groundwater samples were collected from two MSW landfills in Southeastern Wisconsin, USA (Figure 3.1). The landfills each contain at least one phytoremediation buffer planting of hybrid *Populus* and *Salix* genotypes that are part of a regional phytotechnologies network (Zalesny et al., 2021). These plantings were established to serve multiple purposes, including runoff reduction, phytoremediation, groundwater recycling, and stormwater management. At the time of sample collection, the trees in these systems had just completed their third growing season. Contaminant profiles of the leachate and groundwater of these sites are largely unknown, especially regarding CECs and other novel pollutants. Exact locations and names of these landfills

are not reported here due to confidentiality agreements with landfill managers. Hereafter, the landfills will be referred to as Landfill A and Landfill B.

Landfill A is a closed MSW landfill that contains a groundwater intercept trench adjacent to a closed, unlined waste cell (Table 3.1). The cell was in operation from 1976-1986, serving a population of around 39,000 people from rural agricultural communities and one small city (information accessed prior to 2023 using SHWIMS on the Web; refer to WI DNR, 2025b). Groundwater under the waste cell flows toward a sump and is pumped to aboveground storage tanks. From there, it is transported off-site for processing at a Publicly-Owned Treatment Works. Groundwater samples were taken from this collection system for the present study.

Landfill B is a closed MSW zone of saturation landfill (Table 3.1), meaning groundwater flows through the buried waste, and is therefore termed "leachate." The landfill is listed by the Wisconsin DNR as a "post-reg" site, which indicates that waste disposal continued at the site after new sanitary landfill requirements were enacted by state law in 1972 (WI DNR, 2013). Landfill B was closed prior to 1992, and during its operation, it served a population of around 32,000 people from four towns and one small city (information accessed prior to 2023 using SHWIMS on the Web; refer to WI DNR, 2025b). Information on the specific years of operation of Landfill B is not publicly available. At Landfill B, leachate samples were collected directly from an underground collection well at the site using a polyvinylchloride bailer according to the sampling procedures outlined in the WI DNR Groundwater Sampling Field Manual [Karklins, 1996 (M. Prattke, personal communication, June 9, 2020)].

Physical triplicate samples of groundwater or leachate were collected at each landfill. All samples were collected in 500-mL polypropylene bottles (Thermo Fisher Scientific, Waltham, MA, USA) that were rinsed with methanol (HPLC Grade, Fisher Scientific, Pittsburgh, PA) prior to sample collection. Samples were immediately kept on dry ice and then stored at 0°C before being transported to the University of Missouri, Center for Agroforestry (Columbia, MO, USA), where they were stored at 0°C until further analysis. In addition to these samples, three blank control samples were prepared at the Center for Agroforestry by filling empty, pre-rinsed bottles with deionized water and storing them at 0°C with the rest of the samples until sample analysis.

3.2.2 Sample preparation

Prior to extraction, samples were removed from the freezer and allowed to reach room temperature. Samples were extracted by water:chloroform liquid-liquid extraction (LLE), within which 200 mL of each sample was extracted twice with 100 mL of chloroform (HPLC Grade, Fisher Scientific, Pittsburgh, PA). The chloroform fractions were combined and then evaporated to complete dryness with a BUCHI R110 Rotavapor rotary evaporator system (BUCHI Corporation, New Castle, DE). After evaporation, the extracts were resuspended with 5 mL of methanol (HPLC Grade, Fisher Scientific, Pittsburgh, PA). The suspended mixtures were then evaporated under a dry stream of nitrogen at room temperature (Organomation N-EVAP Evaporator, Model 112, Organomation, Berlin, MA). After nitrogen evaporation, extracts were resuspended with 1 mL of methanol.

3.2.3 LC-HRMS analysis

Extracts were analyzed using liquid chromatography coupled with high-resolution mass spectrometry (LC-HRMS) by the University of Missouri Center for Metabolomics (Columbia, MO, USA). Extracts were injected into a Waters Acquity ultra-high performance liquid chromatograph (UHPLC) (Waters Corporation, Milford, MA, USA) coupled with a Bruker maXis impact quadrupole-time-of-flight (Q-TOF) HRMS (Bruker Corporation, Billerica, MA, USA) for non-target analysis. Compounds were separated on a Waters C18 column (2.1×100 mm, BEH C18 column with 1.7-um particles). The mobile phases were A) 0.1% formic acid and B) 100% acetonitrile. The following elution gradient was employed at a column temperature of 60 °C and a flow rate of 0.56 mL min^{-1}: 95%:5% to 30%:70% eluent A:B from 0 – 30 min; 30%:70% to 5%:95% from 30 – 33 min; 5%:95% from 33 – 36 min.; 95%:5% from 36 – 40 min. The HRMS system was operated in both positive and negative electrospray ionization modes, with the nebulization gas pressure at 43.5 psi, dry gas of 12 L min^{-1}, dry temperature of 250 °C and a capillary voltage of 4000 V. Mass spectra data were collected across the range of 100–1,500 m/z (protonated $[M + H]^+$ and deprotonated $[M – H]^-$) and were auto-calibrated after data acquisition with sodium formate.

3.2.4 XCMS data processing

The (*.cdf) files containing raw ion chromatograms obtained from UHPLC-HRMS analysis were uploaded into the cloud-based XCMS Online platform, which performs processing of raw mass spectral data, including automatic peak detection (centWAVE detection), peak grouping, and nonlinear retention time correction/ alignment (Ordered Bijective Interpolated Warping; OBI-Warp alignment) across samples (Forsberg

et al., 2018; Gowda et al., 2014; Mahieu et al., 2016; Smith et al., 2006; Tautenhahn et al., 2012). XCMS Online enables identification of statistically significant differences in annotated features (chemicals) among sample sets through its built-in statistical analyses (Welch's t-test, Mann-Whitney t-test, paired parametric t-test, Wilcoxon signed-rank test, ANOVA, Kruskal-Wallis nonparametric test) (Gowda et al., 2014). Relative intensities of features are compared among sample groups using the selected statistical test, and the resulting p-values are reported in the Results Table in XCMS, which can then be used as search filtration criteria to identify features whose relative intensities are significantly different among sample groups (e.g., filter results for all features with $p < 0.05$) (Forsberg et al., 2018). In the present study, job parameters selected for XCMS data processing are listed in Table B1.

XCMS Online is fully integrated with the METLIN high-resolution mass spectral database, which currently contains mass spectral data for over one million molecular standards (Giera et al., 2024; Xue et al., 2020). METLIN enables library matching and robust annotation of peaks within sample ion chromatograms according to the mass to charge ratios, m/z (Gowda et al., 2014; Tautenhahn et al., 2012). The integrated XCMS Online-METLIN platform was used in the present study to perform putative identification of compounds within the groundwater and leachate samples according to the approaches outlined below, and in Figure 3.2.

3.2.4.1 Reverse searching

The first approach applied to the landfill data was a "reverse searching" approach, in which the data themselves guided the putative identification of candidate compounds. In other literature, this method is referred to as "untargeted" or "nontargeted" data

processing (Guo et al., 2024; Hemmer et al., 2020; Züllig et al., 2020). In such an approach, compound identification is not directed by a predetermined list of compounds to search for, but rather, by search criteria that enable identification of the most significant/disparate compounds among samples. Reverse searching is a broad, data-driven approach that generally provides a much larger number of candidate compounds than forward searching. Pairwise jobs comparing landfill samples against blank controls, as well as landfill samples against each other, were run in XCMS. For all pairwise comparisons, Welch's t-test was selected to statistically compare features among sample groups, as it is the recommended method for pairwise comparison of samples with unequal variances (Gowda et al., 2014). A series of searches were conducted within each pairwise job to identify candidate compounds. Search filters, including fold change, p-value, and retention time, were applied to identify candidate compounds with the characteristics of interest. Details of the applied search filters are presented in Table 3.2.

3.2.4.2 Forward searching

The opposite of reverse searching is "forward searching," which also may be known as "list-based searching" (Züllig et al., 2020). In this case, a list of compounds of interest is defined ahead of time, generally through a review of the literature, and is searched for within samples, whether by name or CASRN. Two lists of compounds were compiled and implemented during forward searching in the present study. The first list contained the top 150 landfill leachate contaminants identified via the literature review and prioritization of Rogers et al. (2021). The second list contained compounds included in Appendices I and II of the Code of Federal Regulations Title 40, Part 258: Criteria for Municipal Solid Waste Landfills (n = 275) (Appendix I to 40 C.F.R. § 258; Appendix II

to 40 C.F.R. § 258). Compounds on both lists were searched for by name within the pairwise XCMS job Results Tables. These searches served to expand the scope of the nontargeted searches by pinpointing those chemicals that had previously been identified in landfill leachate, while also enabling investigation of what compounds would have been found if a targeted search based strictly on regulatory lists had been performed. Like within the Reverse Searching approach, data from the identified candidates (fold change, p-value, direction of fold change, median retention time, maximum intensity, mean intensity for each dataset, adducts, peak group, ppm, putative name, and METLIN identification number) were extracted from the XCMS Results Tables.

3.2.5 Contaminant prioritization

The features putatively identified through forward and reverse searching, which met the criteria in Table 3.2, were compiled into a comprehensive compound list, and duplicates were removed. CASRN for the compounds were identified using PubChem. For those compounds with available CASRN, toxicity data were collected from freely available toxicity databases according to the methods of Rogers et al. (2021). Briefly, gathered data included EC50 (ECOTOX Database; Olker et al., 2022), AC50 and percentage of active assays (ToxCast database; Richard et al., 2016), and predicted values of RfD, OSF, NO(A)EL, CPV, BMDL, and BMD (Conditional Toxicity Value Predictor, CTV Predictor; Wignall et al., 2018). Toxicity databases and associated parameters gathered for the current study are described in further detail in Table B2. Compounds that had available toxicity data from at least two of the three toxicity databases were then prioritized according to potential overall toxicity to human health and/or the environment using the ToxPi Framework (Marvel et al., 2018; Reif et al., 2013). All sources of toxicity

data were given equal weight in ToxPi, following the General Prioritization Scheme of Rogers et al. (2021). For prioritized compounds, relative intensity information was compiled from multigroup jobs in XCMS Online (Landfill A vs. Landfill B vs. Control, positive and negative ion mode). For multigroup jobs, the same retention time range as that applied for pairwise jobs was used ($5 \leq RT \leq 35$).

3.3 Results

3.3.1 Reverse searching

The first step of the comprehensive landfill data processing approach was data-driven reverse searching of HRMS data using XCMS Online (Figure 3.2). Table 3.2 describes the search filters applied in pairwise jobs in XCMS Online, which included landfill samples vs. controls and landfill samples vs. each other, in both positive and negative ion mode. A total of 6,699 features were identified across all pairwise jobs. Of these, there were 4,256 METLIN candidates that met search criteria (≤ 5 METLIN candidates that could be differentiated based on ppm for a particular feature, all candidates ≤ 5 ppm). Landfill B samples (leachate) had a total of 6,293 upregulated features with 4,032 METLIN candidates across all pairwise jobs, while Landfill A samples (groundwater) had a total of 406 upregulated features with 224 METLIN candidates. These trends can be seen in the representative cloud plots of Figure 3.3 (Patti et al., 2013). In pairwise comparisons between Landfill A and B, Landfill B (shown in green) had many more highly significant features ($p < 0.0001$ and fold > 1.5) than Landfill A (shown in red). In particular, Landfill B exhibited 97% of all highly significant features in positive ion mode (Figure 3.3A), and 98% of all highly significant features in

negative ion mode (Figure 3.3B). Differences in chemical space among the samples from the two landfills can also be seen in Figure 3.4.

3.3.2 Forward searching

The next step of the comprehensive landfill data processing approach was list-based forward searching of HRMS data using XCMS Online (Figure 3.2). First, a list of 150 landfill leachate compounds identified in a literature review and prioritized based on toxicity (Rogers et al., 2021) were searched for in the datasets of the present study. Of these 150 compounds, 19 were putatively identified in the samples from Landfill A and B using XCMS Online (Table 3.3). The relative intensities of 17 of the 19 compounds were much higher in Landfill B samples than Landfill A and Control samples, with the folds of upregulated compounds in Landfill B samples ranging from 1.7 (triclosan) to 65 (clotrimazole), compared to Landfill A. Two compounds, Fluoranthene and Pyrene, both putative candidates for the same feature ID (m/z of 203.084749 and RT of 10.8190 min) exhibited similar intensities among Landfill A (46,911 ± 4,228) and B samples (57,600 ± 2,714).

Then, a list of 275 compounds compiled from two regulatory lists (Appendix I and II, 40 C.F.R § 258) was searched for in the Landfill A and B datasets. Eleven of these compounds were putatively identified using XCMS Online (Table 3.4). Again, besides pyrene and fluoranthene, all other compounds had much higher relative intensities in Landfill B samples than Landfill A samples. Folds for upregulated Landfill B compounds (compared to Landfill A) ranged from 4.2 (indeno[1,2,3-cd]pyrene and benzo[ghi]perylene) to 66 (diphenylamine).

3.3.3 Toxicity prioritization

The final step of the comprehensive landfill data processing approach was to prioritize putatively identified compounds with ToxPi based on potential toxicity to humans and/or the environment (Figure 3.2). In total, after removing duplicate compounds, there were 1,321 METLIN candidates with available CASRN across all pairwise jobs. Toxicity data were collected for these compounds from ECOTOX (Olker et al., 2022), ToxCast (Richard et al., 2016), and the CTV Predictor (Wignall et al., 2018). A majority of compounds (81.6%) had low toxicity data availability, with 75.3% of compounds having available data in only one of the three databases, and 7.3% of compounds that did not have available toxicity data in any of the databases (Figure 3.5). 18.4% of compounds (242 total) had available toxicity data from two or all three of the databases and were prioritized with ToxPi.

All prioritized landfill compounds and their associated ToxPi scores and ranks are listed in Table B3. Considering all 242 prioritized compounds, a range in fold changes were observed among the samples. Upregulated features in Landfill A samples with the largest fold changes were putatively identified as benzofuran (fold: 14.9, A vs. Control), clopirac (fold: 10.2, A vs. Control), and bromodiphenhydramine (fold: 8.9, A vs. Control). On the other hand, upregulated features in Landfill B samples had much larger fold changes, the largest being putatively identified as 9-hydroxyrisperidone (fold: 1025.8, B vs. Control; fold: 845.4, B vs. A), benzofuran (fold: 458.8, B vs. Control; fold: 30.9, B vs. A), and D-leucine (fold: 401.5, B vs. Control; fold: 374.8, B vs. A). Overall, the highest relative intensities were demonstrated for potassium acetate (10,972,971 ± 403,947; Landfill B; ToxPi rank: 186), benzofuran (5,454,660 ± 118,385; Landfill B; ToxPi rank:

232), tetraethylammonium chloride (2,341,099 ± 196,496; Landfill B; ToxPi rank: 158), 9-hydroxyrisperidone (965,801 ± 54,578, Landfill B, ToxPi rank: 86), and D-leucine (476,451 ± 58,782, Landfill B, ToxPi rank: 240).

ToxPi scores for the 242 compounds ranged from 0.0296 (cimetidine) to 0.6430 (clotrimazole). The top 25 compounds from ToxPi analysis that are identified as potentially harmful to human health and/or the environment are listed in Table 3.5. Relative intensities for these compounds (according to XCMS Online multigroup jobs) were much higher in Landfill B than Landfill A samples for a majority of the top 25 compounds. For landfill B, highest relative intensities were exhibited by features putatively identified as triparanol (126,507 ± 12,091) clotrimazole (118,848 ± 8,147), and fluoxymesterone (19,749 ± 1,831). For landfill A, highest relative intensities were exhibited by features putatively identified as aldicarb (4,081 ± 268), ipecac (1,936 ± 20), and gliotoxin (1,986 ± 259). Uses for the top 25 compounds include antifungal agents, pharmaceuticals, pesticides, insecticides, amebicides, and reagents, with a few compounds resulting from burning fossil fuels (Table 3.6).

Hierarchical cluster analysis was performed within ToxPi (Marvel et al., 2018) to identify groupings among the 242 compounds based on their toxicity profiles (Figure 3.6). Six clusters were identified in the analysis (Figures 3.6B and 3.7). Clusters A and B were the smallest clusters, containing 17 and 6 compounds, respectively, while also exhibiting the highest toxicity scores among all clusters; each had an average toxicity score of 0.48, while the next highest average was 0.32 for cluster C (Figures 3.6B and 3.7). The ranks of compounds within clusters A and B were also high, with ranks ranging from 1 to 43 in cluster A and 5 to 25 in cluster B. Ranks in other clusters had larger

ranges, ranging from 13 to 149 in cluster C, 24 to 206 in cluster D, 21 to 205 in cluster E, and 130 to 242 in cluster F. Representative ToxPi toxicity profiles for each hierarchical cluster are depicted in Figure 3.7. Cluster A is characterized by relatively high values (scaled) for all toxicity parameters from the CTV Predictor, including cluster-level means greater than overall means for all six CTV Predictor parameters (BMD, BMDL, CPV, NO(A)EL, OSF, and RfD). Cluster B is characterized by the highest values (scaled) for EC50, BMD, BMDL, NO(A)EL, and RfD among all clusters. Cluster C contains compounds with the highest values of percent active assays, high values (scaled) of BMD and BMDL, and moderate values of NO(A)EL and RfD. Cluster D had the highest average (scaled) AC50 and moderate values of percent active assays, BMD, BMDL, NO(A)EL, and RfD. Cluster E had moderate values for all categories except CPV and OSF, which were low. Cluster F exhibited the lowest average values for all categories among all clusters except EC50.

3.4 Discussion

The potential for landfill pollutant prioritization by the comprehensive approach reported here was demonstrated in the present case study on landfill leachate and groundwater samples. Through a multistep process consisting of non-targeted HRMS data acquisition, data-driven reverse searching and list-based forward searching of HRMS data, and finally, prioritization of putatively identified compounds (Figure 3.2), a total of 242 compounds were prioritized. Ranked according to the general prioritization scheme reported in Rogers et al. (2021) which builds upon the methods of Danforth et al. (2020), the top 25 compounds with the greatest potential toxicity to human health and/or the environment included mainly pharmaceuticals (52%) and biocides (28%) (Table 3.6).

These classes of compounds have been identified in other recent landfill scientific literature (Clarke et al., 2015; Kumar et al., 2023; Masoner et al., 2016, 2020; Ochs et al., 2024; Yu et al., 2020). For example, in a scoping review on persistent organic pollutants in Canadian and US landfills, Ochs et al. (2024) reported pesticides to be one of the main components of the contaminant profile of MSW landfills, with pesticides at detectable levels reported for five of 12 Canadian provinces at which landfill sampling occurred. These results are corroborated by Clarke et al. (2015), who reported concentrations of the insecticide DEET (diethyltoluamide) ranging from 6900-143000 ngL^{-1} for leachate samples collected from five United States landfills. The same study also identified pharmaceuticals including carbamazepine, primidone, and gemfibrozil in the leachate samples (Clarke et al., 2015). Masoner et al. (2016) similarly found that out of 190 contaminants of emerging concern analyzed in leachate samples collected from 22 US landfills, a majority of those detected were pharmaceuticals (54% of detections). Contaminants of emerging concern in landfill leachate, including pesticides and pharmaceutical compounds, can pose challenges for conventional means of leachate treatment (Kumar et al., 2023) and may require exploration of integrated, multi-stage leachate treatment approaches. The phytoremediation of such emerging compounds has received increasing study over the past few decades, with the utility of a variety of plant species being tested for remediation of pesticides (Eevers et al., 2017), pharmaceuticals (Carvalho et al., 2014) and antibiotics (McCorquodale-Bauer et al., 2023). Remediation of these classes of pollutants within landfill leachate, specifically, remains an active avenue for growth for future phytoremediation research.

Not surprisingly, more compounds were detected, and with higher relative intensities, in landfill leachate samples than groundwater samples. The highest relative intensities were demonstrated for potassium acetate (variety of uses in the chemical industry, textile processing industry, anti-freeze agents, and pharmaceuticals), benzofuran (formed by processing coal into coal oil, which is then used in the manufacture of paints and varnishes), tetraethylammonium chloride (pharmacological research agent), 9-hydroxyrisperidone (pharmaceutical), and D-leucine (bacterial metabolite; pharmacological research agent). Targeted analysis will be required to confirm the identity and perform absolute quantification of these signals within the mass spectral data. It is important to note that the results presented in the current study represent a single snapshot in time of leachate and groundwater composition at two individual sites. Landfill leachate composition is complex, varying according to landfill age, waste composition, and season (Wang and Qiao, 2024). The samples analyzed in the present study are a starting point for MSW landfill pollutant prioritization upon which other studies can build. Given the considerable variability in leachate chemical composition, the most effective approach for pollutant identification and prioritization will involve sampling at the particular site of interest, rather than relying solely upon regulatory lists such as Appendices I and II of 40 C.F.R. § 258, or on leachate pollutants reported in the literature. Further, conducting sampling events at multiple timepoints will enable researchers to investigate the seasonality of pollutant presence and abundance, important factors to consider in the design of pollutant remediation systems, such as phytoremediation systems. On the other hand, in order to develop a robust database of the current state of landfill contaminants, sampling across a variety of landfills with varying

characteristics, such as geographic location, climatic conditions, landfill age, waste composition, and landfill engineering and design features, will be necessary. A comprehensive database of landfill leachate chemical composition would enhance knowledge of leachate characteristics and could inform decision-making on its treatment and management.

Based on complete-linkage hierarchical cluster analysis performed in ToxPi, six clusters were identified for the 242 prioritized compounds, with clusters defined according to similarities in ToxPi profile components among compounds within a cluster. Clusters A and B contained compounds of consistently higher rank (greater potential toxicity) than the other four clusters (Figure 3.7) and were defined by overall high (scaled) values for all parameters from the CTV Predictor (cluster A), and as well as high (scaled) values of EC50 and a subset of parameters from the CTV Predictor (cluster B). Consistently low values across all toxicity parameters led to predictably low ToxPi scores and toxicity rankings, demonstrated by cluster F. Hierarchical clustering analysis enables visualization of patterns in toxicity data among compounds and could be particularly useful when presenting results to landfill site managers to aid in decision-making on compounds to target with remediation activities. Identified clusters present an additional layer of information beyond ToxPi scores and rankings that could enable researchers and landfill managers to visually inspect the toxicity criteria and associated slices for each prioritized compound, and to make informed decisions on which pollutants to dedicate resources to (e.g., targeted analysis, remediation strategies) in order to meet the needs of the site manager and the community.

Future work can expand upon and improve these efforts through targeted analysis of putatively identified and prioritized compounds using reference analytical standards. This work is limited in that the data it presents are nontargeted, relying on accurate mass-to-charge ratios in order to match compound peaks with putative identities in the METLIN mass spectral reference library (Gowda et al., 2014). The steps outlined here allow for narrowing down potential chemicals to purchase analytical reference standards for and conduct targeted analysis of. Targeted analysis is a critical final step in the pollutant prioritization process that enables compound identify confirmation and absolute quantification. Further studies could also incorporate additional toxicity or physicochemical parameters related to human exposure into prioritization approaches. For example, Ekpe et al. (2025) included parameters related to the environmental fate and transport potential of pollutants, including n-octanol-water partition coefficient (log K_{OW}), water solubility, biodegradation half-life, and soil organic carbon-water partition coefficient (K_{OC}) in their ToxPi prioritization of groundwater contaminants. In the current study, compounds which did not have available toxicity data from at least two of the three toxicity databases are biased against, as they were not included for prioritization. Incorporating a broader range of criteria than those provided by the three databases here could reduce this bias. Similarly, mass spectral reference libraries beyond XCMS-METLIN could also expand the capacity for landfill pollutant identification and prioritization, with a range of both publicly available libraries and commercial libraries (Bittremieux et al., 2022). In addition, incorporating other analytical techniques for sample preparation, such as solid-phase microextraction, thermal desorption, and solid-phase extraction, along with gas chromatography paired with mass spectrometry (GC-

MS) for mass spectral analysis, would enable analysis of volatile contaminants in leachate samples that are not captured with the current approach. Finally, the availability of highly specialized software packages for automated data curation, coupled with advancements in statistical computation and machine learning, could streamline the time-consuming process of toxicity data collection and standardize ToxPi model design. De Vries (2024) recently demonstrated the utility of a specialized R package, ECOTOXr, for automated, transparent, and reproducible extraction of toxicity data from the ECOTOX database (Olker et al., 2022). In another recent study, Ekpe et al. (2025) reported the implementation of random forest machine learning algorithms to select optimized model weighting parameters for toxicity criteria within ToxPi prioritization schemes. Both types of technology could enable implementation of streamlined, efficient, and non-biased prioritization of landfill contaminants that can inform landfill management and phytoremediation planning.

The success of the phytoremediation strategy often depends on the chemical and physical properties of the pollutants that are targeted for remediation (Pilon-Smits, 2005). Properties that influence the bioavailability of pollutants in phytoremediation systems, such as log K_{OW} and Henry's law constant, determine the degree to which phytoremediation can be effective for remediating the pollutants. The unbiased approach presented here represents a first step in pollutant prioritization for phytoremediation. Once priority compounds are identified according to their potential toxicity, their bioavailabilities can be investigated, and those that are most suited to phytoremediation (moderate to high solubility based on log K_{OW} and low to moderate volatility based on Henry's law constant values) can be selected for targeting with remediation. Management

strategies to enhance the bioavailability of the selected compounds, including plant selection (e.g., hyperaccumulators, those with extensive root systems) and agronomic practices (e.g., addition of soil amendments, beneficial microbes) can then be implemented to further enhance the efficacy of the phytoremediation system.

3.5 Conclusion

The selection of priority pollutants is a challenging aspect of phytoremediation system design, particularly when the media to be remediated have complex chemical compositions, such as landfill leachate. The novel approach presented here incorporates list-based and data-based putative compound identification with toxicity-based prioritization to remove ambiguity and improve standardization of pollutant prioritization. Applying data-based reverse searching of non-targeted HRMS data enables a more current, comprehensive analysis of leachate composition than searching for compounds using lists derived from the literature or regulatory lists alone could provide. However, list-based forward searching is complementary to reverse searching in that it ensures priority compounds according to federal and state regulations are accounted for, while providing a means for comparing the outcomes of the two types of searches. The final step of ranking identified compounds according to potential toxicity to human health and/or the environment allows for standardized, quantitative evaluation and selection of priority pollutants. Using the comprehensive approach, the present study putatively identified and prioritized 242 compounds in a case study on landfill leachate and groundwater samples collected at two Wisconsin landfills. Of the top 25 compounds, a majority were pharmaceuticals and pesticides/herbicides/fungicides, which represent newer classes of landfill leachate compounds and expanding avenues for leachate

phytoremediation. In total, 1,321 features were originally putatively identified in the samples using XCMS Online, however, only 18% (242 compounds) had available toxicity data from at least two of the three toxicity databases implemented here (ECOTOX, ToxCast, and CTV Predictor). Further work can expand upon these efforts by incorporating additional toxicity databases, and chemical properties related to environmental fate, transport, and exposure, into the toxicity prioritization model. Doing so would serve to increase the number of compounds that are able to be prioritized and would improve the meaningfulness of ToxPi rankings. Overall, the pollutant prioritization framework developed here is suitable for identifying pollutants to target with landfill leachate phytoremediation systems, but it is also more broadly applicable to pollutant prioritization across the range of phytotechnologies and their diverse site types.

Table 3.1. Landfill characteristics of two landfills in Southeastern Wisconsin, USA, where samples were collected for the present study.

Landfill Characteristics[a]	Landfill A	Landfill B
Site Description	Closed municipal solid waste landfill	Closed municipal solid waste zone of saturation landfill
Population served	~39,000	~32,000
Population demographics	Mixture of rural towns and one small city	Mixture of rural towns and one small city
Hectares	6.9	18.6
Types of waste handled[b]	Demolition; fly ash; garbage; noncombustible; refuse; wood matter	Demolition; garbage; noncombustible; refuse; wood matter
Operational timeframe	1976-1986	Specific timeframe is unknown. Landfill is classified as a "post-reg" site[c]. Waste disposal continued after 1972 but prior to the issuance of a waste disposal license.
Type of sample collected for present study	Contaminated Groundwater	Leachate

[a] Information on both landfills was gathered from a variety of sources, including SHWIMS on the Web (WI DNR, 2025b), BRRTS on the Web (WI DNR, 2025a), and the Historic Registry of Waste Disposal Sites Spreadsheet (WI DNR, 2013).
[b] Classified according to the Wisconsin Department of Natural Resources Waste Type Activity Codes (WI DNR, 2024).
[c] WI DNR (2013)

Table 3.2. XCMS Online pairwise job parameters and feature information for groundwater and leachate samples collected from two landfills in Southeastern Wisconsin. After duplicates were removed, there were 1,321 total METLIN candidates.

XCMS Pairwise Job	Ion Mode	Fold	p-value	Retention Time (rt)	Features Identified	METLIN Candidates*
Landfill A vs Control	+	≥ 2	$p \leq 0.05$	$5 \leq rt \leq 35$	256	148
Landfill A vs Control	-	≥ 2	$p \leq 0.05$	$5 \leq rt \leq 35$	39	10
Landfill B vs Control	+	≥ 5	$p \leq 0.05$	$5 \leq rt \leq 35$	2,453	1,604
Landfill B vs Control	-	≥ 5	$p \leq 0.05$	$5 \leq rt \leq 35$	1,009	511
Landfill A vs Landfill B	+	≥ 2	$p \leq 0.05$	$5 \leq rt \leq 35$	90	65
Landfill A vs Landfill B	-	≥ 2	$p \leq 0.05$	$5 \leq rt \leq 35$	21	1
Landfill B vs Landfill A	+	≥ 5	$p \leq 0.05$	$5 \leq rt \leq 35$	1,975	1,457
Landfill B vs Landfill A	-	≥ 5	$p \leq 0.05$	$5 \leq rt \leq 35$	856	460
				Totals	**6,699**	**4,256**

*Candidates were selected that had the lowest ppm values (≤5 ppm). If there were more than five METLIN candidates per feature, those with the lowest ppm values were selected for further analysis. Features with more than five METLIN candidates that couldn't be separated by ppm were not included in further analyses in order to minimize uncertainties.

Table 3.3. Landfill leachate compounds from the literature review of Rogers et al. (2021) that were putatively identified in the present study. The top 150 compounds in Rogers et al. (2021) according to toxicity prioritization were searched for in groundwater and leachate samples using XCMS Online. Values are mean intensity ± standard error.

Compound	CASRN	m/z	rt (min)	Landfill A	Landfill B	Control	Toxicity Rank in Rogers et al. (2021)	Toxicity Rank in Current Study
Clotrimazole	23593-75-1	367.0976	22.1495	1,820 ± 83	118,848 ± 8,147	1,064 ± 347	4	1
Oxytetracycline	79-57-2	477.1734	22.1745	1,197 ± 91	12,833 ± 5,424	1,101 ± 68	5	2
Indeno[1,2,3-cd]pyrene	193-39-5	299.0835	15.4754	1,338 ± 58	5,607 ± 560	1,114 ± 36	7	3
Benzo[ghi]perylene	191-24-2	299.0835	15.4754	1,338 ± 58	5,607 ± 560	1,114 ± 36	16	4
Benz[a]anthracene	56-55-3	227.0855	10.0315	763 ± 13	4,410 ± 467	643 ± 34	23	21
Tebuconazole	80443-41-0	325.1796	25.3798	952 ± 152	2,382 ± 228	772 ± 188	37	39
Ofloxacin	82419-36-1	362.1512	18.9000	661 ± 9	1,245 ± 195	539 ± 16	39	26
Triclosan	3380-34-5	288.9574	11.1365	592 ± 9	978 ± 42	490 ± 42	49	69
Perfluorooctanesulfonic acid	1763-23-1	498.9318	24.3259	2,089 ± 123	25,933 ± 492	1,503 ± 17	58	71
Ketamine	6740-88-1	238.1002	18.7389	1,348 ± 40	14,143 ± 940	1,206 ± 21	60	68
Ametryn	834-12-8	245.1545	18.1357	896 ± 57	7,748 ± 1,436	716 ± 12	84	66
Fluoranthene	206-44-0	203.0847	10.8190	46,911 ± 4,228	57,600 ± 2,714	14,974 ± 604	86	111
Perfluorooctanoic acid	335-67-1	452.9356	6.8660	691 ± 53	9,956 ± 142	649 ± 20	99	99
Fluconazole	86386-73-4	307.1116	9.1282	834 ± 61	4,416 ± 551	628 ± 63	109	75
Sulfadimidine (Sulfamethazine)	57-68-1	317.0458	16.6538	592.39 ± 9	2,884.83 ± 119	577 ± 38	119	81
Dibenzofuran	132-64-9	169.0640	8.1942	1,853 ± 91	3,242 ± 908	895 ± 133	129	146
Pyrene	129-00-0	203.0847	10.8190	46,911 ± 4,228	57,600 ± 2,714	14,974 ± 604	123	101
Sulfaguanidine	57-67-0	237.0414	10.0820	1,325 ± 54	35,547 ± 4,551	1,187 ± 116	137	78
Phenanthrene	85-01-8	179.0853	7.52345	4,299 ± 634	25,791 ± 6,405	1,763 ± 35	139	171

Table 3.4. Landfill leachate compounds from regulatory lists that were putatively identified in the present study. Landfill leachate compounds included in two regulatory lists (Appendices I and II, 40 C.F.R. § 258) were searched for in groundwater and leachate samples using XCMS Online. Values are mean intensity ± standard error.

Compound	CASRN	m/z	rt (min)	Landfill A	Landfill B	Control	Toxicity Rank
Indeno[1,2,3-cd]pyrene	193-39-5	299.0835	15.4754	1,338 ± 58	5,607 ± 560	1,114 ± 36	3
Benzo[ghi]perylene	191-24-2	299.0835	15.4754	1,338 ± 58	5,607 ± 560	1,114 ± 36	4
Disulfoton	298-04-4	292.0626	15.7600	613 ± 16	3,189 ± 1,084	484 ± 44	5
Parathion	56-38-2	314.0218	24.2807	601 ± 32	3,040 ± 357	581± 90	10
Benz[a]anthracene	56-55-3	227.0855	10.0315	763 ± 13	4,410 ± 467	643 ± 34	21
Pyrene	129-00-0	203.0847	10.8190	46,911 ± 4,228	57,600 ± 2,714	14,974 ± 605	101
Fluoranthene	206-44-0	203.0847	10.8190	46,911 ± 4,228	57,600 ± 2,714	14,974 ± 605	111
4-Biphenylamine	92-67-1	170.0969	17.8400	1,180 ± 250	77,332 ± 8,307	1,088 ± 3	142
Chrysene	218-01-9	227.0855	10.0200	763 ± 13	4,410 ± 467	643 ± 34	147
Diphenylamine	122-39-4	170.0970	17.8703	1,180 ± 250	77,332 ± 8,307	1,088 ± 5	161
Fluorene	86-73-7	167.0862	14.2185	3,134 ± 142	43,687 ± 644	2,117± 256	215

Table 3.5. Top 25 compounds putatively identified in groundwater and leachate samples from two landfills in Southeastern Wisconsin using XCMS Online. Ranks and ToxPi scores were calculated using the ToxPi software. Values are mean intensity ± standard error.

Rank	ToxPi Score	Name	CASRN	m/z	rt (min)	Landfill A	Landfill B	Control
1	0.6430	Clotrimazole[a]	23593-75-1	367.0976	22.1495	1,820 ± 83	118,848 ± 8,147	1,064 ± 347
2	0.6252	Oxytetracycline[a]	79-57-2	477.1734	22.1745	1,197 ± 91	12,833 ± 5,424	1,101 ± 68
3	0.5921	Indeno[1,2,3-cd]pyrene[a,b]	193-39-5	299.0835	15.4754	1,338 ± 58	5,607 ± 560	1,114 ± 36
4	0.5627	Benzo[ghi]perylene[a,b]	191-24-2	299.0835	15.4754	1,338 ± 58	5,607 ± 560	1,114 ± 36
5	0.5534	Disulfoton[b]	298-04-4	292.0626	15.7600	613 ± 16	3,189 ± 1,084	484 ± 44
6	0.5225	Cyproterone acetate	427-51-0	451.1447	19.7439	1,352 ± 149	2,897 ± 493	1,278 ± 37
7	0.4997	Flurandrenolide	1524-88-5	459.2157	23.6126	1,003 ± 278	4,591 ± 604	647 ± 98
8	0.4807	Canrenone	976-71-6	341.2101	19.6276	1,282 ± 148	9,491 ± 837	1,051 ± 75
9	0.4759	Gliotoxin	67-99-2	344.0741	7.2983	1,986 ± 259	2,140 ± 564	968 ± 283
10	0.4740	Parathion[b]	56-38-2	314.0218	24.2807	601 ± 32	3,040 ± 357	581 ± 90
11	0.4734	1-Amino-2,4-dibromoanthraquinone	81-49-2	396.9197	6.8703	484 ± 13	4,191 ± 101	421 ± 45
12	0.4652	Fluoxymesterone	76-43-7	354.2437	16.8723	1,134 ± 107	19,749 ± 1,831	1,337 ± 251
13	0.4609	Clomipramine	303-49-1	315.1626	14.3409	1,366 ± 26	8,314 ± 567	1,172 ± 460
14	0.4430	Ajmaline	4360-12-7	365.1618	11.0470	777 ± 78	2,477 ± 285	429 ± 37
15	0.4424	Trequinsin hydrochloride	78416-81-6	423.2395	8.0521	922 ± 42	8,551 ± 627	772 ± 49
16	0.4370	Phenolphthalein	77-09-8	336.1235	19.3825	1,143 ± 42	6,931 ± 851	818 ± 16
17	0.4367	Ipecac (Emetine)	483-18-1	498.3300	12.3534	1,936 ± 20	18,424 ± 2,834	2,008 ± 82
18	0.4339	Alprazolam	28981-97-7	309.0905	16.1443	1,091 ± 35	7,254 ± 339	1,614 ± 778
19	0.4305	Triparanol	78-41-1	438.2192	22.1533	1,278 ± 42	126,507 ± 12,091	1,110 ± 29
20	0.4304	Diniconazole	83657-24-3	364.0388	8.0088	709 ± 71	8,378 ± 379	636 ± 22
21	0.4281	Benz[a]anthracene[a,b]	56-55-3	227.0855	10.0315	763 ± 13	4,410 ± 467	643 ± 34
22	0.4260	Chlorprothixene	113-59-7	338.0747	10.1706	455 ± 28	4,869 ± 794	286 ± 19
23	0.4250	Aldicarb	116-06-3	191.0851	8.3289	4,081 ± 268	8,995 ± 1,251	1,360 ± 217
24	0.4207	Hydroxyzine	68-88-2	373.1685	17.4235	1,462 ± 52	3,779 ± 502	1,027 ± 88
25	0.4207	Fenitrothion	122-14-5	278.0249	15.7562	1,010 ± 53	13,287 ± 650	828 ± 52

[a] Reported in Rogers et al. (2021) literature review on landfill leachate contaminants.
[b] Included in Appendix II, 40 C.F.R. § 258.

Table 3.6. Uses of top 25 compounds putatively identified in groundwater and leachate samples from two landfills in Southeastern Wisconsin using XCMS Online. Ranks and ToxPi scores were calculated using the ToxPi software.

Rank	ToxPi Score	Name	CASRN	Use[c]
1	0.6430	Clotrimazole[a]	23593-75-1	Pharmaceutical
2	0.6252	Oxytetracycline[a]	79-57-2	Pharmaceutical
3	0.5921	Indeno[1,2,3-cd]pyrene[a,b]	193-39-5	Polycyclic aromatic hydrocarbon; formed during burning of fossil fuels
4	0.5627	Benzo[ghi]perylene[a,b]	191-24-2	Polycyclic aromatic hydrocarbon; formed during burning of fossil fuels
5	0.5534	Disulfoton[b]	298-04-4	Pesticide
6	0.5225	Cyproterone acetate	427-51-0	Pharmaceutical
7	0.4997	Flurandrenolide	1524-88-5	Pharmaceutical
8	0.4807	Canrenone	976-71-6	Pharmaceutical
9	0.4759	Gliotoxin	67-99-2	Mycotoxin, antifungal agent
10	0.4740	Parathion[b]	56-38-2	Insecticide
11	0.4734	1-Amino-2,4-dibromoanthraquinone	81-49-2	Intermediate in the production of anthraquinone dyes (electroplating, pulp and paper processing, farming-pesticides)
12	0.4652	Fluoxymesterone	76-43-7	Pharmaceutical
13	0.4609	Clomipramine	303-49-1	Antidepressant
14	0.4430	Ajmaline	4360-12-7	Pharmaceutical
15	0.4424	Trequinsin hydrochloride	78416-81-6	Research pharmaceutical
16	0.4370	Phenolphthalein	77-09-8	Laboratory reagent; medication; home maintenance
17	0.4367	Ipecac (Emetine)	483-18-1	Amebicide; antinematodal agent
18	0.4339	Alprazolam	28981-97-7	Medication
19	0.4305	Triparanol	78-41-1	Pharmaceutical
20	0.4304	Diniconazole	83657-24-3	Fungicide
21	0.4281	Benz[a]anthracene[a,b]	56-55-3	Polycyclic aromatic hydrocarbon; found in fossil fuels, formed during burning of coal, oil, gas, wood, garbage
22	0.4260	Chlorprothixene	113-59-7	Pharmaceutical
23	0.4250	Aldicarb	116-06-3	Carbamate pesticide
24	0.4207	Hydroxyzine	68-88-2	Pharmaceutical
25	0.4207	Fenitrothion	122-14-5	Insecticide

[a] Reported in Rogers et al. (2021) literature review on landfill leachate contaminants.
[b] Included in Appendix II, 40 C.F.R. § 258.
[c] According to PubChem (https://pubchem.ncbi.nlm.nih.gov/).

Figure 3.1. Location of two landfill sites in Southeastern Wisconsin, USA where samples were collected. Groundwater samples were collected at Landfill A, and leachate samples were collected at Landfill B.

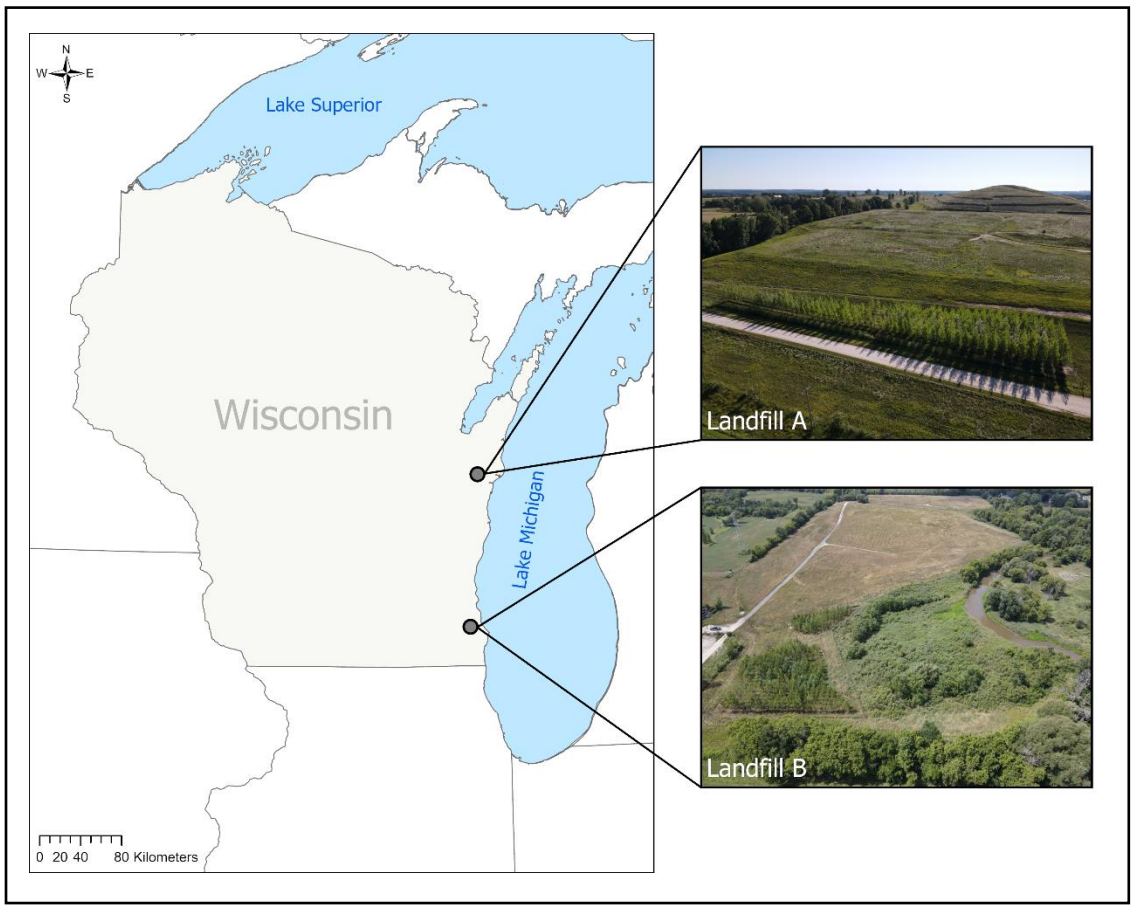

Figure 3.2. Comprehensive approach for putative identification of landfill contaminants. The approach combines data-driven reverse searching and list- and literature-based forward searching of high-resolution mass spectrometry data using XCMS Online. Data acquisition phases are shown in boxes with dashed lines. Data processing steps are shown in boxes with solid lines. Software programs used during data processing are labeled in purple.

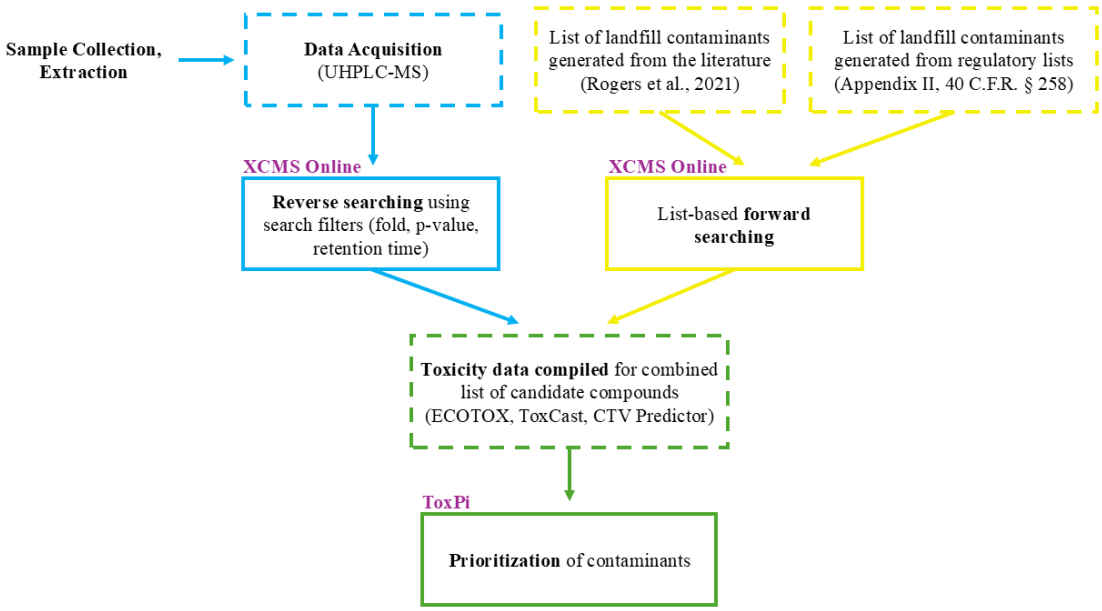

Figure 3.3. Representative cloud plots of pairwise jobs in XCMS Online. (A) Landfill A vs. Landfill B, positive ion mode. (B) Landfill A vs. Landfill B, negative ion mode. In both plots, green features represent features that are upregulated in Landfill B samples compared to Landfill A samples, while red features represent features that are downregulated in Landfill B samples compared to landfill A samples. Both plots display highly significant ($p < 0.0001$) features whose fold change is greater than 1.5 (Patti et al., 2013). In plot (A), 501 features met these criteria. In plot (B), 132 features met the criteria. The size of points in the plots correspond to fold change, with larger points corresponding to larger fold changes. The color of the points corresponds to p-value, with brighter points having lower p-values than darker points (according to Welch's t-test). Points are overlaid on the total ion chromatogram for the samples (shown in grey).

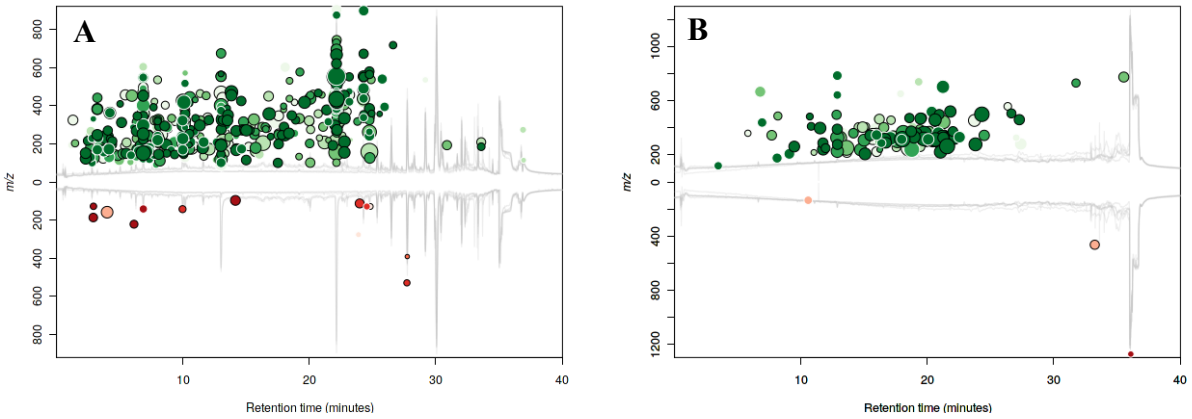

Figure 3.4. Representative 3D PCA plot of Landfill A and Landfill B samples. The samples shown are in positive ion mode. Landfill A samples are shown in red and Landfill B samples are shown in green.

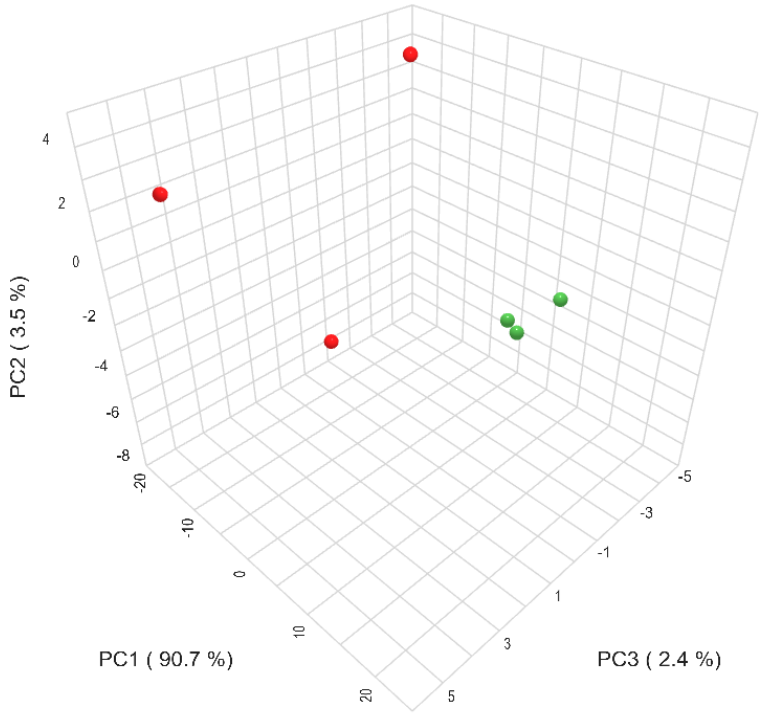

Figure 3.5. Toxicity data availability for 1,321 putatively identified landfill contaminants. Candidate compounds were putatively identified using comprehensive data-driven and list-based searching of XCMS Online. Toxicity data were compiled for candidate compounds with available CASRN. The three toxicity databases of interest were ECOTOX, ToxCast, and the CTV Predictor.

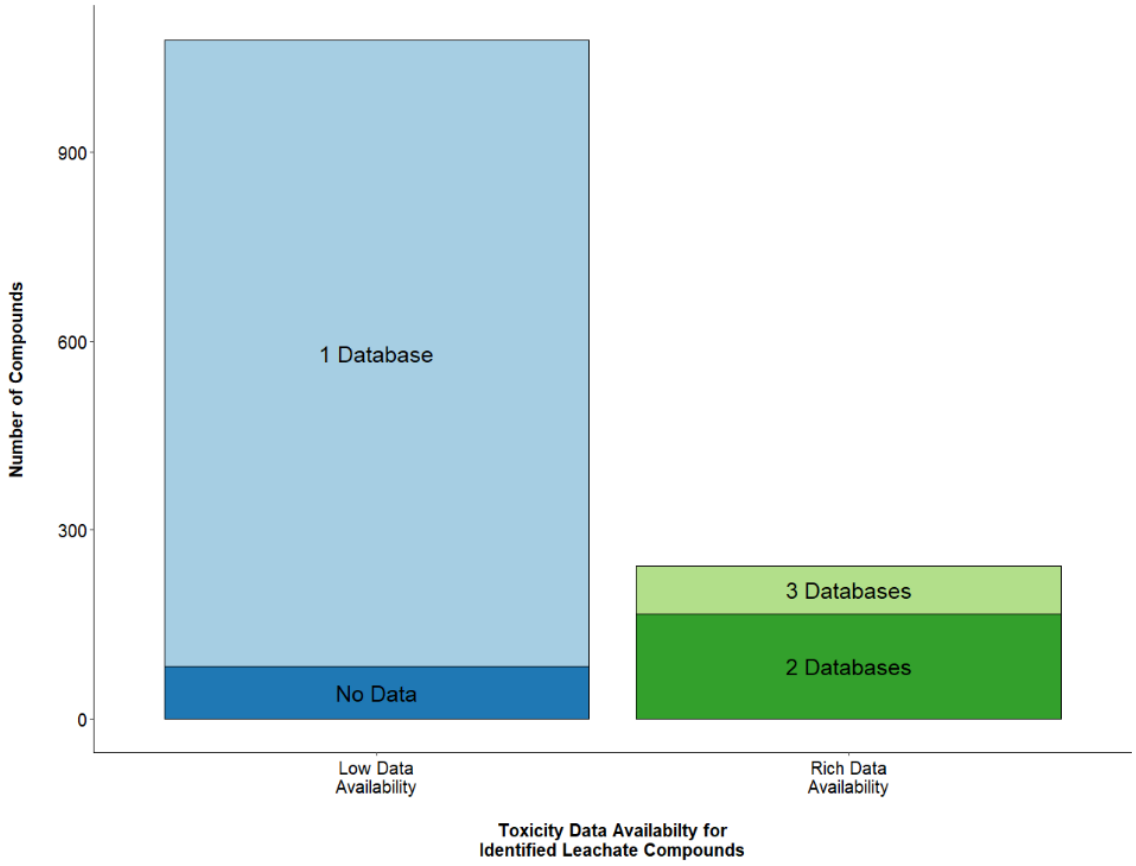

Figure 3.6. ToxPi model (A) and hierarchical cluster analysis for 242 landfill contaminants putatively identified using a comprehensive data-based and list-based approach in XCMS Online (B). Toxicity data were compiled from three toxicity databases: ECOTOX (EC50, shown in blue, representing *in vivo* toxicity data); ToxCast (AC50 and % Active Assays, shown in aqua, representing *in vitro* assay data); and the CTV Predictor (BMD, BMDL, CPV, NO(A)EL, OSF, and RfD, shown in different shades of red and pink, representing calculated *in silico* toxicity data). The size of each slice in a ToxPi profile corresponds to the value of the toxicity endpoint, with larger slices for larger scores. Representative ToxPi profiles for each hierarchical group are shown, as well as average ToxPi toxicity scores for each group.

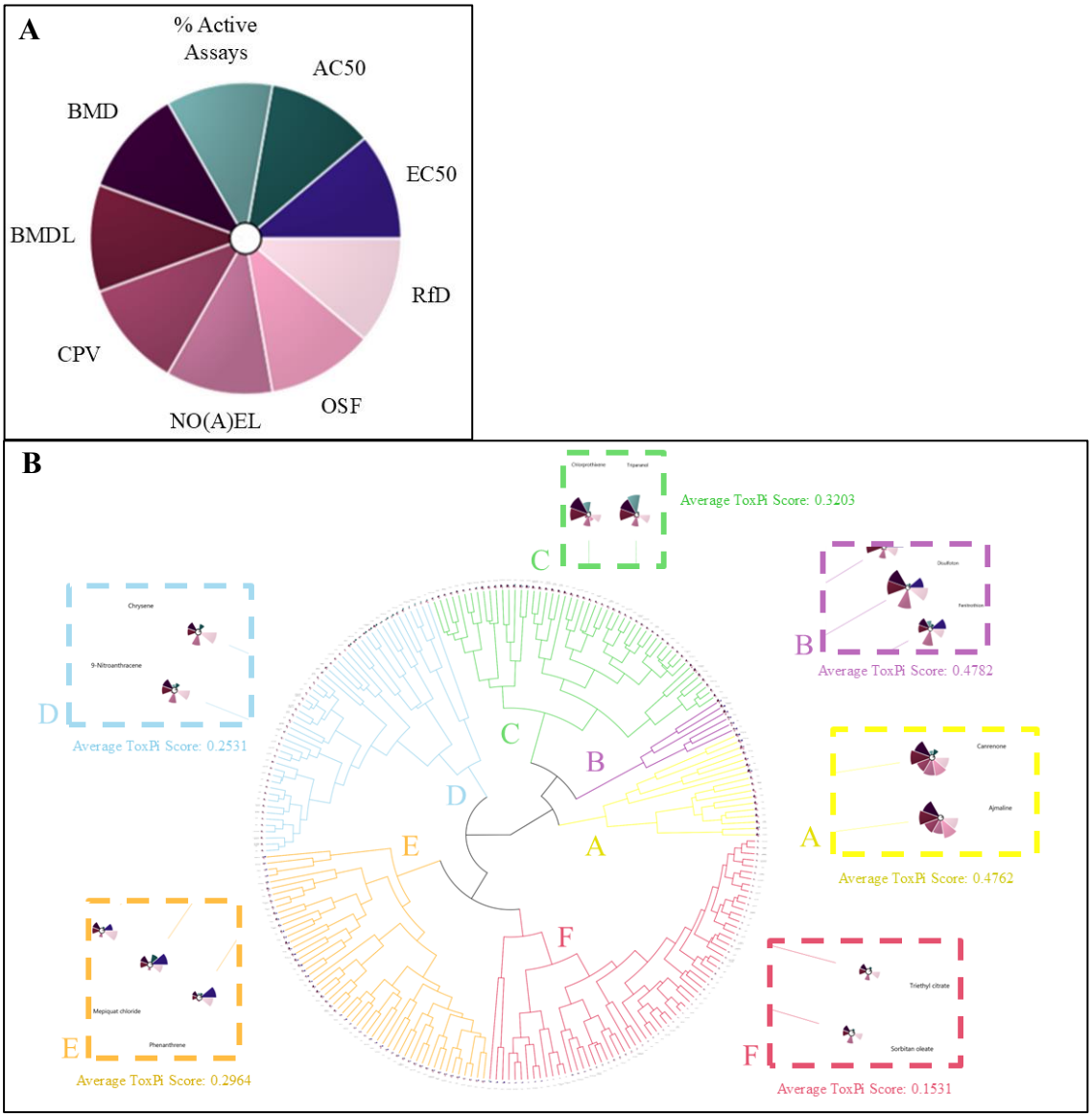

Figure 3.7. ToxPi toxicity score rank plot for 242 putatively identified landfill contaminants. Compounds with lower ranks and higher toxicity scores are more potentially harmful to humans and/or the environment. Hierarchical clustering was performed in ToxPi to visually group compounds based on toxicity profiles. Six groups were identified in clustering analysis. A representative toxicity profile for each hierarchical cluster group is shown within the plot, with colors designating the six groups.

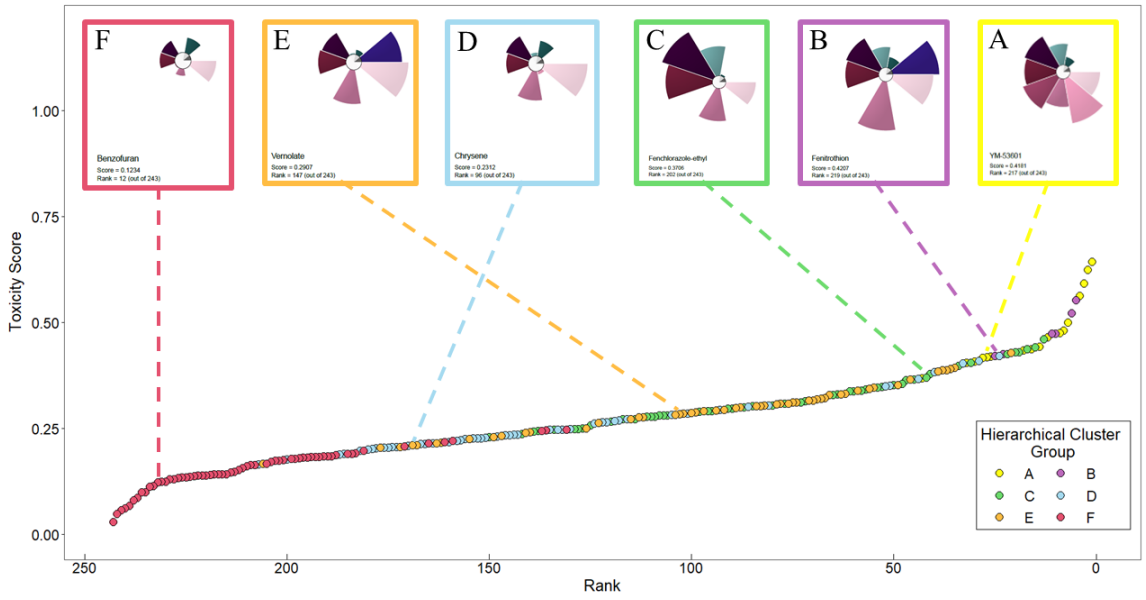

APPENDIX B.

Table B1. Data processing parameters used in XCMS Online jobs.

Parameter	Value
Parameter ID	UPLC / Bruker Q-TOF (6675)
Feature Detection	
method	centWave
maximal tolerated m/z deviation in consecutive scans (ppm)	10
minimum chromatographic peak width (s)	5
maximum chromatographic peak width (s)	20
minimum difference in m/z for peaks with overlapping retention times	0.01
signal/noise threshold	6
integration method	1
prefilter peaks	3
prefilter intensity	100
noise filter	100
Retention Time Correction	
method	obiwarp
step size (m/z) to use for profile generation from raw data files	1
Alignment	
bw (allowable retention time deviations) (s)	5
minfrac (minimum fraction of samples necessary in at least one of the sample groups for it to be a valid group)	0.5
mzwid (width of overlapping m/z slices to use for creating peak density chromatograms and grouping peaks across samples)	0.015
minsamp (minimum number of samples necessary in at least one of the sample groups for it to be a valid group)	1
maximum number of groups to identify in a single m/z slice	100

Table B2. Toxicity parameters, their definitions, and their transformations in ToxPi.

Database	Parameter	Definition	Transformation in ToxPi
ECOTOX[a]			
	EC50	Half-maximal effective concentration.	-log
ToxCast[b]			
	AC50	Half-maximal activity concentration.	-log
	Percent active assays	Percentage of active assays (number of active assays / total number of assays)	linear
CTV Predictor[c]			
	BMD	Benchmark dose	-log
	BMDL	Benchmark dose lower limit	-log
	CPV	Cancer potency value	linear
	NO(A)EL	No observed adverse effect level	-log
	OSF	Oral slope factor	linear
	RfD	Reference dose	-log

[a] https://cfpub.epa.gov/ecotox/

[b] https://comptox.epa.gov/dashboard/chemical-lists/toxcast

[c] https://toxvalue.org/6-CTV/Cover.php

Table B3. ToxPi toxicity rankings, hierarchical cluster groupings, and relative intensities for 242 compounds putatively identified in groundwater and leachate samples.

Rank	ToxPi Score	Hierarchical Cluster	Compound	Relative Intensities		
				Landfill A	Landfill B	Control
1	0.6430	A	Clotrimazole	1,820 ± 83	118,848 ± 8,147	1,064 ± 347
2	0.6252	A	Oxytetracycline	1,197 ± 91	12,833 ± 5,424	1,101 ± 68
3	0.5921	A	Indeno[1,2,3-cd]pyrene	1,338 ± 58	5,607 ± 560	1,114 ± 36
4	0.5627	A	Benzo[ghi]perylene	1,338 ± 58	5,607 ± 560	1,114 ± 36
5	0.5534	B	Disulfoton	613 ± 16	3,189 ± 1,084	484 ± 44
6	0.5225	B	Cyproterone acetate	1,352 ± 149	2,897 ± 493	1,278 ± 37
7	0.4997	A	Flurandrenolide	1,003 ± 278	4,591 ± 604	647 ± 98
8	0.4807	A	Canrenone	1,282 ± 148	9,491 ± 837	1,051 ± 75
9	0.4759	A	Gliotoxin	1,986 ± 259	2,140 ± 564	968 ± 283
10	0.4740	B	Parathion	601 ± 32	3,040 ± 357	581 ± 90
11	0.4734	B	1-Amino-2,4-dibromoanthraquinone	484 ± 13	4,191 ± 101	421 ± 45
12	0.4652	A	Fluoxymesterone	1,134 ± 107	19,749 ± 1,831	1,337 ± 251
13	0.4609	C	Clomipramine	1,366 ± 26	8,314 ± 567	1,172 ± 460
14	0.4430	A	Ajmaline	777 ± 78	2,477 ± 285	429 ± 37
15	0.4424	C	Trequinsin hydrochloride	922 ± 42	8,551 ± 627	772 ± 49
16	0.4370	A	Phenolphthalein	1,143 ± 42	6,931 ± 851	818 ± 16
17	0.4367	C	Ipecac (Emetine)	1,936 ± 20	18,424 ± 2,834	2,008 ± 82
18	0.4339	A	Alprazolam	1,091 ± 35	7,254 ± 339	1,614 ± 778
19	0.4305	C	Triparanol	1,278 ± 42	126,507 ± 12,091	1,110 ± 29
20	0.4304	C	Diniconazole	709 ± 71	8,378 ± 379	636 ± 22
21	0.4281	E	Benz[a]anthracene	763 ± 13	4,410 ± 467	643 ± 34
22	0.4260	C	Chlorprothixene	455 ± 28	4,869 ± 794	286 ± 19
23	0.4250	B	Aldicarb	4,081 ± 268	8,995 ± 1,251	1,360 ± 217
24	0.4207	D	Hydroxyzine	1,462 ± 52	3,779 ± 502	1,027 ± 88
25	0.4207	B	Fenitrothion	1,010 ± 53	13,287 ± 650	828 ± 52
26	0.4201	A	Ofloxacin	661 ± 9	1,245 ± 195	539 ± 16

Rank	ToxPi Score	Hierarchical Cluster	Compound	Relative Intensities		
				Landfill A	Landfill B	Control
27	0.4181	A	YM-53601	1,950 ± 134	19,430 ± 17,368	774 ± 52
28	0.4171	A	Epinastine hydrochloride	1,482 ± 12	8,312 ± 1,416	873 ± 81
29	0.4091	D	Methysergide	960 ± 53	5,521 ± 762	764 ± 75
30	0.4079	A	Olanzapine	457 ± 52	7,409 ± 6,750	407 ± 11
31	0.4059	C	Spiperone	1,031 ± 110	5,262 ± 296	709 ± 26
32	0.4050	A	Azatadine	2,225 ± 102	22,839 ± 2,678	2,180 ± 194
33	0.4043	D	PP242	659 ± 39	3,355 ± 1,155	597 ± 41
34	0.3975	C	2,2,4,4,6,6-Hexamethyl-1,3,5-trithiane	1,204 ± 33	25,627 ± 2,617	1,030 ± 32
35	0.3940	E	GW 9662	1,143 ± 232	28,645 ± 3,291	2,539 ± 677
36	0.3909	E	Isazofos	1,458 ± 47	13,330 ± 272	1,141 ± 32
37	0.3880	E	Enilconazole	1,446 ± 96	4,582 ± 79	834 ± 80
38	0.3874	E	Bromacil	664 ± 113	3,184 ± 332	493 ± 17
39	0.3843	E	Tebuconazole	952 ± 152	2,381 ± 228	772 ± 188
40	0.3840	D	Acarbose (Glucobay)	-	18,596 ± 174	940 ± 47
41	0.3789	C	Indatraline hydrochloride	23,227 ± 14,800	56,009 ± 6,531	10,935 ± 5,080
42	0.3706	C	Fenchlorazole-ethyl	787 ± 22	3,903 ± 108	698 ± 46
43	0.3686	A	Lysergic acid diethylamide	3,126 ± 227	24,163 ± 2,496	2,370 ± 169
44	0.3676	D	Sorafenib tosylate	674 ± 19	2,708 ± 523	466 ± 54
45	0.3661	C	Imipramine hydrochloride	958 ± 77	4,962 ± 1,573	538 ± 18
46	0.3655	E	Dichlorophene	1,178 ± 60	4,977 ± 705	952 ± 41
47	0.3641	C	Bexarotene	660 ± 103	7,411 ± 932	342 ± 69
48	0.3557	C	Spiroxatrine	626 ± 21	3,723 ± 394	581 ± 18
49	0.3525	E	Oryzalin	538 ± 42	2,969 ± 211	423 ± 51
50	0.3521	C	Eletriptan	1,463 ± 73	7,500 ± 1,083	1,410 ± 108
51	0.3518	D	Arotinoid acid (TTNPB)	660 ± 103	7,411 ± 932	342 ± 69
52	0.3495	D	Cannabinol	1,383 ± 65	8,857 ± 830	1,140 ± 35
53	0.3487	C	Benztropine mesylate	556 ± 48	1,955 ± 412	272 ± 33
54	0.3470	C	Estazolam	883 ± 22	7,427 ± 661	729 ± 20
55	0.3463	E	Beta napthoflavone	784 ± 51	11,079 ± 1,999	573 ± 58

Rank	ToxPi Score	Hierarchical Cluster	Compound	Relative Intensities		
				Landfill A	Landfill B	Control
56	0.3437	E	Thifensulfuron-methyl	690 ± 57	3,908 ± 352	556 ± 39
57	0.3421	C	Mecarbam	680 ± 5	3,401 ± 215	512 ± 27
58	0.3394	C	Metconazole	711 ± 21	4,484 ± 387	516 ± 23
59	0.3394	E	Dimethipin	1,404 ± 70	50,222 ± 5,363	1,294 ± 71
60	0.3379	C	C.I. Basic Violet 14, monohydrochloride	1,673 ± 432	25,256 ± 4,011	658 ± 18
61	0.3378	C	N-Cyclohexyl-2-Benzothiazolesulfenamide	1,615 ± 184	3,048 ± 506	617 ± 50
62	0.3320	E	Hydroxyflutamide	4,313 ± 144	34,057 ± 478	4,526 ± 307
63	0.3308	E	Sodium Tetradecyl Sulfate	810 ± 42	17,904 ± 926	544 ± 61
64	0.3301	C	Felodipine	1,253 ± 26	21,571 ± 2,610	1,336 ± 75
65	0.3297	C	Compactin	1,022 ± 105	16,325 ± 1,710	885 ± 41
66	0.3287	E	Ametryn	896 ± 57	7,747 ± 1,436	716 ± 12
67	0.3221	E	4-Acetyl-6-tert-butyl-1,1-dimethylindane	1,374 ± 64	12,455 ± 2,524	780 ± 25
68	0.3198	E	Ketamine	1,348 ± 40	14,143 ± 940	1,206 ± 21
69	0.3185	E	Triclosan	592 ± 9	978 ± 42	490 ± 42
70	0.3164	E	Ampicillin sodium	1,109 ± 61	12,787 ± 1,284	975 ± 70
71	0.3157	E	Perfluorooctanesulfonic acid	2,089 ± 123	25,933 ± 492	1,503 ± 17
72	0.3121	C	Bromodiphenhydramine	7,447 ± 989	7,488 ± 2,796	833 ± 16
73	0.3120	E	Molinate	853 ± 43	6,019 ± 968	604 ± 29
74	0.3113	E	Amitraz	1,890 ± 111	5,189 ± 966	1,643 ± 262
75	0.3087	E	Fluconazole	834 ± 61	4,416 ± 551	628 ± 63
76	0.3086	C	Sclareolide (Norambreinolide)	1,458 ± 391	17,803 ± 609	1,370 ± 14
77	0.3083	E	Omethoate	1,177 ± 229	13,866 ± 1,642	865 ± 32
78	0.3076	E	Sulfaguanidine	1,325 ± 54	35,547 ± 4,551	1,187 ± 116
79	0.3048	C	Sulbactam	663 ± 25	4,004 ± 733	632 ± 47
80	0.3045	D	4-Hydroxybenzenesulfonic acid	576 ± 42	2,753 ± 1,185	495 ± 47
81	0.3044	E	Sulfadimidine (Sulfamethazine)	592 ± 9	2,885 ± 119	577 ± 38
82	0.3035	E	Dimethametryn	2,230 ± 133	25,398 ± 1,078	1,370 ± 80
83	0.3029	E	Tributyl phosphate	1,333 ± 214	103,000 ± 3,022	1,032 ± 59
84	0.3025	C	Sibutramine	2,569 ± 335	2,037 ± 163	1,127 ± 86

Rank	ToxPi Score	Hierarchical Cluster	Compound	Relative Intensities		
				Landfill A	Landfill B	Control
85	0.3009	D	9-Hydroxyrisperidone	1,142 ± 101	965,801 ± 54,578	941 ± 17
86	0.3004	C	Tocoretinate	1,005 ± 606	3,601 ± 522	254 ± 52
87	0.2994	E	Pebulate	3,803 ± 72	22,189 ± 1,867	2,567 ± 91
88	0.2981	E	Pendimethalin	621 ± 40	18,408 ± 13,466	428 ± 42
89	0.2974	C	Atropine methyl bromide	5,996 ± 495	82,741 ± 10,229	4,133 ± 220
90	0.2973	C	Chlormezanone	1,113 ± 123	8,543 ± 530	1,328 ± 190
91	0.2944	E	Sodium lauryl sulfate	1,028 ± 96	26,574 ± 1,498	849 ± 96
92	0.2939	D	Thiosalicylic Acid	1,885 ± 516	19,544 ± 1,855	1,973 ± 166
93	0.2928	E	Vinclozolin	644 ± 57	6,059 ± 193	505 ± 31
94	0.2916	C	Glycopyrrolate	1,227 ± 74	16,512 ± 1,368	900 ± 26
95	0.2908	C	Ethaverine Hydrochloride	304 ± 2	972 ± 184	288 ± 3
96	0.2907	E	Vernolate	3,803 ± 72	22,189 ± 1,867	2,567 ± 91
97	0.2904	C	Octylonium bromide	887 ± 55	13,885 ± 2,514	877 ± 2
98	0.2879	E	Chloroxuron	1,601 ± 304	19,938 ± 1,733	1,177 ± 9
99	0.2873	E	Perfluorooctanoic acid	691 ± 53	9,956 ± 142	649 ± 20
100	0.2852	D	Dicumarol	783 ± 191	5,389 ± 330	718 ± 29
101	0.2848	E	Pyrene	46,911 ± 4,228	57,600 ± 2,714	14,974 ± 604
102	0.2842	E	S-Ethyl dipropylthiocarbamate (EPTC)	1,134 ± 44	10,075 ± 1,585	1,099 ± 116
103	0.2828	E	Bensulfuron-methyl	731 ± 55	6,772 ± 147	707 ± 22
104	0.2825	D	Stiripentol	912 ± 20	4,927 ± 312	780 ± 148
105	0.2811	C	Cloperastine Hydrochloride	1,745 ± 359	5,254 ± 586	457 ± 60
106	0.2811	C	Dibenzepine HCL	800 ± 42	3,417 ± 112	422 ± 7
107	0.2807	C	Phenoxybenzamine hydrochloride	508 ± 57	3,342 ± 239	419 ± 35
108	0.2785	C	Gliclazide	834 ± 53	5,593 ± 533	679 ± 35
109	0.2778	C	Oxyphenonium bromide	1,646 ± 291	2,685 ± 208	1,582 ± 165
110	0.2774	C	Tinoridine	508 ± 20	3,066 ± 157	361 ± 14
111	0.2765	E	Fluoranthene	46,911 ± 4,228	57,600 ± 2,714	14,974 ± 604
112	0.2761	E	Butylate	1,018 ± 52	18,082 ± 1,608	979 ± 76
113	0.2728	C	Piperonyl sulfoxide	13,152 ± 1,833	73,172 ± 9,630	12,053 ± 2,702

Rank	ToxPi Score	Hierarchical Cluster	Compound	Relative Intensities		
				Landfill A	Landfill B	Control
114	0.2725	E	Sulfamerazine	1,781 ± 444	2,225 ± 716	489 ± 28
115	0.2720	D	Cantharidin	1,373 ± 68	12,212 ± 2,481	1,086 ± 44
116	0.2720	C	Pencycuron	203 ± 12	532 ± 71	156 ± 2
117	0.2695	D	Nafcillin Sodium Salt Monohydrate	918 ± 40	4,894 ± 563	919 ± 23
118	0.2677	D	Cytarabine hydrochloride	513 ± 59	2,880 ± 154	326 ± 6
119	0.2669	C	Valdecoxib	1,960 ± 558	78,769 ± 3,278	817 ± 30
120	0.2654	D	Busulfan	1,178 ± 60	4,977 ± 705	952 ± 41
121	0.2651	D	Entecavir	1,655 ± 93	10,328 ± 464	1,493 ± 53
122	0.2631	E	Nitramine	565 ± 54	3,280 ± 330	451 ± 15
123	0.2616	D	Nomifensin	314 ± 37	1,477 ± 254	226 ± 23
124	0.2573	C	DL-alpha-Lipoic Acid	1,264 ± 53	23,234 ± 2,239	1,089 ± 27
125	0.2500	E	Mepiquat chloride	3,940 ± 1,929	8,660 ± 1,289	1,520 ± 385
126	0.2496	C	Valethamate Bromide	5,970 ± 740	160,745 ± 8,350	1,537 ± 514
127	0.2488	C	4,4'-Dichlorobenzophenone	3,651 ± 787	7,610 ± 133	707 ± 29
128	0.2487	C	Clopirac	10,024 ± 2,336	15,666 ± 1,583	982 ± 72
129	0.2486	D	Chloropyramine Hydrochloride	662 ± 15	7,018 ± 349	726 ± 7
130	0.2478	F	Sudan I	472 ± 80	1,280 ± 716	389 ± 39
131	0.2472	D	Dodecanedioic acid	486 ± 36	3,502 ± 99	436 ± 10
132	0.2469	D	Trifluperidol hydrochloride	918 ± 20	5,463 ± 810	786 ± 85
133	0.2467	C	Indecainide	1,348 ± 103	7,701 ± 435	1,116 ± 88
134	0.2467	D	9-Hydroxyphenanthrene	797 ± 33	2,544 ± 425	772 ± 63
135	0.2452	F	C.I. Acid Green 50	372 ± 10	3,599 ± 88	362 ± 36
136	0.2448	F	Zearalenone	856 ± 124	2,190 ± 330	300 ± 17
137	0.2446	C	Sulfacetamide	1,031 ± 58	9,810 ± 750	810 ± 36
138	0.2436	C	Clenbuterol	764 ± 109	9,509 ± 1,469	574 ± 47
139	0.2421	E	Phenothrin	1,336 ± 127	6,409 ± 504	915 ± 99
140	0.2403	E	Fluroxypyr	663 ± 25	4,004 ± 733	632 ± 47
141	0.2366	C	Raclopride	626 ± 6	7,967 ± 248	450 ± 67
142	0.2353	D	4-Biphenylamine	1,180 ± 250	77,332 ± 8,307	1,088 ± 3

Rank	ToxPi Score	Hierarchical Cluster	Compound	Relative Intensities		
				Landfill A	Landfill B	Control
143	0.2352	D	Amprolium	1,264 ± 160	3,827 ± 498	682 ± 47
144	0.2344	D	Zolpidem	1,056 ± 144	7,370 ± 89	597 ± 52
145	0.2343	D	9-Nitroanthracene	2,806 ± 822	29,252 ± 430	1,072 ± 255
146	0.2330	E	Dibenzofuran	1,853 ± 91	3,242 ± 908	895 ± 133
147	0.2312	D	Chrysene	763 ± 13	4,410 ± 467	643 ± 34
148	0.2299	E	Sethoxydim	1,029 ± 28	5,515 ± 788	985 ± 99
149	0.2293	C	3-Thiatetradecanoic Acid	1,056 ± 327	5,130 ± 309	1,114 ± 265
150	0.2289	D	Triprolidine	3,077 ± 258	1,032 ± 356	384 ± 27
151	0.2267	D	Diphenylcyclopropenone	1,275 ± 249	3,037 ± 569	428 ± 18
152	0.2264	D	1-(2,6,6-Trimethyl-2-cyclohexen-1-yl)-1,6-heptadien-3-one	789 ± 123	5,271 ± 411	453 ± 28
153	0.2263	D	Nifurtimox	1,394 ± 147	25,895 ± 2,325	1,061 ± 113
154	0.2251	E	Methoprotryne	3,015 ± 522	21,215 ± 669	1,219 ± 153
155	0.2251	D	Carprofen	1,601 ± 304	19,938 ± 1,733	1,177 ± 9
156	0.2219	D	2-Methyl-2-[(1-oxo-2-propenyl)amino]-1-propanesulfonic acid	4,411 ± 144	17,199 ± 2,284	3,026 ± 1,243
157	0.2210	D	Tetraethylammonium chloride	1,058,538 ± 711,088	2,341,099 ± 196,496	463,634 ± 222,626
158	0.2205	F	cis-Caryophyllene	1,503 ± 234	10,000 ± 724	1,108 ± 30
159	0.2185	D	Cidofovir	4,452 ± 698	5,952 ± 460	1,414 ± 489
160	0.2180	F	2-Aminoanthraquinone	2,806 ± 822	29,252 ± 430	1,072 ± 255
161	0.2169	E	Diphenylamine	1,180 ± 250	77,332 ± 8,307	1,088 ± 3
162	0.2153	E	Isoproturon	2,211 ± 39	25,323 ± 3,389	1,088 ± 53
163	0.2150	D	Thonzylamine Hydrochloride	1,047 ± 192	6,731 ± 1,141	354 ± 13
164	0.2147	F	Etretinate	1,352 ± 29	11,347 ± 1,575	1,029 ± 11
165	0.2142	D	Miltefosine	930 ± 29	8,458 ± 997	891 ± 25
166	0.2137	D	Tulobuterol hydrochloride	1,003 ± 63	46,567 ± 1,607	779 ± 38
167	0.2109	E	Genistein	5,943 ± 991	7,196 ± 517	3,499 ± 1,640
168	0.2100	E	Isoflurophate	7,390 ± 1,925	18,777 ± 1,351	3,554 ± 1,110
169	0.2091	D	Tegafur	2,394 ± 1,089	2,345 ± 334	836 ± 241

Rank	ToxPi Score	Hierarchical Cluster	Compound	Relative Intensities		
				Landfill A	Landfill B	Control
170	0.2083	F	Indigo	4,381 ± 841	14,386 ± 1,040	1,249 ± 49
171	0.2068	E	Phenanthrene	4,299 ± 634	25,791 ± 6,405	1,763 ± 35
172	0.2057	D	Parecoxib sodium	568 ± 4	4,040 ± 743	495 ± 7
173	0.2056	D	Clonixin	1,179 ± 76	2,151 ± 699	811 ± 59
174	0.2050	D	Adefovir	1,127 ± 42	8,714 ± 588	821 ± 58
175	0.2050	D	Cinnamyl cinnamate	2,099 ± 373	10,282 ± 1,253	572 ± 4
176	0.2041	E	Furfural	21,190 ± 978	7,995 ± 5,921	16,283 ± 7,751
177	0.2029	D	5-Chloro-1-piperidin-4-yl-1,3-dihydrobenzimidazol-2-one; R 29676	944 ± 229	7,196 ± 1,186	1,181 ± 138
178	0.2024	D	Nalidixic acid	496 ± 42	9,871 ± 1,150	491 ± 25
179	0.1999	D	7-Aminodesacetoxycephalosporanic acid	1,256 ± 75	7,715 ± 1,374	1,134 ± 85
180	0.1974	F	6-Methyl-2-phenylquinoline-4-carboxylic acid, ethyl ester	811 ± 76	10,121 ± 1,564	571 ± 11
181	0.1971	D	Phenobarbital	496 ± 42	9,871 ± 1,150	491 ± 25
182	0.1922	F	2-Naphthalenol 2-aminobenzoate	1,034 ± 99	7,522 ± 703	656 ± 101
183	0.1904	F	1-tetradecanol	1,380 ± 195	6,271 ± 696	841 ± 152
184	0.1903	F	Cumene hydroperoxide	5,562 ± 436	3,473 ± 65	1,260 ± 96
185	0.1895	D	Potassium acetate	56,080 ± 5,577	10,972,971 ± 403,947	39,512 ± 3,673
186	0.1892	D	Nomifensine maleate	314 ± 37	1,477 ± 254	226 ± 23
187	0.1873	F	Tropisetron	2,547 ± 421	8,134 ± 1,626	474 ± 41
188	0.1850	F	Mupirocin	2,862 ± 104	57,363 ± 6,579	2,408 ± 79
189	0.1847	F	Ganciclovir	281 ± 6	1,279 ± 108	225 ± 12
190	0.1844	F	Drometrizolum	1,458 ± 125	7,122 ± 357	666 ± 6
191	0.1831	F	4,4'-Methylene bis(2-methylaniline)	1,180 ± 36	4,052 ± 678	1,100 ± 40
192	0.1830	F	Azaperone	3,195 ± 1,355	6,052 ± 2,650	1,686 ± 19
193	0.1825	F	4-Benzylphenyl Carbamate	999 ± 27	30,281 ± 2,152	723 ± 40
194	0.1810	F	Asaraldehyde (Asaronaldehyde)	1,373 ± 68	12,212 ± 2,481	1,086 ± 44
195	0.1808	F	2-Phenylethyl 3-phenyl-2-propenoate	2,292 ± 45	87,655 ± 6,265	1,094 ± 47
196	0.1794	F	PHA-543613	4,514 ± 849	7,356 ± 3,314	614 ± 170

Rank	ToxPi Score	Hierarchical Cluster	Compound	Relative Intensities		
				Landfill A	Landfill B	Control
197	0.1789	F	N-(9-Fluorenylmethoxycarbonyl)-L-Leucine	640 ± 17	4,097 ± 519	635 ± 28
198	0.1783	F	Thiacloprid	720 ± 100	2,631 ± 250	399 ± 15
199	0.1768	D	Miglitol	979 ± 45	10,266 ± 869	653 ± 19
200	0.1762	F	Nepafenac	898 ± 43	2,611 ± 349	812 ± 40
201	0.1746	F	Xanthone	1,843 ± 37	5,818 ± 138	898 ± 112
202	0.1745	F	Ibudilast	1,560 ± 406	3,438 ± 592	453 ± 22
203	0.1714	F	Flupirtine maleate	494 ± 75	21,365 ± 2,387	11,472 ± 10,677
204	0.1663	F	Cyazofamid	781 ± 23	4,444 ± 644	786 ± 20
205	0.1663	E	1-Octadecanamine	2,641 ± 334	190,390 ± 22,821	1,676 ± 49
206	0.1655	D	Ethiolate	1,778 ± 124	11,566 ± 1,088	1,554 ± 19
207	0.1636	F	Agaric Acid	963 ± 18	4,820 ± 175	768 ± 19
208	0.1634	F	Theobromine	698 ± 32	4,119 ± 848	412 ± 21
209	0.1605	F	Quinocide	470 ± 17	4,832 ± 182	487 ± 13
210	0.1570	F	Flumioxazin	957 ± 63	25,773 ± 1,256	1,003 ± 41
211	0.1528	F	1,7-Dimethylxanthine	698 ± 32	4,119 ± 848	412 ± 21
212	0.1484	F	Dibutyl succinate	486 ± 36	3,502 ± 99	436 ± 10
213	0.1466	F	Crotamiton	2,707 ± 102	321,306 ± 8,600	2,431 ± 139
214	0.1425	F	Benzhydrol	726 ± 19	4,118 ± 635	450 ± 6
215	0.1421	F	Fluorene	3,134 ± 142	43,687 ± 644	2,117 ± 148
216	0.1415	F	2-Propenyl 2-aminobenzoate	2,110 ± 131	9,352 ± 514	718 ± 92
217	0.1414	F	7,8 Dihydrokawain	5,759 ± 775	8,802 ± 253	2,061 ± 565
218	0.1398	F	Naproxol	21,668 ± 1,043	25,562 ± 991	7,390 ± 2,799
219	0.1393	F	Sorbitan oleate	4,812 ± 802	28,526 ± 2,609	3,825 ± 1,713
220	0.1391	F	8,8-Dimethoxy-2,6-dimethyl-2-octanol	1,465 ± 228	37,876 ± 3,462	1,410 ± 107
221	0.1386	F	Dicyclopentadiene	19,491 ± 11,673	52,183 ± 3,382	8,580 ± 3,558
222	0.1375	F	Dihydrojasmonic Acid, Methyl Ester	166 ± 30	893 ± 82	156 ± 5
223	0.1364	F	Triethyl citrate	1,083 ± 61	9,830 ± 836	841 ± 75
224	0.1350	F	Enalapril	2,369 ± 451	16,784 ± 1,086	2,682 ± 513
225	0.1344	F	4-Phenylpyridine	1,520 ± 42	8,569 ± 1,378	802 ± 10

Rank	ToxPi Score	Hierarchical Cluster	Compound	Relative Intensities		
				Landfill A	Landfill B	Control
226	0.1327	F	Pyrilamine	592 ± 21	10,141 ± 287	470 ± 21
227	0.1309	F	Ethylene brassylate	3,065 ± 1,117	49,621 ± 755	1,676 ± 109
228	0.1308	F	Talinolol	587 ± 34	2,254 ± 160	341 ± 52
229	0.1248	F	Tetralin	19,491 ± 11,673	52,183 ± 3,382	8,580 ± 3,558
230	0.1243	F	Tropicamide	2,547 ± 421	8,134 ± 1,626	474 ± 41
231	0.1234	F	Benzofuran	176,647 ± 32,749	5,454,660 ± 118,385	11,888 ± 2,566
232	0.1142	F	Butacaine	5,214 ± 760	3,336 ± 483	5,856 ± 790
233	0.1125	F	Methenamine	8,497 ± 722	10,626 ± 1,037	3,345 ± 1,629
234	0.0991	F	Diisopropyl adipate	1,031 ± 110	5,262 ± 296	709 ± 26
235	0.0989	F	Dipropyl hexanedioate	486 ± 36	3,502 ± 99	436 ± 10
236	0.0861	F	3-Methylindole	2,244 ± 378	81,132 ± 3,845	2,349 ± 383
237	0.0806	F	(Cis-) Nanophine	1,058 ± 84	7,390 ± 768	953 ± 53
238	0.0668	F	Flonicamid	1,260 ± 54	9,234 ± 189	1,449 ± 97
239	0.0609	F	D-Leucine	1,271 ± 220	476,451 ± 58,782	1,187 ± 80
240	0.0564	F	3-Methyl-1,2-cyclohexanedione	1,722 ± 498	2,177 ± 354	676 ± 157
241	0.0479	F	N-Methyl-2-pyrrolidinone	1,246 ± 226	5,513 ± 1,545	1,181 ± 61
242	0.0296	F	Cimetidine	945 ± 32	11,362 ± 1,086	663 ± 79

3.6 References

40 C.F.R. § 258, 1991. Criteria for municipal solid waste landfills. https://www.ecfr.gov/current/title-40/chapter-I/subchapter-I/part-258.

40 CFR § 258.54, 1991. Detection monitoring program. https://www.ecfr.gov/current/title-40/section-258.54.

40 CFR § 258.55, 1991. Assessment monitoring program. https://www.ecfr.gov/current/title-40/section-258.55.

Appendix I to 40 C.F.R. § 258, 1991. Appendix I to Part 258—Constituents for detection monitoring. https://www.ecfr.gov/current/title-40/part-258/appendix-Appendix I to Part 258.

Appendix II to 40 C.F.R. § 258, 1991. Appendix II to Part 258—List of hazardous inorganic and organic constituents. https://www.ecfr.gov/current/title-40/part-258/appendix-Appendix II to Part 258.

Aronsson, P., Dahlin, T., Dimitriou, I., 2010. Treatment of landfill leachate by irrigation of willow coppice – plant response and treatment efficiency. Environ. Pollut. 158, 795–804. https://doi.org/10.1016/j.envpol.2009.10.003.

Bittremieux, W., Wang, M., Dorrestein, P.C., 2022. The critical role that spectral libraries play in capturing the metabolomics community knowledge. Metabolomics 18, 94. https://doi.org/10.1007/s11306-022-01947-y.

Carvalho, P.N., Basto, M.C.P., Almeida, C.M.R., Brix, H., 2014. A review of plant–pharmaceutical interactions: from uptake and effects in crop plants to

phytoremediation in constructed wetlands. Environ. Sci. Pollut. Res. 21, 11729–11763. https://doi.org/10.1007/s11356-014-2550-3.

Clarke, B.O., Anumol, T., Barlaz, M., Snyder, S.A., 2015. Investigating landfill leachate as a source of trace organic pollutants. Chemosphere 127, 269–275. https://doi.org/10.1016/j.chemosphere.2015.02.030.

Danforth, C., Chiu, W.A., Rusyn, I., Schultz, K., Bolden, A., Kwiatkowski, C., Craft, E., 2020. An integrative method for identification and prioritization of constituents of concern in produced water from onshore oil and gas extraction. Environ. Int. 134, 105280. https://doi.org/10.1016/j.envint.2019.105280.

De Vries, P., 2024. ECOTOXr: an R package for reproducible and transparent retrieval of data from EPA's ECOTOX database. Chemosphere 364, 143078. https://doi.org/10.1016/j.chemosphere.2024.143078.

Dimitriou, I., Aronsson, P., 2010. Landfill leachate treatment with willows and poplars – efficiency and plant response. Waste Manage. 30, 2137–2145. https://doi.org/10.1016/j.wasman.2010.06.013.

Dimitriou, I., Aronsson, P., Weih, M., 2006. Stress tolerance of five willow clones after irrigation with different amounts of landfill leachate. Bioresour. Technol. 97, 150–157. https://doi.org/10.1016/j.biortech.2005.02.004.

Eevers, N., White, J.C., Vangronsveld, J., Weyens, N., 2017. Bio- and phytoremediation of pesticide-contaminated environments, in: Advances in Botanical Research. Elsevier, pp. 277–318. https://doi.org/10.1016/bs.abr.2017.01.001.

Ekpe, O.D., Moon, H., Pyo, J., Oh, J.-E., 2025. Prioritization of monitoring compounds from SNTS identified organic micropollutants in contaminated groundwater using a machine learning optimized ToxPi model. Water Res. 270, 122824. https://doi.org/10.1016/j.watres.2024.122824.

Forsberg, E.M., Huan, T., Rinehart, D., Benton, H.P., Warth, B., Hilmers, B., Siuzdak, G., 2018. Data processing, multi-omic pathway mapping, and metabolite activity analysis using XCMS Online. Nat. Protoc. 13, 633–651. https://doi.org/10.1038/nprot.2017.151.

Giera, M., Aisporna, A., Uritboonthai, W., Hoang, L., Derks, R.J.E., Joseph, K.M., Baker, E.S., Siuzdak, G., 2024. XCMS-METLIN: data-driven metabolite, lipid, and chemical analysis. Mol. Syst. Biol. 20, 1153–1155. https://doi.org/10.1038/s44320-024-00063-4.

Gowda, H., Ivanisevic, J., Johnson, C.H., Kurczy, M.E., Benton, H.P., Rinehart, D., Nguyen, T., Ray, J., Kuehl, J., Arevalo, B., Westenskow, P.D., Wang, J., Arkin, A.P., Deutschbauer, A.M., Patti, G.J., Siuzdak, G., 2014. Interactive XCMS Online: simplifying advanced metabolomic data processing and subsequent statistical analyses. Anal. Chem. 86, 6931–6939. https://doi.org/10.1021/ac500734c.

Guidi Nissim, W., Palm, E., Pandolfi, C., Mancuso, S., Azzarello, E., 2021. Willow and poplar for the phyto-treatment of landfill leachate in Mediterranean climate. J. Environ. Manage. 277, 111454. https://doi.org/10.1016/j.jenvman.2020.111454.

Guidi Nissim, W., Voicu, A., Labrecque, M., 2014. Willow short-rotation coppice for treatment of polluted groundwater. Ecol. Eng. 62, 102–114. https://doi.org/10.1016/j.ecoleng.2013.10.005.

Guo, W., Kwok, H.C., Griffith, S.M., Nagl, S., Milovanović, D., Pavlović, M., Pavlović, N.M., Yu, J.Z., Dedon, P.C., Chan, W., 2024. Combustion-derived pollutants linked with kidney disease in low-lying flood-affected areas in the Balkans. Environ. Sci. Technol. 58, 11301–11308. https://doi.org/10.1021/acs.est.4c02848.

Hemmer, S., Manier, S.K., Fischmann, S., Westphal, F., Wagmann, L., Meyer, M.R., 2020. Comparison of three untargeted data processing workflows for evaluating LC-HRMS metabolomics data. Metabolites 10, 378. https://doi.org/10.3390/metabo10090378.

Jain, P., Wally, J., Tolaymat, T., Krause, M., 2021. State of the practice of onsite leachate treatment at municipal solid waste landfills (No. EPA/600/R-21/182). US Environmental Protection Agency, Washington, D.C., USA. https://cfpub.epa.gov/si/si_public_record_Report.cfm?dirEntryId=358950&Lab=CESER.

Jones, D.L., Williamson, K.L., Owen, A.G., 2006. Phytoremediation of landfill leachate. Waste Manage. 26, 825–837. https://doi.org/10.1016/j.wasman.2005.06.014.

Justin, M.Z., Pajk, N., Zupanc, V., Zupančič, M., 2010. Phytoremediation of landfill leachate and compost wastewater by irrigation of *Populus* and *Salix*: biomass and growth response. Waste Manage. 30, 1032–1042. https://doi.org/10.1016/j.wasman.2010.02.013.

Kafle, A., Timilsina, A., Gautam, A., Adhikari, K., Bhattarai, A., Aryal, N., 2022. Phytoremediation: mechanisms, plant selection and enhancement by natural and synthetic agents. Environ. Adv. 8, 100203. https://doi.org/10.1016/j.envadv.2022.100203.

Karklins, S., 1996. Groundwater sampling field manual (No. PUBL-DG-038 96). Wisconsin Department of Natural Resources Bureau of Drinking Water and Groundwater, Madison, WI, USA. https://dnr.wisconsin.gov/sites/default/files/topic/DrinkingWater/Publications/DG038.pdf.

Krause, M.J., Detwiler, N., Eades, W., Marro, D., Schwarber, A., Tolaymat, T., 2023. Dataset of leachate volumes and surface areas for municipal solid waste (MSW) landfills in Ohio, USA from 1988–2020. Data in Brief 47, 108961. https://doi.org/10.1016/j.dib.2023.108961.

Kumar, V., Sharma, N., Umesh, M., Chakraborty, P., Kaur, K., Duhan, L., Sarojini, S., Thazeem, B., Pasrija, R., Vangnai, A.S., Maitra, S.S., 2023. Micropollutants characteristics, fate, and sustainable removal technologies for landfill leachate: a technical perspective. J. Water Process Eng. 53, 103649. https://doi.org/10.1016/j.jwpe.2023.103649.

Lamb, D.T., Venkatraman, K., Bolan, N., Ashwath, N., Choppala, G., Naidu, R., 2014. Phytocapping: an alternative technology for the sustainable management of landfill sites. Crit. Rev. Env. Sci. Technol. 44, 561–637. https://doi.org/10.1080/10643389.2012.728823.

Mahieu, N.G., Genenbacher, J.L., Patti, G.J., 2016. A roadmap for the XCMS family of software solutions in metabolomics. Curr. Opin. Chem. Biol. 30, 87–93. https://doi.org/10.1016/j.cbpa.2015.11.009.

Marvel, S.W., To, K., Grimm, F.A., Wright, F.A., Rusyn, I., Reif, D.M., 2018. ToxPi Graphical User Interface 2.0: dynamic exploration, visualization, and sharing of integrated data models. BMC Bioinf. 19, 80. https://doi.org/10.1186/s12859-018-2089-2.

Masoner, J.R., Kolpin, D.W., Cozzarelli, I.M., Smalling, K.L., Bolyard, S.C., Field, J.A., Furlong, E.T., Gray, J.L., Lozinski, D., Reinhart, D., Rodowa, A., Bradley, P.M., 2020. Landfill leachate contributes per-/poly-fluoroalkyl substances (PFAS) and pharmaceuticals to municipal wastewater. Environ. Sci.: Water Res. Technol. 6, 1300–1311. https://doi.org/10.1039/D0EW00045K.

Masoner, J.R., Kolpin, D.W., Furlong, E.T., Cozzarelli, I.M., Gray, J.L., 2016. Landfill leachate as a mirror of today's disposable society: pharmaceuticals and other contaminants of emerging concern in final leachate from landfills in the conterminous United States. Environ. Toxicol. Chem. 35, 906–918. https://doi.org/10.1002/etc.3219.

McCorquodale-Bauer, K., Grosshans, R., Zvomuya, F., Cicek, N., 2023. Critical review of phytoremediation for the removal of antibiotics and antibiotic resistance genes in wastewater. Sci. Total Environ. 870, 161876. https://doi.org/10.1016/j.scitotenv.2023.161876.

McCutcheon, S.C., Schnoor, J.L. (Eds.), 2003. Phytoremediation: transformation and control of contaminants, 1st ed. Wiley-Interscience, Hoboken, New Jersey. https://doi.org/10.1002/047127304X.

Ochs, C., Garrison, K., Saxena, P., Romme, K., Sarkar, A., 2024. Contamination of aquatic ecosystems by persistent organic pollutants (POPs) originating from landfills in Canada and the United States: a rapid scoping review. Sci. Total Environ. 924, 171490. https://doi.org/10.1016/j.scitotenv.2024.171490.

Olker, J.H., Elonen, C.M., Pilli, A., Anderson, A., Kinziger, B., Erickson, S., Skopinski, M., Pomplun, A., LaLone, C.A., Russom, C.L., Hoff, D., 2022. The ECOTOXicology knowledgebase: a curated database of ecologically relevant toxicity tests to support environmental research and risk assessment. Environ. Toxicol. Chem. 41, 1520–1539. https://doi.org/10.1002/etc.5324.

Patti, G.J., Tautenhahn, R., Rinehart, D., Cho, K., Shriver, L.P., Manchester, M., Nikolskiy, I., Johnson, C.H., Mahieu, N.G., Siuzdak, G., 2013. A view from above: cloud plots to visualize global metabolomic data. Anal. Chem. 85, 798–804. https://doi.org/10.1021/ac3029745.

Pilon-Smits, E., 2005. Phytoremediation. Annu. Rev. Plant Biol. 56, 15–39. https://doi.org/10.1146/annurev.arplant.56.032604.144214.

Pivato, A., Garbo, F., Moretto, M., Lavagnolo, M.C., 2018. Energy crops on landfills: functional, environmental, and costs analysis of different landfill configurations. Environ. Sci. Pollut. Res. 25, 35936–35948. https://doi.org/10.1007/s11356-018-1452-1.

Reif, D.M., Sypa, M., Lock, E.F., Wright, F.A., Wilson, A., Cathey, T., Judson, R.R., Rusyn, I., 2013. ToxPi GUI: an interactive visualization tool for transparent integration of data from diverse sources of evidence. Bioinf. 29, 402–403. https://doi.org/10.1093/bioinformatics/bts686.

Richard, A.M., Judson, R.S., Houck, K.A., Grulke, C.M., Volarath, P., Thillainadarajah, I., Yang, C., Rathman, J., Martin, M.T., Wambaugh, J.F., Knudsen, T.B., Kancherla, J., Mansouri, K., Patlewicz, G., Williams, A.J., Little, S.B., Crofton, K.M., Thomas, R.S., 2016. ToxCast chemical landscape: paving the road to 21st century toxicology. Chem. Res. Toxicol. 29, 1225–1251. https://doi.org/10.1021/acs.chemrestox.6b00135.

Rogers, E.R., Zalesny, R.S., Lin, C.-H., 2021. A systematic approach for prioritizing landfill pollutants based on toxicity: applications and opportunities. J. Environ. Manage. 284, 112031. https://doi.org/10.1016/j.jenvman.2021.112031.

Smith, C.A., Want, E.J., O'Maille, G., Abagyan, R., Siuzdak, G., 2006. XCMS: processing mass spectrometry data for metabolite profiling using nonlinear peak alignment, matching, and identification. Anal. Chem. 78, 779–787. https://doi.org/10.1021/ac051437y.

Tautenhahn, R., Patti, G.J., Rinehart, D., Siuzdak, G., 2012. XCMS Online: a web-based platform to process untargeted metabolomic data. Anal. Chem. 84, 5035–5039. https://doi.org/10.1021/ac300698c.

Tolaymat, T., Carson, D., 2020. Technical considerations for evaluating the environmental emissions from RCRA subtitle D landfills beyond the 30-year post-

closure care period (No. EPA/600/R-20/346). United States Environmental Protection Agency, Washington, D.C., USA. https://nepis.epa.gov/Exe/ZyPDF.cgi/P1010XDW.PDF?Dockey=P1010XDW.PDF.

Tolaymat, T., Robey, N., Krause, M., Larson, J., Weitz, K., Parvathikar, S., Phelps, L., Linak, W., Burden, S., Speth, T., Krug, J., 2023. A critical review of perfluoroalkyl and polyfluoroalkyl substances (PFAS) landfill disposal in the United States. Sci. Total Environ. 905, 167185. https://doi.org/10.1016/j.scitotenv.2023.167185.

U.S. EPA (United States Environmental Protection Agency), 2024a. Landfill methane outreach program (LMOP): landfill technical data. https://www.epa.gov/lmop/landfill-technical-data (accessed 23 March 2025).

U.S. EPA (United States Environmental Protection Agency), 2024b. National overview: facts and figures on materials, wastes and recycling. https://www.epa.gov/facts-and-figures-about-materials-waste-and-recycling/national-overview-facts-and-figures-materials#NationalPicture (accessed 23 March 2025).

U.S. EPA (United States Environmental Protection Agency), 2024c. Resource Conservation and Recovery Act (RCRA) overview. https://www.epa.gov/rcra/resource-conservation-and-recovery-act-rcra-overview (accessed 23 March 2025).

U.S. EPA (United States Environmental Protection Agency), 2014. RCRA orientation manual 2014 (No. EPA530- F-11– 003). Washington, D.C., USA. https://www.epa.gov/sites/default/files/2015-07/documents/rom.pdf.

Wang, J., Qiao, Z., 2024. A comprehensive review of landfill leachate treatment technologies. Front. Environ. Sci. 12, 1439128. https://doi.org/10.3389/fenvs.2024.1439128.

Wignall, J.A., Muratov, E., Sedykh, A., Guyton, K.Z., Tropsha, A., Rusyn, I., Chiu, W.A., 2018. Conditional Toxicity Value (CTV) predictor: an *in silico* approach for generating quantitative risk estimates for chemicals. Environ. Health Perspect. 126, 057008. https://doi.org/10.1289/EHP2998.

WI DNR (Wisconsin Department of Natural Resources), 2025a. Environmental cleanup & brownfields redevelopment: BRRTS on the web. BOTW Release 4.4. https://apps.dnr.wi.gov/botw/ (accessed 25 March 2025).

WI DNR (Wisconsin Department of Natural Resources), 2025b. Regional licensing, reporting and compliance specialists: waste and materials management program. https://dnr.wisconsin.gov/topic/Waste/EPAs.html (accessed 25 March 2025).

WI DNR (Wisconsin Department of Natural Resources), 2025c. Waste & materials management GEMS on the web (GOTW) public access. https://apps.dnr.wi.gov/gotw/webpages/UserAgreement.aspx (accessed 25 March 2025).

WI DNR (Wisconsin Department of Natural Resources), 2024. Waste types for license applications and renewal forms. https://dnr.wisconsin.gov/sites/default/files/topic/Waste/WasteActivityCodes.pdf (accessed 25 March 2025).

WI DNR (Wisconsin Department of Natural Resources), 2013. The historic registry of waste disposal sites spreadsheet. Historic and current waste disposal sites. https://dnr.wisconsin.gov/topic/Landfills/Registry.html (accessed 25 March 2025).

Xue, J., Guijas, C., Benton, H.P., Warth, B., Siuzdak, G., 2020. METLIN MS^2 molecular standards database: a broad chemical and biological resource. Nat. Methods 17, 953–954. https://doi.org/10.1038/s41592-020-0942-5.

Yu, X., Sui, Q., Lyu, S., Zhao, W., Liu, J., Cai, Z., Yu, G., Barcelo, D., 2020. Municipal solid waste landfills: an underestimated source of pharmaceutical and personal care products in the water environment. Environ. Sci. Technol. 54, 9757–9768. https://doi.org/10.1021/acs.est.0c00565.

Zalesny, J.A., Zalesny, R.S., Coyle, D.R., Hall, R.B., 2007. Growth and biomass of *Populus* irrigated with landfill leachate. For. Ecol. Manage. 248, 143–152. https://doi.org/10.1016/j.foreco.2007.04.045.

Zalesny, J.A., Zalesny, R.S., Wiese, A.H., Sexton, B., Hall, R.B., 2008. Sodium and chloride accumulation in leaf, woody, and root tissue of *Populus* after irrigation with landfill leachate. Environ. Pollut. 155, 72–80. https://doi.org/10.1016/j.envpol.2007.10.032.

Zalesny, R.S., Pilipović, A., Rogers, E.R., Burken, J.G., Hallett, R.A., Lin, C.-H., McMahon, B.G., Nelson, N.D., Wiese, A.H., Bauer, E.O., Buechel, L., DeBauche, B.S., Peterson, M., Seegers, R., Vinhal, R.A., 2021. Establishment of regional phytoremediation buffer systems for ecological restoration in the Great Lakes

Basin, USA. I. Genotype × environment interactions. Forests 12, 430. https://doi.org/10.3390/f12040430.

Zalesny, R.S., Wiese, A.H., Bauer, E.O., Riemenschneider, D.E., 2009. *Ex situ* growth and biomass of *Populus* bioenergy crops irrigated and fertilized with landfill leachate. Biomass Bioenerg. 33, 62–69. https://doi.org/10.1016/j.biombioe.2008.04.012.

Züllig, T., Zandl-Lang, M., Trötzmüller, M., Hartler, J., Plecko, B., Köfeler, H.C., 2020. A metabolomics workflow for analyzing complex biological samples using a combined method of untargeted and target-list based approaches. Metabolites 10, 342. https://doi.org/10.3390/metabo10090342.

CHAPTER 4. INTRINSIC AND EXTRINSIC FACTORS INFLUENCING *POPULUS* WATER USE: A LITERATURE REVIEW

Adapted from: Rogers, E.R., Zalesny, R.S., Lin, C.-H., Vinhal, R.A., 2023. Intrinsic and extrinsic factors influencing *Populus* water use: a literature review. Journal of Environmental Management 348, 119180. https://doi.org/10.1016/j.jenvman.2023.119180

Abstract

Poplars (*Populus* L. spp.) are versatile, productive trees that are used in environmental systems worldwide to provide a variety of benefits. Though poplars are recognized for their elevated water use, summaries of existing data on poplar water use, its influencing factors, and the methodologies used to measure it, are lacking. We sought to 1) summarize the sap flow methodologies used to quantify poplar water use, 2) review sap flow-derived water use data reported in the literature for *Populus* hybrids and non-hybrids, and 3) assess the effects of different intrinsic factors (plant variables) and extrinsic factors (environmental variables) on poplar water use. We identified 133 articles containing information on the methodologies used to measure poplar sap flow. Of these, the thermal dissipation method was used in a majority (55%) of the studies. Poplar water use data were reported in 51 of the articles, with studies taking place in 13 countries, and representing the time period of 1992–2018. Hybrids were studied in 18 articles and included 17 genotypes, while non-hybrids were studied in 33 articles, and included eight species. Hybrid poplar water use ranged from 0.7 to 11.3 mm day^{-1}, with an overall mean of 2.7 ± 0.3 mm day^{-1}. Non-hybrid water use ranged from 0.2 to 19.5 mm day^{-1} with an average of 2.8 ± 0.4 mm day^{-1}. Hybrid poplar water use differed significantly among hybrid types, tree age classes, and water availability classes, and non-hybrid water use

was significantly different among species, experimental context, and water availability classes. While we focused on poplar water use measured by sap flow methodologies, this review builds the foundation for a comprehensive summary of available poplar water use information that has been reported in the literature. Our results on the factors influencing poplar water use can be used to aid in the decision-making process when designing poplar-based environmental systems such as remediation, bioenergy, and agroforestry systems.

4.1 Introduction

Degradation of soil, water, and air resources is a major global concern that is receiving national and international action (United Nations, 2019). Sustainable solutions to degraded natural resources are needed now more than ever before. Trees are an attractive option for rehabilitating degraded lands given lower relative costs compared to other solutions, as well as their ability to provide ecosystem services and contribute to broader sustainability goals. One genus that is used extensively in tree-based environmental systems around the world is *Populus* L. Six taxonomic sections make up the *Populus* genus, with the total number of recognized *Populus* species a topic of debate due to different taxonomic definitions of species and misclassifications of hybrids as species (Eckenwalder, 1996). *Populus* species and their hybrids (i.e., poplars and hybrid poplars) provide important ecosystem services such as erosion control (McIvor et al., 2011), carbon sequestration (Lemus and Lal, 2005), the production of biomass for bioenergy (Kauter et al., 2003), wind protection (Peri and Bloomberg, 2002), and remediation of contaminated sites (Rockwood et al., 2004; Zalesny and Bauer, 2007). As such, poplars and hybrid poplars are broadly implemented in environmental applications

ranging from agroforestry systems (Isebrands et al., 2014; Pavlidis and Tsihrintzis, 2018), to biomass production plantings (Ceulemans and Deraedt, 1999; Njakou Djomo et al., 2015), to phytotechnologies (Dietz and Schnoor, 2001; Zalesny et al., 2019). Key traits such as high yield, rapid growth, vegetative propagation, genetic diversity, extensive rooting, and ability to hybridize for genetic gain make poplars ideal candidates for these environmental systems (Dickmann, 2001; Puri et al., 1994; Stettler et al., 1996).

An important factor to consider when designing and implementing poplar-based environmental systems is water use. Hybrid poplars, in particular, exhibit elevated water use and are used to gain hydraulic control of contaminant plumes in phytoremediation systems (Ferro et al., 2001; Guthrie Nichols et al., 2014). In such instances where water uptake aligns with the objectives of a poplar system, or in cases where there is abundant available water, such as regions near floodplains, elevated water use is primarily an asset. In other cases, elevated *Populus* water use could serve as a liability, such as locations with limited water supply or drought-prone areas where elevated water use may deplete the water table or alter the regional water balance, or in agroecological systems in which high water use can inhibit the productivity of other valuable species (Swieter et al., 2021). In either situation, knowledge of poplar water use, and the factors that can influence it, is key to effective management decisions for poplar-based environmental systems.

Plant water use is a complex physiological process that occurs due to a combination of abiotic and biotic factors. The cohesion-tension theory explains the mechanism for water movement in trees (Tyree and Zimmerman, 2002). Negative pressure is formed when water evaporates from the surface of leaf cells that are in contact

with the atmosphere. As this evaporation occurs, negative pressure (low water potential) develops at the surface of leaves (Taiz and Zeiger, 2006). Water molecules held together by cohesive forces then move through the xylem along a water potential gradient, from areas of higher water potential (roots) to areas of lower water potential (leaves). Transpiration at the leaf surface is driven by the difference in water vapor concentration between the internal leaf air space and the external air. Plant characteristics, such as stomatal resistance and leaf size and pubescence, as well as abiotic factors such as wind speed, air temperature, and relative humidity, all influence the diffusion of water along the transpiration pathway, and therefore, plant water use (Taiz and Zeiger, 2006).

Whole-tree water use has been quantified by a variety of methods involving lysimeters, potometers, chemical tracers, isotopes, and whole-canopy gas exchange chambers (Wullschleger et al., 1998). Tree water use may also be estimated through evapotranspiration modeling (Osroosh et al., 2016), leaf-level gas-exchange measurements, or calculated through a combination of methods such as soil moisture sensors and lysimeters (Girona et al., 2002). However, these methodologies have drawbacks that limit their broad applicability, including technical feasibility (lysimeters, potometers, chemical tracers, isotopes, and gas chambers), data requirements (evapotranspiration modeling), scalability to the tree level (gas-exchange measurements), and costs (lysimeters, potometers, environmental chambers). An alternative approach is to quantify the movement of water in trees, known as sap flow, which enables the quantification of tree transpiration and therefore serves as a proxy for tree water use (Köstner et al., 1998; Peters et al., 2018).

For environmental research, sap flow methodologies offer greater spatial and temporal resolution, lower relative costs, simpler installation, and are less intrusive than other methods of tree water use quantification (Smith and Allen, 1996). Though sap flow methodologies are commonly implemented to quantify *Populus* water use, the different types of sap flow technologies and their frequency of use are not summarized in a comprehensive manner. Further, though poplars are commonly considered as being significant water consumers, a comparative, quantitative assessment of the environmental and management factors influencing hybrid and non-hybrid *Populus* water use (derived from sap flow values) does not exist.

Therefore, the objectives of this paper are to: 1) summarize the sap flow methodologies commonly implemented to measure *Populus* transpiration-based water use, specifically by quantifying their frequency of use; 2) review sap flow-derived water use data reported in the literature for *Populus* hybrids and non-hybrids; and 3) evaluate intrinsic (i.e., genetic background, age) and extrinsic factors (i.e., planting density, experimental context, water availability) that influence sap flow in *Populus*. Researchers and resource managers can use the information presented in this review to guide their decision-making for *Populus*-based environmental projects.

4.2 Materials and methods

4.2.1 Literature review and article selection

First, we conducted a comprehensive literature review of *Populus* sap flow studies. The literature review was performed using the Web of Science database (https://clarivate.com/webofsciencegroup/- solutions/web-of-science/). Web of Science

search logic is as follows: TS=(*Populus* OR poplar OR cottonwood OR "hybrid poplar" OR "hybrid aspen" OR canadensis OR crandon OR eugenii OR eugenei) AND TS=(sapf* OR "sap f*" OR "sap velocity" OR "water use*" OR "heat pulse" OR "heat balance" OR "thermal dissipation") AND Language: (English). Articles were selected for inclusion in the review that 1) directly measured the sap flow of *Populus* trees and 2) explicitly stated the sap flow methodologies used. Web of Science searches were conducted from December 2019 to February 2020. For the quantitative portion of this review, a further criterion was that the articles reported original results of sap flow, sap flux, transpiration, and/or water use from these measurements. From these, only articles that reported data that could be converted to water use in mm d^{-1} (millimeters per day) were selected. This selectivity was to ensure that the results were comparable across studies, and that the units would be relevant to site managers and other decision-makers. Laboratory studies were excluded, as well as studies that included non-*Populus* species in the water use data. Upon selection for inclusion in the review, articles were grouped by the type of *Populus* involved: hybrid or non-hybrid.

4.2.2 Water use data transformation

All average water use data were converted to mm d^{-1}, a unit commonly used to report transpiration, and one that is readily applicable to water budget calculations and water management decision-making (Healy et al., 2007). In the studies reviewed here, multiple different units were used to report *Populus* water use. Some data were reported as the sum of *Populus* water use over a period of time (e.g., mm study $period^{-1}$, mm $growing\ season^{-1}$); in these cases, total water use values were divided by the number of days in the period to arrive at mm d^{-1}. In other cases, water use was reported on an

average hourly basis. These hourly data were multiplied by the number of daylight hours in a day at the particular study site, assuming that flow during non-daylight hours was negligible unless reported otherwise. When the number of daylight hours were not reported in the text, the NOAA Solar Calculator was used to determine location- and time-specific daylight hours (NOAA, 2022). This provides a conservative estimate of daily water use for studies that did not report daily averages. Next, data reported on a leaf area basis were multiplied by leaf canopy per unit ground area, if given. If leaf canopy per unit ground area data were not given, the study was excluded from this review. Further, transpiration data reported as the weight of water taken up by an individual tree (e.g., kg $tree^{-1}$ day^{-1}) were multiplied by stand density data (i.e., trees ha^{-1}) and conversion factors to convert from a weight of water to a volume of water (e.g., mass density of water = 1000 kg H_2O m^{-3}). Finally, where water use data were not directly reported in the text, values were extracted from figures using the open-source software Plot Digitizer (http://plotdigitizer.sourceforge.net; Jelicic Kadic et al., 2016).

4.2.3 Comparative analysis based on experimental factors

To examine the influence of tree-based (i.e., intrinsic factors) and environmental factors (i.e., extrinsic factors) on *Populus* water use, data were classified into qualitative or semi-quantitative categories within each factor (Table 4.1). Factors were selected that could be readily modified by management actions (e.g., clonal selection, planting design, choice to irrigate) or that could provide information useful to *Populus* system management (e.g., water usage as a function of tree age, experimental context). Categories that were data-poor, i.e., those that did not contain at least three water use data points, were excluded from further analysis.

Two intrinsic factors (i.e., those internal to the trees) were evaluated: genetic background (parentage for hybrids and species for non-hybrids) and tree age. In addition, three extrinsic factors were assessed: planting density, experimental context (i.e., natural stand, plantation, riparian buffer, and shelterbelt), and water availability. These factors were classified differently for hybrid and non-hybrid *Populus* due to the differences in life histories, growth habits, and silvicultural prescriptions between hybrids and non-hybrids.

4.2.3.1 Hybrid *Populus*: intrinsic factors

Performance can vary among inter- and intraspecific *Populus* hybrids for aboveground growth parameters [i.e., bud set, leaf number, height, diameter, volume (Li et al., 1998)] and wood characteristics [e.g., lignin content and composition, wood density, fiber length and width (Hart et al., 2013)], which can affect water use. Therefore, hybrid *Populus* water use data were grouped into two categories regarding genetic background: *interspecific hybrids* and *intraspecific hybrids* (Table 4.1). Hybrid categories were not further divided into genomic groups due to a limited number of data points in each group, which would have prevented statistical comparison among groups.

Tree age is another intrinsic factor governing hybrid *Populus* performance. As hybrid poplars age, anatomical properties related to water transport such as fiber length, ray area, and vessel and fiber lumen area and diameter (DeBell et al., 2002; Peszlen, 1994), as well as leaf area index (Dickmann et al., 2001) can change. Rates of growth and biomass production also change over the lifespan of hybrid *Populus* and can influence water use and water uptake (Li et al., 2021). Hybrid water use data were grouped into three semi-quantitative age categories: *saplings* (0–2 years old) in which root systems are

developing and more biomass is allocated to the roots than to shoots (Douglas et al., 2016), *young trees* (3–6 years old) in which trees are established and exhibit rapid growth, and *mature trees* (≥ 7 years old), in which the maximal mean annual increment is reached (Karačić and Weih, 2006; Miller et al., 2016) (Table 4.1).

4.2.3.2 Hybrid *Populus*: extrinsic factors

The planting density of hybrid *Populus* varies depending on the application. For instance, hybrid poplars in agroforestry systems generally have lower planting densities (<1,000 trees ha^{-1}) (Burgess et al., 2005; Fang et al., 2010; Khan and Khaliq Chaudhry, 2007) than do hybrids grown intensively for biomass production (>5,000 trees ha^{-1}) (Armstrong et al., 1999; Cañellas et al., 2012; DeBell et al., 1996). Planting density can have considerable effects on the growth, productivity, and morphology of hybrid poplars (Benomar et al., 2012), which can in turn affect water relations. Hybrid water use data were classified into three planting density categories: *low density* (<1,000 trees ha^{-1}), *medium density* (1,000–5,000 trees ha^{-1}) and *high density* (>5,000 trees ha^{-1}) (Table 4.1).

Hybrid water use was not classified by experimental context as all studies had the same experimental context: hybrid poplar plantations.

Finally, one of the most important factors influencing tree water use is the amount of water that is available for uptake. All but three studies on hybrid poplars relied solely on precipitation for fulfilling tree water needs, and therefore water availability was categorized according to annual precipitation as follows: *low water availability* (<600 mm annual precipitation), *medium water availability* (600–850 mm annual precipitation), and *high water availability* (>850 mm annual precipitation) (Table 4.1). Water availability for the three studies that used irrigation were classified separately to reflect

their use of irrigation. For these three studies, water availability was classified as *medium* if the study location had medium annual precipitation and/or the irrigation supply was not enough to maintain field capacity [occurring at 0.1–0.33 bars of pressure (Walker, 1989)], and *high* if the amount of irrigation supplied was enough to saturate the soil to field capacity or greater for the duration of the study.

4.2.3.3 Non-hybrid *Populus*: intrinsic factors

Like the variation in growth and physiological parameters between inter- and intraspecific poplar hybrids, non-hybrid poplar species also exhibit morphological, phenological, and physiological differences, which can affect water relations (Dillen et al., 2010; Farmer, 1996). Therefore, non-hybrid poplar water use data were grouped by species in order to evaluate the influence of genetic background on non-hybrid water use (Table 4.1).

To account for differences in productivity, growth, and anatomical properties that occur during the lifespan of non-hybrid poplar species, water use data were grouped into three age categories: *juvenile trees* (0–15 years), *middle-aged trees* (16–60 years), and *old trees* (> 60 years old) (Table 4.1). As multiple *Populus* species with different life histories were included in this review, these age classes were selected as representative average classes. A majority of the species in this review exhibit life stages that fall within these three broad age classes. Class boundaries represent: the age that reproductive maturity is reached (in general, occurring within 5–15 years); the age of growth maintenance and reproduction (occurring between 30–75 years); and old age (occurring between 40–200 years), respectively (Braatne et al., 1996; Burns and Honkala, 1990; Corenblit et al., 2014; Taylor, 2001; Thomas et al., 2016; Zihe et al., 2021).

4.2.3.4 Non-Hybrid *Populus*: extrinsic factors

Non-hybrid *Populus* planting density was classified into the same three categories as hybrid density: *low density* (<1,000 trees ha^{-1}), *medium density* (1,000–5,000 trees ha^{-1}), and *high density* (>5,000 trees ha^{-1}) (Table 4.1). These categories captured the range of planting densities exhibited in different environmental contexts of non-hybrid poplars, from natural stands with low density, to shelterbelts with medium density, to plantations (or natural stands) with high densities.

There were four experimental contexts in non-hybrid studies: *natural stands*, *plantations*, *riparian buffers*, and *shelterbelts* (also known as windbreaks) (Table 4.1). This variable accounts for geographical and hydrological variability among locations, scale, and planting designs that may influence poplar water use.

Regarding water availability, more non-hybrid *Populus* studies used irrigation than hybrid *Populus* studies. Therefore, non-hybrid *Populus* water availability was categorized accordingly: *low water availability* in arid to semiarid climates (≤ 600 mm annual precipitation) with no irrigation, *medium water availability* if irrigation was periodically applied in moderate to humid climates (600–850 mm annual precipitation), and *high water availability* if at least one of the following conditions was met: irrigation was constantly supplied, groundwater level was <1 m from the soil surface, or the climate was humid (>850 mm annual precipitation) (Table 4.1).

4.2.4 Exclusion of meteorological variables from the present review

The influence of meteorological parameters besides overall precipitation (e.g., vapor pressure deficit, wind speed, solar radiation, temperature) on *Populus* water use

was not considered in this study for two main reasons. First, because these parameters are among the governing abiotic factors of transpiration, and their effects on tree water use are well documented (Bovard et al., 2005; Huang et al., 2015; Jones, 1985; Katul et al., 2012; Kozlowski and Pallardy, 1997; Kramer and Boyer, 1995; Will et al., 2013; Zhu et al., 2022). Second, because these variables are not directly manipulated by management actions but instead depend on the weather conditions of the site in question. Such comparisons would require temporal resolution of meteorological and physiological data on the order of hours or minutes. Many of the studies included in the present review did not report meteorological or physiological data with this degree of temporal resolution, so making comparisons was not feasible.

4.2.5 Exclusion of soil type from the present review

Soil texture and structure govern soil characteristics that influence water availability for plants, including water holding capacity and hydraulic conductivity (Brady and Weil, 2010). Despite the importance of these factors in plant-water relations, the effects of soil properties on *Populus* water use were not assessed in the present review for multiple reasons. First, some studies did not provide soil information, and instead only provided geographic coordinates of site locations. Although it is possible to use coordinates to identify soil series– and therefore soil characteristics– based upon online soil survey databases, some study locations from the current review do not exist in such databases. Furthermore, soil survey databases oftentimes have low spatial resolution, which can lead to inaccuracies in soil classification, especially when coarse-scale coordinates are given. In other studies, where soil properties were reported using online

soil survey databases and not directly assessed from sites, the same issue of accurate soil classification could be present.

On the other hand, when soil textural data were provided from field sample collections, these data were often reported in different manners. For instance, the depths at which soil samples were collected and analyzed were not consistent across studies, nor were the sampling protocols, or descriptions of textural classes. Given that soil texture and structure can vary significantly with small increases in soil depth (e.g., lithologic discontinuities), this could have introduced substantial error to our comparisons. Additionally, a majority of the studies reviewed here did not assess soil properties to sufficient depths for understanding water use of deep-rooted trees like *Populus*. Thus, only shallow-depth comparisons could have been made, which does not accurately represent the entire soil profile which *Populus* roots can extract water from.

Because many studies included in this review did not report the necessary information to be able to classify soil texture in a standardized, consistent manner, soil properties were not included as an extrinsic factor. Further investigations that account for soil factors such as soil texture, pH, bulk density, and organic matter content are warranted in order to understand how soil characteristics influence *Populus* water use.

4.2.6 Statistical analysis

To determine how *Populus* water use differed within each of the intrinsic and extrinsic factors, we compared water use values among the categories in each factor. We applied the non-parametric Kruskal-Wallis test to compare the relative ranks of water use values among the categories within each factor using the kruskal.test() function of the

native stats() package in R version 4.0.3 (R Core Team, 2020). As the ranks of the values, rather than the values themselves, are used to determine significant differences among groups (Sullivan, N.D.), the Kruskal-Wallis test is not sensitive to outliers, unlike parametric approaches such as ANOVA. Many of the categories included outlier values that would have skewed the results if we had used such an approach. Further, the categories were often unequal, with some containing as little as four data points, and others containing over 15. The Kruskal-Wallis test is suitable for such unbalanced data (Lowry, N.D.). After identifying the significant differences among the factor categories, we performed the Dunn *post hoc* test to identify which specific categories within the factors were significantly different from one another using the dunnTest() function of the FSA package (Ogle et al., 2022) in R. In all analyses, a significance level of $p \leq 0.05$ was used.

4.3 Results

4.3.1 Article selection

The Web of Science literature review yielded 859 articles (Figure 4.1). Additionally, seven more articles were identified by manual Scopus searching for a total of 866 articles. From these, 706 articles were excluded based on title or abstract, leaving 160 articles to be assessed for full-text eligibility. After full-text review, 27 articles were excluded from further analysis. The resulting 133 relevant articles contained information on the sap flow methodologies used to quantify *Populus* water use. These articles were utilized for objective 1 (to review the sap flow methodologies commonly implemented for *Populus* trees).

The final step in the article selection process was to identify the articles that reported water use data in mm day^{-1}, or units that could be transformed to mm day^{-1}. Out of the 133 articles with information on sap flow methodologies, 51 articles reported this type of water use data, and were utilized to fulfill objectives 2 (to review sap flow-derived water use data for *Populus* hybrids and non-hybrids) and 3 (to evaluate intrinsic and extrinsic factors influencing the water use). These 51 articles were then separated according to whether hybrids or non-hybrids were studied.

4.3.2 Sap flow methodologies

Within the 133 articles that contained information on sap flow methodologies used to measure *Populus* water use, seven sap flow methodologies were implemented: thermal dissipation, stem heat balance, trunk heat balance, heat field deformation, heat ratio, heat pulse velocity, and compensation heat pulse methods (Figure 4.2; Table C1). The most common method was thermal dissipation, which was used in 54.8% of the studies. The next most-commonly implemented methodologies included the stem heat balance method (used in 14.8% of studies), heat ratio method (12.6% of studies), and heat pulse velocity method (11.8% of studies). Less-commonly implemented methodologies included the trunk heat balance method (used in 3.7% of studies), heat field deformation method (1.5% of studies), and compensation heat pulse method (0.7% of studies). The total percentage adds up to 99.9% due to rounding.

These seven sap flow methodologies could be split into two categories: constant heat methodologies and pulsed heat methodologies. Within constant heat methodologies, heat is continuously applied, whether to the entire circumference of the tree stem or internally to a portion of the stem via plates or probes (Smith and Allen, 1996). Heat

balance calculations (in the case of stem and trunk heat balance methods) or equations that consider the temperature gradients in sap wood produced by internal sap flow probes (in the case of the thermal dissipation and heat field deformation methods) are then implemented to quantify the rate of sap flow (Nadezhdina, 2018; Smith and Allen, 1996). This contrasts with pulsed heat methodologies, in which short pulses of heat are applied to the tree stem (internally via probes), their velocity is measured, and the velocity of the sap flow is then calculated by compensating for conductive heat dissipation (Smith and Allen, 1996). Of the articles reviewed here, constant heat methodologies (thermal dissipation, stem heat balance, trunk heat balance, and heat field deformation) were used in 75% of the studies, while pulsed heat methodologies (heat ratio, heat pulse velocity, and compensation heat pulse) were used in 25% of studies.

4.3.3 *Populus* water use

The 51 studies that reported *Populus* water use information took place in 13 countries, with data collected during the time period of 1992–2018 (Table 4.2). Hybrids were studied in 18 articles and included 17 genotypes (Tables 4.2 and 4.3). A majority of the hybrid studies (89%) included information on all of the intrinsic and extrinsic factors analyzed here. Non-hybrids were studied in 33 articles, which included eight species (Tables 4.4 and 4.5). Only two instances each of *P. alba* and *P. nigra* were studied, and therefore these species were excluded from the species comparison analysis, as there were not enough data points to calculate the arithmetic mean on a species level. Information on four of the five factors analyzed here was reported in a majority (91%) of the non-hybrid articles.

Average daily water use ranged from low values of below 1 mm day^{-1} to highs of over 11 mm day^{-1} for both hybrid and non-hybrid *Populus* (Tables 4.2 and 4.4). Of the three factors that were similarly assessed among hybrid and non-hybrid water use data (age, planting density, and water availability), water availability was the only factor in which water use differed significantly among its classes for hybrids and non-hybrids (Figures 4.3-4.6). In both types of *Populus*, water use increased with increasing water availability (Figures 4.4 and 4.6). There were also similar overall trends among age classes for hybrids and non-hybrids, with rates of water use peaking during the middle age class of both hybrids and non-hybrids. This peak occurred in the young age class (3- to 6-year-old trees) for hybrid *Populus* (Figure 4.3), and the middle-aged age class (16- to 60-year-old trees) for non-hybrid *Populus* (Figure 4.5). Finally, there were not any discernable trends in water use among planting density classes for hybrids or non-hybrids (Figures 4.4 and 4.6).

4.3.3.1 Hybrids

Based on our analysis of 18 articles that reported 40 independent water use results for hybrid *Populus*, daily water use ranged from 0.7 to 11.3 mm day^{-1}, with an overall mean of 2.7 ± 0.3 mm day^{-1}. In general, the lowest values of water use (< 2 mm day^{-1}) occurred for mature hybrid *Populus* and/or those grown with low water availability (Chen et al., 2014; Meiresonne, 1999; Muller and Lambs, 2009; Xi et al., 2014), with a few exceptions (Allen et al., 1999; Bloemen et al., 2017; Navarro et al., 2018). The highest water use, on the other hand (≥ 5 mm day^{-1}), was reported for saplings (Allen et al., 1999) or young hybrid *Populus* (Ferro et al., 2001; Zalesny et al., 2006) with medium or high water availability.

Water use was significantly different among intrasectional and intersectional hybrids ($p = 0.0010$) (Figure 4.3), with intersectional hybrids having higher water use (3.5 ± 0.5 mm day^{-1}) than intrasectional hybrids (2.1 ± 0.3 mm day^{-1}). Water use for intersectional hybrids ranged from 1.6 mm day^{-1} for 'Dorschkamp' (*P. deltoides* Bartr. Ex Marsh. ´ *P. nigra* L.) (Allen et al., 1999) to 11.3 for 'NM6' (*P. nigra ´ P. maximowiczii* A. Henry) (Zalesny et al., 2006). For intrasectional hybrids, water use ranged from 0.7 mm day^{-1} for *Populus ´ euramericana cv*. '74/76' (Chen et al., 2014) to 6.9 mm day^{-1} for 'DN34' (*P. deltoides* × *P. nigra*) (Ferro et al., 2001).

Water use was also significantly different among hybrid *Populus* age classes ($p = 0.0452$) (Figure 4.3). Mature *Populus* had the lowest water use (1.9 ± 0.1 mm day^{-1}), saplings had moderate water use (2.8 ± 0.6 mm day^{-1}), and young *Populus* had the highest average water use (3.4 ± 0.5 mm day^{-1}). Results of the Dunn post hoc analysis indicated that the young and mature age classes had significantly different water use ($p = 0.0386$), with water use of mature hybrid *Populus* being significantly lower than that of young trees. Young hybrid *Populus* daily water use ranged from 1.4 mm day^{-1} for a mixture of 'DN34' and 'DN2' (both *P. deltoides* × *P. nigra*) trees in their third growing season (Preston and McBride, 2004) to 11.3 mm day^{-1} for 'NM6' (*P. nigra* × *P. maximowiczii*) trees in their fifth growing season (Zalesny et al., 2006). In contrast, water use for mature hybrid *Populus* ranged from 1.4 mm day^{-1} for 7- to 9-year-old 'B301' [(*P. tomentosa* Carrière × *P. bolleana*) × *P. tomentosa*] trees (Xi et al., 2014) to 2.3 mm day^{-1} for 10-year-old 'Max 1' (*P. maximowiczii* × *P. nigra*) trees (Petzold et al., 2011).

Hybrid *Populus* water use was not significantly different among planting density classes (Figure 4.4). Average water use tended to be higher for *Populus* grown in lower

planting densities (4.5 ± 2.3 mm day^{-1}) and moderate for high planting densities (2.8 ± 0.4 mm day^{-1}) and medium planting densities (2.8 ± 0.3 mm day^{-1}).

Hybrid water use was significantly different among water availability classes (p = 0.0004) (Figure 4.4). Average water use was highest in plantings with high water availability (4.4 ± 1.1 mm day^{-1}), moderate for medium water availabilities (2.6 ± 0.3 mm day^{-1}), and low for low water availabilities (1.3 ± 0.2 mm day^{-1}), respectively. Results of the post hoc Dunn test indicated that water use was significantly different among high and low water availabilities (p = 0.0003) and among medium and low water availabilities (p = 0.0075). For the low water availability class, water use ranged from 0.7 mm day^{-1} for '74/76' (*P. × euramericana*) grown at a plantation south of Beijing, China (569 mm annual precipitation with no irrigation) (Chen et al., 2014) to 2.4 mm day^{-1} for 'J-105' (*P. nigra* × *P. maximowiczii*) grown near Erfurt in central Germany (549 mm annual precipitation with no irrigation) (Schmidt-Walter et al., 2014). The medium water availability class exhibited more variation in water use. Values ranged from 1.1 mm day^{-1} for clones 'Skado' (*P. trichocarpa* × *P. maximowiczii*), 'Oudenberg' (*P. deltoides* × *P. nigra*), and 'Grimminge' [*P. deltoides* × (*P. trichocarpa* × *P. deltoides*)] grown in Flanders, Belgium (726 mm annual precipitation with no irrigation) (Bloemen et al., 2017) to 6.9 mm day^{-1} for 'DN34' (*P. deltoides* × *P. nigra*) grown in Utah, USA (610 mm annual precipitation with no irrigation) (Ferro et al., 2001). Within the high water availability class, hybrid *Populus* water use ranged from 2.0 mm day^{-1} for 'Bakan' (*P. trichocarpa* × *P. maximowiczii*) trees grown in Lochristi, Belgium (860 mm annual precipitation with no irrigation) (Navarro et al., 2020) to 11.3 mm day^{-1} for 'NM6' trees

grown at a former landfill in Rhinelander, WI, USA (610 mm annual precipitation with drip irrigation) (Zalesny et al., 2006).

4.3.3.2 Non-hybrids

For the 33 articles that reported 63 independent water use results, daily water use among non-hybrid poplars ranged from 0.2 to 19.5 mm day^{-1} with an average of 2.8 ± 0.4 mm day^{-1}. In general, the lowest values of water use (< 1 mm day^{-1}) occurred for natural *Populus* stands (Angstmann et al., 2012; Chen et al., 2004; Lang et al., 2016) and/or those grown with low water availability (Fu et al., 2016; Samuelson et al., 2007; Venturas et al., 2018; Voigt et al., 2018). In some instances, juvenile *P. deltoides* exhibited low water use (Engel et al., 2004; Samuelson et al., 2007), as did middle-aged *P. nigra* (Nadal-Sala et al., 2017) and old *P. euphratica* (Yu et al., 2019). The greatest water use (≥ 5 mm day^{-1}) was reported for *Populus* grown with high water availability within plantations (Nagler et al., 2007), shelterbelt plantings (Strenge et al., 2018; Thevs et al., 2019), and in riparian settings (Pataki et al., 2005).

Water use was significantly different among *Populus* species ($p = 0.0007$) (Figure 4.5). The lowest average water use was reported for *P. deltoides* (0.9 ± 0.1 mm day^{-1}) and the highest was reported for *P. fremontii* (8.5 ± 2.2 mm day^{-1}). Results of the Dunn post hoc analysis indicated that there were significant differences in water use among *P. fremontii* and *P. deltoides* ($p = 0.0087$), among *P. fremontii* and *P. euphratica* ($p = 0.0007$), and among *P. fremontii* and *P. tremuloides* ($p = 0.0088$). Water use ranged from 0.7 mm day^{-1} (Engel et al., 2004; Samuelson et al., 2007) to 1.2 mm day^{-1} (Samuelson et al., 2007) for *P. deltoides*, 0.2 mm day^{-1} (Lang et al., 2016) to 3.7 mm day^{-1} (Si et al.,

2015) for *P. euphratica*, and 2.7 mm day^{-1} (Gazal et al., 2006) to 19.5 mm day^{-1} (Nagler et al., 2003) for *P. fremontii*.

Water use did not differ significantly among non-hybrid *Populus* age classes (Figure 4.5). However, water use tended to be lower for old trees (1.5 ± 0.2 mm day^{-1}) than juvenile (3.0 ± 1.1 mm day^{-1}) and middle-aged trees (3.3 ± 0.7 mm day^{-1}).

Water use did not vary significantly among planting density categories for non-hybrid *Populus* (Figure 4.6). On average, non-hybrids grown at high densities had the lowest water use (1.6 ± 0.3 mm day^{-1}) and those grown at low densities (2.7 ± 0.7 mm day^{-1}) and medium densities (2.8 ± 0.8 mm day^{-1}) had moderate water use.

Non-hybrid *Populus* exhibited significantly different water use among experimental contexts (p = 0.0239) (Figure 4.6). Natural stands and plantations had lower levels of water use (means of 1.9 ± 0.3 and 2.2 ± 0.8 mm day^{-1}, respectively), while riparian and shelterbelt plantings had greater water use (means of 3.5 ± 1.2 and 3.9 ± 0.6 mm day^{-1}, respectively). Results of the Dunn post hoc analysis indicated that natural stands and shelterbelts had significantly different water use (p = 0.0410). Water use of non-hybrid *Populus* grown in natural stands ranged from 0.2 mm day^{-1} (Lang et al., 2016) to 5.1 mm day^{-1} (Gazal et al., 2006), while that of *Populus* grown in shelterbelts ranged from 0.5 mm day^{-1} (Fu et al., 2016) to 7.8 mm day^{-1} (Strenge et al., 2018).

Water use of non-hybrids also varied significantly among water availability classes (p = 0.0003) (Figure 4.6). Water use was highest in plantings with high water availability (6.3 ± 1.6 mm day^{-1}), moderate in plantings with medium water availability (2.5 ± 0.3 mm day^{-1}), and low in plantings with low water availability (1.5 ± 0.2 mm

day^{-1}). Results of the post hoc analysis Dunn test indicated that water use was significantly different among high and low water availabilities (p = 0.0003), and among medium and low water availabilities (p = 0.0483). For the low water availability class, water use ranged from 0.2 mm day^{-1} for *P. euphratica* grown in Xinjiang, China (< 50 mm annual precipitation, trees located with varying groundwater levels and distances to a nearby river) (Lang et al., 2016) to 3.3 mm day^{-1} for *P. tremuloides* grown in Saskatchewan, Canada (462 mm annual precipitation) (Hogg and Hurdle, 1997). Within the medium water availability class, water use ranged from 0.7 mm day^{-1} for *P. deltoides* grown in a mesocosm in Arizona, USA (irrigated to maintain soil water content at 75% field capacity for part of the experiment) (Engel et al., 2004) to 6.2 mm day^{-1} for *P. fremontii* grown in the Cibola National Wildlife Refuge in California, USA (97 mm annual precipitation, flood irrigation of the experimental field until the start of the study, natural water table at 2-3 m soil depth) (Nagler et al., 2007). Finally, water use within the high water availability class ranged from 0.2 mm day^{-1} for *P. nigra* grown in the Montseny Natural Park in northeastern Spain (924 mm annual precipitation with no irrigation) (Nadal-Sala et al., 2017) to 19.5 mm day^{-1} for *P. fremontii* grown in pots outside and watered to saturation daily (Nagler et al., 2003).

4.4 Discussion

4.4.1 Sap flow methodologies

Of the seven methodologies used to measure *Populus* sap flow in the articles reviewed here, the thermal dissipation methodology was implemented most frequently. Thermal dissipation sap flow methodologies are easy to install, do not require complex calculations, and are relatively inexpensive compared to other sap flow methodologies

(Smith and Allen, 1996). The original Granier calibration for calculating tree sap flow has also been demonstrated to be accurate for species that have diffuse porous wood anatomy (Bush et al., 2010), like *Populus* species. However, errors in calculated sap flow can still arise for *Populus*; Sun et al. (2012) compared *Populus* water uptake measured using potometers and calculated using thermal dissipation probes and found that the values derived from the thermal dissipation method were 34% lower than the measured values using potometers. They suggested developing species-specific calibrations to enhance the accuracy of the thermal dissipation method (Sun et al., 2012). The benefits of the thermal dissipation approach will likely ensure its continued use in *Populus* water use studies, though calibrations may need to be developed for the species in question.

4.4.2 Hybrid *Populus* water use

Hybrid *Populus* water use varied significantly among hybrid types, age classes, and water availability classes. To begin, hybrid vigor could be related to the higher rates of water use observed among intersectional than intrasectional hybrids in the current review. Elevated heterosis in intersectional compared to intrasectional *Populus* hybrids has been reported for a variety of traits. Li et al. (1998) observed greater juvenile stem growth (height, diameter, and growth rate) for one-year-old interspecific crosses of *P. tremuloides* and *P. tremula* than an intraspecific cross of *P. tremuloides*. Li and Wu (1996) corroborated these results and found the volume growth of *P. tremula* × *P. tremuloides* hybrids to be significantly greater than that of a pure *P. tremuloides* cross in the first three years after establishment. Similar results have been reported elsewhere, with interspecific hybrids also found to exhibit greater basal area increments (Rood et al., 2017), overall growth, and biomass production (Novotná et al., 2020) than intraspecific counterparts.

Such hybrid vigor makes interspecific hybrids ideal candidates for tree breeding and tree improvement programs (Nelson et al., 2018). Further, greater growth and biomass production of interspecific hybrids could be a factor contributing to the higher water use among interspecific than intraspecific hybrids seen here.

The differences observed among age classes, in which water use first increased as trees grew, then decreased with age (beyond six years), are likely due to *Populus* growth and development with time. For example, DeBell et al. (1996) reported leaf area index (LAI) values for hybrid *Populus* over seven years. They found that LAI peaked at around three or four years of age among two different clones, followed by steady or decreasing values. As the surface area of leaves affects rates of stomatal conductance, changes in LAI over the life of hybrid *Populus* can therefore affect transpiration rates. The initial trend reported by DeBell et al. (1996) is consistent with the results of this review in that increasing LAI values during the first four years of growth correspond with concurrent increases in water use. The increased water use that we observed from saplings to young hybrids has also been documented directly. Li et al. (2021) reported that both yearly cumulative values and daily rates of transpiration increased consistently as hybrid *P. tomentosa* trees aged from two- to five-years-old.

In the current study, hybrid *Populus* water use was also significantly different among water availability classes. Not surprisingly, hybrids exhibited the greatest water use when grown in conditions of high water availability, while rates did not differ significantly among medium and low water availability classes. Hybrid *Populus* are recognized for their ability to exploit available water resources by increasing their growth under conditions of plentiful water (Shock et al., 2002). This opportunistic water use

strategy likely influenced the results seen here of *Populus* grown under higher water availability conditions exhibiting increased water use. Not all hybrids respond in this way to varying levels of water availability, however; *Populus* genotypes exhibit different degrees of plasticity in aboveground and belowground responses to water availability. For instance, the observed increase in shallow fine root development by clone 'Eugenei' [*Populus* × *euramericana* (Dode) Guinier] in response to irrigation reported by Dickmann et al. (1996) would allow it to take more full advantage of elevated water availability than clones that are less plastic in their responses. More recently, Pilipović et al. (2021) reported broad variation in water use strategies (i.e., water consumers versus water conservers) of seven poplar genotypes belonging to three genomic groups [*P. deltoides* 'C916000', 'C916400', 'C918001'; (*P. trichocarpa* × *P. deltoides*) × *P. deltoides* 'NC13563', 'NC13624', 'NC13649'; *P. nigra* × *P. maximowiczii* 'NM2') growing at three sites in the Midwestern United States for ten years. Though out of the scope of the present work, further studies on genotypic variation in the ability to respond plastically to water availability could enhance decision-making for poplar-based environmental projects. Poplars identified as luxury consumers of water can then be selected for outplanting in floodplains, or other areas of abundant water, while poplars that exhibit conservative water use may be more suited to agroforestry systems or areas where irrigation is not feasible.

4.4.3 Non-hybrid *Populus* water use

Non-hybrid water use varied significantly among *Populus* species, with *P. fremontii* exhibiting the greatest rates, which were significantly higher than those of *P. deltoides*, *P. euphratica*, and *P. tremuloides*. The observed differences among species

likely had to do with differences in water availability of the species' habitats as well as different water use strategies of the species. To begin, the lower rates of water use exhibited by *P. euphratica* likely are related to the arid habitat that they are common to (Xu et al., 2016). Species native to dry areas can become drought tolerant and limit their growth, photosynthesis, and gas exchange to reduce their water requirements (Arntz and Delph, 2001). Opposite to *P. euphratica* is *P. fremontii*, whose riparian habitat (USDA NRCS, 2005) is likely a major factor influencing the high levels of transpiration exhibited by the species in the articles reviewed here. The interaction between water availability and species and its effect on non-hybrid *Populus* water use was not investigated in this study. However, exploring this interaction (and the interactions between all the factors evaluated here) in further detail could shed light on the interrelationships within the factors affecting *Populus* water use.

The experimental contexts in which non-hybrid *Populus* are grown also influenced water use, with shelterbelts exhibiting significantly greater water use than natural stands. This difference may be due to differences in water or nutrient availability among the two contexts. Natural stands are subject to the amount of water available from precipitation, while shelterbelts are generally located adjacent to agricultural fields, and may have increased water or nutrient availability because of the nearby agricultural irrigation and fertilization activities. Depending on the proximity of the shelterbelts to the agricultural operations, *Populus* grown in shelterbelts likely took advantage of the increased water and nutrient supplies, leading to the increased rates of water use exhibited here.

Like hybrid *Populus*, non-hybrids also exhibited significant differences in water use among water availability classes. The same reasons are relevant for these differences as for hybrids, namely, that water availability is a limiting factor of transpiration, and that increased water availability (below levels of water-logging) cause increased water use. *Populus* species differ in their abilities to respond to varying water availabilities (Braatne et al., 1992), as do genotypes within species (Possen et al., 2011). Specifically, differences in physiological parameters governing water use efficiency among species and genotypes can cause variable responses to water availability. Some species, for instance, are more water efficient during water stress conditions, and can make effective tradeoffs between water use and biomass production, while others do not limit their transpiration as much under water stress conditions (Cao et al., 2012).

4.5 Conclusions

Though *Populus* are commonly used in environmental applications around the world, information summarizing the methods used to quantify *Populus* sap flow, and the intrinsic and extrinsic factors influencing it are lacking. Based on our review of 133 articles, the thermal dissipation method was used most often to quantify *Populus* sap flow due to its ease of use and relative affordability. We also found that *Populus* water use varied among different intrinsic and extrinsic factors. Specifically, hybrid *Populus* water use varied significantly among hybrid type, tree age, and water availability. On the other hand, non-hybrid water use varied significantly among *Populus* species, experimental context, and water availability. Based on these results, water availability and genetic background (hybrid type for hybrids and species for non-hybrids) are important factors that dictate overall poplar water use and are important to consider when designing poplar-

based environmental systems. Our results indicate that for hybrid poplars, intersectional hybrids may be more suitable for use in pollution remediation systems or in locations with abundant water, while intrasectional hybrids may be more suited to areas with less available water. For non-hybrids, *P. fremontii* may be better suited to areas with abundant water, while *P. deltoides*, *P. euphratica*, and *P. tremuloides* may be more suited to drier areas or those without irrigation. An important methodological consideration for the present work regards the statistical method employed. While the Kruskal-Wallis test is suitable for comparing poplar water use within each of the intrinsic and extrinsic variables, this approach does not capture the interactions that exist among multiple factors. Such interactions could exist among the factors defined in this study and could also involve additional factors not included in the present analysis, such as fertilization regime. This, in addition to our choice not to include soil textural, physical, and chemical properties in our quantitative comparisons of water use, could affect the interpretation of the results presented here. Future work could expand upon this research by conducting a more comprehensive statistical analysis of variables and their interactions, and through the inclusion of soil properties. This study builds the foundation on some of the key factors that influence *Populus* water use by providing a standardized summary of available information. We set the stage for further research directions that investigate the effects of additional factors on *Populus* water use, such as soil properties, as well as the interactions that exist among factors.

4.6 Funding and acknowledgements

This work was supported by the Great Lakes Restoration Initiative, Template Number 738 (Landfill Runoff Reduction), the Center for Agroforestry at the University

of Missouri, and the USDA/ARS Dale Bumpers Small Farm Research Center under cooperative agreement (58- 6020-6-001) with the USDA Agricultural Research Service.

The findings and conclusions in this publication are those of the authors and should not be construed to represent any official USDA or U.S. Government determination or policy. We thank C. Li, S. Ghezehei, and anonymous journal reviewers for reviewing earlier versions of this manuscript. We would also like to thank the USDA Forest Service, the Great Lakes Restoration Initiative, the Center for Agroforestry at the University of Missouri, and the USDA/ARS Dale Bumpers Small Farm Research Center for their support.

Table 4.1. Definitions of intrinsic and extrinsic factors analyzed in a quantitative comparison of *Populus* water use reported in the literature. Studies were separated based on whether they assessed the water use of hybrid or non-hybrid *Populus*. Water use data were then classified according to the corresponding intrinsic and extrinsic factors.

Factor Type	Factor	Categories	Description
Hybrids			
Intrinsic Factors	Hybrid Type	Intersectional Hybrid	See Table 4.3 for list of *Populus* genotypes
		Intrasectional Hybrid	
	Tree Age	Sapling	0–2 years
		Young	3–6 years
		Mature	≥ 7 years
Extrinsic Factors	Planting Density	Low	< 1,000 trees/ha
		Medium	1,000–5,000 trees/ha
		High	> 5,000 trees/ha
	Water Availability	Low	< 600 mm annual precipitation
		Medium	600–850 mm annual precipitation
		High	> 850 mm annual precipitation
Non-Hybrids			
Intrinsic Factors	Species	8 species	See Table 4.5 for list of *Populus* species
	Tree Age	Juvenile	0–15 years
		Middle-aged	16–60 years
		Old	> 60 years
Extrinsic Factors	Planting Density	Low	< 1,000 trees/ha
		Medium	1,000–5,000 trees/ha
		High	> 5,000 trees/ha
	Experimental Context	Natural Stand	
		Plantation	
		Shelterbelt	
		Riparian	
	Water Availability	Low	≤ 600 mm annual precipitation, no irrigation
		Medium	600–850 mm annual precipitation, periodic irrigation
		High	>850 mm annual precipitation or constant irrigation or groundwater level < 1 m from soil surface

Table 4.2. Summary of studies that used sap flow methodologies to quantify hybrid *Populus* water use (n = 18 articles). Water use data were compiled from these studies and were quantitatively compared among intrinsic and extrinsic factors affecting hybrid *Populus* water use.

Reference	Country	Length of Data Collection	Number of Trees	Genotype[a]	Average Water Use (mm/day)
Allen et al. (1999)	United Kingdom	46 days	16 total (8 trees/genotype)	Beaupré	1.9-5.0
				Dorschkamp	1.6-3.0
Bloemen et al. (2017)	Belgium	39 days	3 total (1 tree/genotype)	Skado, Oudenberg, Grimminge	1.1
Chen et al. (2014)	China	April-October, 6 years	3-15 trees/year	74/76	0.7-1.6[b]
Ferro et al. (2001)	USA	18 days	4	DN34	6.9
Fischer et al. (2013)	Czech Republic	121 days	4	J-105	2.3[b]
Hall et al. (1998)	United Kingdom	40 days (SHB); 95 days (HPV)	10 total (5 trees/method)	Beaupré	6.0
Hinckley et al. (1994)	USA	53 days	6	50-194	3.6
Kim et al. (2008)	USA	126 days	10 total (2 monitoring periods, 5 trees/period)	*P. trichocarpa* Torr. & A. Gray × *P. deltoides* Bartr. Ex Marsh	3.4
Meiresonne (1999)	Belgium	26 days	6	Beaupré	1.9
Muller and Lambs (2009)	France	84 days	2	I-214	1.8
Navarro et al. (2018)	Belgium	217 days	12 total (3 trees/genotype)	Bakan	1.5
				Grimminge	2.9
				Koster	1.6
				Oudenberg	2.2
Navarro et al. (2020)	Belgium	~200 days	12 total (3 trees/genotype)	Bakan, Grimminge, Koster, Oudenberg	2.0-4.1[b]
Petzold et al. (2011)	Germany	2 growing seasons	6	Max 1	2.2-2.3
Preston and McBride (2004)	Canada	2 growing seasons	8 trees in 2001; 6 trees in 2002	DN2; DN34	1.4-3.8[b]
Schmidt-Walter et al. (2014)	Germany	200 days	7	J-105	2.4
Xi et al. (2014)	China	~200 days	12 total (3 trees/treatment)	B301	1.4-2.4
Zalesny et al. (2006)	USA	18 days/year (2 years)	15 trees in 2002; 9 trees in 2003	NM6	2.8-11.3
Zhang et al. (1999)	United Kingdom	~100	2	TT32	2.7-3.8

[a] See Table 4.3 for list of hybrid *Populus* genotype parentages.
[b] Data extracted from figures.

Table 4.3. Hybrid *Populus* genotype parentages from *Populus* water use studies (n = 18) reported in the literature.

Genotype	Parentage
Beaupré	*Populus trichocarpa* × *P. deltoides*
Dorschkamp	*P. deltoides* × *P. nigra*
Skado	*P. trichocarpa* × *P. maximowiczii*
Oudenberg	*P. deltoides* × *P. nigra*
Grimminge	*P. deltoides* × (*P. trichocarpa* × *P. deltoides*)
74/76	*Populus* × *euramericana*
DN34	*P. deltoides* × *P. nigra*
J-105	*P. nigra* × *P. maximowiczii*
50-194	*P. trichocarpa* × *P. deltoides* (F_1 hybrid)
I214	*P. deltoides* × *P. nigra*
Bakan	*P. trichocarpa* × *P. maximowiczii*
Koster	*P. deltoides* × *P. nigra*
Max 1	*P. maximowiczii* × *P. nigra*
DN2	*P. deltoides* × *P. nigra*
B301	(*P. tomentosa* × *P. bolleana*) × *P. tomentosa*
NM6	*P. nigra* × *P. maximowiczii*
TT32	*P. trichocarpa* × *P. tacamahaca*

Table 4.4. Summary of studies that used sap flow methodologies to quantify non-hybrid *Populus* water use (n = 33 articles). Water use data were compiled from these studies and were quantitatively compared among intrinsic and extrinsic factors affecting non-hybrid P*opulus* water use.

Reference	Country	Length of Data Collection	Number of Trees	Species[a]	Average Water Use (mm/day)
Angstmann et al. (2012)	Canada	2 growing seasons	25 trees	*P. tremuloides*	0.3-0.9[b]
Butler et al. (2007)	USA	2 growing seasons	NA	*Populus* spp.	4.2
Chang et al. (2006)	China	43 days	8 trees	*P. gansuensis*	3.9
Chen et al. (2004)	China	104 days (*P. gansuensis*)	2 total (1 tree/species)	*P. gansuensis*	2.6
		73 days (*P. euphratica*)		*P. euphratica*	0.8
Engel et al. (2004)	USA	24 days	12 total (6 trees/treatment)	*P. deltoides*	0.7-1.0
Ewers et al. (2007)	USA	2 growing seasons	8 trees	*P. tremuloides*	1.0-2.0
Fu et al. (2016)	China	172 days	NA	*P. simonii*	0.5
Fu et al. (2017)	China	167 days	6 trees	*P. simonii*	3.8
Gazal et al. (2006)	USA	218 days	8 total (4 trees/site)	*P. fremontii*	2.7-5.1[b]
Hogg and Hurdle (1997)	Canada	1-2 growing seasons (2 sites)	18 total (2 sites)	*P. tremuloides*	2.3-3.3[b]
Hogg et al. (1997)	Canada	231 days; 147 days	9 trees (CHP); 6 trees (HPV)	*P. tremuloides*	2.0-2.6
Hogg et al. (2000)	Canada	1 growing season	4 total trees	*P. tremuloides*	0.5-2.6
Hu et al. (2018)	China	2 growing seasons	6 trees	*P. simonii*	1.5-4.6
LaMalfa and Ryle (2008)	USA	1 growing season	12 trees	*P. tremuloides*	3.6
Lang et al. (2016)	China	1 growing season/site	2-6 trees/plot	*P. euphratica*	0.2-0.9
Nadal-Sala et al. (2017)	Spain	206 days	6 trees	*P. nigra*	0.2
Nagler et al. (2003)	USA	11 days	6 trees	*P. fremontii*	19.5
Nagler et al. (2007)	USA	45 days	20 total (10 trees/treatment)	*P. fremontii*	6.2-11.8
Ntshidi et al. (2018)	South Africa	1 year	3 trees	*P. alba* var. *canescens*	1.0-4.0
Pataki et al. (2000)	USA	70 days	5 trees	*P. tremuloides*	2.6
Pataki et al. (2005)	USA	66 days	36 total (18 trees/site)	*P. fremontii*	4.8-9.3
Samuelson et al. (2007)	USA	1 growing season	48 trees	*P. deltoides*	0.7-1.2
Shen et al. (2015)	China	2 growing seasons	8 trees	*P. gansuensis*	4.8-4.9
Si et al. (2015)	China	1 growing season	3 trees	*P. euphratica*	3.7
Strenge et al. (2018)	Kazakhstan	49 days	3 trees	*P. alba*	7.8
Thevs et al. (2019)	Kyrgyzstan	NA	NA	*P. nigra*	7.3
Uddling et al. (2008)	USA	2 growing seasons	108 trees	*P. tremuloides*	1.2-1.6
Venturas et al. (2018)	USA	~100 days	16 total trees (4 trees/treatment)	*P. tremuloides*	0.8-1.2
Voigt et al. (2018)	Uzbekistan	2 growing seasons	2 trees	*P. euphratica*	0.5-2.0
Xiao and Huang (2016)	China	152 days	6 trees	*P. gansuensis*	1.3-4.4
Yu et al. (2019)	China	1 year	NA	*P. euphratica*	0.9-1.3
Zhang et al. (2008)	China	1 growing season	4 trees	*P. euphratica*	1.0
Zhao et al. (2019)	China	3 growing seasons	9 trees	*P. euphratica*	2.0-3.2

[a] For species authorities, see Table 4.5.
[b] Data extracted from figures.

Table 4.5. *Populus* species and authorities from non-hybrid *Populus* water use studies (n = 33).

***Populus* Species**
P. alba L.
P. alba var. *canescens* Ait.
P. deltoides Bartr. ex Marsh.
P. euphratica Oliv.
P. fremontii S. Wats.
P. gansuensis Z. Wang & H.L. Yang
P. nigra L.
P. simonii Carr.
P. tremuloides Michx.

Figure 4.1. Flow chart of literature review article selection process.

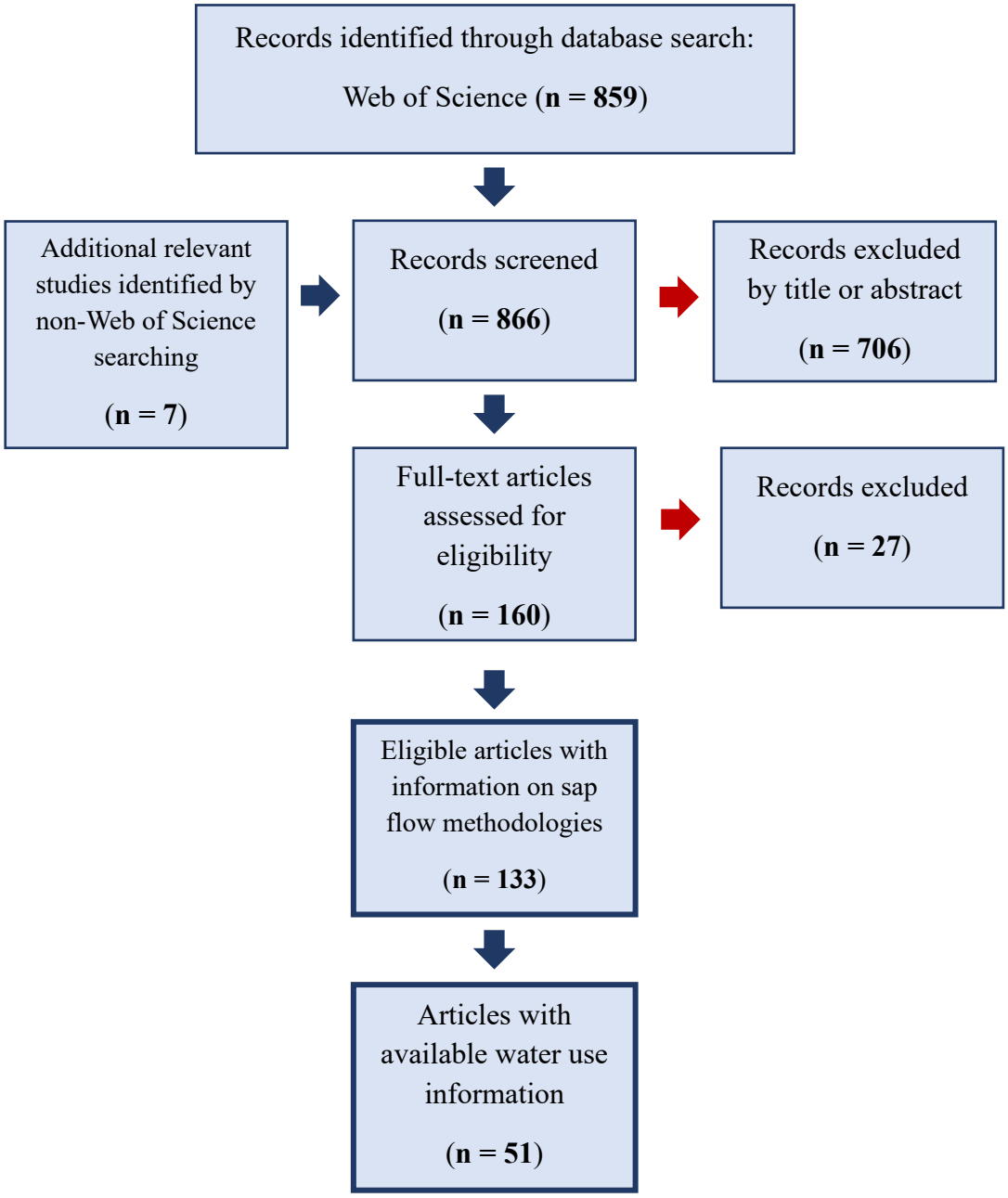

Figure 4.2. Sap flow methodologies used to quantify *Populus* sap flow reported in the literature (n = 133 articles). Constant heat methodologies (i.e., thermal dissipation, stem heat balance, trunk heat balance, and heat field deformation) are shown in blue, and pulsed heat methodologies (i.e., heat ratio, heat pulse velocity, and compensation heat pulse) are shown in green. The total percentage adds up to 99.9% due to rounding.

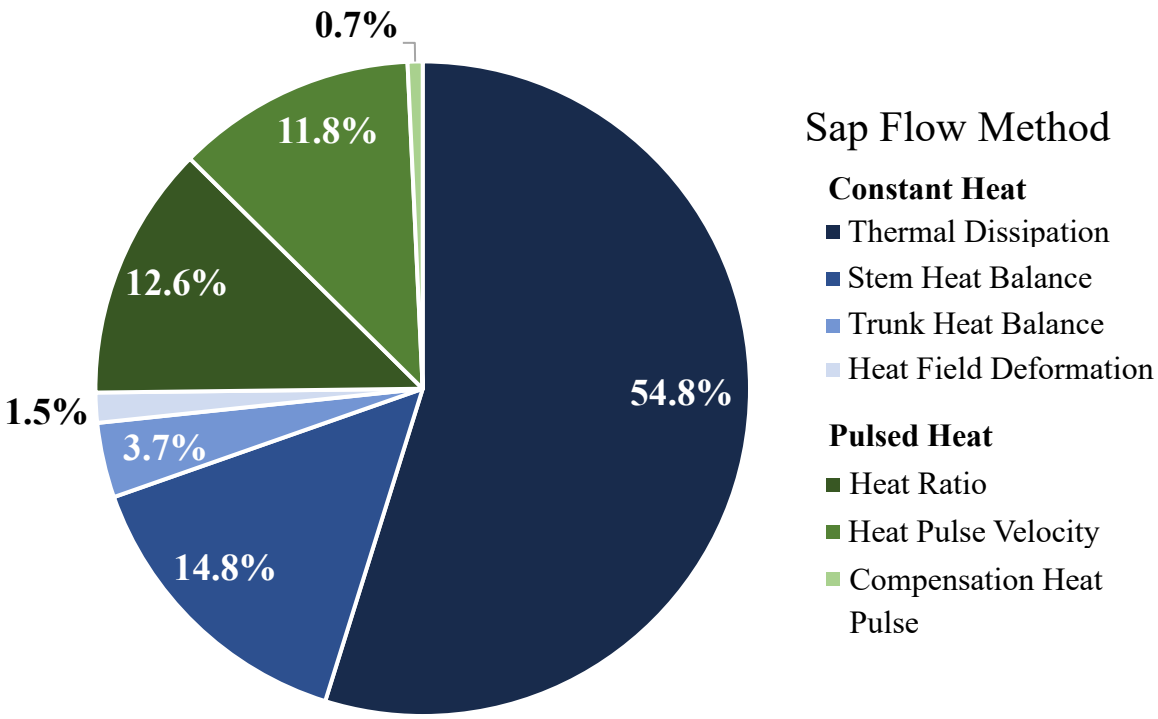

Figure 4.3. Hybrid *Populus* transpiration rates (mm/day) reported in 18 articles according to intrinsic factors (i.e., hybrid type and tree age). The black square within each plot represents the average water use for that factor. Significance levels identified using the Dunn post hoc test are given by stars: p-values < 0.05 are shown as '*', p-values < 0.01 are shown as '**', and p-values < 0.001 are shown as '***'.

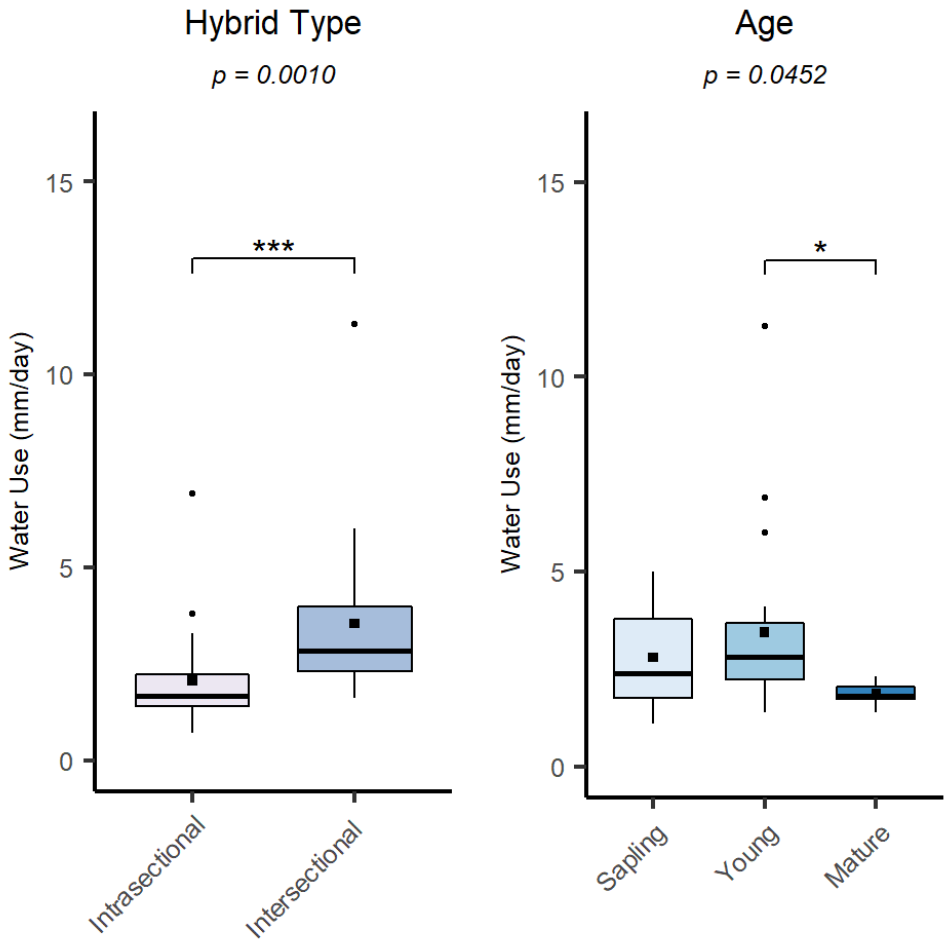

Figure 4.4. Hybrid *Populus* transpiration rates (mm/day) reported in 18 articles according to extrinsic factors (i.e., planting density and water availability). The black square within each plot represents the average water use for that factor. Significance levels identified using the Dunn post hoc test are given by stars: p-values < 0.05 are shown as '*', p-values < 0.01 are shown as '**', and p-values < 0.001 are shown as '***'.

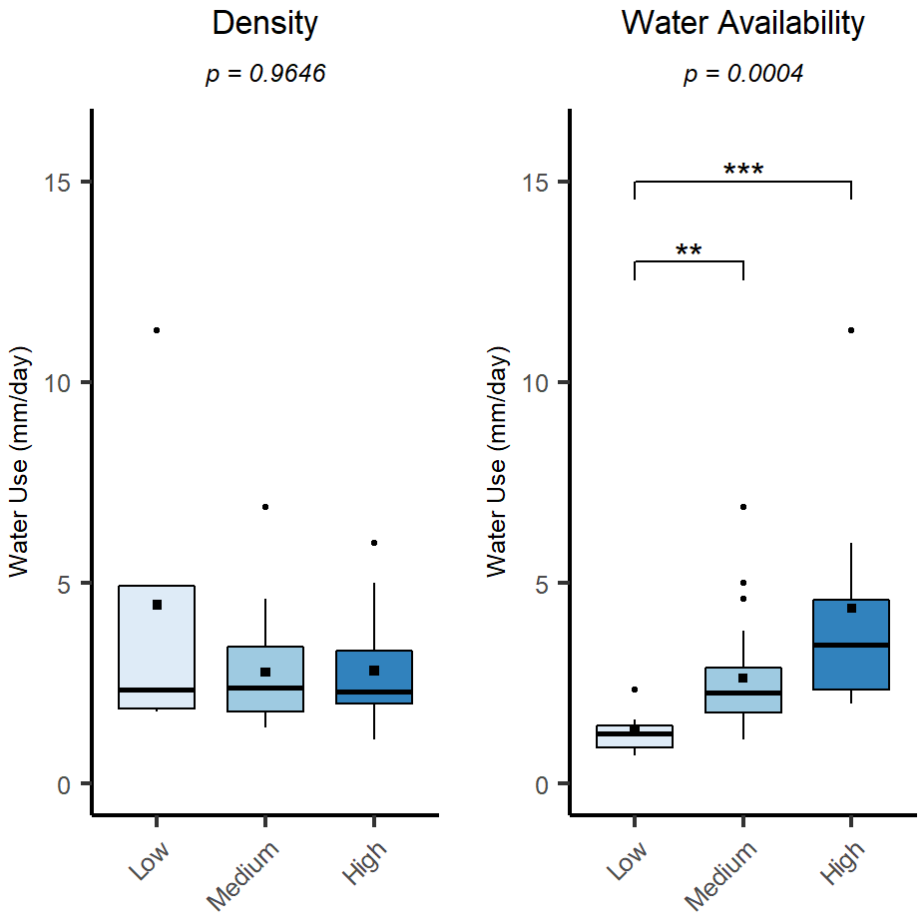

Figure 4.5. Non-hybrid *Populus* transpiration rates (mm/day) reported in 33 articles according to intrinsic factors (i.e., species and tree age). The black square within each plot represents the average water use for that factor. Significance levels identified using the Dunn post hoc test are given by stars: p-values < 0.05 are shown as '*', p-values < 0.01 are shown as '**', and p-values < 0.001 are shown as '***'.

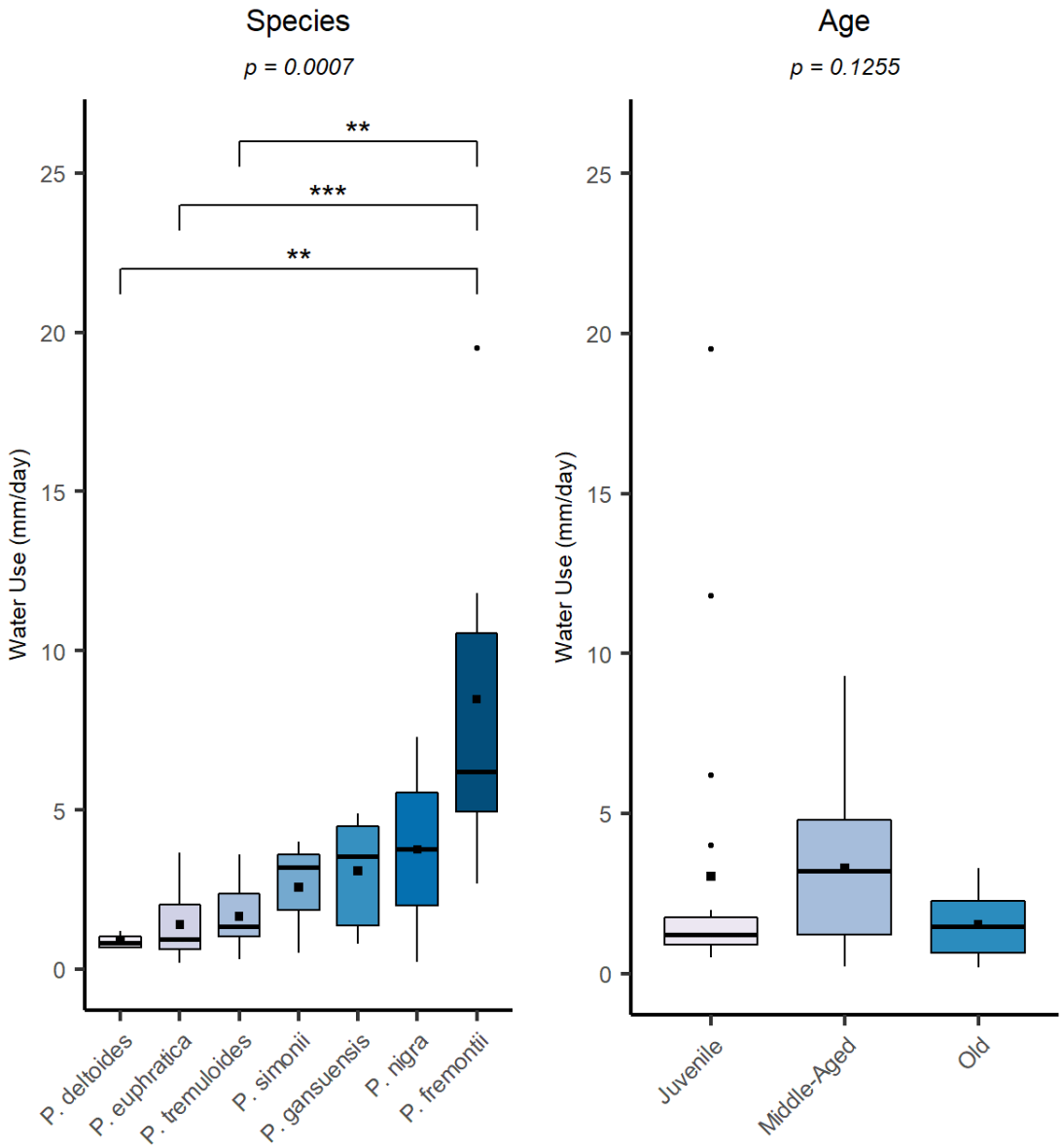

Figure 4.6. Non-hybrid *Populus* transpiration rates (mm/day) reported in 33 articles according to extrinsic factors (i.e., planting density, experimental context, and water availability). The black square within each plot represents the average water use for that factor. Significance levels identified using the Dunn post hoc test are given by stars: p-values < 0.05 are shown as '*', p-values < 0.01 are shown as '**', and p-values < 0.001 are shown as '***'.

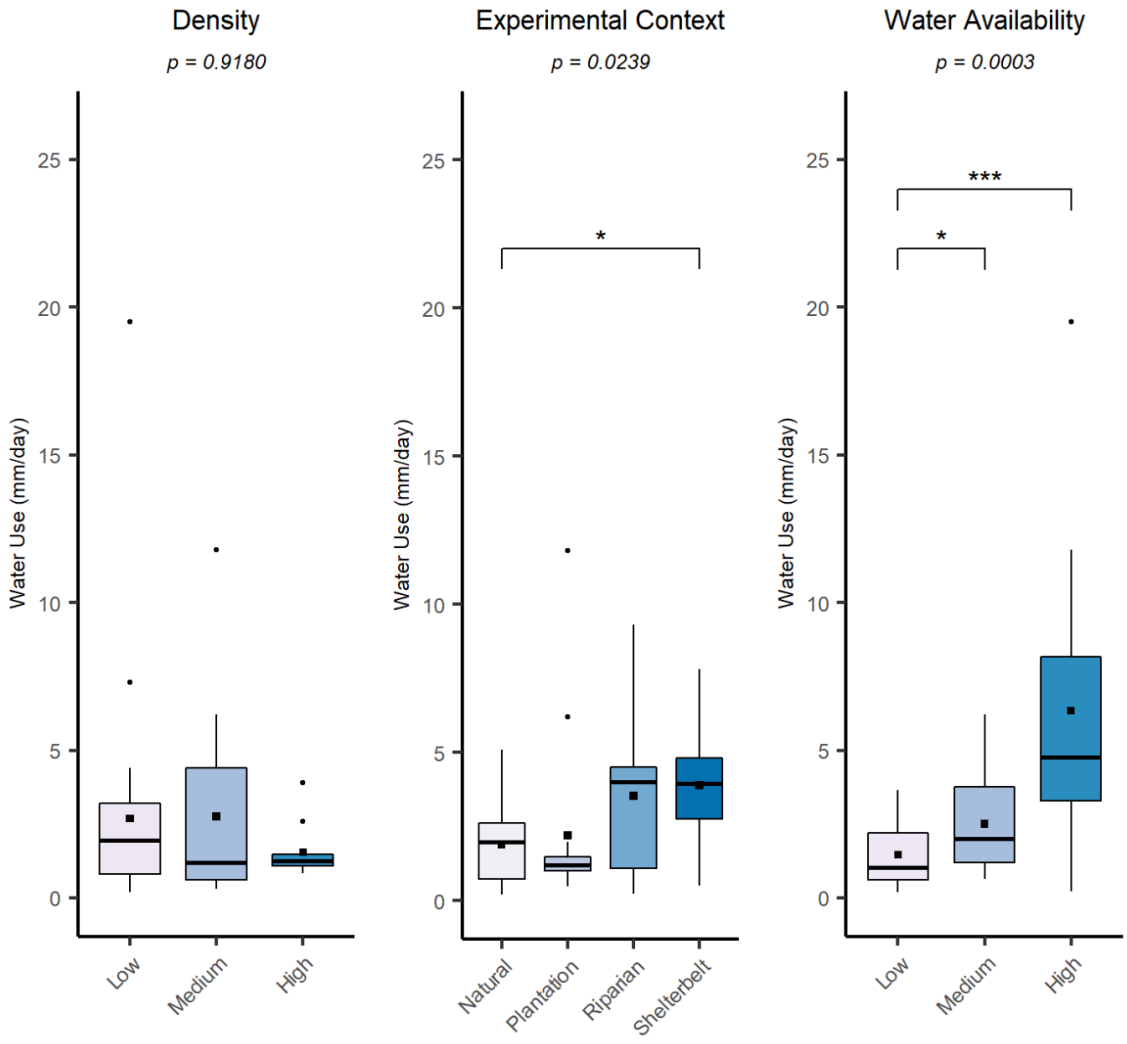

APPENDIX C.

Table C1. Sap flow methodologies implemented in *Populus* water use studies.

Method	References
Constant Heat	
Thermal Dissipation	Adelman et al. (2008); Anderegg et al. (2014); Angstmann et al. (2012); Bai et al. (2017); Barron-Gafford et al. (2007); Bladon et al. (2006); Bobich et al. (2010); Bovard et al. (2005); Bush et al. (2010); L. Chen et al. (2014); R. Chen et al. (2004); Clinton et al. (2004); Cox et al. (2005); Di Baccio et al. (2012); Di et al. (2019); Engel et al. (2004); Ewers et al. (2005, 2007); Ewers and Oren (2000); Ferro et al. (2001, 2013); D. Fischer et al. (2004); M. Fischer et al. (2013); Fu et al. (2016, 2017); Gazal et al. (2006); Gibert et al. (2006); Giovannelli et al. (2019); Guan et al. (2012); Hogg et al. (1997); Hoppe et al. (2020); Hu et al. (2018); Hultine et al. (2010); Kim et al. (2008); Kort and Blake (2007); LaMalfa and Ryle (2008); Lambs et al. (2006); Lambs and Muller (2002); Lang et al. (2016); Li et al. (2013); Loranty et al. (2008); Lu et al. (2013); Mackay et al. (2010); Maier et al. (2019); Moore and Owens (2012); Muller and Lambs (2009); Nadal-Sala et al. (2017); Nagler et al. (2003, 2007); Pataki et al. (2000, 2005); Samuelson et al. (2007); Sánchez-Pérez et al. (2008); Saveyn et al. (2008); Schmidt-Walter et al. (2014); Shen et al. (2015); Steppe et al. (2007); Strenge et al. (2018); Sun et al. (2012); Thevs et al. (2017, 2019); Tie et al. (2017); Uddling et al. (2008, 2009); H. Wang et al. (2017); S. Wang et al. (2019); Y. Wang et al. (2018); Xi et al. (2013, 2014, 2017); Xiao and Huang (2016); Yan et al. (2015); Zalesny et al. (2006); Zhou et al. (2013)
Stem Heat Balance	Allen et al. (1999); Bloemen et al. (2017); Bretfeld et al. (2017); Domenicano et al. (2011); Ewers et al. (2005); Hall et al. (1998); Kupper et al. (2011, 2012); Love and Sperry (2018); Meinzer et al. (1997); Navarro et al. (2018); Preston and McBride (2004); Ruan et al. (2009); Siebrecht et al. (2003); Thitihanakul et al. (2012); Tricker et al. (2009); Venturas et al. (2018); Vose et al. (2000); Zhang et al. (1997, 1999)
Trunk Heat Balance	Hinckley et al. (1994); Niglas et al. (2014); Petzold et al. (2011); Preston and McBride (2004); Salomón et al. (2019)
Heat Field Deformation	Meiresonne (1999); Nadezhdina et al. (2002)
Pulsed Heat	
Heat Ratio Method	Chen et al. (2017); Hao et al. (2010, 2013); Keyimu, Halik, Rouzi (2017); Li, Si et al. (2016); Li, Yu et al. (2016); Merlin and Landhäusser (2019); Ntshidi et al. (2018); Salomón et al. (2018); Si et al. (2015); Yu et al. (2013, 2016, 2018); Yu, Feng, Si, Pinkard (2019); Yu, Feng, Si, Xi et al. (2019); Zhao et al. (2017, 2019)
Heat Pulse Velocity	Butler et al. (2007); Chang et al. (2006); Cohen et al. (1981); Green et al. (2003); Guerva-Escobar et al. (2000); Hall et al. (1998); Hogg and Hurdle (1997); Hogg et al. (1997); Keyimu, Halik, Kurban (2017); Ma et al. (2012); Schaeffer et al. (2000); Si et al. (2007); Smith (1992); Xu et al. (2011); Zhang et al. (2008); Zhu et al. (2011)
Compensation Heat Pulse Method	Ma et al. (2013)

4.7 References

Adelman, J.D., Ewers, B.E., MacKay, D.S., 2008. Use of temporal patterns in vapor pressure deficit to explain spatial autocorrelation dynamics in tree transpiration. Tree Physiol. 28, 647–658. https://doi.org/10.1093/treephys/28.4.647.

Allen, S.J., Hall, R.L., Rosier, P.T.W., 1999. Transpiration by two poplar varieties grown as coppice for biomass production. Tree Physiol. 19, 493–501. https://doi.org/10.1093/treephys/19.8.493.

Anderegg, W.R.L., Anderegg, L.D.L., Berry, J.A., Field, C.B., 2014. Loss of whole-tree hydraulic conductance during severe drought and multi-year forest die-off. Oecologia 175, 11–23. https://doi.org/10.1007/s00442-013-2875-5.

Angstmann, J.L., Ewers, B.E., Kwon, H., 2012. Size-mediated tree transpiration along soil drainage gradients in a boreal black spruce forest wildfire chronosequence. Tree Physiol. 32, 599–611. https://doi.org/10.1093/treephys/tps021.

Armstrong, A., Johns, C., Tubby, I., 1999. Effects of spacing and cutting cycle on the yield of poplar grown as an energy crop. Biomass Bioenergy 17, 305–314. https://doi.org/10.1016/S0961-9534(99)00054-9.

Arntz, M.A., Delph, L.F., 2001. Pattern and process: evidence for the evolution of photosynthetic traits in natural populations. Oecologia 127, 455–467. https://doi.org/10.1007/s004420100650.

Bai, Y., Li, X., Liu, S., Wang, P., 2017. Modelling diurnal and seasonal hysteresis phenomena of canopy conductance in an oasis forest ecosystem. Agric. For. Meteorol. 246, 98–110. https://doi.org/10.1016/j.agrformet.2017.06.006.

Barron-Gafford, G.A., Grieve, K.A., Murthy, R., 2007. Leaf- and stand-level responses of a forested mesocosm to independent manipulations of temperature and vapor pressure deficit. New Phytol. 174, 614–625. https://doi.org/10.1111/j.1469-8137.2007.02035.x.

Benomar, L., DesRochers, A., Larocque, G.R., 2012. The effects of spacing on growth, morphology and biomass production and allocation in two hybrid poplar clones growing in the boreal region of Canada. Trees 26, 939–949. https://doi.org/10.1007/s00468-011-0671-6.

Bladon, K.D., Silins, U., Landhäusser, S.M., Lieffers, V.J., 2006. Differential transpiration by three boreal tree species in response to increased evaporative demand after variable retention harvesting. Agric. For. Meteorol. 138, 104–119. https://doi.org/10.1016/j.agrformet.2006.03.015.

Bloemen, J., Fichot, R., Horemans, J.A., Broeckx, L.S., Verlinden, M.S., Zenone, T., Ceulemans, R., 2017. Water use of a multigenotype poplar short-rotation coppice from tree to stand scale. GCB Bioenergy 9, 370–384. https://doi.org/10.1111/gcbb.12345.

Bobich, E.G., Barron-Gafford, G.A., Rascher, K.G., Murthy, R., 2010. Effects of drought and changes in vapour pressure deficit on water relations of *Populus deltoides* growing in ambient and elevated CO2. Tree Physiol. 30, 866–875. https://doi.org/10.1093/treephys/tpq036.

Bovard, B.D., Curtis, P.S., Vogel, C.S., Su, H.-B., Schmid, H.P., 2005. Environmental controls on sap flow in a northern hardwood forest. Tree Physiol. 25, 31–38. https://doi.org/10.1093/treephys/25.1.31.

Braatne, J.H., Hinckley, T.M., Stettler, R.F., 1992. Influence of soil water on the physiological and morphological components of plant water balance in *Populus trichocarpa*, *Populus deltoides* and their F1 hybrids. Tree Physiol. 11, 325–339. https://doi.org/10.1093/treephys/11.4.325.

Braatne, J.H., Rood, S.B., Heilman, P.E., 1996. Life history, ecology, and conservation of riparian cottonwoods in North America, in: Stettler, R.F., Bradshaw Jr., H.D., Heilman, P.E., Hinckley, T.M. (Eds.), Biology of *Populus* and Its Implications for Management and Conservation. NRC Research Press, Ottawa, Ontario.

Brady, N.C., Weil, R.R., 2010. Soil water: characteristics and behavior, in: Elements of the Nature and Properties of Soils. Pearson Prentice Hall, Upper Saddle River, N.J., pp. 132–164.

Bretfeld, M., Franklin, S.B., Hubbard, R.M., 2017. Initial evidence for simultaneous, bi-directional sap flow in roots of interconnected aspen ramets (*Populus tremuloides*). Folia Geobot. 52, 345–352. https://doi.org/10.1007/s12224-017-9285-0.

Burgess, P.J., Incoll, L.D., Corry, D.T., Beaton, A., Hart, B.J., 2005. Poplar (*Populus* spp) growth and crop yields in a silvoarable experiment at three lowland sites in England. Agrofor. Syst. 63, 157–169. https://doi.org/10.1007/s10457-004-7169-9.

Burns, R.M., Honkala, B.H. (Eds.), 1990. Silvics of North America: Volume 2. Hardwoods, Agricultural Handbook. United States Department of Agriculture (USDA), Forest Service. https://research.fs.usda.gov/treesearch/1548.

Bush, S.E., Hultine, K.R., Sperry, J.S., Ehleringer, J.R., 2010. Calibration of thermal dissipation sap flow probes for ring- and diffuse-porous trees. Tree Physiol. 30, 1545–1554. https://doi.org/10.1093/treephys/tpq096.

Butler, J.J., Kluitenberg, G.J., Whittemore, D.O., Loheide, S.P., Jin, W., Billinger, M.A., Zhan, X., 2007. A field investigation of phreatophyte-induced fluctuations in the water table. Water Resour. Res. 43. https://doi.org/10.1029/2005WR004627.

Cañellas, I., Huelin, P., Hernández, M.J., Ciria, P., Calvo, R., Gea-Izquierdo, G., Sixto, H., 2012. The effect of density on short rotation *Populus* sp. plantations in the Mediterranean area. Biomass and Bioenergy 46, 645–652. https://doi.org/10.1016/j.biombioe.2012.06.032.

Cao, X., Jia, J.B., Li, H., Li, M.C., Luo, J., Liang, Z.S., Liu, T.X., Liu, W.G., Peng, C.H., Luo, Z.B., 2012. Photosynthesis, water use efficiency and stable carbon isotope composition are associated with anatomical properties of leaf and xylem in six poplar species: poplar photosynthesis and δ ^{13} C associated with anatomy. Plant Biol. 14, 612–620. https://doi.org/10.1111/j.1438-8677.2011.00531.x.

Ceulemans, R., Deraedt, W., 1999. Production physiology and growth potential of poplars under short-rotation forestry culture. For. Ecol. Manage. 121, 9–23. https://doi.org/10.1016/S0378-1127(98)00564-7.

Chang, X., Zhao, W., Zhang, Z., Su, Y., 2006. Sap flow and tree conductance of shelter-belt in arid region of China. Agric. For. Meteorol. 138, 132–141. https://doi.org/10.1016/j.agrformet.2006.04.003.

Chen, L., Zhang, Z., Zha, T., Mo, K., Zhang, Y., Fang, X., 2014. Soil water affects transpiration response to rainfall and vapor pressure deficit in poplar plantation. N. For. 45, 235–250. https://doi.org/10.1007/s11056-014-9405-0.

Chen, R., Kang, E., Zhang, Z., Zhao, W., Song, K., Zhang, J., Lan, Y., 2004. Estimation of tree transpiration and response of tree conductance to meteorological variables in desert-oasis system of Northwest China. Sci. China Earth Sci. 47, 9–20. https://doi.org/10.1360/04zd0002.

Chen, Y., Li, W., Zhou, H., Chen, Yapeng, Hao, X., Fu, A., Ma, J., 2017. Experimental study on water transport observations of desert riparian forests in the lower reaches of the Tarim River in China. Int. J. Biometeorol. 61, 1055–1062. https://doi.org/10.1007/s00484-016-1285-x.

Clinton, B.D., Vose, J.M., Vroblesky, D.A., Harvey, G.J., 2004. Determination of the relative uptake of ground vs. surface water by *Populus deltoides* during phytoremediation. Int. J. Phytoremediat. 6, 239–252. https://doi.org/10.1080/16226510490496438.

Cohen, Y., Fuchs, M., Green, G.C., 1981. Improvement of the heat pulse method for determining sap flow in trees. Plant Cell Environ. 4, 391–397. https://doi.org/10.1111/j.1365-3040.1981.tb02117.x.

Corenblit, D., Steiger, J., González, E., Gurnell, A.M., Charrier, G., Darrozes, J., Dousseau, J., Julien, F., Lambs, L., Larrue, S., Roussel, E., Vautier, F., Voldoire, O., 2014. The biogeomorphological life cycle of poplars during the fluvial biogeomorphological succession: a special focus on *Populus nigra* L. Earth Surf. Process. Landforms 39, 546–563. https://doi.org/10.1002/esp.3515.

Cox, G., Fischer, D., Hart, S.C., Whitham, T.G., 2005. Nonresponse of native cottonwood trees to water additions during summer drought. W. N. Am. Nat. 65, 175–185. https://www.jstor.org/stable/41717444 (accessed 24 April 2022).

DeBell, D.S., Clendenen, G.W., Harrington, C.A., Zasada, J.C., 1996. Tree growth and stand development in short-rotation *Populus* plantings: 7-year results for two clones at three spacings. Biomass Bioenergy 11, 253–269. https://doi.org/10.1016/0961-9534(96)00020-7.

DeBell, D.S., Singleton, R., Harrington, C.A., Gartner, B.L., 2002. Wood density and fiber length in young *Populus* stems relation to clone, age, growth rate, and pruning. Wood Fiber Sci. 34, 529–539.

Di, N., Wang, Y., Clothier, B., Liu, Y., Jia, L., Xi, B., Shi, H., 2019. Modeling soil evaporation and the response of the crop coefficient to leaf area index in mature *Populus tomentosa* plantations growing under different soil water availabilities. Agric. Forest Meteorol. 264, 125–137. https://doi.org/10.1016/j.agrformet.2018.10.004.

Di Baccio, D., Minnocci, A., Sebastiani, L., Carraro, V., Grani, F., Anfodillo, T., Tognetti, R., 2012. Sap flow measurements for the evaluation of poplar clone performance

in remediation of soil polluted with olive mill wastewater. Acta Hortic. 175–181. https://doi.org/10.17660/ActaHortic.2012.951.21.

Dickmann, D.I., 2001. An overview of the genus *Populus*, in: Dickmann, Donald I., Isebrands, J.G., Eckenwalder, J.E., Richardson, J. (Eds.), Poplar Culture in North America, NRC Monograph Publishing Program. NRC Research Press, Ottawa, pp. 1–41.

Dickmann, D.I., Isebrands, J.G., Blake, T.J., Kosola, K., Kort, J., 2001. Physiological ecology of poplars, in: Dickmann, Donald I., Isebrands, J.G., Eckenwalder, J.E., Richardson, J. (Eds.), Poplar Culture in North America, NRC Monograph Publishing Program. NRC Research Press, Ottawa, pp. 77–115.

Dickmann, D.I., Nguyen, P.V., Pregitzer, K.S., 1996. Effects of irrigation and coppicing on above-ground growth, physiology, and fine-root dynamics of two field-grown hybrid poplar clones. For. Ecol. Manage. 80, 163–174. https://doi.org/10.1016/0378-1127(95)03611-3.

Dietz, A.C., Schnoor, J.L., 2001. Advances in phytoremediation. Environ. Health Perspect. 109, 163–168. https://doi.org/10.1289/ehp.01109s1163.

Dillen, S.Y., Rood, S.B., Ceulemans, R., 2010. Growth and physiology, in: Jansson, S., Bhalerao, R., Groover, A. (Eds.), Genetics and Genomics of *Populus*. Springer New York, New York, NY, pp. 39–63. https://doi.org/10.1007/978-1-4419-1541-2_3.

Domenicano, S., Coll, L., Messier, C., Berninger, F., 2011. Nitrogen forms affect root structure and water uptake in the hybrid poplar. New For. 42, 347–362. https://doi.org/10.1007/s11056-011-9256-x.

Douglas, G.B., McIvor, I.R., Lloyd-West, C.M., 2016. Early root development of field-grown poplar: effects of planting material and genotype. N. Z. J. For. Sci. 46, 1. https://doi.org/10.1186/s40490-015-0057-4.

Eckenwalder, J.E., 1996. Systematics and evolution of *Populus*, in: Stettler, R.F., Bradshaw Jr., H.D., Heilman, P.E., Hinckley, T.M. (Eds.), Biology of *Populus* and Its Implications for Management and Conservation. NRC Research Press, Ottawa, Ontario.

Engel, V.C., Griffin, K.L., Murthy, R., Patterson, L., Klimas, C., Potosnak, M., 2004. Growth CO_2 concentration modifies the transpiration response of *Populus deltoides* to drought and vapor pressure deficit. Tree Physiol. 24, 1137–1145. https://doi.org/10.1093/treephys/24.10.1137.

Ewers, B.E., Gower, S.T., Bond-Lamberty, B., Wang, C.K., 2005. Effects of stand age and tree species on canopy transpiration and average stomatal conductance of boreal forests. Plant Cell Environ. 28, 660–678. https://doi.org/10.1111/j.1365-3040.2005.01312.x.

Ewers, B.E., Mackay, D.S., Samanta, S., 2007. Interannual consistency in canopy stomatal conductance control of leaf water potential across seven tree species. Tree Physiol. 27, 11–24. https://doi.org/10.1093/treephys/27.1.11.

Ewers, B.E., Oren, R., 2000. Analyses of assumptions and errors in the calculation of stomatal conductance from sap flux measurements. Tree Physiol. 20, 579–589. https://doi.org/10.1093/treephys/20.9.579.

Fang, S., Li, H., Sun, Q., Chen, L., 2010. Biomass production and carbon stocks in poplar-crop intercropping systems: a case study in northwestern Jiangsu, China. Agrofor. Syst. 79, 213–222. https://doi.org/10.1007/s10457-010-9307-x.

Farmer Jr., R.E., 1996. The genecology of *Populus*, in: Stettler, R.F., Bradshaw Jr., H.D., Heilman, P.E., Hinckley, T.M. (Eds.), Biology of *Populus* and Its Implications for Management and Conservation. NRC Research Press, Ottawa.

Ferro, A.M., Adham, T., Berra, B., Tsao, D., 2013. Performance of deep-rooted phreatophytic trees at a site containing total petroleum hydrocarbons. Int. J. Phytoremediat. 15, 232–244. https://doi.org/10.1080/15226514.2012.687195.

Ferro, A., Chard, J., Kjelgren, R., Chard, B., Turner, D., Montague, T., 2001. Groundwater capture using hybrid poplar trees: evaluation of a system in Ogden, Utah. Int. J. Phytoremediat. 3, 87–104. https://doi.org/10.1080/15226510108500051.

Fischer, D.G., Hart, S.C., Whitham, T.G., Martinsen, G.D., Keim, P., 2004. Ecosystem implications of genetic variation in water-use of a dominant riparian tree. Oecologia 139, 288–297. https://doi.org/10.1007/s00442-004-1505-7.

Fischer, M., Orság, M., Trnka, M., Pohanková, E., Hlavinka, P., Tripathi, A.M., Zalud, Z., 2013. Annual and intra-annual water balance components of a short rotation poplar coppice based on sap flow and micrometeorological and hydrological approaches. Acta Hortic. 991, 401–408. https://doi.org/10.17660/ActaHortic.2013.991.49.

Fu, S., Sun, L., Luo, Y., 2016. Combining sap flow measurements and modelling to assess water needs in an oasis farmland shelterbelt of *Populus simonii* Carr in Northwest China. Agric. Water Manage. 177, 172–180. https://doi.org/10.1016/j.agwat.2016.07.015.

Fu, S., Sun, L., Luo, Y., 2017. Canopy conductance and stand transpiration of *Populus simonii* Carr in response to soil and atmospheric water deficits in farmland shelterbelt, Northwest China. Agrofor. Syst. 91, 1165–1180. https://doi.org/10.1007/s10457-016-0002-4.

Gazal, R.M., Scott, R.L., Goodrich, D.C., Williams, D.G., 2006. Controls on transpiration in a semiarid riparian cottonwood forest. Agric. For. Meteorol. 137, 56–67. https://doi.org/10.1016/j.agrformet.2006.03.002.

Gibert, D., Le Mouël, J.-L., Lambs, L., Nicollin, F., Perrier, F., 2006. Sap flow and daily electric potential variations in a tree trunk. Plant Sci. 171, 572–584. https://doi.org/10.1016/j.plantsci.2006.06.012.

Giovannelli, A., Traversi, M.L., Anichini, M., Hoshika, Y., Fares, S., Paoletti, E., 2019. Effect of long-term vs. short-term ambient ozone exposure on radial stem growth, sap flux and xylem morphology of O3-sensitive poplar trees. Forests 10, 396. https://doi.org/10.3390/f10050396.

Girona, J., Mata, M., Fereres, E., Goldhamer, D.A., Cohen, M., 2002. Evapotranspiration and soil water dynamics of peach trees under water deficits. Agric. Water Manage. 54, 107–122. https://doi.org/10.1016/S0378-3774(01)00149-4.

Green, S., Clothier, B., Jardine, B., 2003. Theory and practical application of heat pulse to measure sap flow. Agron. J. 95, 1371–1379. https://doi.org/10.2134/agronj2003.1371.

Guan, D.-X., Zhang, X.-J., Yuan, F.-H., Chen, N.-N., Wang, A.-Z., Wu, J.-B., Jin, C.-J., 2012. The relationship between sap flow of intercropped young poplar trees (*Populus×euramericana* cv. N3016) and environmental factors in a semiarid region of northeastern China. Hydrol. Process. 26, 2925–2937. https://doi.org/10.1002/hyp.8250.

Guevara-Escobar, A., Edwards, W.R.N., Morton, R.H., Kemp, P.D., Mackay, A.D., 2000. Tree water use and rainfall partitioning in a mature poplar-pasture system. Tree Physiol. 20, 97–106. https://doi.org/10.1093/treephys/20.2.97.

Guthrie Nichols, E., Cook, R.L., Landmeyer, J.E., Atkinson, B., Malone, D.R., Shaw, G., Woods, L., 2014. Phytoremediation of a petroleum-hydrocarbon contaminated shallow aquifer in Elizabeth City, North Carolina, USA: phytoremediation of a petroleum-hydrocarbon contaminated shallow aquifer. Remediation 24, 29–46. https://doi.org/10.1002/rem.21382

Hall, R.L., Allen, S.J., Rosier, P.T.W., Hopkins, R., 1998. Transpiration from coppiced poplar and willow measured using sap-flow methods. Agric. For. Meteorol. 90, 275–290. https://doi.org/10.1016/S0168-1923(98)00059-8

Hao, X., Chen, Y., Li, W., Guo, B., Zhao, R., 2010. Hydraulic lift in *Populus euphratica* Oliv. from the desert riparian vegetation of the Tarim River Basin. J. Arid Environ. 74, 905–911. https://doi.org/10.1016/j.jaridenv.2010.01.005.

Hao, X.-M., Chen, Y.-N., Guo, B., Ma, J.-X., 2013. Hydraulic redistribution of soil water in *Populus euphratica* Oliv. in a central Asian desert riparian forest. Ecohydrol. 6, 974–983. https://doi.org/10.1002/eco.1338.

Hart, J.F., de Araujo, F., Thomas, B.R., Mansfield, S.D., 2013. Wood quality and growth characterization across intra- and inter-specific hybrid aspen clones. Forests 4, 786–807. https://doi.org/10.3390/f4040786

Healy, R.W., Winter, T.C., LaBaugh, J.W., Franke, O.L., 2007. Water budgets: foundations for effective water resources and environmental management (Circular 1308). U.S. Geological Survey, Reston, Virginia. https://doi.org/10.3133/cir1308.

Hinckley, T.M., Brooks, J.R., Čermák, J., Ceulemans, R., Kučera, J., Meinzer, F.C., Roberts, D.A., 1994. Water flux in a hybrid poplar stand. Tree Physiol. 14, 1005–1018. https://doi.org/10.1093/treephys/14.7-8-9.1005.

Hogg, E.H., Black, T.A., den Hartog, G., Neumann, H.H., Zimmermann, R., Hurdle, P.A., Blanken, P.D., Nesic, Z., Yang, P.C., Staebler, R.M., McDonald, K.C., Oren, R., 1997. A comparison of sap flow and eddy fluxes of water vapor from a boreal deciduous forest. J. Geophys. Res. Atmos. 102, 28929–28937. https://doi.org/10.1029/96JD03881.

Hogg, E.H., Hurdle, P.A., 1997. Sap flow in trembling aspen: implications for stomatal responses to vapor pressure deficit. Tree Physiol. 17, 501–509. https://doi.org/10.1093/treephys/17.8-9.501.

Hogg, E.H., Price, D.T., Black, T.A., 2000. Postulated feedbacks of deciduous forest phenology on seasonal climate patterns in the western Canadian interior. J. Clim. 13, 4229–4243. https://doi.org/10.1175/1520-0442(2000)013<4229:PFODFP>2.0.CO;2.

Hoppe, J., Zhang, X., Thomas, F.M., 2020. Belowground inter-ramet water transport capacity in *Populus euphratica*, a Central Asian desert phreatophyte. Plant Biol. 22, 38–46. https://doi.org/10.1111/plb.13042.

Hu, G., Liu, H., Shangguan, H., Wu, X., Xu, X., Williams, M., 2018. The role of heartwood water storage for sem-arid trees under drought. Agric. For. Meteorol. 256–257, 534–541. https://doi.org/10.1016/j.agrformet.2018.04.007.

Huang, C.-W., Chu, C.-R., Hsieh, C.-I., Palmroth, S., Katul, G.G., 2015. Wind-induced leaf transpiration. Adv. Water Resour. 86, 240–255. https://doi.org/10.1016/j.advwatres.2015.10.009.

Hultine, K.R., Bush, S.E., Ehleringer, J.R., 2010. Ecophysiology of riparian cottonwood and willow before, during, and after two years of soil water removal. Ecol. Appl. 20, 347–361. https://doi.org/10.1890/09-0492.1.

Isebrands, J.G., Aronsson, P., Carlson, M., Ceulemans, R., Coleman, M., Dickinson, N., Dimitriou, J., Doty, S., Gardiner, E., Heinsoo, K., Johnson, J.D., Koo, Y.B., Kort, J., Kuzovkina, J., Licht, L., McCracken, A.R., McIvor, I., Mertens, P., Perttu, K., Riddell-Black, D., Robinson, B., Scarascia-Mugnozza, G., Schroeder, W.R., Stanturf, J., Volk, T.A., et al., 2014. Environmental applications of poplars and willows, in: Isebrands, J.G., Richardson, J. (Eds.), Poplars and Willows: Trees for

Society and the Environment. CABI, Wallingford, pp. 258–336. https://doi.org/10.1079/9781780641089.0258.

Jelicic Kadic, A., Vucic, K., Dosenovic, S., Sapunar, D., Puljak, L., 2016. Extracting data from figures with software was faster, with higher interrater reliability than manual extraction. J. Clin. Epidemiol. 74, 119–123. https://doi.org/10.1016/j.jclinepi.2016.01.002.

Jones, M.B., 1985. Plant microclimate, in: Coombs, J., Hall, D.O., Long, S.P., Scurlock, J.M.O. (Eds.), Techniques in Bioproductivity and Photosynthesis. Elsevier, pp. 26–40. https://doi.org/10.1016/B978-0-08-031999-5.50013-3.

Karačić, A., Weih, M., 2006. Variation in growth and resource utilisation among eight poplar clones grown under different irrigation and fertilisation regimes in Sweden. Biomass Bioenergy 30, 115–124. https://doi.org/10.1016/j.biombioe.2005.11.007.

Katul, G.G., Oren, R., Manzoni, S., Higgins, C., Parlange, M.B., 2012. Evapotranspiration: a process driving mass transport and energy exchange in the soil-plant-atmosphere-climate system. Rev. Geophys. 50. https://doi.org/10.1029/2011RG000366.

Kauter, D., Lewandowski, I., Claupein, W., 2003. Quantity and quality of harvestable biomass from *Populus* short rotation coppice for solid fuel use—a review of the physiological basis and management influences. Biomass Bioenergy 24, 411–427. https://doi.org/10.1016/S0961-9534(02)00177-0.

Keyimu, M., Halik, Ü., Kurban, A., 2017. Estimation of water consumption of riparian forest in the lower reaches of Tarim River, northwest China. Environ. Earth Sci. 76, 547. https://doi.org/10.1007/s12665-017-6801-8.

Keyimu, M., Halik, Ü., Rouzi, A., 2017. Relating water use to tree vitality of *Populus euphratica* Oliv. in the Lower Tarim River, NW China. Water 9, 622. https://doi.org/10.3390/w9080622.

Khan, G.S., Khaliq Chaudhry, A., 2007. Effect of spacing and plant density on the growth of poplar (*Populus deltoides*) trees under agro-forestry system. Pakistan J. Agric. Sci. 44, 321–327.

Kim, H.-S., Oren, R., Hinckley, T.M., 2008. Actual and potential transpiration and carbon assimilation in an irrigated poplar plantation. Tree Physiol. 28, 559–577. https://doi.org/10.1093/treephys/28.4.559.

Kort, J., Blake, T.J., 2007. Sap velocity as an indicator of diurnal and long-term hydraulic resistance changes in mature 'Walker' hybrid poplar trees. Can. J. Bot. 85, 1033–1041. https://doi.org/10.1139/B07-030.

Köstner, B., Granier, A., Cermák, J., 1998. Sapflow measurements in forest stands: methods and uncertainties. Ann. For. Sci. 55, 13–27. https://doi.org/10.1051/forest:19980102.

Kozlowski, T.T., Pallardy, S.G., 1997. Transpiration and plant water balance, in: Physiology of Woody Plants. Academic Press, San Diego, pp. 270–308.

Kramer, P.J., Boyer, J.S., 1995. Water Relations of Plants and Soils. Academic Press, San Diego.

Kupper, P., Rohula, G., Saksing, L., Sellin, A., Lõhmus, K., Ostonen, I., Helmisaari, H.-S., Sõber, A., 2012. Does soil nutrient availability influence night-time water flux of aspen saplings? Environ. Exp. Bot. 82, 37–42. https://doi.org/10.1016/j.envexpbot.2012.03.013.

Kupper, P., Sõber, J., Sellin, A., Lõhmus, K., Tullus, A., Räim, O., Lubenets, K., Tulva, I., Uri, V., Zobel, M., Kull, O., Sõber, A., 2011. An experimental facility for free air humidity manipulation (FAHM) can alter water flux through deciduous tree canopy. Environ. Exp. Bot. 72, 432–438. https://doi.org/10.1016/j.envexpbot.2010.09.003.

LaMalfa, E.M., Ryle, R., 2008. Differential snowpack accumulation and water dynamics in aspen and conifer communities: implications for water yield and ecosystem function. Ecosystems 11, 569–581. https://doi.org/10.1007/s10021-008-9143-2.

Lambs, L., Loubiat, M., Girel, J., Tissier, J., Peltier, J.-P., Marigo, G., 2006. Survival and acclimatation of *Populus nigra* to drier conditions after damming of an alpine river, southeast France. Ann. For. Sci. 63, 377–385. https://doi.org/10.1051/forest:2006018.

Lambs, L., Muller, É., 2002. Sap flow and water transfer in the Garonne River riparian woodland, France: first results on poplar and willow. Ann. For. Sci. 59, 301–315. https://doi.org/10.1051/forest:2002026.

Lang, P., Ahlborn, J., Schäfer, P., Wommelsdorf, T., Jeschke, M., Zhang, X., Thomas, F.M., 2016. Growth and water use of *Populus euphratica* trees and stands with different water supply along the Tarim River, NW China. For. Ecol. Manage. 380, 139–148. https://doi.org/10.1016/j.foreco.2016.08.049.

Lemus, R., Lal, R., 2005. Bioenergy crops and carbon sequestration. Crit. Rev. Plant Sci. 24, 1–21. https://doi.org/10.1080/07352680590910393.

Li, B., Wu, R., 1996. Genetic causes of heterosis in juvenile aspen: a quantitative comparison across intra- and inter-specific hybrids. Theor. Appl. Genet. 93, 380–391. https://doi.org/10.1007/BF00223180.

Li, B., Howe, G.T., Wu, R., 1998. Developmental factors responsible for heterosis in aspen hybrids (*Populus tremuloides* × *P. tremula*). Tree Physiol. 18, 29–36. https://doi.org/10.1093/treephys/18.1.29.

Li, D., Liu, J., Verhoef, A., Xi, B., Hernandez-Santana, V., 2021. Understanding the relationship between biomass production and water use of *Populus tomentosa* trees throughout an entire short-rotation. Agric. Water Manage. 246, 106710. https://doi.org/10.1016/j.agwat.2020.106710.

Li, S., Chen, B., Lu, S., Pan, Q., Zhang, Y., Yang, X., 2013. Water use characteristics of artificial poplar forest based on Granier's thermal dissipation probe method. J Food Agric. Environ. 11, 1255–1261.

Li, W., Si, J., Yu, T., Li, X., 2016. Response of *Populus euphratica* Oliv. sap flow to environmental variables for a desert riparian forest in the Heihe River Basin,

Northwest China. J. Arid Land 8, 591–603. https://doi.org/10.1007/s40333-016-0045-4.

Li, W., Yu, T., Li, X., Zhao, C., 2016. Sap flow characteristics and their response to environmental variables in a desert riparian forest along lower Heihe River Basin, Northwest China. Environ. Monit. Assess. 188, 561. https://doi.org/10.1007/s10661-016-5570-2.

Loranty, M.M., Mackay, D.S., Ewers, B.E., Adelman, J.D., Kruger, E.L., 2008. Environmental drivers of spatial variation in whole-tree transpiration in an aspen-dominated upland-to-wetland forest gradient. Water Resour. Res. 44, W02441. https://doi.org/10.1029/2007WR006272.

Love, D.M., Sperry, J.S., 2018. In situ embolism induction reveals vessel refilling in a natural aspen stand. Tree Physiol. 38, 1006–1015. https://doi.org/10.1093/treephys/tpy007.

Lowry, R., n.d. Subchapter 14a. The kruskal-wallis test for 3 or more independent samples, in: Concepts and Applications of Inferential Statistics. http://vassarstats.net/textbook/ (accessed 7 April 2022).

Lu, S., Chen, B., Li, S., Pan, Q., Zhang, Y., Yang, X., 2013. Variations of whole-tree transpiration of poplar with different diameters in the wet and dry seasons. J. Food Agric. Environ. 11, 1262–1267.

Ma, J.-X., Chen, Y.-N., Li, W.-H., Huang, X., Zhu, C.-G., Ma, X.-D., 2012. Sap flow characteristics of four typical species in desert shelter forest and their responses to

environmental factors. Environ. Earth Sci. 67, 151–160. https://doi.org/10.1007/s12665-011-1488-8.

Ma, J.-X., Huang, X., Li, W.-H., Zhu, C.-G., 2013. Sap flow and trunk maximum daily shrinkage (MDS) measurements for diagnosing water status of *Populus euphratica* in an inland river basin of Northwest China. Ecohydrol. 6, 994–1000. https://doi.org/10.1002/eco.1439.

Mackay, D.S., Ewers, B.E., Loranty, M.M., Kruger, E.L., 2010. On the representativeness of plot size and location for scaling transpiration from trees to a stand. J. Geophys. Res. 115, G02016. https://doi.org/10.1029/2009JG001092

Maier, C., Burley, J., Cook, R., Ghezehei, S.B., Hazel, D.W., Nichols, E.G., 2019. Tree water use, water use efficiency, and carbon isotope discrimination in relation to growth potential in *Populus deltoides* and hybrids under field conditions. Forests 10, 993. https://doi.org/10.3390/f10110993

McIvor, I., Douglas, G., Dymond, J., Eyles, G., Marden, M., 2011. Pastoral hill slope erosion in New Zealand and the role of poplar and willow trees in its reduction, in: Godone, D. (Ed.), Soil Erosion Issues in Agriculture. InTech. https://doi.org/10.5772/24365.

Meinzer, F.C., Hinckley, T.M., Ceulemans, R., 1997. Apparent responses of stomata to transpiration and humidity in a hybrid poplar canopy. Plant Cell Environ. 20, 1301–1308. https://doi.org/10.1046/j.1365-3040.1997.d01-18.x.

Meiresonne, L., 1999. Measured sap flow and simulated transpiration from a poplar stand in Flanders (Belgium). Agric. For. Meteorol. 96, 165–179. https://doi.org/10.1016/S0168-1923(99)00066-0.

Merlin, M., Landhäusser, S.M., 2019. Seasonal patterns of water uptake in *Populus tremuloides* and *Picea glauca* on a boreal reclamation site is species specific and modulated by capping soil depth and slope position. Plant Soil 439, 487–504. https://doi.org/10.1007/s11104-019-04029-6.

Miller, R.O., Bender, B.A., Irving, P.N., Zuidema, K.T., 2016. Common short rotation poplar growth patterns observed in ten trials over 18 years in Michigan, USA (No. 2016(e)). in: Forest Biomass Innovation Center Research Report. Michigan State University.

Moore, G.W., Owens, M.K., 2012. Transpirational water loss in invaded and restored semiarid riparian forests. Restor. Ecol. 20, 346–351. https://doi.org/10.1111/j.1526-100X.2011.00774.x.

Muller, E., Lambs, L., 2009. Daily variations of water use with vapor pressure deficit in a plantation of I214 poplars. Water 1, 32–42. https://doi.org/10.3390/w1010032.

Nadal-Sala, D., Sabaté, S., Sánchez-Costa, E., Poblador, S., Sabater, F., Gracia, C., 2017. Growth and water use performance of four co-occurring riparian tree species in a Mediterranean riparian forest. For Ecol. Manage. 396, 132–142. https://doi.org/10.1016/j.foreco.2017.04.021.

Nadezhdina, N., 2018. Revisiting the Heat Field Deformation (HFD) method for measuring sap flow. iForest 11, 118–130. https://doi.org/10.3832/ifor2381-011.

Nadezhdina, N., Čermák, J., Ceulemans, R., 2002. Radial patterns of sap flow in woody stems of dominant and understory species: scaling errors associated with positioning of sensors. Tree Physiol. 22, 907–918. https://doi.org/10.1093/treephys/22.13.907.

Nagler, P.L., Glenn, E.P., Lewis Thompson, T., 2003. Comparison of transpiration rates among saltcedar, cottonwood and willow trees by sap flow and canopy temperature methods. Agric. For. Meteorol. 116, 73–89. https://doi.org/10.1016/S0168-1923(02)00251-4.

Nagler, P., Jetton, A., Fleming, J., Didan, K., Glenn, E., Erker, J., Morino, K., Milliken, J., Gloss, S., 2007. Evapotranspiration in a cottonwood (*Populus fremontii*) restoration plantation estimated by sap flow and remote sensing methods. Agric. For. Meteorol. 144, 95–110. https://doi.org/10.1016/j.agrformet.2007.02.002.

Navarro, A., Portillo-Estrada, M., Arriga, N., Vanbeveren, S.P.P., Ceulemans, R., 2018. Genotypic variation in transpiration of coppiced poplar during the third rotation of a short-rotation bio-energy culture. GCB Bioenergy 10, 592–607. https://doi.org/10.1111/gcbb.12526.

Navarro, A., Portillo-Estrada, M., Ceulemans, R., 2020. Identifying the best plant water status indicator for bio-energy poplar genotypes. GCB Bioenergy 12, 426–444. https://doi.org/10.1111/gcbb.12687.

Nelson, N.D., Berguson, W.E., McMahon, B.G., Cai, M., Buchman, D.J., 2018. Growth performance and stability of hybrid poplar clones in simultaneous tests on six

sites. Biomass Bioenergy 118, 115–125. https://doi.org/10.1016/j.biombioe.2018.08.007.

Niglas, A., Kupper, P., Tullus, A., Sellin, A., 2014. Responses of sap flow, leaf gas exchange and growth of hybrid aspen to elevated atmospheric humidity under field conditions. AoB PLANTS 6, plu021. https://doi.org/10.1093/aobpla/plu021.

Njakou Djomo, S., Ac, A., Zenone, T., De Groote, T., Bergante, S., Facciotto, G., Sixto, H., Ciria Ciria, P., Weger, J., Ceulemans, R., 2015. Energy performances of intensive and extensive short rotation cropping systems for woody biomass production in the EU. Renew. Sustain. Energy Rev. 41, 845–854. https://doi.org/10.1016/j.rser.2014.08.058.

NOAA (National Oceanic and Atmospheric Administration), 2022. NOAA Solar Calculator: Sunrise, sunset, and noon for any place on Earth. National Oceanic and Atmospheric Administration, Washington. https://www.esrl.noaa.gov/gmd/grad/solcalc/ (accessed 7 April 2022).

Novotná, K., Štochlová, P., Benetka, V., 2020. Verification of new *Populus nigra* L. clone improvement based on their performance over three rotations. iForest 13, 185–193. https://doi.org/10.3832/ifor3171-013.

Ntshidi, Z., Gush, M., Dzikiti, S., Le Maitre, D., 2018. Characterising the water use and hydraulic properties of riparian tree invasions: a case study of *Populus canescens* in South Africa. WSA 44. https://doi.org/10.4314/wsa.v44i2.18.

Ogle, D.H., Doll, J.C., Wheeler, P., Dinno, A., 2022. FSA: Fisheries Stock Analysis. R package version 0.9.3, https://github.com/fishR-Core-Team/FSA.

Osroosh, Y., Peters, R.T., Campbell, C.S., Zhang, Q., 2016. Comparison of irrigation automation algorithms for drip-irrigated apple trees. Comput. Electron. Agric. 128, 87–99. https://doi.org/10.1016/j.compag.2016.08.013.

Pataki, D.E., Oren, R., Smith, W.K., 2000. Sap flux of co-occurring species in a western subalpine forest during seasonal soil drought. Ecology 81, 2557–2566. https://doi.org/10.1890/0012-9658(2000)081[2557:SFOCOS]2.0.CO;2.

Pataki, D.E., Bush, S.E., Gardner, P., Solomon, D.K., Ehleringer, J.R., 2005. Ecohydrology in a Colorado river riparian forest: implications for the decline of *Populus Fremontii*. Ecol. Appl. 15, 1009–1018. https://doi.org/10.1890/04-1272.

Pavlidis, G., Tsihrintzis, V.A., 2018. Environmental benefits and control of pollution to surface water and groundwater by agroforestry systems: a review. Water Resour. Manage. 32, 1–29. https://doi.org/10.1007/s11269-017-1805-4.

Peri, P.L., Bloomberg, M., 2002. Windbreaks in southern Patagonia, Argentina: a review of research on growth models, windspeed reduction, and effects on crops. Agrofor. Syst. 56, 129–144. https://doi.org/10.1023/A:1021314927209.

Peszlen, I., 1994. Influence of age on selected anatomical properties of *Populus* clones. IAWA J. 15, 311–321. https://doi.org/10.1163/22941932-90000613.

Peters, R.L., Fonti, P., Frank, D.C., Poyatos, R., Pappas, C., Kahmen, A., Carraro, V., Prendin, A.L., Schneider, L., Baltzer, J.L., Baron-Gafford, G.A., Dietrich, L., Heinrich, I., Minor, R.L., Sonnentag, O., Matheny, A.M., Wightman, M.G., Steppe, K., 2018. Quantification of uncertainties in conifer sap flow measured

with the thermal dissipation method. New Phytol. 219, 1283–1299. https://doi.org/10.1111/nph.15241.

Petzold, R., Schwärzel, K., Feger, K.-H., 2011. Transpiration of a hybrid poplar plantation in Saxony (Germany) in response to climate and soil conditions. Eur. J. For. Res. 130, 695–706. https://doi.org/10.1007/s10342-010-0459-z.

Pilipović, A., Headlee, W.L., Zalesny, R.S., Pekeč, S., Bauer, E.O. 2021., Water use efficiency of poplars grown for biomass production in the Midwestern United States. GCB Bioenergy 14, 287–306. https://doi.org/10.1111/gcbb.12887.

Possen, B.J.H.M., Oksanen, E., Rousi, M., Ruhanen, H., Ahonen, V., Tervahauta, A., Heinonen, J., Heiskanen, J., Kärenlampi, S., Vapaavuori, E., 2011. Adaptability of birch (*Betula pendula* Roth) and aspen (*Populus tremula* L.) genotypes to different soil moisture conditions. For. Ecol. Manage. 262, 1387–1399. https://doi.org/10.1016/j.foreco.2011.06.035.

Preston, G.M., McBride, R.A., 2004. Assessing the use of poplar tree systems as a landfill evapotranspiration barrier with the SHAW model. Waste Manage. Res. 22, 291–305. https://doi.org/10.1177/0734242X04045429.

Puri, S., Singh, V., Bhushan, B., Singh, S., 1994. Biomass production and distribution of roots in three stands of *Populus deltoides*. For. Ecol. Manage. 65, 135–147. https://doi.org/10.1016/0378-1127(94)90165-1.

R Core Team, 2020. R: A Language and Environment for Statistical Computing. R Foundation for Statistical Computing, Vienna, Austria. https://www.R-project.org/.

Rockwood, D.L., Naidu, C.V., Carter, D.R., Rahmani, M., Spriggs, T.A., Lin, C., Alker, G.R., Isebrands, J.G., Segrest, S.A., 2004. Short-rotation woody crops and phytoremediation: opportunities for agroforestry? Agrofor. Syst. 61–62, 51–63. https://doi.org/10.1023/B:AGFO.0000028989.72186.e6.

Rood, S.B., Goater, L.A., McCaffrey, D., Montgomery, J.S., Hopkinson, C., Pearce, D.W., 2017. Growth of riparian cottonwoods: heterosis in some intersectional *Populus* hybrids and clonal expansion of females. Trees 31, 1069–1081. https://doi.org/10.1007/s00468-017-1531-9.

Ruan, X., Wang, Q., Pan, C.-D., Chen, Y.-N., Jiang, H., 2009. Physiological acclimation strategies of riparian plants to environment change in the delta of the Tarim River, China. Environ. Geol. 57, 1761–1773. https://doi.org/10.1007/s00254-008-1461-3.

Salomón, R.L., De Roo, L., Bodé, S., Boeckx, P., Steppe, K., 2019. Isotope ratio laser spectroscopy to disentangle xylem-transported from locally respired CO_2 in stem CO_2 efflux. Tree Physiol. 39, 819–830. https://doi.org/10.1093/treephys/tpy152.

Salomón, R.L., De Schepper, V., Valbuena-Carabaña, M., Gil, L., Steppe, K., 2018. Daytime depression in temperature-normalised stem CO_2 efflux in young poplar trees is dominated by low turgor pressure rather than by internal transport of respired CO2. New Phytol. 217, 586–598. https://doi.org/10.1111/nph.14831.

Samuelson, L.J., Stokes, T.A., Coleman, M.D., 2007. Influence of irrigation and fertilization on transpiration and hydraulic properties of *Populus deltoides*. Tree Physiol. 27, 765–774. https://doi.org/10.1093/treephys/27.5.765.

Sánchez-Pérez, J.M., Lucot, E., Bariac, T., Trémolières, M., 2008. Water uptake by trees in a riparian hardwood forest (Rhine floodplain, France). Hydrol. Process. 22, 366–375. https://doi.org/10.1002/hyp.6604.

Saveyn, A., Steppe, K., McGuire, M.A., Lemeur, R., Teskey, R.O., 2008. Stem respiration and carbon dioxide efflux of young *Populus deltoides* trees in relation to temperature and xylem carbon dioxide concentration. Oecologia 154, 637–649. https://doi.org/10.1007/s00442-007-0868-y.

Schaeffer, S.M., Williams, D.G., Goodrich, D.C., 2000. Transpiration of cottonwood/willow forest estimated from sap flux. Agric. For. Meteorol. 105, 257–270. https://doi.org/10.1016/S0168-1923(00)00186-6.

Schmidt-Walter, P., Richter, F., Herbst, M., Schuldt, B., Lamersdorf, N.P., 2014. Transpiration and water use strategies of a young and a full-grown short rotation coppice differing in canopy cover and leaf area. Agric. For. Meteorol. 195–196, 165–178. https://doi.org/10.1016/j.agrformet.2014.05.006.

Shen, Q., Gao, G., Fu, B., Lü, Y., 2015. Sap flow and water use sources of shelter-belt trees in an arid inland river basin of Northwest China. Ecohydrol. 8, 1446–1458. https://doi.org/10.1002/eco.1593.

Shock, C.C., Feibert, E.B.G., Seddigh, M., Saunders, L.D., 2002. Water requirements and growth of irrigated hybrid poplar in a semi-arid environment in eastern Oregon. West. J. Appl. For. 17, 46–53. https://doi.org/10.1093/wjaf/17.1.46.

Si, J., Feng, Q., Yu, T., Zhao, C., 2015. Nighttime sap flow and its driving forces for *Populus euphratica* in a desert riparian forest, Northwest China. J. Arid Land 7, 665–674. https://doi.org/10.1007/s40333-015-0009-0.

Si, J.-H., Feng, Q., Zhang, X.-Y., Chang, Z.-Q., Su, Y.-H., Xi, H.-Y., 2007. Sap flow of Populus euphratica in a desert riparian forest in an extreme arid region during the growing season. J. Integr. Plant Biol. 49, 425–436. https://doi.org/10.1111/j.1744-7909.2007.00388.x.

Siebrecht, S., Herdel, K., Schurr, U., Tischner, R., 2003. Nutrient translocation in the xylem of poplar - diurnal variations and spatial distribution along the shoot axis. Planta 217, 783–793. https://doi.org/10.1007/s00425-003-1041-4.

Smith, R.E., 1992. The heat pulse velocity technique for determining water uptake of *Populus deltoides*. S. Afr. J. Bot. 58, 100–104. https://doi.org/10.1016/S0254-6299(16)30879-1.

Smith, D.M., Allen, S.J., 1996. Measurement of sap flow in plant stems. J. Exp. Bot. 47, 1833–1844. https://doi.org/10.1093/jxb/47.12.1833.

Steppe, K., Saveyn, A., McGuire, M.A., Lemeur, R., Teskey, R.O., 2007. Resistance to radial CO_2 diffusion contributes to between-tree variation in CO_2 efflux of *Populus deltoides* stems. Funct. Plant Biol. 34, 785–792. https://doi.org/10.1071/FP07077.

Stettler, R.F., Zsuffa, L., Wu, R., 1996. The role of hybridization in the genetic manipulation of *Populus*, in: Stettler, R.F., Bradshaw Jr., H.D., Heilman, P.E.,

Hinckley, T.M. (Eds.), Biology of *Populus* and Its Implications for Management and Conservation. NRC Research Press, Ottawa, Ontario.

Strenge, E., Thevs, N., Kumar Aliev, K., Eraaliev, M., Lang, P., Baibagysov, A., 2018. Water consumption of *Populus alba* trees in tree shelterbelt systems in Central Asia – a case study in the Chui Valley, South Eastern Kazakhstan. Cent. Asian J. Water Res. 4 (1), 48–62. https://doi.org/10.29258/CAJWR/2018-RI.v4-1/48-62.eng.

Sullivan, L., n.d. Nonparametric Tests. Boston University School of Public Health Online Learning Modules. https://sphweb.bumc.bu.edu/otlt/mph-modules/bs/bs704_nonparametric/BS704_Nonparametric_print.html (accessed 7 April 2022).

Sun, H., Aubrey, D.P., Teskey, R.O., 2012. A simple calibration improved the accuracy of the thermal dissipation technique for sap flow measurements in juvenile trees of six species. Trees 26, 631–640. https://doi.org/10.1007/s00468-011-0631-1.

Swieter, A., Langhof, M., Lamerre, J., 2021. Competition, stress and benefits: trees and crops in the transition zone of a temperate short rotation alley cropping agroforestry system. J. Agron. Crop Sci. 208, 209–224. https://doi.org/10.1111/jac.12553.

Taiz, L., Zeiger, E., 2006. Water balance of plants, in: Plant Physiology. Sinauer Associates, Sunderland, Massachusetts, USA, pp. 53–71.

Taylor, J., 2001. *Populus deltoides*. U.S. Department of Agriculture, Forest Service, Rocky Mountain Research Station, Fire Sciences Laboratory, Fire Effects

Information System. https://www.fs.fed.us/database/feis/plants/tree/popdel/all.html (accessed 7 April 2022).

Thevs, N., Gombert, A., Strenge, E., Lleshi, R., Aliev, K., Emileva, B., 2019. Tree wind breaks in Central Asia and their effects on agricultural water consumption. Land 8, 167. https://doi.org/10.3390/land8110167.

Thevs, N., Strenge, E., Aliev, K., Eraaliev, M., Lang, P., Baibagysov, A., Xu, J., 2017. Tree shelterbelts as an element to improve water resource management in Central Asia. Water 9, 842. https://doi.org/10.3390/w9110842.

Thitithanakul, S., Pétel, G., Chalot, M., Beaujard, F., 2012. Supplying nitrate before bud break induces pronounced changes in nitrogen nutrition and growth of young poplars. Funct. Plant Biol. 39, 795–803. https://doi.org/10.1071/FP12129.

Thomas, F.M., Jeschke, M., Zhang, X., Lang, P., 2016. Stand structure and productivity of *Populus euphratica* along a gradient of groundwater distances at the Tarim River (NW China). J. Plant Ecol. 10, 753–764. https://doi.org/10.1093/jpe/rtw078.

Tie, Q., Hu, H., Tian, F., Guan, H., Lin, H., 2017. Environmental and physiological controls on sap flow in a subhumid mountainous catchment in North China. Agric. For. Meteorol. 240–241, 46–57. https://doi.org/10.1016/j.agrformet.2017.03.018.

Tricker, P.J., Pecchiari, M., Bunn, S.M., Vaccari, F.P., Peressotti, A., Miglietta, F., Taylor, G., 2009. Water use of a bioenergy plantation increases in a future high CO_2 world. Biomass Bioenergy 33, 200–208. https://doi.org/10.1016/j.biombioe.2008.05.009.

Tyree, M.T., Zimmermann, M.H., 2002. The cohesion-tension theory of sap ascent, in: Xylem Structure and the Ascent of Sap, Springer Series in Wood Science. Springer Berlin Heidelberg, Berlin/Heidelberg, Germany, pp. 49–81. https://doi.org/10.1007/978-3-662-04931-0.

Uddling, J., Teclaw, R.M., Kubiske, M.E., Pregitzer, K.S., Ellsworth, D.S., 2008. Sap flux in pure aspen and mixed aspen-birch forests exposed to elevated concentrations of carbon dioxide and ozone. Tree Physiol. 28, 1231–1243. https://doi.org/10.1093/treephys/28.8.1231.

Uddling, J., Teclaw, R.M., Pregitzer, K.S., Ellsworth, D.S., 2009. Leaf and canopy conductance in aspen and aspen-birch forests under free-air enrichment of carbon dioxide and ozone. Tree Physiol. 29, 1367–1380. https://doi.org/10.1093/treephys/tpp070.

United Nations, 2019. The Sustainable Development Goals Report 2019. United Nations, New York. https://unstats.un.org/sdgs/report/2019/The-Sustainable-Development-Goals-Report-2019.pdf.

USDA Natural Resources Conservation Service (NRCS), 2005. Fremont's Cottonwood *Populus femontii* S. Wats., NRCS Plant Guide. USDA Natural Resources Conservation Service.

Venturas, M.D., Sperry, J.S., Love, D.M., Frehner, E.H., Allred, M.G., Wang, Y., Anderegg, W.R.L., 2018. A stomatal control model based on optimization of carbon gain versus hydraulic risk predicts aspen sapling responses to drought. New Phytol. 220, 836–850. https://doi.org/10.1111/nph.15333.

Voigt, H., Khamzina, A., Diekkrüger, B., 2018. Quantifying stand water use of a multi-species afforestation site through sap flow and groundwater measurements. Acta Hortic. 1222, 119–124. https://doi.org/10.17660/ActaHortic.2018.1222.16.

Vose, J.M., Swank, W.T., Harvey, G.J., Clinton, B.D., Sobek, C., 2000. Leaf water relations and sapflow in Eastern Cottonwood (*Populus deltoides* Bartr.) trees planted for phytoremediation of a groundwater pollutant. Int. J. Phytoremediat. 2, 53–73. https://doi.org/10.1080/15226510008500030.

Walker, W.R., 1989. Field measurements, in: Guidelines for Designing and Evaluating Surface Irrigation Systems, FAO Irrigation and Drainage Paper. Food and Agriculture Organization of the United Nations, Rome. https://www.fao.org/4/t0231e/t0231e05.htm#3.%20field%20measurements.

Wang, H., He, K., Li, R., Sheng, Z., Tian, Y., Wen, J., Chang, B., 2017. Impact of time lags on diurnal estimates of canopy transpiration and canopy conductance from sap-flow measurements of *Populus cathayana* in the Qinghai–Tibetan Plateau. J. For. Res. 28, 481–490. https://doi.org/10.1007/s11676-016-0333-z.

Wang, S., Fan, J., Ge, J., Wang, Q., Fu, W., 2019. Discrepancy in tree transpiration of *Salix matsudana*, *Populus simonii* under distinct soil, topography conditions in an ecological rehabilitation area on the Northern Loess Plateau. For. Ecol. Manage. 432, 675–685. https://doi.org/10.1016/j.foreco.2018.10.011.

Wang, Y., Li, G., Di, N., Clothier, B., Duan, J., Li, D., Jia, L., Xi, B., Ma, F., 2018. Leaf phenology variation within the canopy and its relationship with the transpiration

of *Populus tomentosa* under plantation conditions. Forests 9, 603. https://doi.org/10.3390/f9100603.

Will, R.E., Wilson, S.M., Zou, C.B., Hennessey, T.C., 2013. Increased vapor pressure deficit due to higher temperature leads to greater transpiration and faster mortality during drought for tree seedlings common to the forest–grassland ecotone. New Phytol. 200, 366–374. https://doi.org/10.1111/nph.12321.

Wullschleger, S.D., Meinzer, F.C., Vertessy, R.A., 1998. A review of whole-plant water use studies in trees. Tree Physiol. 18, 499–512. https://doi.org/10.1093/treephys/18.8-9.499.

Xi, B., Di, N., Wang, Y., Duan, J., Jia, L., 2017. Modeling stand water use response to soil water availability and groundwater level for a mature *Populus tomentosa* plantation located on the North China Plain. For. Ecol. Manage. 391, 63–74. https://doi.org/10.1016/j.foreco.2017.02.016.

Xi, B., Li, G., Bloomberg, M., Jia, L., 2014. The effects of subsurface irrigation at different soil water potential thresholds on the growth and transpiration of *Populus tomentosa* in the North China Plain. Aust. For. 77, 159–167. https://doi.org/10.1080/00049158.2014.920552.

Xi, B., Wang, Y., Jia, L., Bloomberg, M., Li, G., Di, N., 2013. Characteristics of fine root system and water uptake in a triploid *Populus tomentosa* plantation in the North China Plain: implications for irrigation water management. Agric. Water Manage. 117, 83–92. https://doi.org/10.1016/j.agwat.2012.11.006.

Xiao, Q., Huang, M., 2016. Fine root distributions of shelterbelt trees and their water sources in an oasis of arid northwestern China. J. Arid Environ. 130, 30–39. https://doi.org/10.1016/j.jaridenv.2016.03.004.

Xu, X., Tong, L., Li, F., Kang, S., Qu, Y., 2011. Sap flow of irrigated *Populus alba* var. *pyramidalis* and its relationship with environmental factors and leaf area index in an arid region of Northwest China. J. For. Res. 16, 144–152. https://doi.org/10.1007/s10310-010-0220-y.

Xu, X., Xiao, L., Feng, J., Chen, N., Chen, Y., Song, B., Xue, K., Shi, S., Zhou, Y., Jenks, M.A., 2016. Cuticle lipids on heteromorphic leaves of *Populus euphratica* Oliv. growing in riparian habitats differing in available soil moisture. Physiol. Plantarum 158, 318–330. https://doi.org/10.1111/ppl.12471.

Yan, X.-L., Xi, B.-Y., Jia, L.-M., Li, G.-D., 2015. Response of sap flow to flooding in plantations of irrigated and non-irrigated triploid poplar. J. For. Res. 20, 375–385. https://doi.org/10.1007/s10310-015-0485-2.

Yu, T., Feng, Q., Si, J., Mitchell, P.J., Forster, M.A., Zhang, X., Zhao, C., 2018. Depressed hydraulic redistribution of roots more by stem refilling than by nocturnal transpiration for *Populus euphratica* Oliv. in situ measurement. Ecol. Evol. 8, 2607–2616. https://doi.org/10.1002/ece3.3875.

Yu, T., Feng, Q., Si, J., Pinkard, E.A., 2019. Coordination of stomatal control and stem water storage on plant water use in desert riparian trees. Trees 33, 787–801. https://doi.org/10.1007/s00468-019-01816-7.

Yu, T., Feng, Q., Si, J., Xi, H., Li, Z., Chen, A., 2013. Hydraulic redistribution of soil water by roots of two desert riparian phreatophytes in northwest China's extremely arid region. Plant Soil 372, 297–308. https://doi.org/10.1007/s11104-013-1727-8.

Yu, T., Feng, Q., Si, J., Xi, H., O'Grady, A.P., Pinkard, E.A., 2019. Responses of riparian forests to flood irrigation in the hyper-arid zone of NW China. Sci. Total Environ. 648, 1421–1430. https://doi.org/10.1016/j.scitotenv.2018.08.287.

Yu, T., Feng, Q., Si, J., Zhang, X., Alec, D., Zhao, C., 2016. Evidences and magnitude of nighttime transpiration derived from *Populus euphratica* in the extreme arid region of China. J. Plant Biol. 59, 648–657. https://doi.org/10.1007/s12374-015-0536-4.

Zalesny, R.S., Bauer, E.O., 2007. Selecting and utilizing *Populus* and *Salix* for landfill covers: implications for leachate irrigation. Int. J. Phytoremediat. 9, 497–511. https://doi.org/10.1080/15226510701709689.

Zalesny, R.S., Headlee, W.L., Gopalakrishnan, G., Bauer, E.O., Hall, R.B., Hazel, D.W., Isebrands, J.G., Licht, L.A., Negri, M.C., Nichols, E.G., Rockwood, D.L., Wiese, A.H., 2019. Ecosystem services of poplar at long-term phytoremediation sites in the Midwest and Southeast, United States. WIREs Energy Environ. 8, e349. https://doi.org/10.1002/wene.349.

Zalesny, R.S., Wiese, A., Bauer, E., Riemenschneider, D., 2006. Sapflow of hybrid poplar (*Populus nigra* L. × *P. maximowiczii* A. Henry 'NM6') during phytoremediation

of landfill leachate. Biomass Bioenergy 30, 784–793. https://doi.org/10.1016/j.biombioe.2005.08.006.

Zhang, H., Morison, J.I.L., Simmonds, L.P., 1999. Transpiration and water relations of poplar trees growing close to the water table. Tree Physiol. 19, 563–573. https://doi.org/10.1093/treephys/19.9.563.

Zhang, H., Simmonds, L.P., Morison, J.I. l., Payne, D., 1997. Estimation of transpiration by single trees: comparison of sap flow measurements with a combination equation. Agric. For. Meteorol. 87, 155–169. https://doi.org/10.1016/S0168-1923(97)00017-8.

Zhang, X., Meng, T., Kang, E., 2008. Conversion of water consumption of a single tree and a forest stand of *Populus euphratica*. For. Stud. China 10, 81–87. https://doi.org/10.1007/s11632-008-0026-6.

Zhao, C., Si, J., Feng, Q., Yu, T., Li, P., Forster, M.A., 2019. Nighttime transpiration of *Populus euphratica* during different phenophases. J. For. Res. 30, 435–444. https://doi.org/10.1007/s11676-018-0672-z.

Zhao, C.Y., Si, J.H., Feng, Q., Yu, T.F., Li, P.D., 2017. Comparative study of daytime and nighttime sap flow of *Populus euphratica*. Plant Growth Regul. 82, 353–362. https://doi.org/10.1007/s10725-017-0263-6.

Zhou, Y., Wenninger, J., Yang, Z., Yin, L., Huang, J., Hou, L., Wang, X., Zhang, D., Uhlenbrook, S., 2013. Groundwater–surface water interactions, vegetation dependencies and implications for water resources management in the semi-arid

Hailiutu River catchment, China – a synthesis. Hydrol. Earth Syst. Sci. 17, 2435–2447. https://doi.org/10.5194/hess-17-2435-2013.

Zhu, C., Chen, Yaning, Li, W., Chen, Yapeng, Ma, J., Fu, A., 2011. Effects of groundwater decline on *Populus euphratica* at hyper-arid regions: the lower reaches of the Tarim River in Xinjiang, China. Fresenius Environ. Bull. 20, 3326–3337.

Zhu, Y., Cheng, Z., Feng, K., Chen, Z., Cao, C., Huang, J., Ye, H., Gao, Y., 2022. Influencing factors for transpiration rate: a numerical simulation of an individual leaf system. Therm. Sci. Engin. Prog. 27, 101110. https://doi.org/10.1016/j.tsep.2021.101110.

Zihe, L., Guodong, J., Xinxiao, Y., Weiwei, L., Libo, S., Yusong, W., Baheti, Z., 2021. Morphological trait as a determining factor for *Populus simonii* Carr. to survive from drought in semi-arid region. Agric. Water Manage. 253, 106943. https://doi.org/10.1016/j.agwat.2021.106943.

CHAPTER 5. WATER RELATIONS OF THREE HYBRID *POPULUS* GENOTYPES GROWN FOR PHYTOREMEDIATION IN EASTERN WISCONSIN, USA

Abstract

Tree water use, a major factor affecting the efficacy of tree-based pollution remediation systems, is governed by stomatal response to co-occurring changes in atmospheric evaporative demand and soil moisture conditions. Projected drier climatic conditions, including elevated vapor pressure deficit (VPD) and decreased soil moisture, will require selection of genotypes across the isohydricity continuum to both maximize water use and productivity in the short-term and to promote system survival in the long-term. The overarching objective of the present study was to compare the water use strategies of three hybrid poplar clones ('DN34', *Populus deltoides* Bartr. ex. Marsh × *P. nigra* L.; '9732-11', *P. deltoides* × *P. nigra*; 'NM2', *P. nigra* × *P. maximowiczii* A. Henry) in their fourth growing season and grown for pollution remediation in Eastern Wisconsin. In addition to their isohydricities being unknown, these three genotypes exhibit a range in specialist and generalist performance and are geographically relevant for environmental applications in the midwestern United States. We measured daily water use of 18 trees using thermal dissipation sap flow probes, measured monthly leaf area index with a plant canopy analyzer, and collected climate and soils data from a weather station and soil probes on-site. Water use during the study (75 days) differed among genotypes, with '9732-11' having significantly greater water use than both 'NM2' ($p = 0.0011$) and 'DN34' ($p < 0.0001$). Average daily water use across the study period was 18 ± 0.4 kg tree^{-1} day^{-1} for '9732-11', 13 ± 0.3 kg tree^{-1} day^{-1} for 'NM2', and 10 ± 0.2 kg tree^{-1} day^{-1} for 'DN34'.

Total water use over the 75-day study exhibited a similar trend, with '9732-11' having the greatest total water use (1,335 ± 55 kg tree^{-1}), followed by 'NM2' (1,002 ± 83 kg tree^{-1}) and 'DN34' (780 ± 79 kg tree^{-1}). Stomatal sensitivity to VPD was higher for '9732-11' than 'NM2' ($p = 0.0373$) under average-to-high soil moisture conditions ($\theta > 0.2$ m^3 m^{-3}). On the other hand, 'NM2' exhibited plasticity in response to different soil moisture conditions, with its scaled stomatal sensitivity being significantly higher ($p = 0.0202$) under lower soil moisture than high soil moisture. These and other findings of this study provide evidence that the water use strategies of these genotypes may vary. Such information can inform the selection of resilient poplar genotypes for environmental applications, including pollution remediation.

5.1 Introduction

Maintaining clean, non-polluted air, water, and soil resources is necessary for promoting human health. Yet pollution of these resources remains a major challenge facing the modern world (Fuller et al., 2022). Pollution originates from a range of sources, including industrial processes, waste dumping activities, deforestation, mining operations, and traditional agricultural practices that promote the extensive use of fertilizers, pesticides, and herbicides. Phytoremediation, the strategic implementation of trees on degraded landscapes to remediate environmental pollution, is a sustainable, cost-effective, and aesthetically pleasing option for pollution mitigation (McCutcheon and Schnoor, 2003; Salt et al., 1998). Phytoremediation systems utilize principles of tree growth and physiology such as sorption, uptake and translocation, metabolism, and evapotranspiration, to manage pollution through stabilization, uptake and degradation, accumulation, or volatilization of contaminants (Dietz and Schnoor, 2001; Gerhardt et al.,

2017). Short rotation woody crops (SRWCs), particularly *Populus* L. hybrids, have been commonly implemented in phytoremediation systems since the 1990s (Marmiroli et al., 2011; McCutcheon and Schnoor, 2003; Zalesny et al., 2019) to remediate heavy metals (Kovačević et al., 2025; Li et al., 2024; Prouzová et al., 2024) and organic contaminants (Gordon et al., 1998; Ferro et al., 2013; Doty et al., 2017; Landmeyer and Effinger, 2016; BenIsrael et al., 2019). Hybrid poplars exhibit rapid growth (Bradshaw et al., 2000), extensive biomass production (see supplementary information, Laurent et al., 2015), and the ability to propagate from dormant unrooted cuttings (Dickmann et al., 2001), which are all important factors for communities seeking rapid groundcover establishment over degraded areas. These beneficial traits, along with genetic diversity and ease of hybridization, have made the *Populus* genus the subject of numerous tree breeding and tree improvement programs (Riemenschneider et al., 2001; Isebrands and Zalesny, 2021; Nelson et al., 2021). Poplar genotypes resulting from such programs exhibit tremendous variability in functional traits, and the expression of genotype × environment interactions (Zalesny et al., 2021), necessitating standardized genotype selection approaches to promote phytoremediation efficacy (Marmiroli et al., 2011; Zalesny and Bauer, 2007; Pietrini et al., 2009).

One of the major remediation mechanisms of phytoremediation systems is tree water use (Vose et al., 2000). This mechanism is important for three main reasons. First, as trees transpire and take up water from the soil, bioavailable contaminants may also be taken up, and can then be further broken down, sequestered, volatilized, or otherwise metabolized within the tree (Davis et al., 2002; Landmeyer, 2012). Next, depending on the amount of water that trees use, trees can also act like a pump, pulling contaminated

groundwater toward the rhizosphere, and reducing its movement off-site, known as hydraulic control (Ferro et al., 2003). Finally, as trees transpire and draw water toward their roots, they stimulate mass flow toward the rhizosphere, thereby concentrating contaminants at a site of increased microbial activity, and promoting rhizodegradation (Ferro et al., 1994; Wenzel, 2009; Trapp and Karlson, 2001). Hybrid poplars are obligate phreatophytes often recognized for their elevated water use. In a recent literature review, Rogers et al. (2023) reported hybrid poplar transpiration to range from 0.7 to 11.3 mm day^{-1} across inter- and intraspecific hybrids, planting densities, and water availabilities. In phytoremediation settings, water use of hybrid poplars varies considerably among genotypes, water availabilities, and tree ages. For instance, non-irrigated 'DN34' (*Populus deltoides* Bartr. ex. Marsh × *P. nigra* L.) trees in their fourth growing season and established for remediation of petroleum hydrocarbons used an average of 49 kg water day^{-1} $tree^{-1}$ (Ferro et al., 2001), while drip-irrigated 'NM6' (*Populus nigra* × *P. maximowiczii* A. Henry) trees in their fourth growing season established for phytoremediation of landfill leachate had an average total daily water use of 34 kg $tree^{-1}$ day^{-1} (Zalesny et al., 2006).

Tree water use is driven by the water potential gradient along the soil-plant-atmosphere continuum. At the leaf level, stomatal functioning dictates gas exchange between the leaf and the atmosphere. Stomatal conductance enables carbon dioxide to enter leaves in order to power photosynthesis, with water lost from leaves during stomatal conductance occurring as the cost of assimilation. Transpiration rates, thus, are governed by stomatal response to co-occurring changes in atmospheric evaporative demand and soil moisture conditions (Grossiord et al., 2020; Sperry et al., 2002). Tree stomatal

regulation strategies fall on an isohydricity spectrum (McDowell et al., 2008; Tardieu and Simonneau, 1998). On one end of the spectrum, trees that have an isohydric strategy maintain strict control over their stomatal regulations, closing their stomata under conditions of elevated moisture stress, such as low soil moisture, and/or high vapor pressure deficit (VPD). On the other end is anisohydricity. Trees with this water use strategy are not as restrictive regarding stomatal conductance, but instead, allow gas and water exchange via stomatal conductance to continue under moisture stress conditions. Both strategies involve tradeoffs regarding productivity and water use. Trees with more of an anisohydric strategy are able to maintain higher levels of gas exchange, and thus, photosynthesis, as well as water use, during water stress as compared to isohydric trees (McDowell et al., 2008). However, this ability to maintain productivity comes at the risk of cavitation, and in severe cases, hydraulic failure (McDowell et al., 2008). On the other hand, trees with more of an isohydric strategy limit both their photosynthetic productivity and water use during water stress by closing their stomata in order to maintain a relatively stable leaf water potential (Attia et al., 2015).

Broad variability in water use strategies has been reported among species and genotypes in the *Populus* genus, with some exhibiting isohydric responses to periods of water stress, characterized by relatively rapid stomatal closure and relatively constant leaf water potential (Attia et al., 2015; Lüttschwager et al., 2016; Navarro et al., 2018; Schmidt-Walter et al., 2014; Tardieau and Simonneau, 1998), others that exhibit an anisohydric strategy, maintaining stomatal conductance and experiencing declining leaf water potentials throughout dry periods (Attia et al., 2015; Babi et al., 2019; Kojima et al., 2024; Lüttschwager et al., 2016; Navarro et al., 2018; Orság et al., 2024; Zenone et

al., 2015), and others falling somewhere in the middle, with near-isohydric, and near-anisohydric responses (Rovida Kojima et al., 2023; 2024; Tang et al., 2024). Such different water use strategies can lead to differences in productivity among poplars (Tang et al., 2024). Rovida Kojima et al. (2024) found anisohydric poplar clones to have the lowest reductions in stem growth under moderate water restrictions, and to exhibit significantly greater stem growth under moderate water restriction, compared to their isohydric counterparts. These trends are corroborated by González-González et al. (2017) who reported anisohydric poplars to exhibit lower reductions in biomass production under water-limited conditions, though lower productivity under optimal conditions, and lower water use efficiency than productive isohydric clones. Regarding transpiration, some isohydric poplars can recover transpiration rates after severe water stress sooner and more completely than more anisohydric genotypes (Attia et al., 2015). Elevated transpiration in general has also been documented for anisohydric trees compared to isohydric trees. For example, when grown under field conditions, anisohydric clones 'Oudenberg' (*P. deltoides* × *P. nigra*) and 'Grimminge' (*P. deltoides* × (*P. trichocarpa* Torr. & Gray × *P. deltoides*)) had daily average transpiration values of 2.5 mm day^{-1} and 3.1 mm day^{-1} compared to values of 1.6 mm day^{-1} and 1.8 mm day^{-1} for isohydric clones 'Bakan' (*P. trichocarpa* × *P. maximowiczii*) and 'Koster' (*P. deltoides* × *P. nigra*), respectively (Navarro et al., 2018). Such differences have implications for genotype selection for phytoremediation systems and will require weighing tradeoffs in water use and productivity against site climatic conditions and remediation objectives.

Management decisions that affect the water potential gradient for trees in phytoremediation systems, such as irrigation and planting density, can largely influence

tree water use (Rogers et al., 2023). Additionally, projected drier conditions in future climatic scenarios, including extended periods of elevated VPD and decreased soil moisture, have potential to greatly impact tree water relations (Fu et al., 2022; Rigden et al., 2020; Yuan et al., 2019). Changes in VPD and soil water content will not only affect the quantity of water that is used within phytoremediation systems, but could also affect tree productivity and survival if the selected genotypes are not tolerant to the dry conditions (Yuan et al., 2019). Successful phytoremediation systems will require the selection of resilient genotypes that are able to withstand such conditions while maintaining an adequate level of water use to meet remediation objectives. Anisohydric poplars are more likely to have greater overall water use, especially during times of water stress (Attia et al., 2015; Navarro et al., 2018), which may benefit phytoremediation systems that require constant "pumping" by trees via their elevated water use. However, sole use of anisohydric genotypes may lead to reduced productivity and water use efficiency compared to strictly using isohydric genotypes (González-González et al., 2017) and may also increase the risk of cavitation and hydraulic failure (Attia et al., 2015; McDowell et al., 2008). All these outcomes could reduce overall water use, and therefore efficacy, of a phytoremediation system. Isohydric poplars may be a less risky option under severe drought conditions (Attia et al., 2015; Schmidt-Walter et al., 2014) and therefore may be a more suitable option for sites that do not have irrigation. However, their lower water use relative to that of anisohydric trees is another factor to be considered (Navarro et al., 2018). Design of resilient phytoremediation systems may therefore include poplar genotypes of water use strategies across the anisohydric to isohydric continuum, to both maximize water use and productivity in the short-term and

to promote system survival in the long-term. Few studies investigate the relationships between poplar isohydricity and phytoremediation implications (Babi et al., 2019; Stojnić et al., 2021; Grimond et al., 2024). Information on water use strategies for the multitude of genotypes resulting from breeding and improvement programs is also incomplete but it will be necessary to inform the selection of regionally relevant genotypes for phytoremediation systems.

Our overarching objective was to compare the water use strategies of three hybrid poplar clones ('DN34', *P. deltoides* × *P. nigra*; '9732-11', *P. deltoides* × *P. nigra*; 'NM2', *P. nigra* × *P. maximowiczii*) in their fourth growing season and grown for phytoremediation in Eastern Wisconsin, USA. In addition to their isohydricities being unknown, these three genotypes were selected for study as they exhibit a range in specialist and generalist performance, have different genomic and clone groups, and are geographically relevant for use in phytoremediation applications in the midwestern United States (Zalesny et al., 2021). Our specific objectives were to: 1) quantify and compare thermal dissipation-based whole-tree water use of the three poplar clones, 2) investigate clone-specific responses of canopy conductance to driving environmental factors, specifically VPD and soil moisture, throughout the growing season, and 3) assess the response of leaf water potential and whole-tree hydraulic conductance to varying moisture availabilities. We hypothesized that whole-tree water use would vary among genotypes according to their morphology, with genotypes exhibiting larger diameters having the greatest water use. We also hypothesized that tree-level and leaf-level physiological responses to environmental driving factors will vary among the genotypes and will enable identification of their relative degrees of isohydricity. Information on the

physiological response of different poplar varieties to environmental gradients will aid in designing remediation systems to sustain projected future conditions. While genotypes with greater water use may be desired for phytoremediation applications, those that exhibit a range of isohydricities may be a preferable option to minimize risk associated with increasingly dry conditions.

5.2 Materials and methods

5.2.1 Experimental site, poplar material, establishment

The field site is located in Eastern Wisconsin near Manitowoc, WI (Figure 5.1). The site has a humid continental climate that is moderated by Lake Michigan. Average annual precipitation according to 30-year climate normals is 799 mm (NOAA, 2025), which occurs mainly as snow in the winter months (December – March) and rain during the rest of the year. Average daily temperature during the growing season (May – October) is 15.8 °C, with average daily minimum and maximum temperatures of 11.3 °C and 20.2 °C, respectively (NOAA, 2025). On average, there are 2,112 growing degree days (base temperature of 10 °C) each year (NOAA, 2025). Soils are classified as Hochheim loam, with 6 to 12 percent slopes, eroded (NRCS, 2025).

Historically, the field site was used for dumping of municipal and industrial wastes during the 1960s-1970s (AECOM, 2023). Ongoing environmental monitoring activities at the site have identified soil and groundwater contamination by a range of organic and inorganic compounds, including volatile organic compounds (VOCs), polychlorinated biphenyls (PCBs), and Resource Conservation and Recovery Act (RCRA) metals (AECOM, 2023). In 2017, an engineered cap and an engineered

groundwater treatment pond were implemented at the site, followed by hybrid *Populus* and *Salix* phytoremediation buffers in 2018 (Pilipović et al., 2021; Zalesny et al., 2021), to mitigate site contamination and potential off-site transport of contaminants. The poplar planting was strategically located downgradient from the treatment pond to augment site remediation efforts. A total of 356 trees, consisting of 12 hybrid *Populus* genotypes, were established within the planting. *Populus* genotypes were selected for field establishment following greenhouse trials of phyto-recurrent selection (see Rogers et al., 2019 and Zalesny et al. 2021 for more information on genotype selection). The current study focuses on a subset of three hybrid *Populus* genotypes (Table 5.1) that were established within the larger *Populus* planting at the site, including 'DN34' (*P. deltoides* × *P. nigra*), '9732-11' (*P. deltoides* × *P. nigra*), and 'NM2' (*P. nigra* × *P. maximowiczii*).

Methods for site preparation, plant material processing, and establishment, are described in Zalesny et al. (2021). Briefly, the field site was tilled to a 30 cm depth and large rocks were removed. One-year-old whips were obtained from nurseries (Table 5.1) during the dormant season, and brought to the USDA Forest Service Northern Research Station, Institute for Applied Ecosystem Studies, where they were processed into 25.4 cm cuttings, and stored in the dark at 5 °C. Prior to planting, the dormant, hardwood cuttings were soaked in water, in the dark, at 21 °C for 48 h (Zalesny et al., 2021). Cuttings were planted at the site on June 6, 2018 at a spacing of 2.44 m × 2.44 m (1,680 trees ha^{-1}). The three genotypes of the current study (Table 5.1) were originally established in three sets of 16-tree monoclonal blocks in a randomized complete block design. A subset of two of these blocks were the focus of this study. The entire *Populus* planting at the site (0.25 ha) was fenced with 2.3 m tall Trident extra strength deer fencing (DeerBusters, Waynesboro,

PA, USA) to prevent browse by white-tailed deer. Competition from other vegetation at the site was minimized through an intensive maintenance regime (Zalesny et al., 2021), consisting of monthly tilling to a depth of 30 cm and hand weeding to a diameter of 0.61 m around each tree during the first two growing seasons, followed by monthly tilling during the third growing season, and monthly mowing during the fourth growing season. A cover crop species mixture including white clover (*Trifolium repens* L.), red clover (*T. pratense* L.), meadow fescue (*Festuca pratensis* Huds.), spring oats (*Avena sativa* L.), and brassicas (Cruciferae family) was established at the site under the trees during the fourth growing season to enhance nitrogen availability in the phytoremediation planting. Site soil physicochemical properties are reported in Table 5.2. Tree survival for the 96 trees within the two monoclonal blocks selected for this study was 98% after the third growing season.

5.2.2 Environmental measurements

In June 2021, we installed climatic, soil, and sap flow sensors at the site (Figure 5.2). Climatic, soil, and sap flow data were collected for a 75-day period from June 25 (DOY 176) to September 8 (DOY 251) 2021. A weather station containing all the components of a WxPRO weather station (Campbell Scientific, Inc., Logan, UT, USA) was installed in a clearing ~4 m from the *Populus* planting. All meteorological instruments were mounted to a 3.05-m tripod with a 1.22-m crossarm. A HygroVUE5 sensor (Sensirion AG, Stäfa, Switzerland) protected by a RAD06 6-Plate Radiation Shield (MetSpec, Oakham, England) measured air temperature and relative humidity. Barometric pressure was measured with a CS100 Barometric Pressure Sensor (Model 278; Setra, Boxborough, ME, USA), and total sun and sky radiation was measured with a

pyranometer (Apogee Instruments, Logan, UT, USA). A tipping bucket gage with 0.254 mm per tip (TE525; Texas Electronics, Dallas, TX, USA) mounted to a 58.4-cm mounting pole and tripod measured rainfall totals. Additionally, soil volumetric water content was measured using three SoilVUE 10 1-m soil profile probes (Campbell Scientific, Inc.). SoilVUE probes were installed throughout the planting using a 5-cm hand auger. Due to an impervious layer at ~50-60 cm below the soil surface, SoilVUE probes could only be installed to a depth of 50 cm. Surface layer soil volumetric water content was calculated by averaging the measurements from all three probes for the three measurement depths closest to the soil surface (i.e., depths of 0, 10, and 25 cm). Climatic and soils data were measured every 30 s, and 1-min averages were recorded using a CR-310 datalogger (Campbell Scientific, Inc.). Data were offloaded from the datalogger and managed with PC400 Datalogger Support Software, version 4.7 (Campbell Scientific, Inc.). All climatic and soil sensors were powered by a 12 V deep-cycle marine battery and a solar panel.

5.2.3 Sap flow measurements

A subset of three trees from the inner four trees of each block were chosen for sap flow measurements (Figure 5.3A), for a total of 18 trees measured, with six from each genotype (2 blocks, 3 genotypes, 3 trees per genotype per block). The inner trees of the blocks were chosen to ensure that the trees were bordered on all sides by trees of the same genotype, thereby minimizing edge effects and heterogeneity in competition. Sap flow was measured using a Dynamax FLGS-TDP XM1000 Sap Velocity System (Dynamax, Inc., Houston, TX, USA). One 30-mm-long Granier-style, thermal dissipation probe (TDP-30; Dynamax Inc.) was installed on the north side of each tree at 51 cm

above the ground surface. Each TDP consists of two thermocouple-containing needles that are inserted radially into the tree, one 40 mm directly above the other. The upper needle is heated, while the lower needle measures the temperature difference between the heated needle and the non-heated needle.

Sap flux is calculated from the temperature differences between the needles using the following equation, developed by Granier (1987):

$$J_S = 0.119 \times \left(\frac{\Delta T_{Max} - \Delta T}{\Delta T}\right)^{1.231}$$

Where J_S is sap flux (kg H_2O m^{-2} $_{\text{sapwood area}}$ s^{-1}), ΔT_{Max} is the maximum temperature difference between probes when sap flow is zero, and ΔT is the temperature difference between probes at a particular timepoint, when sap flow is > 0.

Putty was applied around the base of each needle to prevent moisture damage, and probes were held in place using foam quarter eggs that were taped to the tree. Probes were protected from insolation using reflective thermal bubble foil insulation and an outer layer of aluminum foil (Figure 5.2). Probes were inspected monthly throughout the growing season to ensure they were functioning properly. Rapid tree growth could cause trees to grow over the TDP sensors, and therefore, probes were checked monthly for position within the trees, as well as inspected for any damage due to insects, rodents, or other wildlife. Sensors were connected to a CR-1000X datalogger (Campbell Scientific, Inc.), where data were collected every 60 s and averaged every 15 min. Raw sap flow senor output data (15-min averages in °C) were baseline corrected using Baseliner version 4 software (Oishi et al., 2016). Baseliner enables selection of the zero-flow baseline at which ΔT_{Max} occurs. The software automatically selects ΔT_{Max} on a nightly

basis according to user-defined biophysical thresholds below which zero-flow is expected to occur (e.g., certain values of VPD, solar radiation). Then the user manually inspects the baseline anchor points, and makes modifications as needed. Biophysical parameter thresholds used in the present study are shown in Table D1. J_S was then calculated using the baseline-corrected values of ΔT_{Max} and Granier's empirical equation (Granier, 1987). Tree-level sap flow (kg per unit time) was calculated by multiplying J_S by sapwood area (m^2) of each individual tree.

Sapwood area was determined during a biomass harvest near the end of the growing season in September. Trees instrumented for sap flow measurements were not harvested in order to allow long-term monitoring and data collection. Instead, trees grown at the site that were of the same age and the same or closely related genotypes were harvested, including 'DN34', 'NM2', and '9732-24' (used as a proxy for '9732-11'; like '9732-11', '9732-24' also was developed by the Natural Resources Research Institute of the University of Minnesota, Duluth breeding program and has a parentage of *P. deltoides* × *P. nigra*). Three trees of each genotype were harvested, and the proportions of the diameter occupied by bark and sapwood were calculated from discs cut from each tree. Sapwood was visually delineated from bark based on color differences (Wullschleger et al., 2000). Bark thickness for each harvested tree was measured at four points (cardinal directions) along the circumference of each tree disc, and clonal values were calculated by averaging the corresponding individual tree data. The calculated clonal proportions of tree diameter occupied by bark were used to adjust diameter values of the non-harvested sap flow trees. Diameters of sap flow trees were measured at probe installation and monthly thereafter, and a linear growth rate was assumed between measurements. Cross

sectional sapwood area was calculated using diameter measurements adjusted for bark thickness. All sapwood area in contact with the sap flow probes was assumed to be functional, with uniform sap flux across the sapwood area (Samuelson et al., 2007; Telewski et al., 1996).

5.2.4 Leaf area index

For a separate study, block-level leaf area index (LAI) was measured weekly at the study site in 2021 (end of May – beginning of November) using an LAI 2200-C Plant Canopy Analyzer (LI-COR Environmental Inc., Lincoln, NE, USA). Measurements were taken at all three monoclonal blocks at the site (Figure 5.3). For the current study, only a subset of these measurements were assessed, including monthly measurements (May – September) for the two blocks containing trees instrumented with TDPs. Measurements were taken at five locations within each 16-tree plot: at each of the four corners of the plot, and at the center of the plot (Figure 5.3B). Six readings were taken at each measuring location. A 90-degree view cap was placed onto the sensor lens for measurements taken at plot corners to limit the sensor's field of view to the plot being measured, while a 180-degree view cap was placed onto the sensor for measurements taken at plot centers. For measurements taken at plot corners, the sensor was aimed toward the plot center, while for measurements taken at plot centers, the sensor was aimed toward the east. All measurements were taken at predawn when the sun was below the horizon, and there were uniform sky light conditions. Care was taken to ensure the sensor was level during measurements. A second sensor was set up on a tripod in an open area outside of the poplar planting (~40 m from the planting) to record above canopy light conditions. This above canopy sensor was set to "autonomous configuration" mode

to automatically log data points every 30 seconds. The position of the above canopy sensor was adjusted throughout data collection to ensure that both sensors were always viewing the same part of the sky, and that both sensors had the same view cap. Data from above canopy and below canopy readings were interpolated to calculate plot-level LAI data using the FV2200 software version 2.1.1 (LI-COR Environmental, Inc.). The outer two rings were masked in order to reduce the minimum plot size (LI-COR, 2023).

5.2.5 Canopy conductance

Leaf-level transpiration (E_l; kg m^{-2} $_{leaf\ area}$ s^{-1}) was determined by dividing tree-level sap flow (kg s^{-1}) by tree leaf area. Tree leaf area values were calculated using LAI values. Block-level LAI was multiplied by the ground area occupied by the block to obtain block leaf area (m^2). Block leaf area was scaled to individual tree leaf area by multiplying block leaf area by the proportion of the summed total block diameter that was occupied by the individual tree within the block. Canopy conductance (G_S; m s^{-1}) was then calculated using the following equation (Renninger et al., 2022):

$$G_S = \frac{K_G \times E_l}{VPD}$$

Where K_G is a coefficient calculated as 115.8 + 0.4226 × air temperature (°C) according to Phillips and Oren (1998). Canopy conductance was scaled to units of mol m^{-2} s^{-1} by multiplying values by the molar density of air (mol m^{-3}) that was calculated according to the ideal gas law using pressure and temperature data measured at the site.

5.2.6 Leaf water potential and hydraulic conductance

Leaf water potential was measured on leaves taken from the lower third of the canopy at predawn (Ψ_{pd}, 0400 – 0600 h) and midday (Ψ_{md}, 1200 – 1400 h) using a pressure chamber (Model 615D, PMS Instrument Company, Albany, OR, USA). Leaf water potential was measured on four days that represent two time periods of different soil moisture content. The first two days (DOY 194-195) occurred at the end of a dry period, in which >93% of Manitowoc County was under a moderate drought (U.S. Drought Monitor, 2025) for 11 consecutive weeks (April – July). Soil volumetric water content (VWC) at the site had been < 0.2 $m^3\ m^{-3}$ since the soil probes were installed at the end of June. On the night of DOY 195 and into the early morning of DOY 196, a large rainfall event occurred, which produced 13.6 cm precipitation in a 12-hour period. Following this event, Manitowoc County was no longer under a drought (U.S. Drought Monitor, 2025). Leaf water potential was then measured on the two days directly following this rainfall event (DOY 197-198). Soil VWC after the rainfall event increased to $\theta > 0.3\ m^3\ m^{-3}$. Leaf-specific whole-plant hydraulic conductance (K_l; kg $m^{-2}\ h^{-1}\ MPa^{-1}$) was calculated for the four days of leaf water potential measurements according to Chen et al. (2023) using the following equation:

$$K_l = \frac{E_l}{\Delta\Psi}$$

Where E_l is transpiration per unit leaf area (kg $m^{-2}_{\text{leaf area}}\ h^{-1}$) during midday (average of values from 1200-1400 h) and $\Delta\Psi$ is the difference in water potential between Ψ_{pd} and Ψ_{md} and serves as a proxy for the leaf water potential gradient between the soil and the leaf (Maier et al., 2019). The values of K_l were further corrected for gravitational effects

on the pressure gradient due to tree height (Chen et al., 2023; Maier et al., 2019). Values for Ψ_{pd}, Ψ_{md}, $\Delta\Psi$, and K_l, were averaged by soil moisture content category (i.e., $\theta > 0.2$ m^3 m^{-3}, "high" and $\theta < 0.2$ m^3 m^{-3}, "low") on an individual tree basis, resulting in one value per tree for each soil moisture content category.

5.2.7 Statistical analysis

Data organization, preparation, and preprocessing for all datasets were performed in R statistical software version 4.0.3 (R Core Team, 2020). Figures were created using the "ggplot2" R package (Wickham, 2016). Statistical analyses were conducted in Excel, R, and SAS version 9.4 (SAS Institute, Inc., 2023), with specific analyses and associated functions and packages described below. Unless otherwise noted, a significance level of $\alpha = 0.05$ was used for all analyses. One tree (Tree 106, '9732-11') had a faulty sap flow probe which produced inconsistent data and was removed from further analyses. Daily water use and sap flux were analyzed using repeated measures ANOVA (PROC MIXED, SAS Institute, Inc., 2023). For both water use and sap flux, a first-order autoregressive covariance structure was selected, as this structure provided a balance between optimal AIC fit statistics and model parsimony. In these models, Genotype was a fixed factor, Day was the repeated measure, and Tree was the experimental unit. One-way ANOVA was used to analyze the effect of Genotype on stand characteristics (height, diameter, sapwood area, LAI, tree leaf area), monthly water use (June and July), and study period water use. A two-way ANOVA was used to analyze the effect of Genotype, Soil Water Content (low and average-to-high), and their interaction on leaf water potential variables (Ψ_{pd}, Ψ_{md}, $\Delta\Psi$, and K_l) (PROC GLM, SAS Institute, Inc., 2023). For significant fixed

effects identified in the ANOVAs, the Tukey-Kramer post-hoc test was used to make pairwise comparisons within response variables.

The sensitivity of stomata to VPD was estimated by fitting linear regressions to the relationship between G_S and ln(VPD) (Oren et al., 1999). The slope of these equations represents G_S sensitivity to VPD, the y-intercept represents the reference G_S at VPD = 1 kPa ($G_{S,ref}$), and the ratio of G_S sensitivity / $G_{S,ref}$ represents scaled G_S sensitivity. G_S values (VPD > 0.6 kPa and solar radiation > 200 W m^{-2}) were first split into two separate datasets according to soil moisture, low soil moisture ($\theta < 0.2$ m^3 m^{-3}) and average-to-high soil moisture ($\theta > 0.2$ m^3 m^{-3}), based on observation of inflection points in the data (Renninger et al., 2021). To determine if regression equations differed among genotypes, contrasts were applied to full models, and a Bonferroni corrected alpha level was used (Zarnoch, 2009). Linear regressions between G_S and ln(VPD) were further fitted for individual trees using the lm() function in R ("stats" package, R Core Team, 2019). One-way ANOVA (PROC GLM, SAS Institute, Inc., 2023) was then used to compare slopes, y-intercepts, and scaled G_S sensitivity values from the individual tree equations among genotypes. For significant fixed effects identified in the ANOVAs, the Tukey-Kramer post-hoc test again was used to make pairwise comparisons within response variables. Scaled G_S sensitivity values were compared between low soil moisture and high soil moisture conditions for each genotype using paired t-tests (two-tailed and paired by tree) in Excel (Data Analysis Tool).

5.3 Results

5.3.1 Environmental conditions

The mean air temperature during the study period was 20°C, with an average daily low of 16°C and an average daily high of 25°C (Figure 5.4A). These values were similar to the 30-year averages for June – September in Manitowoc, WI, which are 18.4°C average daily temperature, 22.9°C daily maximum, and 13.9°C daily minimum (NOAA, 2025). Total rainfall during the study period (DOY 176-251) was 399 mm, with daily totals during precipitation events generally 2.5 cm or less, except for one severe thunderstorm in July which produced 13.6 cm of rain in less than a 24-hour period (Figure 5.4E). Precipitation totals were 19.2 cm in July and 16.4 cm in August, both of which were much greater than the 30-year normals of 8.9 cm for July and 8.7 cm for August. Mean vapor pressure deficient was low, generally staying below 1 kPa, while daily VPD maximums reached above 2 kPa (Figure 5.4B). On the other hand, relative humidity was generally over 70%, with an overall average of 82% (Figure 5.4C). Average daily soil volumetric water content in the upper 25 cm of soil ranged from 0.12 to 0.18 $m^3\ m^{-3}$ at the beginning of the study period (DOY 176-195), corresponding to the end of an 11-week drought that began in April for Manitowoc County (National Drought Mitigation Center, 2025). During the rest of the study period, soil water content increased appreciably in the days preceding rainfall events, while decreasing to average values of 0.13 to 0.23 $m^3\ m^{-3}$ in the periods between precipitation (Figure 5.4D).

5.3.2 Stand characteristics

Growth characteristics varied significantly among genotypes. During the middle of the study (DOY 207; 7/26/21), '9732-11' and 'NM2' had average heights of 8.07 ± 0.37

m and 8.52 ± 0.17 m, respectively (Table 5.3), both of which were significantly greater than the average height of 'DN34' (6.84 ± 0.31 m) ($p = 0.0239$ for '9732-11'; $p = 0.0020$ for 'NM2'). For diameter at breast height (DBH), '9732-11' had the largest average DBH of 9.60 ± 0.36 cm, 'NM2' had a moderate DBH of 8.05 ± 0.34 cm, and 'DN34' had the smallest DBH of 6.68 ± 0.46 cm. The DBH of '9732-11' was significantly larger than that of both 'NM2' ($p = 0.0434$) and 'DN34' ($p = 0.0005$). Not surprisingly, sapwood area followed this trend, with '9732-11' exhibiting the largest sapwood area (65.83 ± 5.01 cm^2) which was significantly larger than the sapwood area of both 'NM2' (45.97 ± 3.99 cm^2; $p = 0.0200$) and 'DN34' (32.45 ± 4.41 cm^2; $p = 0.0004$). Over the course of the study period (DOY 176-251), sapwood areas increased by 45% for '9732-11', 39% for 'NM2', and 72% for 'DN34' from the first to the last day of the study.

Monthly LAI followed different seasonal trends among the three genotypes. The LAI of '9732-11' reached peak values in July, followed by a relatively steep decrease over the remainder of the growing season (Figure 5.5). 'DN34', also a DN genotype, reached a seasonal maximum LAI in August, with a more gradual decrease in September. 'NM2' also exhibited seasonal maximum LAI in August, followed by a slight decrease in September. The LAI of 'NM2' was consistently larger than that of both '9732-11' and 'DN34' over the entire growing season. In the middle of the study period (DOY 207), the average LAI was significantly different among all three genotypes. 'NM2' had the highest average LAI of 6.37 ± 0.59 $m^2\ m^{-2}$, which was significantly greater than the LAI of '9732-11' (4.81 ± 0.23 $m^2\ m^{-2}$; $p = 0.0169$) and 'DN34' (2.78 ± 0.22 $m^2\ m^{-2}$; $p < 0.0001$). The LAI of '9732-11' was also significantly greater than that of 'DN34' ($p = 0.0011$).

5.3.3 Water use and sap flux

Daily water use ranged from < 1 to 38 kg tree^{-1} day^{-1} with an overall average of 13 kg tree^{-1} day^{-1}. The lowest water use values for all genotypes occurred on days that experienced precipitation events (Figure 5.4E), such as DOY 188, in which water use had genotype-level averages of 1 kg tree^{-1} for '9732-11', 0.4 kg tree^{-1} for 'DN34', and 0.8 kg tree^{-1} for 'NM2'. Daily water use was highest on days with greatest VPD, such as DOY 184, in which water use reached an average of 29 kg tree^{-1} for '9732-11'. Over the study period, '9732-11' had the greatest average daily water use (18 ± 0.4 kg tree^{-1} day^{-1}) which was significantly greater than that of 'NM2' (13 ± 0.3 kg tree^{-1} day^{-1}; $p = 0.0011$) and 'DN34' (10 ± 0.2 kg tree^{-1} day^{-1}; $p < 0.0001$), while 'NM2' daily water use was also greater than that of 'DN34' ($p = 0.0165$). Average daily sap flux during daytime hours (0400 – 1900 h) ranged from lows near 1 to over 120 g m^{-2} s^{-1}. Unlike water use, sap flux was highest for 'DN34', followed by 'NM2', and finally, by '9732-11'. 'DN34' had significantly greater sap flux than '9732-11' ($p = 0.0465$).

Daily water use summed to monthly water use (kg tree^{-1} month^{-1}) revealed different trends for the two complete months of the study, July and August (Figure 5.6). In July, monthly tree-level water use varied among the three clones, with '9732-11' having the greatest water use (690 ± 55 kg tree^{-1}), which was significantly greater than the water use of both 'NM2' (449 ± 38 kg tree^{-1}; $p = 0.0027$) and 'DN34' (332 ± 28 kg tree^{-1}; $p < 0.001$). In August, there were not any significant differences in monthly water use among the genotypes (Figure 5.6). Water use summed over the course of the 75-day study period (DOY 176-251) had an overall average of 1,022 kg tree^{-1}. '9732-11' had the greatest water use over the study period (1,335 ± 55 kg tree^{-1}), which was significantly greater than that

of 'NM2' (1,002 ± 83 kg tree^{-1}; $p = 0.0218$) and 'DN34' (780 ± 79 kg tree^{-1}; p = *0.0005*) (Figure 5.6).

5.3.4 Stomatal sensitivity to vapor pressure deficit

Stomatal sensitivity (G_S) to VPD was assessed by regressing G_S against ln(VPD). The data were first divided into two categories according to soil moisture: low soil moisture ($\theta < 0.2$ m^3 m^{-3}) and average-to-high soil moisture ($\theta > 0.2$ m^3 m^{-3}), based on observation of inflection points within the data. A linear model for the G_S vs. ln(VPD) relationship was fitted for each tree, using sample sizes of 1,263 datapoints per tree for the low soil moisture dataset and 728 datapoints per tree for the average-to-high soil moisture dataset. The y-intercept parameter for the models, $G_{S,ref}$ (G_S at VPD = 1 kPa), had the same trend among genotypes in both soil moisture groups. At both low and average-to-high soil moistures, $G_{S,ref}$ was significantly higher for '9732-11' ($p = 0.0006$ in low soil moisture; $p = 0.0030$ in high soil moisture) and 'DN34' ($p = 0.0002$ in low soil moisture; $p = 0.0026$ in high soil moisture) than 'NM2' (Table 5.4). This trend did not hold for G_S sensitivity (the slope of the lines, $-\Delta G_S/\Delta lnVPD$). At low soil moistures, G_S sensitivity did not differ among genotypes (Table 5.4). However, at average-to-high soil moistures, G_S sensitivity was significantly higher for '9732-11' than 'NM2' ($p = 0.0373$), with 'DN34' falling in the middle (Table 5.4). Scaled G_S sensitivity (G_S sensitivity$/G_{S,ref}$) did not differ statistically among genotypes for either soil moisture regime (Table 5.4), with scaled G_S sensitivity averaging 0.50 ± 0.03 at low soil moisture and 0.45 ± 0.03 at high soil moisture. Across both soil moisture categories, 'NM2' consistently had the lowest $G_{S,ref}$, G_S sensitivity, and scaled G_S sensitivity (Table 5.4, Figure 5.7), while '9732-11' consistently had the highest G_S sensitivity and scaled G_S

sensitivity, and 'DN34' consistently had moderate values in between those of the other two genotypes for G_S sensitivity and scaled G_S sensitivity. According to paired t-tests, both '9732-11' and 'DN34' exhibited statistically similar scaled G_S sensitivity at low and high soil moisture conditions, while 'NM2' had significantly greater scaled sensitivity at low soil moisture than high soil moisture conditions ($p = 0.0202$) (Table 5.4).

5.3.5 Leaf water potential and hydraulic conductance

There was a significant genotype × soil moisture interaction for Ψ_{pd} ($p = 0.0474$) (Table 5.5). Specifically, the 'NM2' × high soil moisture interaction had significantly greater (less negative) Ψ_{pd} than 'NM2' × low soil moisture ($p = 0.0032$) and '9732-11' × low soil moisture ($p = 0.0043$). The soil moisture content main effect was also significant for Ψ_{pd}, with $\theta < 0.2$ having lower Ψ_{pd} than $\theta > 0.2$ ($p = 0.0002$). There were no significant effects of genotype, soil moisture, or their interaction for Ψ_{md}. There was a significant soil moisture content main effect for $\Delta\Psi$, with $\Delta\Psi$ being significantly greater for high soil moisture conditions than low ($p = 0.0278$). There were no significant effects of genotype, soil moisture, or their interaction for K_l.

5.4 Discussion

5.4.1 Water use and sap flux

There was a range in water use among the three hybrid *Populus* genotypes in their fourth growing season. Water use appeared to be related to tree size, with the largest genotype (according to diameter and sapwood area), '9732-11', having the greatest water use of 1,335 kg tree^{-1} over the course of the study period (DOY 176-251). For a 1-ha monoclonal planting of '9732-11' established with the same spacing as this study (1,680

trees ha^{-1}), this converts to 224 mm water used during the study. The moderately-sized 'NM2' had the next highest water use of 1,002 kg tree^{-1} during the study period, or 168 mm per hectare. Finally, the smallest genotype, 'DN34', had the lowest water use of 780 kg tree^{-1} during the study period, or 131 mm per hectare. These cumulative values are comparable to others reported for hybrid poplar water use, though they are at the lower end of the spectrum, which can be attributed to the shorter length of this study period compared to other studies. For instance, Schmidt-Walter et al. (2014) observed cumulative transpiration of 387 mm for 'J-105' (*P. nigra* × *P. maximowiczii*) in their sixth growing season (study period of DOY 105-305), grown in Germany. Similarly, DN trees in their second growing season were reported to use 534 kg tree^{-1} of water over the course of a growing season (May – October) in Mississippi, with other poplar genotypes (*P. deltoides* × *P. maximowiczii*) of the same age reaching 944 kg tree^{-1} (Renninger et al., 2022).

During the study period, the study site received 399 mm of rainfall, and accordingly, the transpiration of the three genotypes accounted for 56% ('9732-11'), 42% ('NM2'), and 33% ('DN34') of this rainfall. These estimates are in line with Renninger et al. (2021), who similarly quantified the proportion of growing season precipitation that was accounted for by hybrid poplar transpiration and found a range of 20-61% for TD (*P. trichocarpa* Torr. & Gray ex Hook. × *P. deltoides*) and DM (*P. deltoides* × *P. maximowiczii*) hybrids. Focusing on the two complete months of the current study, July and August, total water use for these two months was 1,163 kg tree^{-1}, or 195 mm ('9732-11'), 853 kg tree^{-1}, or 143 mm ('NM2'), and 671 kg tree^{-1}, or 113 mm ('DN34'). The 30-year average rainfall summed for these two months is 176 mm for the site (NOAA,

2025), so it would appear that '9732-11' has the potential to transpire more water than what is received as rainfall. However, upon further investigation, the year that this study took place (2021) experienced significant rainfall events which led to a much greater total precipitation than is expected for the location. A total of 355 mm of rainfall was measured at the site for July and August during the study. Therefore, based on the rainfall that was measured at the site during the study year, a monoclonal plantation with the same spacing of the current study could expect to transpire around 55% of the precipitation during July and August for '9732-11', 40% for 'NM2', and 32% for 'DN34', if climatic conditions are similar to those observed during the study period.

Average daily water use was 18 kg tree^{-1} day^{-1} (3.0 mm day^{-1}) for '9732-11', followed by 13 kg tree^{-1} day^{-1} (2.2 mm day^{-1}) for 'NM2', and 10 kg tree^{-1} day^{-1} (1.7 mm day^{-1}) for 'DN34'. These water use values reported are lower than those reported by Zalesny et al. (2006) who found daily water use of 'NM6' (*P. nigra* × *P. maximowiczii*) trees in their fourth growing season to be 34 kg day^{-1}. This difference may be related to the timing of that study, which was 18 days in length, and took place at the peak of the growing season from DOY 206-223. The present study was longer and contained days outside of the peak of the growing season, with those days having lower water use, and contributing to an overall lower mean daily water use, than that of Zalesny et al. (2006). Others have observed similar daily water use values to those in the present study, including Schmidt-Walter et al. (2014) who reported average stand transpiration (May – September) of 2.35 mm day^{-1} for 'J-105' (*P. nigra* × *P. maximowiczii*) in their sixth growing season. Sap flux did not follow the same genotypic trends as water use ('9732-11' > 'NM2' > 'DN34'), and unlike water use, does not include sapwood area in its

calculation. On the contrary, 'DN34' exhibited the greatest average daily sap flux, followed by 'NM2', and '9732-11', respectively. Therefore, it can be reasoned that differences in water use among the genotypes of the present study can be attributed to the size differences of the trees, and not the sap flux itself.

Though out of the scope of the current study, future work to generate genotype-specific data on the physiological and anatomical components underlying sap flow calculations could improve estimates of whole-tree water use. Specifically, studies to characterize the radial sap flow profile of the genotypes (Meiresonne et al., 1999), better quantify the active sapwood areas of the genotypes, such as with dye injection studies (Schmidt-Walter et al., 2014), and develop genotype-specific coefficients for the Granier thermal dissipation sap flow equation (Sun et al., 2012), could all serve to increase the accuracy of their water use estimates.

5.4.2 Water use and leaf retention

In addition to differing in overall water usage, the three genotypes also differed in terms of the seasonal patterns of their water use. '9732-11' exhibited peak water use during July, after which its values steadily declined for the rest of the study period. On the other hand, 'NM2' and 'DN34' both had peak water use in mid-August, with values decreasing after that. These trends are paralleled in the monthly LAI values for the genotypes. '9732-11' had its greatest LAI values in July, after which it declined at a relatively steep rate compared to the other two genotypes. 'NM2' and 'DN34' both exhibited their highest LAI values in August, with values decreasing, more gradually than those of '9732-11', from August to September. The declining water use observed after a July peak for '9732-11' could be related to leaf loss of the genotype, though it is unknown

if this genotype naturally loses its leaves earlier than the other two genotypes, or if there were factors other than phenology that contributed to quicker leaf loss of the genotype. To the author's knowledge, no studies exist to date on the leaf area phenology of '9732-11'. However, studies have assessed the leaf area dynamics of other DN genotypes (Ceulemans and Deraedt, 1999; Fontenla-Razzetto et al., 2023). At two sites with contrasting water regimes, maximum LAI was observed at the beginning of August for uncoppiced 'AF2' (*P. deltoides* × *P. nigra*) in their fourth growing season (Fontenla-Razzetto et al., 2023). The earlier reduction in LAI of '9732-11' seen in the present study may be related to geographic origin, with genotypes native to more northern latitudes exhibiting shorter growing seasons and earlier leaf fall than more southerly genotypes (Ceulemans and Deraedt, 1999). '9732-11' originates from northern Minnesota, USA (46.8069° N), which may contribute to a shorter growing season of this genotype. On the other hand, the leaf area trends for 'NM2' seen in the present study have also been reported elsewhere for other NM genotypes. Tripathi et al. (2016; 2018) found the LAI of uncoppiced 'J-105' (*P. nigra* × *P. maximowiczii*) trees in their 8th and 9th years of growth to reach peak values later in the growing season, in late August into September, with values reaching highs of over 6 m^2 m^{-2}. Tharakan (1999) found LAI of another related NM genotype, 'NM6', to peak in early August following coppice. The earlier leaf loss of '9732-11' could also be an adaptive response to water stress. Leaf senescence (Munné-Bosch and Alegre, 2004), leaf shedding (Wolfe et al., 2016) and other decreases in leaf area (Marron et al., 2003) are mechanisms used by plants to increase survival during times of drought through the reduction of plant water demand. Drought-induced reductions in leaf area have been reported for poplars, including leaf desiccation of

Populus tremula L. × *P. tremuloides* Michx. (Hennig et al., 2015), as well as clonal differences in leaf area reductions among *Populus* × *canadensis* (Moench) (*P. deltoides* × *P. nigra*) genotypes subjected to drought stress (Marron et al., 2003). Further work on the seasonal leaf area dynamics of the three genotypes studied here, particularly to investigate the timing of senescence and leaf drop for '9732-11', as well as the correlations between its leaf area and drought conditions, could be beneficial to better understand the relationship between leaf area index and seasonal water use dynamics of the genotypes.

5.4.3 Stomatal sensitivity

Scaled stomatal sensitivity did not differ statistically among genotypes under either lower soil moisture conditions ($\theta < 0.2$ m^3 m^{-3}) or average-to-high soil moisture conditions ($\theta > 0.2$ m^3 m^{-3}). Inability to detect a statistically significant difference among the genotypes may be the result of the limited sample size of the study (n = five and six trees per genotype) more so than a lack of physiological differences. However, there was an observable trend that scaled G_S sensitivity was marginally higher for '9732-11' than 'NM2' and 'DN34' for both soil moisture regimes, with its average values of 0.562 ($\theta <$ 0.2 m^3 m^{-3}) and 0.535 ($\theta > 0.2$ m^3 m^{-3}) being reasonably close to the theoretical universal value of 0.6 for an isohydric stomatal regulation strategy (Oren et al., 1999). The (marginally) lower scaled G_S sensitivity values for 'NM2' (0.463 for low soil moisture and 0.410 for high soil moisture) and 'DN34' (0.490 for low soil moisture and 0.427 for high soil moisture) indicate slightly more anisohydric strategies of the two genotypes than for '9732-11'. Though the stomatal sensitivity is unknown for the three genotypes studied here, other hybrid poplars have been investigated. Maier et al. (2019) found an average

scaled sensitivity of 0.63 across nine poplar genotypes in their fourth year of growth, while one group of the genotypes, considered “low growth performance” genotypes, had significantly lower scaled stomatal sensitivity of 0.54 when compared to the intermediate and high growth performance groups. Maier et al. (2019) further observed that the “low performance” genotypes were less sensitive to decreasing soil relative extractable water (i.e., they maintained higher levels of stomatal conductance at lower levels of soil moisture). Schmidt-Walter et al. (2014) found values for scaled sensitivity to range from a low of 0.471 in May to values between 0.6-0.7 for the rest of the growing season for 'J-105' (*P. nigra* × *P. maximowiczii*) in their sixth growing season. Similar values were observed by Renninger et al. (2021), who found an overall average scaled stomatal sensitivity of 0.59 across all trees in their study (a mixture of *Populus* genotypes), though results were nuanced according to site and soil moisture.

Results of paired t-tests indicated different responses of genotypes to soil moisture levels. Plasticity in stomatal sensitivity was demonstrated for 'NM2', whose scaled G_S sensitivity was significantly greater for low soil moisture conditions than higher soil moisture conditions ($p = 0.0202$). Renninger et al. (2021) similarly identified '8019' (*P. deltoides* × *P. maximowiczii*) and '110412' (*P. deltoides* × *P. deltoides*) genotypes as exhibiting plasticity in G_S sensitivity in response to variable soil moisture regimes. Statistically significant differences among soil moisture conditions were not observed for '9732-11' nor 'DN34' (i.e., their scaled G_S sensitivities remained consistent among soil moisture conditions). These results point toward the potential for 'NM2' to be more poised to adapt to changes in soil moisture conditions, though further investigation to confirm these results, including through the use of larger sample sizes, is warranted.

5.4.4 Hydraulic conductance and leaf water potential

There were no significant genotype main effects observed for tree leaf water potential parameters (Ψ_{pd}, Ψ_{md}, $\Delta\Psi$), nor leaf-specific whole-plant hydraulic conductance (K_l). The only significant differences that were observed in these parameters resulted from differences in soil moisture content. This is not unexpected for Ψ_{pd}, as this variable is tightly linked to soil moisture conditions, and is considered a proxy for soil moisture content (Améglio et al., 1999). Relatedly, as there were not significant differences among soil moisture regimes for Ψ_{md}, the significantly greater $\Delta\Psi$ seen for high soil moisture than low soil moisture conditions can be attributed to the significantly higher Ψ_{pd} under high soil moisture conditions, which led to greater differences between predawn and midday Ψ. A conclusion on the hydraulic conductance of the three genotypes in the current study cannot yet be reached, again due to the limited sample size of the study (n = five and six trees per genotype for each soil moisture category). However, if the trends observed here, namely, no significant difference in leaf-specific whole-plant hydraulic conductance among genotypes, remain true under larger sample sizes, it could be reasoned that differences in stomatal conductance or transpiration among the genotypes may not be due to differences in hydraulic properties.

It is important to note that with the Ψ measurements being conducted using leaves from the lower third of the canopy, rather than the upper canopy, the leaf water potential gradient (ΔΨ) reported in this study may be underestimated as a result. It has been reported that Ψ decreases with increasing crown heights (Fang et al., 2021), which is due to the greater gravitational forces and resistances along the path from roots to leaves that must be overcome by Ψ in order for water to be transported to the canopy. Comparisons

among genotypes for the Ψ-related variables (Ψ_{pd}, Ψ_{md}, $\Delta\Psi$, and K_l) in this study can be made on a relative basis, but if comparisons of absolute values are desired, further work incorporating leaves from the upper canopy will be necessary.

5.5 Conclusion

In a 75-day field study on hybrid *Populus* water use, we found that overall water use as well as seasonal trends of water use varied among three *Populus* genotypes in their fourth growing season. '9732-11' had the greatest water use on all temporal scales assessed (daily, monthly, total study period), followed by 'NM2', with 'DN34' having the lowest water use across all temporal scales. These results can be attributed to the size differences of the genotypes, with '9732-11' having the largest DBH and sapwood area, followed by 'NM2', and 'DN34' with the smallest values. Over the course of the study, '9732-11' water use peaked in July, with values steadily declining after that, while 'NM2' and 'DN34' water use did not peak until mid-August. These seasonal trends in water use were reflected by similar trends in LAI, with peak LAI observed in July for '9732-11', while 'NM2' and 'DN34' both exhibited their highest LAI values in August. Further investigation into leaf phenology of these genotypes and its association with tree water use are warranted. There were variable results for water use strategies of the genotypes. Scaled G_S sensitivity did not differ statistically among genotypes for either soil moisture regime, though 'NM2' consistently had the lowest values, '9732-11' had the highest values, and 'DN34' had moderate values of scaled G_S sensitivity. However, 'NM2' appeared to exhibit greater plasticity to soil moisture conditions, with significantly greater scaled sensitivity at low soil moisture than high soil moisture conditions. Neither '9732-11' nor 'DN34' exhibited statistically significant differences in scaled G_S sensitivity

between low and high soil moisture conditions, which could suggest that 'NM2' may be better able to modify its water use strategy in response to different soil moisture conditions. Finally, there were not any genotypic differences in tree leaf water potential parameters, nor leaf-specific whole-plant hydraulic conductance. These results could indicate that differences in water use among the genotypes are not due to differences in hydraulic properties, though further studies containing larger samples sizes will be necessary to validate this result, and the results on other water use parameters reported here. Based on our findings, '9732-11' is a promising candidate for phytoremediation systems that require elevated water use to reach remediation objectives. '9732-11' had much greater water use than the other two genotypes studied. However, its water use declined after a peak in July. On the other hand, 'NM2' had lower, yet comparable, water use to '9732-11', exhibited peak values of LAI and water use that occurred later in the growing season, and greater plasticity in stomatal response to changing soil moisture conditions. Utilizing *Populus* genotypes with complementary water use strategies, such as '9732-11' and 'NM2', may be a prudent option for maximizing water use of phytoremediation systems while also promoting resiliency against variable climatic conditions.

Table 5.1. Genomic groups and plant material sources for the three hybrid poplar genotypes investigated in the current study. Dormant hardwood cuttings were obtained from the nurseries listed and were kept in cold storage (5 °C, in darkness) until planting.

Genomic Group	Genotype	Nursery
Populus deltoides Bartr. ex. Marsh × *P. nigra* L. 'DN'	DN34	Michigan State University Clonal Orchard at the Tree Research Center (Lansing, MI, USA)
	9732-11	University of Minnesota NRRI Clonal Orchard at the North Central Research and Outreach Center Nursery (Grand Rapids, Minnesota, USA)
P. nigra × *P. maximowiczii* A. Henry 'NM'	NM2	Michigan State University Clonal Orchard at the Tree Research Center (Lansing, MI, USA)

Table 5.2. Soil physicochemical properties of the study site in Eastern Wisconsin.

	Depth	
	0-27.9 cm	**27.9-58.4 cm**
pH	6.67 ± 0.03	7.07 ± 0.09
Texture	Sandy Loam	Loam
	Percent	
Clay	14	18
Sand	53	49
Silt	33	33
C	10.51 ± 1.11	6.06 ± 0.20
N	0.56 ± 0.05	0.25 ± 0.03
	mg kg^{-1}	
Cd	0.48 ± 0.03	0.34 ± 0.02
Cr	17.96 ± 0.53	18.85 ± 0.68
Cu	25.45 ± 0.67	22.95 ± 1.68
Na	137.71 ± 2.26	126.68 ± 4.45
Ni	10.55 ± 0.33	12.61 ± 0.74
Mn	229.30 ± 7.03	277.00 ± 7.03
Pb	14.09 ± 0.19	13.48 ± 0.33
S	874.46 ± 55.22	471.49 ± 33.47
Zn	66.97 ± 5.67	58.81 ± 3.96
	g kg^{-1}	
Ca	56.78 ± 7.60	57.96 ± 2.94
Fe	14.22 ± 0.53	16.11 ± 0.84
K	2.62 ± 0.46	3.36 ± 0.16
P	1.19 ± 0.03	0.71 ± 0.03
Mg	33.28 ± 4.16	37.52 ± 1.50

Table 5.3. Tree growth and leaf area characteristics in the middle of the study period (DOY 207; 7/26/21) for 'NM2' (*Populus nigra* × *P. maximowiczii*), '9732-11' (*P. deltoides* × *P. nigra*), and 'DN34' (*P. deltoides* × *P. nigra*) in their fourth growing season. Values are means followed by standard errors in parentheses. Within a column, means with different superscript letters are significantly different at $p < 0.05$. These data represent the middle of the study period; height (m), diameter at breast height (DBH; cm), and leaf area index (LAI; $m^2\ m^{-2}$) were measured on DOY 207. Tree leaf area (m^2) was calculated from block-level LAI data. Sapwood area (cm^2) was calculated from DBH data and adjusted for bark thickness according to results from a subsample full-tree harvest.

Genotype	Height (m)	DBH (cm)	Sapwood Area (cm^2)	LAI (m^2/m^2)	Tree Leaf Area (m^2)
9732-11	8.07 (0.37)[a]	9.60 (0.36)[a]	65.83 (5.01)[a]	4.81 (0.23)[b]	32.60 (1.25)[a]
DN34	6.84 (0.31)[b]	6.68 (0.46)[b]	32.45 (4.41)[b]	2.78 (0.22)[c]	19.16 (2.80)[b]
NM2	8.52 (0.17)[a]	8.05 (0.34)[b]	45.97 (3.99)[b]	6.37 (0.59)[a]	37.08 (1.99)[a]

Table 5.4. Parameters estimated from linear regression equations fitted to the canopy stomatal conductance (G_S; mol m^{-2} s^{-1}) vs. natural log of vapor pressure deficit [ln(VPD); kPa] relationship for 'NM2' (*Populus nigra* × *P. maximowiczii*), '9732-11' (*P. deltoides* × *P. nigra*), and 'DN34' (*P. deltoides* × *P. nigra*). Separate equations were fitted for low soil moisture ($\theta < 0.2$ m^3 m^{-3}) and average-to-high soil moisture conditions ($\theta > 0.2$ m^3 m^{-3}). Values are means of all trees within genotypes, followed by standard errors in parentheses. Within a column, means with different superscript letters are significantly different at $p < 0.05$. Parameters include $G_{S,ref}$, the reference G_S when VPD = 1 kPa (mol m^{-2} s^{-1}; y-intercept), G_S sensitivity (mol m^{-2} s^{-1} ln kPa^{-1}; slope), and scaled G_S sensitivity (slope / y-intercept). The "Low vs. High θ" column includes p-values for paired, two-tailed t-tests between scaled G_S sensitivity for low soil moisture and average-to-high soil moisture conditions. Significant p-values ($p < 0.05$) are bolded.

	Low Soil Moisture (θ)			Average-to-High Soil Moisture (θ)			
Genotype	**$G_{S,ref}$**	**G_S sensitivity**	**Scaled G_S sensitivity**	**$G_{S,ref}$**	**G_S sensitivity**	**Scaled G_S sensitivity**	**Low vs. High θ**
9732-11	0.096 (0.004)^{a}	0.055 (0.010)^{a}	0.562 (0.078)^{a}	0.099 (0.004)^{a}	0.053 (0.008)^{a}	0.535 (0.067)^{a}	0.6470
DN34	0.099 (0.008)^{a}	0.051 (0.010)^{a}	0.490 (0.065)^{a}	0.098 (0.010)^{a}	0.044 (0.010)^{ab}	0.427 (0.067)^{a}	0.0647
NM2	0.056 (0.004)^{b}	0.026 (0.002)^{a}	0.463 (0.015)^{a}	0.059 (0.004)^{b}	0.024 (0.002)^{b}	0.410 (0.018)^{a}	**0.0202**

Table 5.5. Tree leaf water potential (Ψ; MPa) and leaf-specific whole-plant hydraulic conductance (K_l; kg m^{-2} h^{-1} MPa^{-1}) for 'NM2' (*Populus nigra* × *P. maximowiczii*), '9732-11' (*P. deltoides* × *P. nigra*), and 'DN34' (*P. deltoides* × *P. nigra*) measured within low (θ < 0.2 m^3 m^{-3}) and high (θ > 0.2 m^3 m^{-3}) soil moisture conditions. Leaf water potential was measured at predawn (Ψ_{pd}; 0400-0600 h) and midday (Ψ_{md}; 1200-1400 h), with ΔΨ representing their difference (Ψ_{pd} - Ψ_{md}). Data are means followed by standard errors in parentheses. Probability values from the two-way ANOVAs relating genotype, soil moisture, and their interaction are reported at the bottom. Significant p-values (*p < 0.05*) are bolded.

Genotype	Soil Moisture	Ψ_{pd}	Ψ_{md}	ΔΨ	K_l
9732-11	Low	-0.82 (0.05)	-1.67 (0.10)	0.85 (0.10)	0.11 (0.01)
	High	-0.64 (0.04)	-1.83 (0.07)	1.19 (0.08)	0.07 (0.01)
DN34	Low	-0.67 (0.04)	-1.60 (0.08)	0.93 (0.09)	0.08 (0.004)
	High	-0.64 (0.03)	-1.76 (0.19)	1.12 (0.20)	0.08 (0.01)
NM2	Low	-0.82 (0.06)	-1.62 (0.09)	0.81 (0.08)	0.08 (0.02)
	High	-0.56 (0.04)	-1.50 (0.08)	0.94 (0.08)	0.06 (0.01)
Two-Way ANOVA (p-values)					
Genotype		0.2427	0.2539	0.3468	0.2069
Soil Moisture		**0.0002**	0.4737	**0.0278**	0.0873
Genotype × Soil Moisture		**0.0474**	0.3660	0.6651	0.2566

Figure 5.1. Location of the sap flow study site. Hybrid poplars were established in a phytoremediation buffer system at the site in 2018.

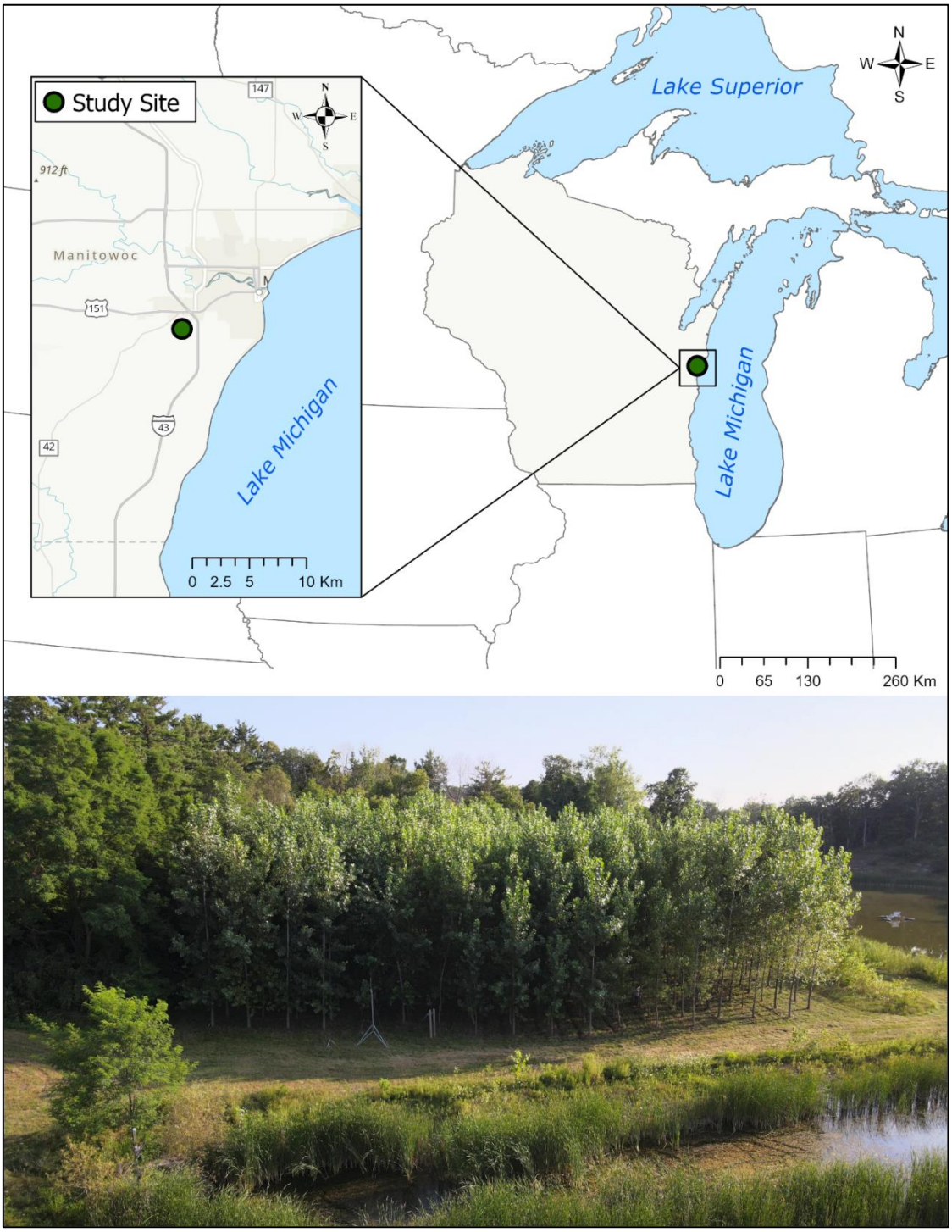

Figure 5.2. Installation of thermal dissipation sap flow probes in hybrid poplar trees. Thermal dissipation probes consist of two 30 mm thermocouples inserted radially into the trees (A). Once installed, probes were secured with putty, protected with quarter-moon styrofoam eggs (B), and shielded from solar radiation with reflective bubble wrap and aluminum foil (C). A climatic station was also installed at the site to collect climatic data throughout the study (D).

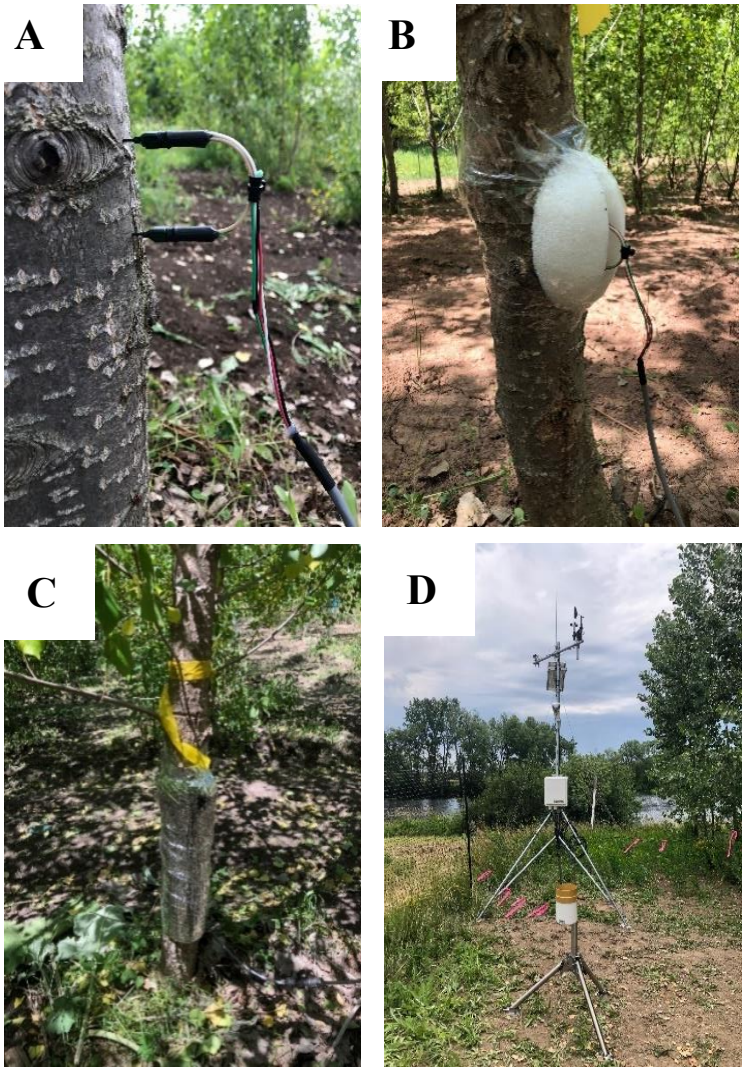

Figure 5.3. Map of phytoremediation buffer planting (A) and schematic of LAI measurement scheme (B-C). Each rectangle (light green, dark grey, orange, and blue) represents a poplar tree (A). Trees were established at 2.44 m × 2.44 m spacing. Monoclonal blocks of the three genotypes assessed in the current study are shown in dark grey ('NM2'), orange ('9732-11'), and blue ('DN34'). Trees instrumented with sap flow probes are numbered (101-118). An aerial view of the planting, taken during the trees' second growing season, is shown below (B). The inset (C) depicts the measurement scheme for LAI. Five leaf area index measurements were taken per block using an LAI-2200C plant canopy analyzer: four corners (90° view cap, depicted as black and white circles) and one middle (180° view cap). Aerial photo courtesy of Paul Manley, Missouri University of Science and Technology.

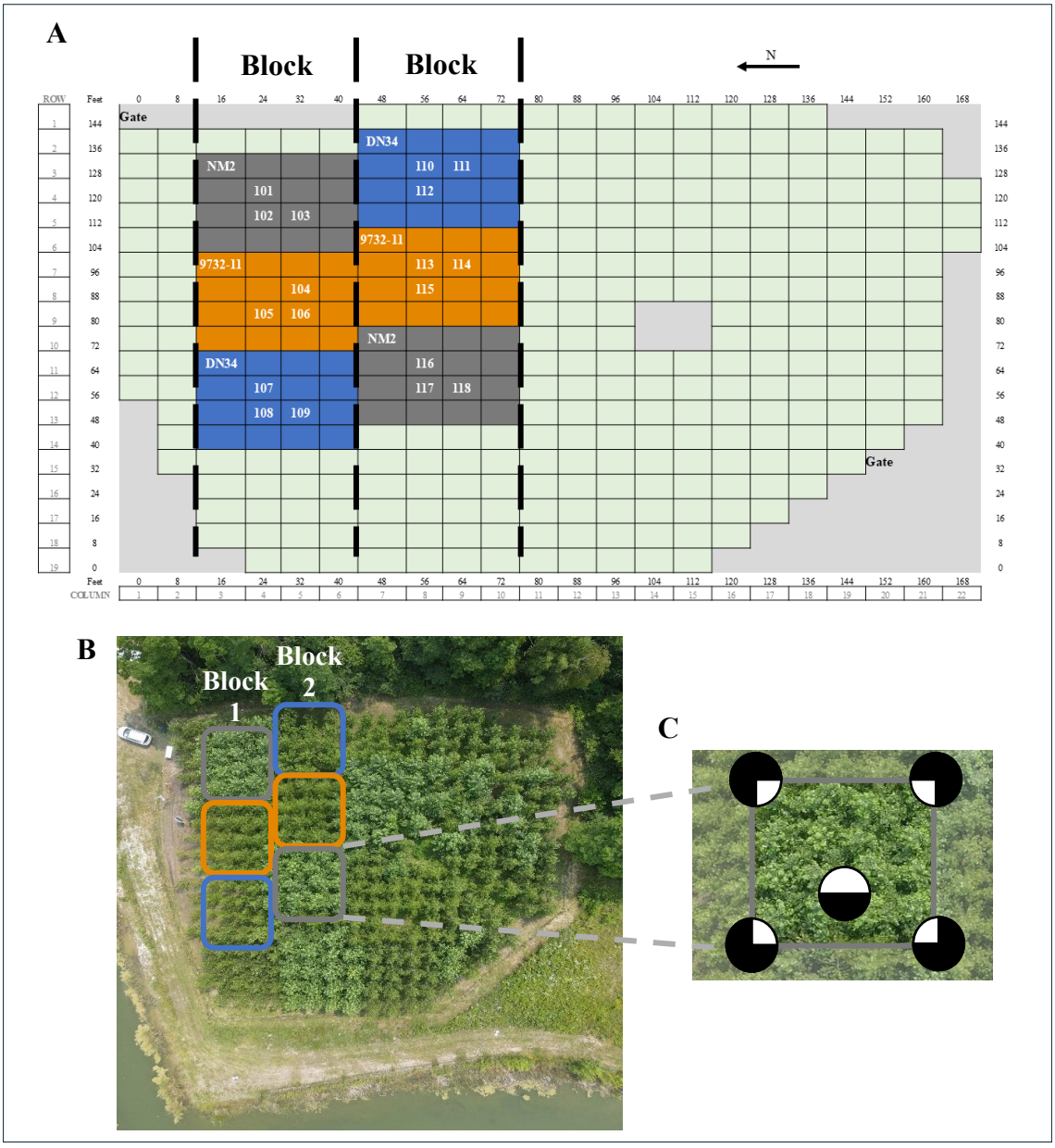

Figure 5.4. Climatic conditions measured at the study site in Eastern Wisconsin, USA during the study period (DOY 176-251, 6/25/21-9/8/21).

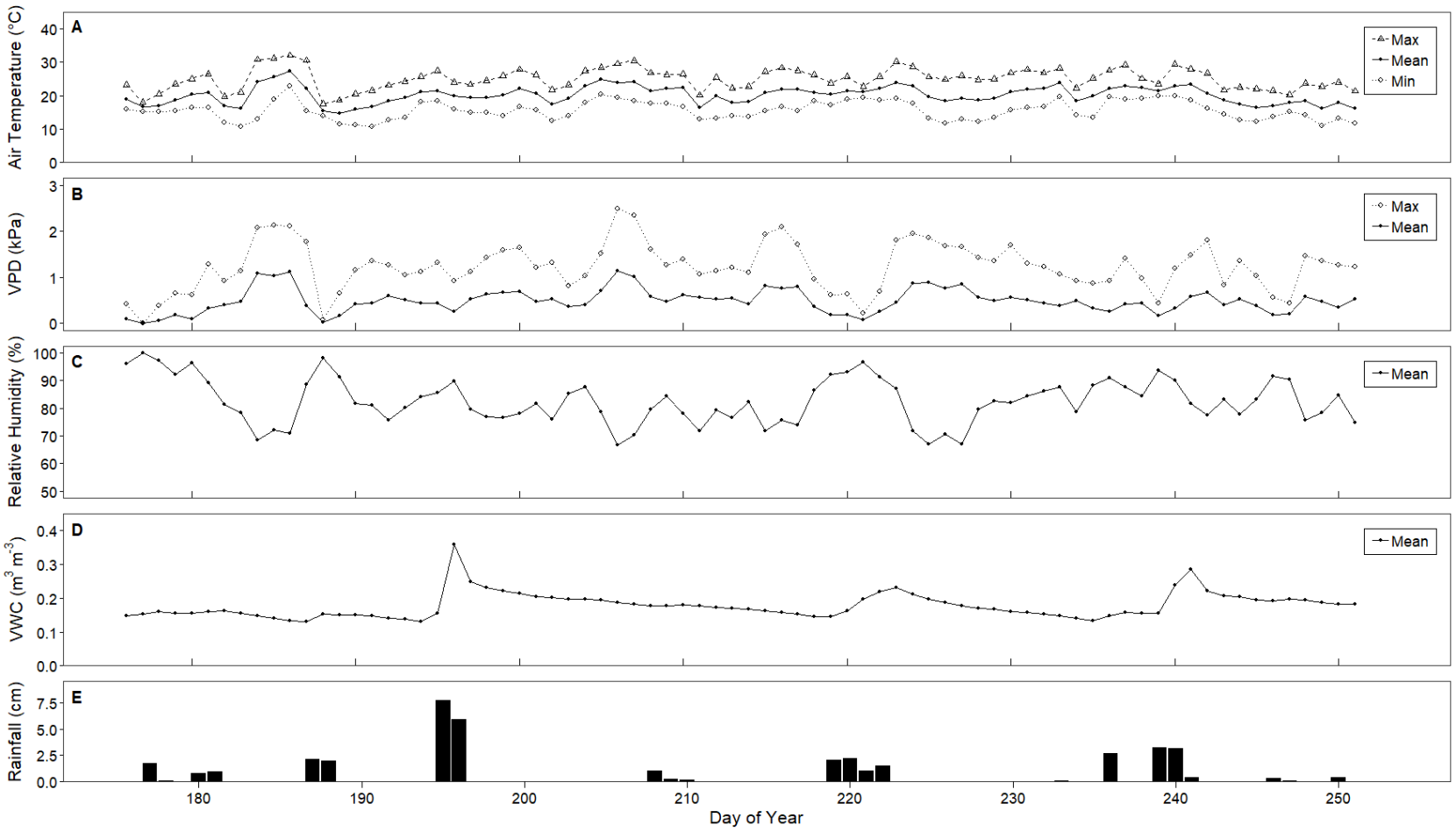

Figure 5.5. Monthly leaf area index (LAI; m^2 m^{-2}) of 'NM2' (*Populus nigra* × *P. maximowiczii*), '9732-11' (*P. deltoides* × *P. nigra*), and 'DN34' (*P. deltoides* × *P. nigra*) in their fourth growing season. Mean values are plotted as points, and standard errors are shown as bars extending from the means.

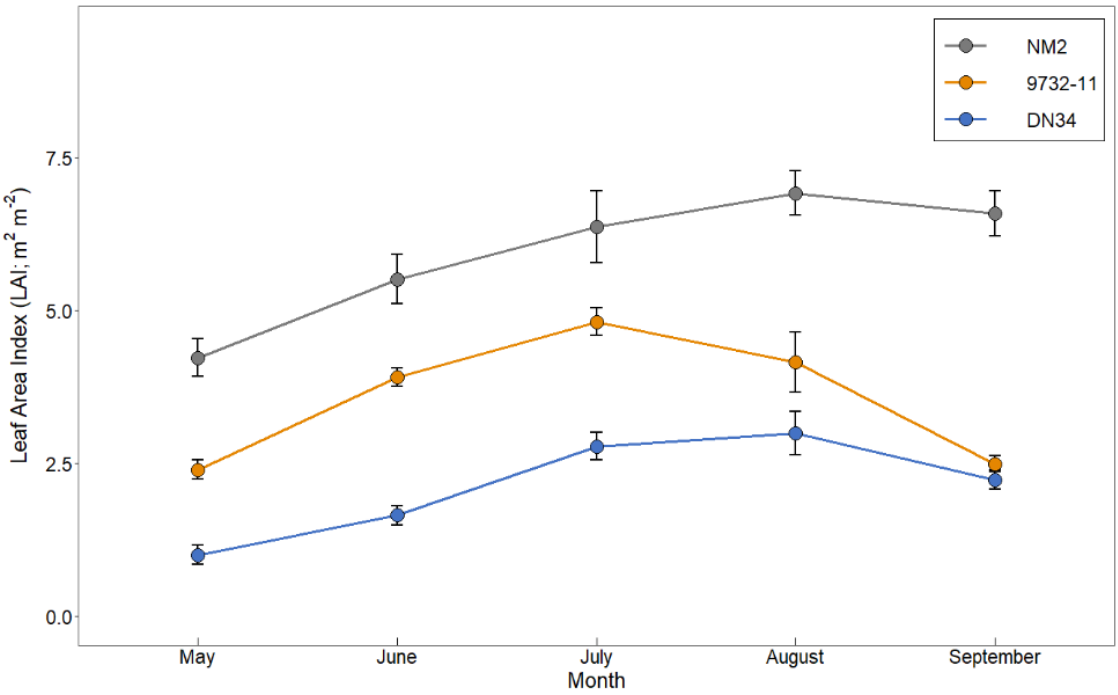

Figure 5.6. Tree-level monthly (A, B) and season (C) water use (kg tree^{-1}) of three hybrid poplars ('9732-11', 'DN34', and 'NM2') in their fourth growing season. Season water use is the total water use over the study period (DOY 176-251, 6/25/21-9/8/21). Within a panel, genotypes with different letters differ significantly at $p < 0.05$. Means are represented as stars and standard errors as bold bars extending from the means.

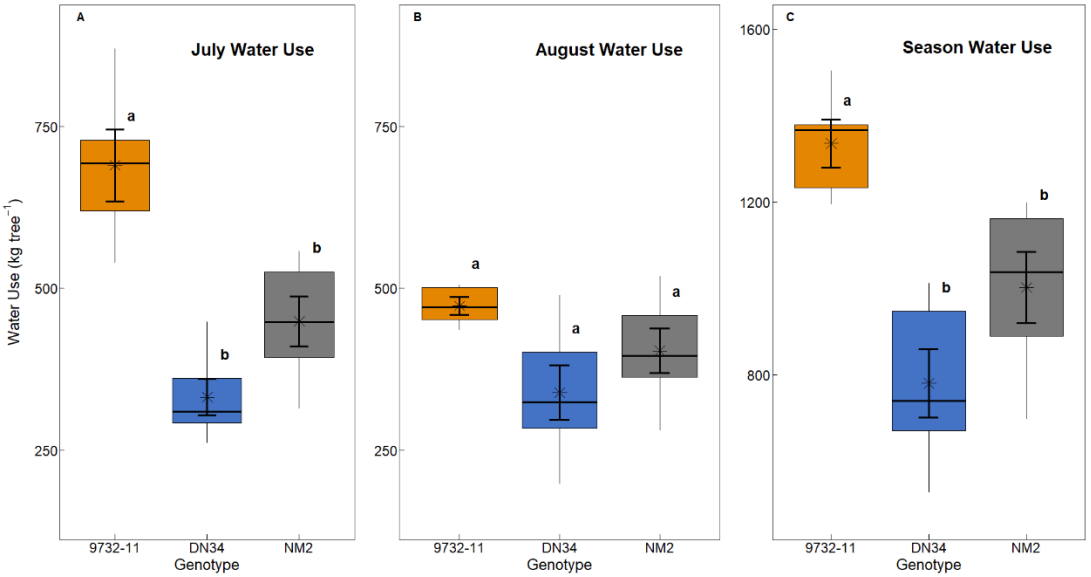

Figure 5.7. Canopy stomatal conductance (G_S; mol m^{-2} s^{-1}) vs. the natural log of vapor pressure deficit (ln VPD; ln kPa) for three poplar genotypes ('9732-11', 'DN34', and 'NM2') within (A) low soil moisture conditions ($\theta < 0.2$ m^3 m^{-3}) and (B) average-to-high soil moisture conditions ($\theta > 0.2$ m^3 m^{-3}). For plotting purposes, G_S values were binned into 16 and 14 ln VPD bins (low θ and high θ, respectively). Each point represents the mean G_S value for all trees of the corresponding genotype, within that particular ln(VPD) bin. Standard errors are shown as bars extending from the means. Linear regression lines were fitted for each genotype using all available data (non-binned). Slope (G_S sensitivity) and intercept ($G_{S,ref}$) values for the linear regressions are reported in Table 5.4. R^2 values for the regressions are as follows for the low θ category: $R^2 = 0.1871$ ('9732-11'); $R^2 = 0.1538$ ('DN34'); $R^2 = 0.1110$ ('NM2'). R^2 values for the high θ category are as follows: $R^2 = 0.1996$ ('9732-11'); $R^2 = 0.1364$ ('DN34'); $R^2 = 0.1242$ ('NM2').

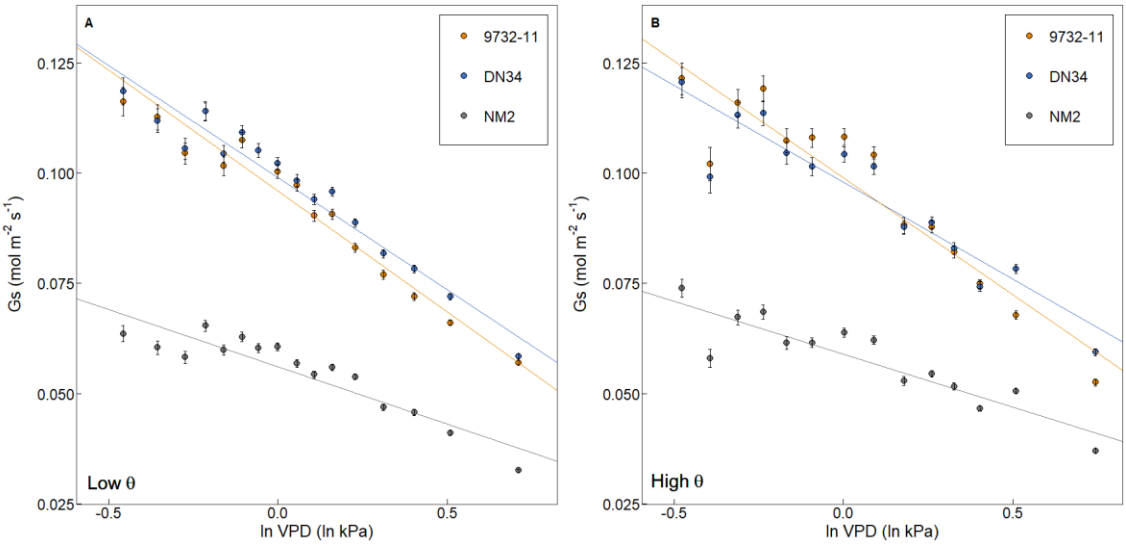

APPENDIX D.

Table D1. Parameters used in Baseliner preprocessing of sap flow data.

Parameter	Value
Time step increments (minutes)	15
Minimum valid sap flow value	0.5
Maximum valid sap flow value	30
Maximum change per interval	2
Delete data segments shorter than X points	4
Solar radiation threshold: values below this are considered nighttime (Watts m^{-2})	10
VPD threshold: values below this are considered zero (kPa)	0.2
VPD time: length in hours of time segment of low-VPD conditions	2

5.6 References

AECOM, 2023. 2021 Annual VOC groundwater monitoring report, Project Number: 60135471. https://apps.dnr.wi.gov/botw/DownloadBlobFile.do?docSeqNo=265053&docName=20230815_43_GW_Monitor_2021.pdf&docDsn=33760.

Améglio, T., Archer, P., Cohen, M., Valancogne, C., Daudet, F.-A., Dayau, S., Cruiziat, P., 1999. Significance and limits in the use of predawn leaf water potential for tree irrigation. Plant Soil 207, 155–167. https://doi.org/10.1023/A:1026415302759.

Attia, Z., Domec, J.-C., Oren, R., Way, D.A., Moshelion, M., 2015. Growth and physiological responses of isohydric and anisohydric poplars to drought. J. Exp. Bot. 66, 4373–4381. https://doi.org/10.1093/jxb/erv195.

Babi, K., Guittonny, M., Larocque, G.R., Bussière, B., 2019. Effects of spacing and herbaceous hydroseeding on water stress exposure and root development of poplars planted in soil-covered waste rock slopes. Écoscience 26, 149–163. https://doi.org/10.1080/11956860.2018.1538591.

BenIsrael, M., Wanner, P., Aravena, R., Parker, B.L., Haack, E.A., Tsao, D.T., Dunfield, K.E., 2019. Toluene biodegradation in the vadose zone of a poplar phytoremediation system identified using metagenomics and toluene-specific stable carbon isotope analysis. Int. J. Phytoremediat. 21, 60–69. https://doi.org/10.1080/15226514.2018.1523873.

Bradshaw, H.D., Ceulemans, R., Davis, J., Stettler, R., 2000. Emerging model systems in plant biology: poplar (*Populus*) as a model forest tree. J. Plant Growth. Regul. 19, 306–313. https://doi.org/10.1007/s003440000030.

Ceulemans, R., Deraedt, W., 1999. Production physiology and growth potential of poplars under short-rotation forestry culture. For. Ecol. Manage. 121, 9–23. https://doi.org/10.1016/S0378-1127(98)00564-7.

Chen, S., Chen, Z., Kong, Z., Zhang, Z., 2023. The increase of leaf water potential and whole-tree hydraulic conductance promotes canopy conductance and transpiration of *Pinus tabulaeformis* during soil droughts. Trees 37, 41–52. https://doi.org/10.1007/s00468-022-02322-z.

Davis, L.C., Castro-Diaz, S., Zhang, Q., Erickson, L.E., 2002. Benefits of vegetation for soils with organic contaminants. Crit. Rev. Plant Sci. 21, 457–491. https://doi.org/10.1080/0735-260291044322.

Dickmann, D.I., Isebrands, J.G., Eckenwalder, J.E., Richarson, J. (Eds.), 2001. Poplar culture in North America. NRC Research Press, Ottawa, Ontario.

Dietz, A.C., Schnoor, J.L., 2001. Advances in phytoremediation. Environ. Health Perspect. 109, 163–168. https://doi.org/10.1289/ehp.01109s1163.

Doty, S.L., Freeman, J.L., Cohu, C.M., Burken, J.G., Firrincieli, A., Simon, A., Khan, Z., Isebrands, J.G., Lukas, J., Blaylock, M.J., 2017. Enhanced degradation of TCE on a superfund site using endophyte-assisted poplar tree phytoremediation. Environ. Sci. Technol. 51, 10050–10058. https://doi.org/10.1021/acs.est.7b01504.

Fang, L.-D., Ning, Q.-R., Guo, J.-J., Gong, X.-W., Zhu, J.-J., Hao, G.-Y., 2021. Hydraulic limitation underlies the dieback of *Populus pseudo-simonii* trees in water-limited areas of northern China. For. Ecol. Manage. 483, 118764. https://doi.org/10.1016/j.foreco.2020.118764.

Ferro, A., Chard, J., Kjelgren, R., Chard, B., Turner, D., Montague, T., 2001. Groundwater capture using hybrid poplar trees: evaluation of a system in Ogden, Utah. Int. J. Phytoremediat. 3, 87–104. https://doi.org/10.1080/15226510108500051.

Ferro, A., Gefell, M., Kjelgren, R., Lipson, D.S., Zollinger, N., Jackson, S., 2003. Maintaining hydraulic control using deep rooted tree systems, in: Tsao, D.T. (Ed.), Phytoremediation. Springer Berlin Heidelberg, Berlin, Heidelberg, pp. 125–156.

Ferro, A.M., Adham, T., Berra, B., Tsao, D., 2013. Performance of deep-rooted phreatophytic trees at a site containing total petroleum hydrocarbons. Int. J. Phytoremediat. 15, 232–244. https://doi.org/10.1080/15226514.2012.687195.

Ferro, A.M., Sims, R.C., Bugbee, B., 1994. Hycrest crested wheatgrass accelerates the degradation of pentachlorophenol in soil. J. Environ. Qual. 23, 272–279. https://doi.org/10.2134/jeq1994.00472425002300020008x.

Fontenla-Razzetto, G., Wahren, F.T., Heilig, D., Heil, B., Kovacs, G., Feger, K.-H., Julich, S., 2023. Water use of hybrid poplar (*Populus deltoides* Bart. ex Marsh × *P. nigra* L. "AF2") growing across contrasting site and groundwater conditions in Western Slovakia. Bioenerg. Res. 16, 379–397. https://doi.org/10.1007/s12155-022-10445-x.

Fu, Z., Ciais, P., Prentice, I.C., Gentine, P., Makowski, D., Bastos, A., Luo, X., Green, J.K., Stoy, P.C., Yang, H., Hajima, T., 2022. Atmospheric dryness reduces photosynthesis along a large range of soil water deficits. Nat. Commun. 13, 989. https://doi.org/10.1038/s41467-022-28652-7.

Fuller, R., Landrigan, P.J., Balakrishnan, K., Bathan, G., Bose-O'Reilly, S., Brauer, M., Caravanos, J., Chiles, T., Cohen, A., Corra, L., Cropper, M., Ferraro, G., Hanna, J., Hanrahan, D., Hu, H., Hunter, D., Janata, G., Kupka, R., Lanphear, B., Lichtveld, M., Martin, K., Mustapha, A., Sanchez-Triana, E., Sandilya, K., Schaefli, L., Shaw, J., Seddon, J., Suk, W., Téllez-Rojo, M.M., Yan, C., 2022. Pollution and health: a progress update. The Lancet Planetary Health 6, e535–e547. https://doi.org/10.1016/S2542-5196(22)00090-0.

Gerhardt, K.E., Gerwing, P.D., Greenberg, B.M., 2017. Opinion: taking phytoremediation from proven technology to accepted practice. Plant Sci. 256, 170–185. https://doi.org/10.1016/j.plantsci.2016.11.016.

González-González, B.D., Oliveira, N., González, I., Cañellas, I., Sixto, H., 2017. Poplar biomass production in short rotation under irrigation: a case study in the Mediterranean. Biomass Bioenerg. 107, 198–206. https://doi.org/10.1016/j.biombioe.2017.10.004.

Gordon, M., Choe, N., Duffy, J., Ekuan, G., Heilman, P., Muiznieks, I., Ruszaj, M., Shurtleff, B.B., Strand, S., Wilmoth, J., Newman, L.A., 1998. Phytoremediation of trichloroethylene with hybrid poplars. Environ. Health Perspect. 106, 1001–1004. https://doi.org/10.1289/ehp.98106s41001.

Granier, A., 1987. Evaluation of transpiration in a Douglas-fir stand by means of sap flow measurements. Tree Physiol. 3, 309–320. https://doi.org/10.1093/treephys/3.4.309.

Grimond, L., Rivest, D., Bilodeau-Gauthier, S., Khlifa, R., Elferjani, R., Bélanger, N., 2024. Novel soil reconstruction leads to successful afforestation of a former asbestos mine in southern Quebec, Canada. New Forest. 55, 477–503. https://doi.org/10.1007/s11056-023-09989-3.

Grossiord, C., Buckley, T.N., Cernusak, L.A., Novick, K.A., Poulter, B., Siegwolf, R.T.W., Sperry, J.S., McDowell, N.G., 2020. Plant responses to rising vapor pressure deficit. New Phytol. 226, 1550–1566. https://doi.org/10.1111/nph.16485.

Hennig, A., Kleinschmit, J.R.G., Schoneberg, S., Löffler, S., Janßen, A., Polle, A., 2015. Water consumption and biomass production of protoplast fusion lines of poplar hybrids under drought stress. Front. Plant Sci. 6. https://doi.org/10.3389/fpls.2015.00330

Isebrands, J.G., Zalesny Jr., R.S., 2021. Reflections on the contributions of *Populus* research at Rhinelander, Wisconsin, USA. Can. J. For. Res. 51, 139–153. https://doi.org/10.1139/cjfr-2020-0248.

Kovačević, B., Milović, M., Kesić, L., Pajnik, L.P., Pekeč, S., Stanković, D., Orlović, S., 2025. Interclonal variation in heavy metal accumulation among poplar and willow clones: implications for phytoremediation of contaminated landfill soils. Plants 14, 567. https://doi.org/10.3390/plants14040567.

Landmeyer, J.E., 2012. Introduction to phytoremediation of contaminated groundwater: historical foundation, hydrologic control, and contaminant remediation. Springer Netherlands, Dordrecht. https://doi.org/10.1007/978-94-007-1957-6.

Landmeyer, J.E., Effinger, T.N., 2016. Effect of phytoremediation on concentrations of benzene, toluene, naphthalene, and dissolved oxygen in groundwater at a former manufactured gas plant site, Charleston, South Carolina, USA, 1998–2014. Environ. Earth Sci. 75, 605. https://doi.org/10.1007/s12665-016-5408-9.

Laurent, A., Pelzer, E., Loyce, C., Makowski, D., 2015. Ranking yields of energy crops: a meta-analysis using direct and indirect comparisons. Renew. Sustain. Energ. Rev. 46, 41–50. https://doi.org/10.1016/j.rser.2015.02.023.

Li, M., Heng, Q., Hu, C., Wang, Z., Jiang, Y., Wang, X., He, X., Yong, J.W.H., Dawoud, T.M., Rahman, S.U., Fan, J., Zhang, Y., 2024. Phytoremediation efficiency of poplar hybrid varieties with diverse genetic backgrounds in soil contaminated by multiple toxic metals (Cd, Hg, Pb, and As). Ecotoxicol. Environ. Safe. 283, 116843. https://doi.org/10.1016/j.ecoenv.2024.116843.

LI-COR, 2023. Section 6: Canopy Types, in: LAI 2200C Plant Canopy Analyzer Instruction Manual, 4th Edition (Publication No. 984-14112). LI-COR Environmental, Lincoln, Nebraska.

Lüttschwager, D., Ewald, D., Atanet Alía, L., 2016. Consequences of moderate drought stress on the net photosynthesis, water-use efficiency and biomass production of three poplar clones. Acta Physiol. Plant. 38, 27. https://doi.org/10.1007/s11738-015-2057-7.

Maier, C.A., Burley, J., Cook, R., Ghezehei, S.B., Hazel, D.W., Nichols, E.G., 2019. Tree water use, water use efficiency, and carbon isotope discrimination in relation to growth potential in *Populus deltoides* and hybrids under field conditions. Forests 10, 993. https://doi.org/10.3390/f10110993.

Marmiroli, M., Pietrini, F., Maestri, E., Zacchini, M., Marmiroli, N., Massacci, A., 2011. Growth, physiological and molecular traits in Salicaceae trees investigated for phytoremediation of heavy metals and organics. Tree Physiol. 31, 1319–1334. https://doi.org/10.1093/treephys/tpr090.

Marron, N., Dreyer, E., Boudouresque, E., Delay, D., Petit, J.-M., Delmotte, F.M., Brignolas, F., 2003. Impact of successive drought and re-watering cycles on growth and specific leaf area of two *Populus x canadensis* (Moench) clones, "Dorskamp" and "Luisa_Avanzo." Tree Physiol. 23, 1225–1235. https://doi.org/10.1093/treephys/23.18.1225.

McCutcheon, S.C., Schnoor, J.L. (Eds.), 2003. Phytoremediation: transformation and control of contaminants, 1st ed. Wiley-Interscience, Hoboken, New Jersey. https://doi.org/10.1002/047127304X.

McDowell, N., Pockman, W.T., Allen, C.D., Breshears, D.D., Cobb, N., Kolb, T., Plaut, J., Sperry, J., West, A., Williams, D.G., Yepez, E.A., 2008. Mechanisms of plant survival and mortality during drought: why do some plants survive while others succumb to drought? New Phytol. 178, 719–739. https://doi.org/10.1111/j.1469-8137.2008.02436.x.

Meiresonne, L., 1999. Measured sap flow and simulated transpiration from a poplar stand in Flanders (Belgium). Agric. For. Meteorol. 96, 165–179. https://doi.org/10.1016/S0168-1923(99)00066-0.

Munné-Bosch, S., Alegre, L., 2004. Die and let live: leaf senescence contributes to plant survival under drought stress. Functional Plant Biol. 31, 203–216. https://doi.org/10.1071/FP03236.

National Drought Mitigation Center, 2025. U.S. drought monitor. https://droughtmonitor.unl.edu/DmData/DataDownload/ComprehensiveStatistics.aspx (accessed 4 March 2025).

Navarro, A., Portillo-Estrada, M., Arriga, N., Vanbeveren, S.P.P., Ceulemans, R., 2018. Genotypic variation in transpiration of coppiced poplar during the third rotation of a short-rotation bio-energy culture. GCB Bioenergy 10, 592–607. https://doi.org/10.1111/gcbb.12526.

Nelson, N.D., Berguson, W.E., McMahon, B.G., Jackson, J., Buchman, D., DuPlissis, J., White, T.W., 2021. Intellectual property in the NRRI hybrid poplar program – inventory, commercialization plan, and progress report (Technical Report No. NRRI/TR-2021/07). University of Minnesota Duluth, Duluth, Minnesota. https://conservancy.umn.edu/items/b5cb6f2f-ccbe-4a63-a057-b3c57f1e0a30.

NOAA (National Oceanic and Atmospheric Administration) National Centers for Environmental Information, 2025. U.S climate normals. https://www.ncei.noaa.gov/products/land-based-station/us-climate-normals (accessed 6 March 2025).

Oishi, A.C., Hawthorne, D.A., Oren, R., 2016. Baseliner: an open-source, interactive tool for processing sap flux data from thermal dissipation probes. SoftwareX 5, 139–143. https://doi.org/10.1016/j.softx.2016.07.003.

Oren, R., Sperry, J.S., Katul, G.G., Pataki, D.E., Ewers, B.E., Phillips, N., Schäfer, K.V.R., 1999. Survey and synthesis of intra- and interspecific variation in stomatal sensitivity to vapour pressure deficit. Plant Cell Environ. 22, 1515–1526. https://doi.org/10.1046/j.1365-3040.1999.00513.x.

Orság, M., Berhongaray, G., Fischer, M., Klem, K., Ceulemans, R., King, J.S., Hlaváčová, M., Trnka, M., 2024. Elevated CO_2 concentration alleviates the negative effect of vapour pressure deficit and soil drought on juvenile poplar growth. Centr. Eur. For. J. 70, 51–61. https://doi.org/10.2478/forj-2024-0017.

Phillips, N., Oren, R., 1998. A comparison of daily representations of canopy conductance based on two conditional time-averaging methods and the dependence of daily conductance on environmental factors. Ann. For. Sci. 55, 217–235. https://doi.org/10.1051/forest:19980113.

Pietrini, F., Zacchini, M., Iori, V., Pietrosanti, L., Bianconi, D., Massacci, A., 2009. Screening of poplar clones for cadmium phytoremediation using photosynthesis, biomass and cadmium content analyses. Int. J. Phytoremediat. 12, 105–120. https://doi.org/10.1080/15226510902767163.

Pilipović, A., Zalesny, R.S., Rogers, E.R., McMahon, B.G., Nelson, N.D., Burken, J.G., Hallett, R.A., Lin, C.-H., 2021. Establishment of regional phytoremediation buffer

systems for ecological restoration in the Great Lakes Basin, USA. II. New clones show exceptional promise. Forests 12, 474. https://doi.org/10.3390/f12040474.

Prouzová, N., Kubátová, P., Mercl, F., Száková, J., Najmanová, J., Tlustoš, P., 2024. Biomass yield and metal phytoextraction efficiency of *Salix* and *Populus* clones harvested at different rotation lengths in the field experiment. Chem. Biol. Technol. Agric. 11, 78. https://doi.org/10.1186/s40538-024-00600-1.

R Core Team, 2020. R: a language and environment for statistical computing. R Foundation for Statistical Computing, Vienna, Austria. https://www.R-project.org/.

R Core Team, 2019. The R stats package. https://www.rdocumentation.org/packages/stats/versions/3.6.2.

Renninger, H.J., Pitts, J.J., Rousseau, R.J., 2022. Comparisons of biomass, water use efficiency and water use strategies across five genomic groups of *Populus* and its hybrids. GCB Bioenergy 15, 99–112. https://doi.org/10.1111/gcbb.13014.

Renninger, H.J., Stewart, L.F., Rousseau, R.J., 2021. Water use, efficiency, and stomatal sensitivity in eastern cottonwood and hybrid poplar varietals on contrasting sites in the southeastern United States. Front. For. Glob. Change 4, 704799. https://doi.org/10.3389/ffgc.2021.704799.

Riemenschneider, D.E., Isebrands, J.G., Berguson, W.E., Dickmann, D.I., Hall, R.B., Mohn, C.A., Stanosz, G.R., Tuskan, G.A., 2001. Poplar breeding and testing strategies in the north-central U.S.: demonstration of potential yield and

consideration of future research needs. Forest. Chron. 77, 245–253. https://doi.org/10.5558/tfc77245-2.

Rigden, A.J., Mueller, N.D., Holbrook, N.M., Pillai, N., Huybers, P., 2020. Combined influence of soil moisture and atmospheric evaporative demand is important for accurately predicting US maize yields. Nat. Food 1, 127–133. https://doi.org/10.1038/s43016-020-0028-7.

Rogers, E.R., Zalesny, R.S., Hallett, R.A., Headlee, W.L., Wiese, A.H., 2019. Relationships among root–shoot ratio, early growth, and health of hybrid poplar and willow clones grown in different landfill soils. Forests 10, 49. https://doi.org/10.3390/f10010049.

Rogers, E.R., Zalesny, R.S., Lin, C.-H., Vinhal, R.A., 2023. Intrinsic and extrinsic factors influencing *Populus* water use: a literature review. J. Environ. Manage. 348, 119180. https://doi.org/10.1016/j.jenvman.2023.119180.

Rovida Kojima, E.A., Gonzalez, C.V., Mundo, I.A., Guevara, A., Biruk, L.N., Giordano, C.V., 2023. Differential responses of *Populus deltoides* and *Populus* × *canadensis* clones to short-term water deficit. New Forest. 54, 421–437. https://doi.org/10.1007/s11056-022-09929-7.

Rovida Kojima, E.A., González, C.V., Mundo, I.A., Guevara, A., Giordano, C.V., 2024. Mechanisms of drought resistance in *Populus deltoides* and *P.* × *canadensis* clones to possible situations of water restriction in irrigated systems in drylands. Trees 38, 1267–1281. https://doi.org/10.1007/s00468-024-02551-4.

Salt, D.E., Smith, R.D., Raskin, I., 1998. Phytoremediation. Annu. Rev. Plant. Physiol. Plant. Mol. Biol. 49, 643–668. https://doi.org/10.1146/annurev.arplant.49.1.643.

Samuelson, L.J., Stokes, T.A., Coleman, M.D., 2007. Influence of irrigation and fertilization on transpiration and hydraulic properties of *Populus deltoides*. Tree Physiol. 27, 765–774. https://doi.org/10.1093/treephys/27.5.765.

SAS Institute, Inc., 2023. SAS/STAT® 15.3 user's guide. Carey, North Carolina. https://documentation.sas.com/doc/en/pgmsascdc/9.4_3.5/statug/titlepage.htm.

Schmidt-Walter, P., Richter, F., Herbst, M., Schuldt, B., Lamersdorf, N.P., 2014. Transpiration and water use strategies of a young and a full-grown short rotation coppice differing in canopy cover and leaf area. Agric. Forest Meteorol. 195–196, 165–178. https://doi.org/10.1016/j.agrformet.2014.05.006.

Sperry, J.S., Hacke, U.G., Oren, R., Comstock, J.P., 2002. Water deficits and hydraulic limits to leaf water supply. Plant Cell Environ. 25, 251–263. https://doi.org/10.1046/j.0016-8025.2001.00799.x.

Stojnić, S., Bojović, M., Pilipović, A., Orlović, S., 2021. Selecting tree species for reclamation of coal mine tailings based on physiological parameters. Topola 27–38. https://doi.org/10.5937/topola2108027S.

Sun, H., Aubrey, D.P., Teskey, R.O., 2012. A simple calibration improved the accuracy of the thermal dissipation technique for sap flow measurements in juvenile trees of six species. Trees 26, 631–640. https://doi.org/10.1007/s00468-011-0631-1.

Tang, L., Cao, P., Zhang, S., Liu, X., Ge, X., Tang, L., 2024. Two male poplar clones (*Populus* × *euramericana* 'Siyang-1' and *Populus deltoides* 'Nanlin 3804') exhibit distinctly different physiological responses to soil water deficit. Forests 15, 1142. https://doi.org/10.3390/f15071142.

Tardieu, F., Simonneau, T., 1998. Variability among species of stomatal control under fluctuating soil water status and evaporative demand: modelling isohydric and anisohydric behaviours. J. Exp. Bot. 49, 419–432. https://doi.org/10.1093/jxb/49.Special_Issue.419.

Telewski, F., Aloni, R., Sauter, J., 1996. Physiology of secondary tissues of *Populus*, in: Stettler, R., Bradshaw Jr., H., Heilman, P., Hinckley, T. (Eds.), Biology of *Populus* and Its Implications for Management and Conservation. NRC Research Press, Ottawa, Ontario, pp. 301–329.

Tharakan, P.J., 1999. Clonal performance evaluation and production physiology of willow and poplar bioenergy crops. State University of New York College of Environmental Science and Forestry. https://www.proquest.com/dissertations-theses/clonal-performance-evaluation-production/docview/304526829/se-2.

Trapp, S., Karlson, U., 2001. Aspects of phytoremediation of organic pollutants. J. Soils Sediments 1, 37–43. https://doi.org/10.1007/BF02986468.

Tripathi, A., Pohanková, E., Fischer, M., Orság, M., Trnka, M., Klem, K., Marek, M., 2018. The evaluation of radiation use efficiency and leaf area index development for the estimation of biomass accumulation in short rotation poplar and annual field crops. Forests 9, 168. https://doi.org/10.3390/f9040168.

Tripathi, A.M., Fischer, M., Orság, M., Marek, M.V., Žalud, Z., Trnka, M., 2016. Evaluation of indirect measurement method of seasonal patterns of leaf area index in a high-density short rotation coppice culture of poplar. Acta Univ. Agric. Silvic. Mendelianae Brun. 64, 549–556. https://doi.org/10.11118/actaun201664020549.

USDA-NRCS (United States Department of Agriculture Natural Resources Conservation Service), 2025. Web soil survey. https://websoilsurvey.sc.egov.usda.gov/app/ (accessed 14 January 2025).

Vose, J.M., Swank, W.T., Harvey, G.J., Clinton, B.D., Sobek, C., 2000. Leaf water relations and sapflow in eastern cottonwood (*Populus deltoides* Bartr.) trees planted for phytoremediation of a groundwater pollutant. Int. J. Phytoremediat. 2, 53–73. https://doi.org/10.1080/15226510008500030.

Wenzel, W.W., 2009. Rhizosphere processes and management in plant-assisted bioremediation (phytoremediation) of soils. Plant Soil 321, 385–408. https://doi.org/10.1007/s11104-008-9686-1.

Wickham, H., 2016. ggplot2: elegant graphics for data analysis, Use R! Springer International Publishing, New York, USA. https://doi.org/10.1007/978-3-319-24277-4.

Wolfe, B.T., Sperry, J.S., Kursar, T.A., 2016. Does leaf shedding protect stems from cavitation during seasonal droughts? A test of the hydraulic fuse hypothesis. New Phytol. 212, 1007–1018. https://doi.org/10.1111/nph.14087

Wullschleger, S., Wilson, K.B., Hanson, P.J., 2000. Environmental control of whole-plant transpiration, canopy conductance and estimates of the decoupling coefficient for

large red maple trees. Agric. Forest Meteorol. 104, 157–168. https://doi.org/10.1016/S0168-1923(00)00152-0.

Yuan, W., Zheng, Y., Piao, S., Ciais, P., Lombardozzi, D., Wang, Y., Ryu, Y., Chen, G., Dong, W., Hu, Z., Jain, A.K., Jiang, C., Kato, E., Li, S., Lienert, S., Liu, S., Nabel, J.E.M.S., Qin, Z., Quine, T., Sitch, S., Smith, W.K., Wang, F., Wu, C., Xiao, Z., Yang, S., 2019. Increased atmospheric vapor pressure deficit reduces global vegetation growth. Sci. Adv. 5, eaax1396. https://doi.org/10.1126/sciadv.aax1396.

Zalesny, R., Wiese, A., Bauer, E., Riemenschneider, D., 2006. Sapflow of hybrid poplar (*Populus nigra* L. × *P. maximowiczii* A. Henry 'NM6') during phytoremediation of landfill leachate. Biomass Bioenerg. 30, 784–793. https://doi.org/10.1016/j.biombioe.2005.08.006.

Zalesny, R.S., Bauer, E.O., 2007. Selecting and utilizing *Populus* and *Salix* for landfill covers: implications for leachate irrigation. Int. J. Phytoremediat. 9, 497–511. https://doi.org/10.1080/15226510701709689.

Zalesny, R.S., Headlee, W.L., Gopalakrishnan, G., Bauer, E.O., Hall, R.B., Hazel, D.W., Isebrands, J.G., Licht, L.A., Negri, M.C., Nichols, E.G., Rockwood, D.L., Wiese, A.H., 2019. Ecosystem services of poplar at long-term phytoremediation sites in the Midwest and Southeast, United States. WIREs Energy Environ. 8, e349. https://doi.org/10.1002/wene.349.

Zalesny, R.S., Pilipović, A., Rogers, E.R., Burken, J.G., Hallett, R.A., Lin, C.-H., McMahon, B.G., Nelson, N.D., Wiese, A.H., Bauer, E.O., Buechel, L., DeBauche, B.S., Peterson, M., Seegers, R., Vinhal, R.A., 2021. Establishment of regional

phytoremediation buffer systems for ecological restoration in the Great Lakes Basin, USA. I. Genotype × environment interactions. Forests 12, 430. https://doi.org/10.3390/f12040430.

Zarnoch, S.J., 2009. Testing hypotheses for differences between linear regression lines (No. SRS-RN-17). U.S. Department of Agriculture, Forest Service, Southern Research Station, Asheville, NC. https://doi.org/10.2737/SRS-RN-17.

Zenone, T., Fischer, M., Arriga, N., Broeckx, L.S., Verlinden, M.S., Vanbeveren, S., Zona, D., Ceulemans, R., 2015. Biophysical drivers of the carbon dioxide, water vapor, and energy exchanges of a short-rotation poplar coppice. Agric. Forest Meteorol. 209–210, 22–35. https://doi.org/10.1016/j.agrformet.2015.04.009.

CHAPTER 6. CONCLUSIONS AND FUTURE WORK

6.1 Conclusions

In the first study a comprehensive landfill leachate pollutant prioritization method was developed. The tool incorporates ToxPi to quantitatively rank landfill pollutants based on their potential toxicity to human health and/or the environment using publicly available toxicity data from *in vitro* and *in vivo* toxicity assays and *in silico* predicted human toxicity values. The developed approach was implemented to prioritize leachate contaminants reported in the literature. Multiple toxicity endpoint weighting schemes were tested to demonstrate the flexibility and customizable nature of the approach. A total of 322 leachate contaminants identified from the literature were prioritized using the approach. The highest ranked pollutants according to the general weighting scheme (equal weights for all endpoints) consisted mainly of pesticides, pharmaceuticals, and industrial byproducts. When compared to landfill leachate regulatory lists, none of the compounds in the top 40 are contained in Appendix I of 40 C.F.R § 258, while 63% are included in Appendix II of the same section. The developed approach, with its customizable and flexible nature, in addition to its toxicity data being from publicly available sources, holds promise as a method for cost-effective identification of contaminants that are most relevant to community priorities and concerns, and which may warrant remediation measures, including phytotechnologies.

The second study built upon the pollutant prioritization method and added non-targeted high-resolution mass spectrometry-based data processing with the XCMS Online platform. The resulting framework for comprehensive landfill leachate evaluation was

applied to landfill groundwater and leachate samples from two Wisconsin landfills. Out of 6,699 total features, 242 compounds were putatively identified and prioritized using the framework. ToxPi scores for the 242 compounds ranged from 0.0296 (cimetidine) to 0.6430 (clotrimazole). The top 25 compounds with the greatest potential toxicity to human health and/or the environment included mainly pharmaceuticals and biocides, which represent newer classes of landfill leachate compounds and expanding avenues for leachate phytoremediation. Further work can expand upon these efforts by incorporating additional toxicity databases, and chemical properties related to environmental fate, transport, and exposure, into the toxicity prioritization model. This framework is a first step towards standardized pollutant prioritization for phytotechnologies applications.

The third study performed a meta-analysis of poplar water use reported in the literature. Out of 133 identified articles that reported information on the methodologies used to measure poplar sap flow, a proxy for water use, 51 reported poplar water use data, which were extracted from the manuscripts for analysis. Hybrid poplars were studied in 18 articles and included 17 genotypes, while non-hybrids were studied in 33 articles and included eight species. Hybrid poplar water use ranged from 0.7 to 11.3 mm day^{-1} with an overall mean of 2.7 ± 0.3 mm day^{-1}, and differed significantly among hybrid types, tree age classes, and water availability classes. Non-hybrid water use ranged from 0.2 to 19.5 mm day^{-1} with a mean of 2.8 ± 0.4 mm day^{-1}, and differed significantly among species, experimental context, and water availability classes. Results indicated that for hybrid poplars, intersectional hybrids, with their significantly greater water use than intrasectional hybrids, may be more suitable for use in pollution remediation systems or in locations with abundant water, while intrasectional hybrids may be more suited to

areas with less available water, or non-irrigated plantings. For non-hybrids, *P. fremontii* exhibited the greatest water use values and may be better suited to remediation applications, while *P. deltoides*, *P. euphratica*, and *P. tremuloides* had significantly lower water use, and may be more suited to drier areas or those without irrigation. This study provides a standardized summary of available information on *Populus* water use and some of its key influencing factors. The work could be built upon by incorporating soil properties into the analyses of water use, and through investigating the interactions that exist among the influencing factors.

The fourth study assessed the water relations of three hybrid poplar genotypes ('DN34', *P. deltoides* × *P. nigra*; '9732-11', *P. deltoides* × *P. nigra*; 'NM2', *P. nigra* × *P. maximowiczii*) in their fourth growing season and grown for phytoremediation in Eastern Wisconsin. Water use was measured over a 75-day study period using thermal dissipation sap flow probes. Physiological and morphological parameters related to water use (i.e., leaf area index, stomatal sensitivity to vapor pressure deficit (VPD), leaf-level hydraulic conductance, leaf water potential) were also measured during the study. Average daily water use differed among the genotypes, with '9732-11' having significantly greater water use (mean of 18 ± 0.4 kg tree^{-1} day^{-1}) than both 'NM2' (mean of 13 ± 0.3 kg tree^{-1} day^{-1}; $p = 0.0011$) and 'DN34' (mean of 10 ± 0.2 kg tree^{-1} day^{-1}; $p < 0.0001$). Total water use over the 75-day study exhibited a similar trend, with '9732-11' having the greatest total water use (1,335 ± 55 kg tree^{-1}), followed by 'NM2' (1,002 ± 83 kg tree^{-1}) and 'DN34' (780 ± 79 kg tree^{-1}). Stomatal sensitivity to VPD was higher for '9732-11' than 'NM2' ($p = 0.0373$) under average-to-high soil moisture conditions ($\theta > 0.2$ m^3 m^{-3}). On the other hand, 'NM2' exhibited plasticity in response to different soil moisture conditions, with its scaled

stomatal sensitivity being significantly higher ($p = 0.0202$) under lower soil moisture than high soil moisture. These findings provide evidence that the water use strategies of these genotypes may vary. Such information on tree water relations can inform the selection of resilient poplar genotypes for environmental applications, including pollution remediation.

6.2 Future work

The work presented here has motivated me to make the following suggestions for future work to build upon these efforts.

6.2.1 Targeted analysis of landfill leachate

The landfill leachate pollutant identification and prioritization framework presented here is useful for putative identification of candidate priority pollutants, a first step in the design of phytoremediation systems that target the pollutants. A necessary second step will be targeted analysis, in which the identities of the pollutants are confirmed, and their absolute concentrations are determined, using LC-MS analysis. Reference analytical standards of high purity (>98%) will enable peak annotation for identity confirmation, and calibration curves generated using the analytical standards will enable quantification. Identity confirmation and absolute quantification are critical for informed decision-making on contaminants to select for remediation. Analysis of leachate samples collected at multiple timepoints will further allow assessment of the seasonality of its composition, and would provide additional insight into the most appropriate remediation strategy. For the landfills within the studies presented here, targeted analysis will enable identification of contaminants with highest concentrations. Combined with the results of toxicity prioritization, it will be possible to identify contaminants for

remediation that exhibit both high concentrations and high potential toxicity. In a broader sense, results of landfill leachate targeted analysis will inform the testing and selection of suitable poplar genotypes to remediate the identified pollutants. In addition, results can be used to promote effective remediation system design according to the seasonality of the chemical composition, and to implement long-term monitoring approaches to evaluate the effectiveness of phytoremediation on priority compounds over time.

Proposed approach

Objective 1: Conduct targeted analysis of landfill leachate samples.

Task 1: Confirm identities of putatively identified compounds through LC-MS analysis of reference analytical standards.

Task 2: Quantify identified compounds using LC-MS analysis with calibration curves developed from reference analytical standards.

Objective 2: Assess the seasonality of landfill leachate composition.

Task 1: Collect landfill leachate samples at different timepoints throughout the year, and over multiple years.

Task 2: Perform non-targeted analysis, prioritization, and targeted analysis of the collected samples.

6.2.2 Investigations of the phytoremediation efficacy of poplars

Understanding the water use strategies of different hybrid poplar genotypes is important for informing the selection of genotypes to maximize remediation objectives while promoting resilience to variable climatic conditions. However, to better understand

the differences in phytoremediation efficacy among genotypes, further work on pollutant fate that incorporates both pollutant characteristics and tree physiological and morphological characteristics will be necessary. Hydrological modeling is an option for minimally destructive analysis of potential phytoremediation efficacy. The HYDRUS hydrological model and software package enables numerical simulation of water and solute transport in variably saturated media through solving the Richards equation and advection-dispersion equations, respectively. An additional Dynamic Plant Uptake (DPU) module further enables simulation of pollutant fate (i.e., transformation and translocation) in the soil-plant continuum. Results from targeted pollutant analysis described above (e.g., pollutant concentration data), coupled with genotype-specific data (e.g., water use, LAI, growth) are among the necessary input parameters for HYDRUS simulations. Such simulations would provide researchers and practitioners with information on pollutant fate and transport in poplar-based phytoremediation systems, including comparisons among poplar genotypes. This information could help to inform decision-making in phytoremediation system design for minimizing environmental risks from pollutants.

Proposed approach

Objective 1: Obtain input parameters necessary to perform HYDRUS modeling.

Task 1: Perform non-targeted analysis and toxicity-based prioritization of leachate, groundwater, and soil samples from phytoremediation site.

Task 2: Perform targeted analysis of leachate, groundwater, and soil samples for compound identity confirmation and quantitation.

Task 3: Identify pollutant physical and chemical properties (e.g., log K_{OW}, molar mass) and main bacterial and plant metabolites reported in the literature.

Task 4: Perform laboratory experiments to measure hydraulic properties of soil collected from phytoremediation site.

Task 5: Conduct poplar root growth experiments in greenhouse and field settings to quantify rooting depth and lateral growth of different genotypes over time.

Task 6: Conduct poplar growth and water content experiments in the greenhouse and field settings to quantify growth (in terms of mass) of tree components (leaves, stems, roots) and their water content over time.

Objective 2: Compare pollutant fate and transport among poplar genotypes in phytoremediation systems.

Task 1: Perform simulation modeling using HYDRUS – DPU to assess the differences in pollutant fate and transport within phytoremediation systems comprised of different poplar genotypes.

Task 2: Perform validation experiments to compare simulated and measured concentrations of different pollutants and their metabolites within soils, roots, leaves, and stems of different poplar genotypes.

VITA

Ms. Elizabeth Rogers was born in Rhinelander, Wisconsin on August 10th, 1995. She received her Bachelor of Science in both Environmental Science and Elementary Education from Northern Michigan University in Marquette, Michigan in 2018. Ms. Rogers began working at the USDA Forest Service, Northern Research Station, Institute for Applied Ecosystem Studies as a Biological Science Aid in the summer of 2016. It was in this position that she first learned about phytotechnologies, and her interest in environmental remediation was ignited. She continued working at the Forest Service on phytotechnologies research during every summer, winter, and school break from that summer on. Ms. Rogers became a Pathways Intern with the Forest Service in 2018, a position she has been honored to hold since. Her passion for environmental science then led her to pursue a PhD of Natural Resources (phytoremediation) at the University of Missouri, Center for Agroforestry.

Ms. Rogers married in 2024 in a small, beautiful winter ceremony in Michigan's Upper Peninsula. She currently lives in Rhinelander, WI with her spunky, easy-going husband. In her free time, she enjoys outdoor activities in the Northwoods including hiking, camping, kayaking, running, cross-country skiing, and disc golfing.